Haptic Gas Pedal Feedback for Active Car-Following Support

Cover foto: Regional Air Quality Council website (www.raqc.org)

ISBN-10: 90-8559-266-6
ISBN-13: 978-90-8559-266-2

Haptic Gas Pedal Feedback for Active Car-Following Support

Proefschrift

ter verkrijging van de graad van doctor
aan de Technische Universiteit Delft,
op gezag van de Rector Magnificus prof. dr. ir. J.T. Fokkema,
voorzitter van het College voor Promoties,
in het openbaar te verdedigen
op dinsdag 30 januari 2007 om 15:00 uur

door

Mark MULDER

ingenieur luchtvaart en ruimtevaart

geboren te Vlaardingen

Dit proefschrift is goedgekeurd door de promotoren:
Prof. dr. ir. J.A. Mulder
Prof. dr. F.C.T. van der Helm

Toegevoegd promotor:
Dr. ir. M. Mulder

Samenstelling promotiecommissie:

Rector Magnificus,	voorzitter
Prof. dr. ir. J.A. Mulder,	Technische Universiteit Delft, promotor
Prof. dr. F.C.T. van der Helm,	Technische Universiteit Delft, promotor
Dr. ir. M. Mulder,	Technische Universiteit Delft, toegevoegd promotor
Prof. dr. ir. P.A. Wieringa,	Technische Universiteit Delft
Prof. dr. J.M. Flach,	Wright State University, USA
Prof. dr. F.M. Cardullo,	Binghamton University, USA
Dr. ir. E.R. Boer,	LUEBEC, USA
Prof. dr. ir. H.G. Stassen,	Technische Universiteit Delft, reservelid

Dr. ir. M.M. van Paassen heeft als begeleider in belangrijke mate aan de totstandkoming van het proefschrift bijgedragen.

Dit proefschrift is verder in belangrijke mate tot stand gekomen door de wetenschappelijke, materiële en financiële bijdragen van Nissan Motor Company, Ltd., Japan.

"*To me it is of very little importance whether they [Masters] exist or whether they do not exist, because when you have to walk to the camp or to the station from here, there are people ahead of you, nearer the station, people who have started earlier. What is more important – to get to the station or to sit down and worship the man who is ahead of you?*"

Henry Miller
(quoting Krishnamurti)

Summary

With the increased importance of the car as a personal means of transportation, non-driving related devices, such as car-stereos, mobile phones, and more recently navigation systems, divert drivers' attention more and more away from the primary sources of information necessary for safe operation of the vehicle: the road and other road users. With traffic accident statistics attributing driver inattention as one of the major causes of traffic accidents (Campbell, Smith and Najm, 2003; Wang, Knipling, and Goodman, 1996; Treat *et al.,* 1979), this increase of in-vehicle devices is worrisome at least – if not dangerous.

To bridge the gap between the gain in improved passive safety (for example airbags and anti-crash bodies) and the increasing development of non-driving related in-vehicle devices, car safety systems research is directed more towards systems that actively support drivers in their driving task. Ultimately active support systems aim to prevent drivers from getting into accidents. This is a radically different approach compared to that of passive safety systems, which help to lessen the impact of driving accidents but do nothing to contribute to preventing drivers from getting into an accident.

Intelligent transportation systems (ITS) currently available can be labelled as what Goodrich and Boer (2000) call the primary purpose of task automation: "safely promoting comfort". By automating routine skills that were previously required of drivers, for example, speed regulation and car-following which are taken care of by Adaptive Cruise Control (ACC) upon initiation by the driver, driving is made easier without compromising safety. Task automation systems perform driver tasks to maintain the safe field of travel automatically, under a very limited set of circumstances. More recent ITS's are focusing more on what Goodrich and Boer (2000) call response automation: "comfortably promoting safety". This type of automation automatically informs drivers when their safe field of travel is degrading seriously, urging them to take swift action to restore this situation to an acceptable level of safety. So, rather than taking over particular driving tasks, response automation monitors the environment, car state variables, and perhaps driver state variables (for example, drowsiness, gaze, intent) based upon which safety judgments are passed on to the driver who, ultimately, is responsible for taking appropriate corrective actions.

The research presented in this dissertation focuses on supporting drivers in the longitudinal control of their vehicle during car-following. In April 2002, Delft University of Technology started participating in a multi-university research project, initiated by Nissan Motor Company, on human-centred development of a future intelligent driver support system (IDSS). The aim of the project was to develop a system that would cooperate with the driver in comfortably maintaining safe separation with surrounding vehicles. The goal of the research presented in this dissertation is the human-centred development of a haptic gas pedal interface that comfortably supports drivers in maintaining a safe separation with a leading vehicle during car-following.

Two different approaches were found to be suitable for implementation as haptic information providers through the gas pedal. The first approach was to add a force to the gas

pedal dynamics which would have to be related to the safe-field-of-travel ahead of the own vehicle and changes therein. The gas pedal dynamics, that is, the force/pedal-position relationship is not changed by this approach. The second approach was to change the stiffness of the gas pedal by adding a virtual stiffness to the inherent stiffness of the gas pedal. By doing so, the dynamics of the gas pedal are changed depending on the changes detected in the safe-field-of-travel. In both approaches, an electrical actuator provides the additional force or stiffness.

The complementary haptic control loop that is obtained by feeding back environmental parameters with these additional forces or dynamics is based, however, on one major assumption: environmental parameters can be converted into meaningful haptic information in a car-following context.

From the investigations into the environmental variables that are most suitable to represent the safe-field-of-travel and its changes, the link between the mechanisms to provide haptic gas pedal feedback and these environmental variables was established by three haptic gas pedal feedback algorithms. One of these algorithms was designed to provide force feedback, with environmental information based on time-headway (*THW*) and time-to-contact (*TTC*). This algorithm was called the force feedback algorithm. The other two algorithms used stiffness feedback as their means of generating haptic feedback and differed only in the use of the environmental variables. One of the algorithms, which made use of *THW* only as the source of environmental information was called the THW-stiffness algorithm. The other stiffness algorithm made use mainly of *TTC*, which was scaled, however, by *THW*. This algorithm was called the TTC-algorithm.

Because the transformation of environmental information (*THW* and *TTC*) into a haptic feedback signal does not have any natural equivalents, it was impossible to know beforehand how drivers would respond to this kind of support. Therefore, the different algorithms were tested in a number of experiments under a variety of environmental conditions.

It was expected first and most importantly that drivers would adopt a force-task strategy in controlling the gas pedal when haptic feedback was available. The force-task strategy entails that drivers try to maintain the force they experience from the gas pedal at a constant level. Because the haptic feedback algorithms are designed to increase the amount of haptic feedback with decreasing separation with a lead vehicle, trying to keep the force constant will automatically lead to drivers applying the desired control input to their vehicle: reducing gas pedal input when a lead vehicle approaches and increasing gas pedal input when a lead vehicle moves away again.

Analysis of the distributions of the measured gas pedal forces, together with the statistical analysis of variance of the standard deviations, show there is reason to accept the hypothesis that drivers adopt a force task strategy in driving with haptic gas pedal feedback. Not for all haptic feedback algorithms, though. The THW-stiffness algorithm shows little signs of force-task strategy in close following conditions. The differences between the force feedback and the TTC-stiffness feedback seem negligible and it might be concluded for both algorithms that the haptic feedback leads to the adoption of a force-task strategy in controlling the gas pedal during car-following. This conclusion is based on the fact that for almost all experiments described in

this thesis, the standard deviation of the measured pedal force for the conditions with haptic feedback was lower than the conditions without haptic feedback.

A reduction of control effort when using haptic feedback, which was found in all experiments that were conducted, shows that drivers obtain valuable information not only of the changes in the safe-field-of-travel based on the movement of the lead vehicle alone, but also based on the dynamics of the own vehicle.

The cost of reducing control effort is, however, paid in increased physical load during close following with the haptic feedback support system activated. All haptic feedback algorithms showed a highly-significant increase in the physical load.

The results of the experiments show that the force feedback and TTC-stiffness feedback algorithms yield the least increase in physical load with similar reductions in control effort as the THW-stiffness algorithm compared to the base-line no feedback condition.

To conclude, drivers have indicated subjectively to feel that they benefit from the presence of haptic feedback during car-following, indicating the trust they have in the information that is transmitted to them via the haptic gas pedal. The combination of increased driver confidence and decreased control effort could well be an excellent combination in the increased complexity and busyness of our highway traffic today and in the future.

Contents

SUMMARY **VII**

INTRODUCTION **1**

1.1 DRIVER SUPPORT SYSTEMS RESEARCH 3
1.1.1 Intelligent speed adaptation 3
1.1.2 Collision avoidance 4
1.1.3 Car-following 4
1.1.4 The Nissan Intelligent Driver Support System 4
1.2 GOAL OF THE RESEARCH 7
1.3 RESEARCH APPROACH 8
1.4 THESIS ORGANISATION 9

HAPTIC GAS PEDAL FEEDBACK **11**

2.1 HAPTIC FEEDBACK IN THE CONTROL LOOP 11
2.2 DYNAMICS OF DRIVER – GAS PEDAL INTERACTION 13
2.2.1 Passive gas pedal dynamics 13
2.2.2 Neuromusculoskeletal dynamics of the foot 16
2.2.3 Longitudinal control with a passive gas pedal 18
2.3 VIRTUAL GAS PEDAL DYNAMICS 20
2.3.1 Force feedback 21
2.3.2 Stiffness feedback 22
2.3.3 Car-following control with an active gas pedal 23
2.4 FROM FORCE TO INFORMATION 25

HAPTIC FEEDBACK ALGORITHMS **27**

3.1 CAR-FOLLOWING KINEMATICS 28
3.1.1 Following behaviour 29
3.1.2 Time-headway and time-to-contact 31
3.2 GENERALISED OBSTACLE AVOIDANCE ALGORITHMS 34
3.2.1 Generalised potential fields 34
3.2.2 Impedance control for obstacle avoidance 37
3.3 HAPTIC FEEDBACK ALGORITHMS 38
3.3.1 Nissan force feedback 39
3.3.2 THW-stiffness feedback 42
3.3.3 TTC-stiffness feedback 44
3.3.4 Human response to haptic gas-pedal feedback 46

EXPERIMENTAL METHOD **49**

4.1 APPARATUS 50
4.1.1 The active gas-pedal 51
4.2 THE CAR-FOLLOWING TASK 52
4.2.1 Time-headway indicator 53
4.2.2 Lead vehicle speed disturbance characteristics 55
4.3 DATA ACQUISITION AND PROCESSING 56
4.3.1 Time domain data analysis 58
4.3.2 Frequency domain data analysis 60

CAR-FOLLOWING EXPERIMENTS WITH MAXIMAL VISUAL ATTENTION 65

5.1 COMPARISON BETWEEN FORCE FEEDBACK AND STIFFNESS FEEDBACK 66
5.1.1 Method 66
5.1.2 Hypotheses 68
5.1.3 Results 68
5.1.4 Discussion of the results 71
5.1.5 Conclusions 72
5.2 SUPPORTED CAR-FOLLOWING AT DIFFERENT TIME-HEADWAYS 73
5.2.1 Method 73
5.2.2 Hypotheses 75
5.2.3 Results 75
5.2.4 Discussion of the results 78
5.2.5 Conclusions 81
5.3 LEAD VEHICLE SPEED EFFECTS ON SUPPORTED CAR-FOLLOWING 81
5.3.1 Method 81
5.3.2 Hypotheses 83
5.3.3 Time-domain results 84
5.3.4 Frequency-domain results 88
5.3.5 Discussion of the results 90
5.3.6 Conclusions 94
5.4 OVERALL DISCUSSION AND CONCLUSIONS 94

CAR-FOLLOWING EXPERIMENTS WITH SECONDARY TASKS 97

6.1 REACTION-TIME TASK WITH CENTRAL AND PERIPHERAL VISUAL STIMULI 99
6.1.1 Method 99
6.1.2 Hypotheses 101
6.1.3 Results 101
6.1.4 Discussion of the results 105
6.1.5 Conclusions 107
6.2 AUDIO SYSTEM TRACK SELECTION TASK 107
6.2.1 Method 108
6.2.2 Hypotheses 110
6.2.3 Results 111
6.2.4 Discussion of the results 117
6.2.5 Conclusions 121
6.3 OVERALL DISCUSSION AND CONCLUSIONS 121

CONCLUSIONS 123

7.1 THE USE OF HAPTIC FEEDBACK IN CAR-FOLLOWING 125
7.2 HAPTIC FEEDBACK INFORMATION CONTENT 126
7.3 THE FUTURE OF HAPTIC GAS PEDAL FEEDBACK 127

DERIVATION OF GENERALIZED POTENTIAL FIELD PARAMETERS 131

A.1 THE RESERVE AVOIDANCE TIME 131
A.2 THE OBSTACLE AVOIDANCE VECTOR 132

CAR-FOLLOWING DATA DISTRIBUTIONS 135

B.1 CALCULATION OF THE CAR-FOLLOWING SPIRAL DISTRIBUTIONS 135
B.1.1 Distributions for different lead vehicle speed disturbances 135
B.1.2 Distributions for different feedback algorithms 137

B.2 DISTRIBUTION OF GAS PEDAL CHARACTERISTICS 139
B.3 DISTRIBUTION OF GAS PEDAL FORCES 142
B.3.1 Distributions for different lead vehicle speed characteristics 142
B.3.2 Distributions for different haptic feedback algorithms 143

NOMENCLATURE 147

SYMBOLS 147
SUBSCRIPTS 149
ACRONYMS 150

REFERENCES 151

SAMENVATTING 157

ACKNOWLEDGEMENTS 161

CURRICULUM VITAE 163

Chapter 1

Introduction

As early as 1938, James J. Gibson and Laurence E. Crooks (1938) realized that the ability to drive an automobile is a skill that, although acquired with remarkable ease, *"is certainly the most important to the individual, in the sense at least that a defect in it is the greatest threat to his life."* Today, with an almost more than tenfold increase in annual vehicle kilometers travelled since 1938 this statement is more true than ever. That the motor vehicle fatality rate only doubled in this same period is most certainly the result of improved driver safety regulations, higher driver training standards, better road design, and advancements in car-safety systems. From the early seatbelts and anti-crash bodies to airbags and side impact protection systems (SIPS) car manufacturers have come up with a broad range of passive safety improvements that significantly reduce the severity of driver, passenger, and pedestrian or cyclist injury when involved in a traffic accident. However, with the increased importance of the car as a personal means of transportation, non-driving related devices, such as car-stereos, mobile phones, and more recently navigation systems, divert drivers' attention more and more away from the primary sources of information necessary for safe operation of the vehicle: the road and other road users. With traffic accident statistics attributing driver inattention as one of the major causes of traffic accidents (Campbell, Smith and Najm, 2003; Wang, Knipling, and Goodman, 1996; Treat *et al.,* 1979), this increase of in-vehicle devices is worrisome at least – if not dangerous.

To bridge the gap between the gain in improved passive safety and the increasing development of non-driving related in-vehicle devices, car safety systems research is directed more towards systems that actively support drivers in their driving task. Ultimately active support systems aim to prevent drivers from getting into accidents. This is a radically different approach compared to that of passive safety systems, which help to lessen the impact of driving accidents but do nothing to contribute to preventing drivers from getting into an accident. Current existing support systems include for example anti-lock braking systems (ABS), electronic brake force distribution (EBD), advanced cruise control systems[1] (ACC), and more recently lane departure warning systems (LWD) and vehicle dynamics control (VDC) which

[1] Adaptive or Active Cruise Control (ACC) is a control system which can automatically maintain either a selected speed or a distance with a leading vehicle. The speed or distance is selected by the driver. No other driver inputs are required to make the system work (within its operational boundaries). Many modern cars today are equipped with ACC.

actively adjusts the vehicle dynamics demanded by the driving conditions. Although these systems do not explicitly help to improve drivers' ability to detect impending safety threats, they do help improve controllability and handling of cars, greatly enhancing drivers' capabilities of maintaining their safe field of travel in general and in emergency situations in particular. However, as Smiley (2000) points out in discussing behavioural adaptation to new in-vehicle support systems, it can be expected that drivers will attempt to increase their productivity in other tasks while driving, which might reduce the benefits these systems were designed to provide. Furthermore, Rudin-Brown and Parker (2004) showed that when drivers are taken out of the control loop by automation (ACC in this particular paper) their freed up attentional resources allowed them to spend more time on secondary tasks while response times to a hazard detection task decreased and variability in lane position increased. This suggests that the increase in comfort and safety that is offered by new systems might possibly be exploited by drivers to increase their non-driving related activities, diminishing the safety benefits of new intelligent transportation systems (ITS).

ITS systems currently available can be labelled as what Goodrich and Boer (2000) call the primary purpose of task automation: "safely promoting comfort". By automating routine skills that were previously required of drivers, for example, speed regulation and car-following which are taken care of by ACC upon initiation by the driver, driving is made easier without compromising safety. Task automation systems perform driver tasks to maintain the safe field of travel automatically, under a very limited set of circumstances. More recent ITS systems are focusing more on what Goodrich and Boer (2000) call response automation: "comfortably promoting safety". This type of automation automatically informs drivers when their safe field of travel is degrading seriously, urging them to take swift action to restore this situation to an acceptable level of safety. Lane departure warning systems (LDWS), for example, warn drivers that they are deviating dangerously from their current lane, urging them to make corrective actions towards the lane centre. Collision warning systems (CWS) warn drivers when a vehicle in front of their own vehicle is getting dangerously close. So, rather than taking over particular driving tasks, response automation monitors the environment, car state variables, and perhaps driver state variables (for example, drowsiness, gaze, intent) based upon which safety judgments are passed on to the driver who, ultimately, is responsible for taking appropriate corrective actions.

The limited set of operational circumstances of task automation and the discrete on/off nature of currently available and proposed future response automation pose serious problems to the effectiveness of these systems in enhancing safety. When operational constraints of task automation are not clear or not easily identifiable, driver performance might actually worsen in the most critical situations (Rudin-Brown and Parker, 2004). Binary warning systems need to be balanced between false alarm rates and missed detections. Because of the severe consequences of a missed detection, it is important that the number of missed detections is near-zero. This implicates that, theoretically, collision warnings should rarely occur (Dingus *et al.*, 1997), removing the possibilities for drivers to familiarise themselves with the system. Without familiarisation drivers might not be able to respond quickly and appropriately to warnings.

These are severe limitations of existing response and task automation systems that might even be detrimental to the purpose they were designed for: enhancing safety.

1.1 Driver support systems research

The research presented in this dissertation focuses on supporting drivers in the longitudinal control of their vehicle during car-following. Other research projects have investigated longitudinal control support before, focussing on speed adaptation and collision warning support. These investigations are briefly discussed below. Little literature has been found on support systems for car-following. Automatic control of inter-vehicle separation, however, has been thoroughly investigated and a huge body of literature is available (for example, Rudin-Brown and Parker, 2004; Young and Stanton, 2004; Goodrich and Boer, 2003; Higashimata *et al.*, 2001). The focus of the research in this dissertation, however, is on providing support to the driver such that she/he has improved *manual* control over the vehicle she/he is driving.

1.1.1 Intelligent speed adaptation

A haptic gas pedal, providing a counterforce when a local speed limit is exceeded, has been under investigation in a number of research projects. In the Generic Intelligent Driver Support (GIDS) project the use of an active gas pedal was investigated for a range of situations. In the speed control situation, the active gas pedal with a continuous counterforce on the gas pedal related to the speed error relative to a normative speed limit, yielded the lowest speed error compared with alternative displays (Godthelp and Schumann, 1993; Verwey *et al*, 1993). These findings led Godthelp and Schumman (1993) to suggest that active control information "*...may serve as an efficient information system.*" However, haptic gas pedal support for speed control during curve negotiation was found to have been a potential distracting factor in the lateral tracking task (Verwey *et al.*, 1993).

In a more recent European research project - Project for Research On Speed adaptation Policies on European Roads (PROSPER) – an extensive study has been carried out with an active gas pedal support system during speed control. The active gas pedal provides a counter-force whenever the driver tries to depress it beyond a pre-set speed limit. Additionally, the active gas pedal also restricts the engine's fuel injection when the vehicle reaches the actual speed limit. The long term- and large scale effects of using this active gas pedal were evaluated with regard to speed, traffic safety, driver behaviour, travel time, emissions and acceptance using 290 modified vehicles in Lund (Sweden).

Results show that compliance with speed limits improve, that is, speed deviations from the speed limits decreased. Hjälmdahl, Almqvist and Várhelyi (2002) indicate that variance in speed decreased which, according to a review of literature done by Várhelyi (2002), could positively impact on traffic safety. Furthermore, drivers showed improved behaviour towards other road users. In subjective evaluations test drivers mentioned less frequent speedometer observations and less gas and brake pedal usage when using an active gas pedal for speed control (Hjälmdahl and Várhelyi, 2004).

1.1.2 Collision avoidance

The GIDS research on collision avoidance support with a haptic gas pedal used an increase in force on the pedal of 25 [N] when and for as long as the activation criterion is above a pre-determined threshold value (Verwey *et al.*, 1993). The system was compared to two other systems, a buzz and a light. The haptic gas pedal with a 4 [s] time-to-contact[2] (*TTC*) activation criterion resulted in the largest decrease in following separation, and the least increase in driving speed and time spent in the left lane (that is, less overtaking). The side-effects that were found for all tested displays for collision avoidance included increased overall driving speed and speed variability. These results appear to be contradictory to the results found with the haptic speed control interface discussed above. Also, there was a tendency for driving in the left lane more often with all of the collision avoidance systems.

Although some other research projects on collision avoidance mention the GIDS project (for example Tijerina *et al.*, 2000), surprisingly, no literature was found that reports on a similar system, using haptic gas pedal feedback for collision avoidance information.

1.1.3 Car-following

Car-following support was briefly mentioned in the GIDS project (Verwey *et al.*, 1993), but not systematically investigated. A very recent system, Active Distance Support (ACDIS) has been announced by Continental Temic, to be launched by the end of 2005[3]. This system provides a counterforce on the gas pedal to encourage the driver to release the gas pedal when a leading vehicle is getting too close. This force feedback pedal is also engaged when an Active Cruise Control system (ACC) is engaged. Then, the position of the gas pedal is fixed, so that drivers can rest their foot on it, while the ACC is controlling the separation with a leading vehicle. While ACC is engaged "*gentle pedal motion informs the driver of system activities, such as throttling the engine output and automatic braking…*" (Continental, 2004).

Other literature – besides the literature produced by other members of the research project (for example Goodrich and Quigley, 2004) of which this thesis is but a small part – in which a haptic gas pedal display was specifically designed for the use in car-following situations has not been found. This thesis intends to fill in this gap in research on the successful application of haptic feedback via the gas pedal.

1.1.4 The Nissan Intelligent Driver Support System

In April 2002, Delft University of Technology started participating in a multi-university[4] research project, initiated by Nissan Motor Company, on human-centred development of a future intelligent driver support system (IDSS). The aim of the project was to develop a system

[2] Time-to-contact (*TTC*) is defined as the time in which collision will occur if in the current following situation nothing changes. Mathematically *TTC = (inter-vehicle distance) / (inter-vehicle speed difference)*.

[3] On the web: www.conti-online.com/generator/www/de/en/cas/cas/general/home/index_en.html

[4] University of Iowa (IA, USA), University of Minnesota (MN, USA), Brigham Young University (UT, USA), University of California San Diego (CA, USA), Drexel University (PA, USA), University of British Columbia (BC, Canada), Delft University of Technology (the Netherlands), and Nissan Motor Company Ltd (Japan).

that would cooperate with the driver in comfortably maintaining safe separation with surrounding vehicles. A prerequisite of this system was that drivers always remain responsible for decision making and control of the vehicle, while the IDSS provided drivers with the necessary information at the right moment for them to make the required decisions to comfortably and safely control their vehicle. This prerequisite more or less ruled out the development of a task automation system, since that would effectively take over a selected control task once initiated by the driver.

To overcome the potential negative human factors aspects that come with binary warning systems, it was decided to develop an interface that would display support information continuously, much like the warning display suggested by Horowitz and Dingus (1992), who proposed a graded warning from mild to severe as a function of time-to-collision (TTC) for a front-to-rear-end collision warning system. Because of this requirement to present information continuously, the auditory channel was ruled out as an interface modality since continuous auditory information easily leads to irritation and adaptation by humans (USDoT, 1996). Both vision and touch are suitable for comfortably presenting continuous information. However, presenting drivers with a visual display would require them to frequently reallocate their attention from the road to the display to monitor it. Since driving already is a visually highly demanding task, this would only add to the demands of visual processing. Furthermore, other currently available in-vehicle systems, like navigation systems also demand visual attention increasing drivers' visual information processing demands even further. Finally, the benefits of using haptic information are expected to be found in faster processing and faster, reflexive responses to this information compared to the processing and reaction to the same visual information. It was therefore decided to use haptics to communicate support information to drivers.

The best possible manner by which the envisioned haptic display of separation information could be described was that it would enable the driver to virtually "touch" his/her environment (Kitazaki, 2002) – metaphorically named 'Magic Bumper'. In other words, the haptic interface would have to allow the driver to determine his safe-field-of-travel through his sensations of touch. Like obtaining visual information from the driving scene by continuously scanning the road and other road users, the haptic information would have to be easily available as an integral part of the control task of driving an automobile, whenever necessary. By providing the haptic information through the control channels, drivers would feel the consequences of their control actions immediately, allowing them to easily incorporate this information into their understanding of the current situation. Since the necessity of executing corrective control actions becomes more acute the less time is available to avoid a collision (see Figure 1), the saliency of the haptic information should increase with decreasing time to collision. The operational boundaries of the proposed IDSS would extend both into the driver warning systems and normal driving areas of Figure 1.

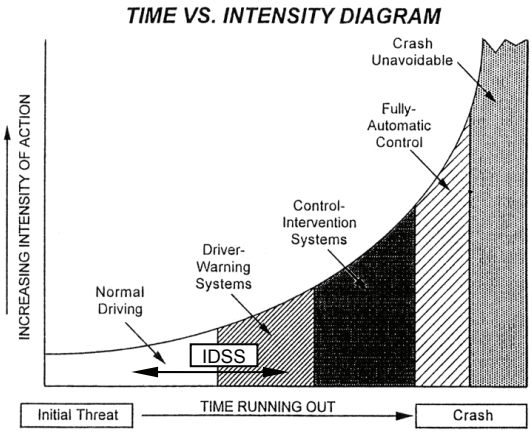


Figure 1: The increasing intensity of action as the time to crash is running out. The IDSS operational boundaries stretch from normal driving to more hazardous situations (adapted from NHTSA, 1992)

Schematically, the system architecture for the IDSS looks like Figure 2. An environment sensing system takes care of detecting surrounding vehicles and the road with features such as lane markers and curves. This information is processed by the control logic which determines what kind and how much haptic feedback needs to be displayed by the interfaces. Since it was decided to present haptic information through the control channels, that is, the gas pedal and the steering wheel, these devices need to be equipped with force actuators to provide the desired haptic feedback to the driver. Tentatively, driver state information could be made available to the control logic to adjust the haptic feedback depending on the inferred driver state.

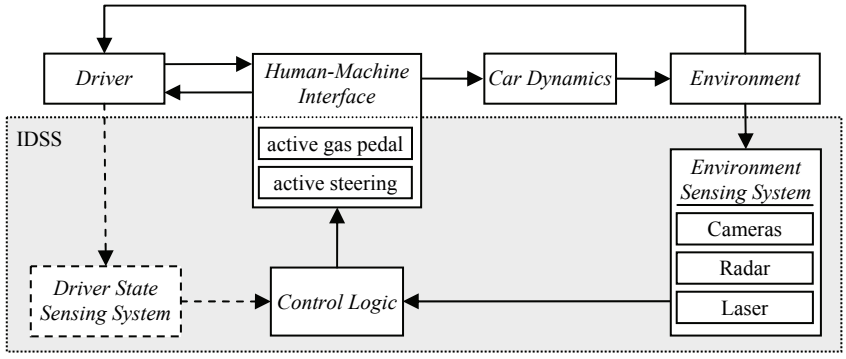


Figure 2: Schematic IDSS architecture (adapted from Kitazaki, 2002). The heart of the IDSS consists of the Environment Sensing System, Control Logic, and active control devices for the Human-Machine Interface. The Driver State Sensing System is a tentative subsystem.

1.2 Goal of the research

Delft University of Technology has been actively involved in developing the control logic and the haptic feedback properties of the actuated gas pedal. The department of Mechanical Engineering investigated the biodynamic properties of the foot – gas pedal system (Abbink, 2006). Human limitations and capabilities in controlling a system cannot be determined properly without the dynamics of the system that is interacted with. For example, a light and little damped control device requires different handling than a heavy and over-damped control device. The human performance in using a control device is thus limited by both the human and control device dynamics. Therefore, a powerful, electrically actuated experimental gas pedal facility was developed, to be able to apply high-bandwidth force and position disturbances to the foot during control tasks in order to determine the dynamics of the combined foot/gas-pedal system. Foot admittance, that is, the capability of humans to yield to forces on the foot, as well dynamic just-noticeable-difference (JND) measurements were conducted with this facility to determine influences of (changing) pedal dynamics on human capabilities to detect and react to haptic feedback (Abbink and van der Helm, 2004). Furthermore, possible interaction on neural level between the simultaneous processing of haptic and visual information was investigated.

At the department of Aerospace Engineering, the investigations focused on the mapping of environmental variables onto haptic feedback variables, that is, the development of the control logic. This was limited to the logic required for feedback through the gas pedal during car-following. What environmental variables and what haptic feedback properties of the actuated gas pedal were to be mapped onto each other to form the control logic has been a recurring research problem that will be addressed in detail in this dissertation. To test the IDSS logic in realistic driving situations a fixed-base driving simulator was built. The driving simulator gas pedal was electrically actuated and could be fully controlled with the simulation software. The sensing system components for detecting vehicles ahead of the own car were assumed to be available and capable of delivering the variables deemed necessary for determining the required haptic gas pedal feedback.

The goal of the research presented in this dissertation is the human-centred development[5] of a haptic gas pedal interface that comfortably supports drivers in maintaining a safe separation with a leading vehicle during car-following. Four major research questions were formulated to guide the research.

1. What possibilities are available and can be usefully exploited to provide drivers with continuous haptic feedback through the gas pedal?
2. Which environmental variables can be related best to haptic gas pedal feedback and how, such that drivers are optimally supported in their car-following task, without decreasing both comfort and safety of that task?

[5] The term human-centered development is used in this thesis with reference to the philosophy that "*…tools are there to assist human operators in carrying out their mission*" (Billings, 1997). In the development of new automation the human operator ought to be the locus of design, such that when using that new automation the human operator remains the locus of control of her/his vehicle.

3. How can the efficiency of the developed feedback algorithms with regard to driver control behaviour and car-following performance be evaluated?
4. What is the influence of the haptic gas pedal interface on driver car-following performance during visually undisrupted and visually disrupted driving?

1.3 Research approach

To arrive at a systematic design of the intended IDSS, a research development cycle consisting of three steps has been used. Each step is iterated a number of times to refine the interface design based on newly acquired knowledge and insight in the interaction of the haptic gas pedal feedback system and the driver (see Figure 3).

First, a theoretical understanding of all elements involved in the design of the support system is required: haptic feedback, driver perception of force, driver interaction with the gas pedal, drivers' visual perception of the car-following situation, driver car-following behaviour, and so on. Based on this theoretical framework hypotheses can be formulated that need to be tested.

Next, this understanding is also used to derive cybernetic control models which clearly show the relations and interactions between the different system elements, leading to a system design. Especially the dynamics of the driver – gas pedal interaction form an important part in this model: they determine the quality of the intended driver support for car-following. Modelling the interaction between driver, car, and haptic gas pedal based on control-theoretic principles allows for the application of system identification methods to investigate driver control behaviour in the frequency domain (see Section 4.3.2 of this dissertation; Abbink, 2006; Mulder *et al.*, 2005a; Mulder *et al.*, 2005b). Overall performance of the driver and his/her interaction with the car and the haptic gas pedal is expressed in control theoretic terms.

Cybernetic models can be divided in manual control and supervisory control models (Blaauw, 1984). In manual control, drivers are actively engaged in controlling the system (that is, closed-loop driver control behaviour), while in supervisory control drivers monitor the control actions and system behaviour of the automation that is actively engaged in controlling the system. The models used in this document are based on manual control.

Third, the system design is tested in a driving simulator. The results of the simulator experiments will affect the understanding of the relation and interaction between the elements of the system, allowing for new ideas to be incorporated to improve the system further.

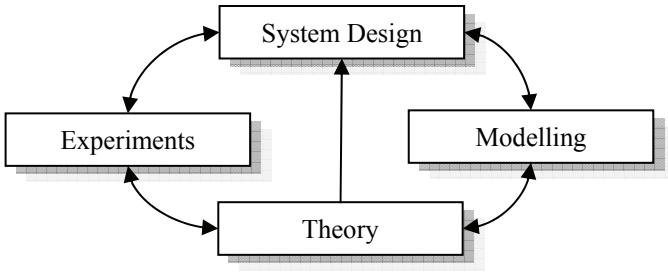


Figure 3: Research development cycle.

1.4 Thesis organisation

This thesis is organised as follows. Chapters two and three form the theoretical basis of the control logic for the haptic gas pedal feedback. In Chapter two, the concepts of haptics in general and that of haptic gas pedal feedback in particular are explained. A car-following model is used to show how the haptic feedback channel fits in with the existing visual feedback which drivers use to control car-following. This model shows the dynamics of driver – gas pedal interaction and how that can be exploited to provide drivers with separation information. Different options of providing drivers with continuous tactile information are discussed. Chapter three presents the selection of suitable environmental variables that, when properly related to haptic feedback variables, determine the quality and effectiveness of the haptic feedback.

Before presenting the results of driving experiments that were conducted in the fixed-base driving simulator at the department of Aerospace Engineering, Chapter four is devoted to the discussion of the basic experimental set-up and the evaluation methods used.

Chapters five and six present the results of car-following experiments. The chronology in which the experiments have been conducted has been altered in favour of grouping similar experiments in the same Chapter. In three of the experiments, all described in Chapter five, drivers were given a maximal car-following task to which they should devote all their visual attention. The main goal of these experiments was to investigate the effects of different haptic feedback designs on driver car-following behaviour. Two experiments, described in Chapter six, were conducted in which drivers were given a secondary task that required them to temporarily re-allocate their visual attention from the driving scene to other parts of the visual environment. The main goal of these two experiments was to investigate the effectiveness of haptic gas pedal feedback when visual attention to the driving scene was distracted.

Finally, Chapter seven summarizes the results of the research presented in the preceding Chapters. Conclusions are drawn with regard to the use and generation of haptic gas pedal feedback and its implications on driver car-following behaviour.

Chapter 2

Haptic Gas Pedal Feedback

Being able to touch and feel the environment is a rich and essential source of information for humans. Touch allows us to determine material characteristics such as surface roughness, stiffness, and object contours. Furthermore, it helps us to determine the proximity of objects and by pushing or pulling them it is possible to get an idea of the resistance to movement. Touching, pushing and pulling enable us to actively investigate properties of the environment. It is precisely this important property – being able to actively investigate properties of the environment – that will be tried to be exploited in the development of haptic gas pedal feedback.

When Gibson and Crooks wrote about their safe-field-of-travel in 1938 they were describing physical safety constraints that drivers needed to conceptualise mentally from the information they were able to collect visually from the environment they were driving in. Today, this situation isn't much different. Drivers are capable of acting in their environment through their gas pedal, but the information they use to base these actions on can only be acquired visually: by looking through the windscreen (see Figure 4[1]). There are other cues, such as engine sounds, vibrations, the speed indicator, etc. that drivers use while controlling their vehicle, but these are mainly related to the state of the own vehicle and tell them little about the environment.

2.1 Haptic feedback in the control loop

The haptic gas pedal interface is an in-vehicle device that does not inform the driver about the state of the vehicle itself, but about the state of the vehicle in the environment. To help drivers form a mental image of their safe-field-of-travel, haptic information of the field boundaries first of all provides them with a complementary channel, besides vision, to

[1] The designation of the signs in this and following block diagrams of car-following deviate from standards in block diagram notation in that the through-going signals are negative (-) and the feedback signals are positive (+). Standard notation is the opposite. It was chosen to deviate from standard block diagram notation in order to adhere to the widely used sign notations of the signals in automotive research.

determine these boundaries (see Figure 5). Second, if the haptic information is presented continuously rather than binary (on/off) as with a warning system, the field boundaries can be perceived continuously.

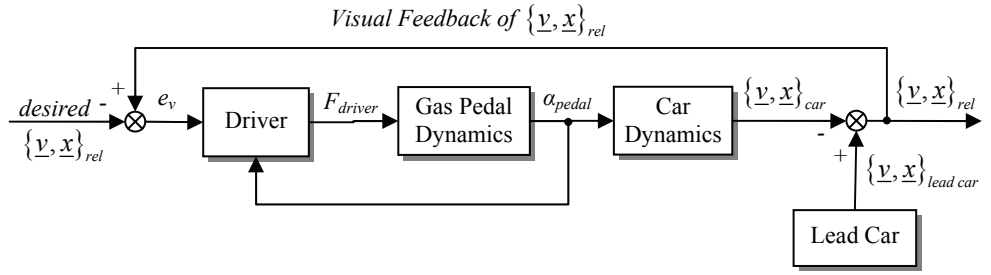


Figure 4: Block diagram of longitudinal control of the car. By pressing the gas pedal with a force F_{driver}, the displacement of the pedal, α_{pedal}, determines the speed and longitudinal position of the car in the environment. The visually perceived information from the environment allows the driver to determine the required amount of gas pedal depression to maintain the desired safe-field-of-travel, closing the control loop.

Third, because the haptic information is presented through the longitudinal control channel, the consequences of control actions can be felt too, as they will induce changes in the safe-field-of-travel. Furthermore, the stimulus-response compatibility (Sheridan and Ferrell, 1975; Wickens, 1992) of haptic gas pedal feedback is expected to be high, that is, an increased force on the pedal is already suggesting the correct control action required of the human to improve the current safe-field-of-travel. Fourth, as will be shown below in Section 2.3, the haptic feedback interface also allows probing of the environment, that is, active investigation of the properties of the safe-field-of-travel, by selecting appropriate characteristics of the haptic gas pedal.

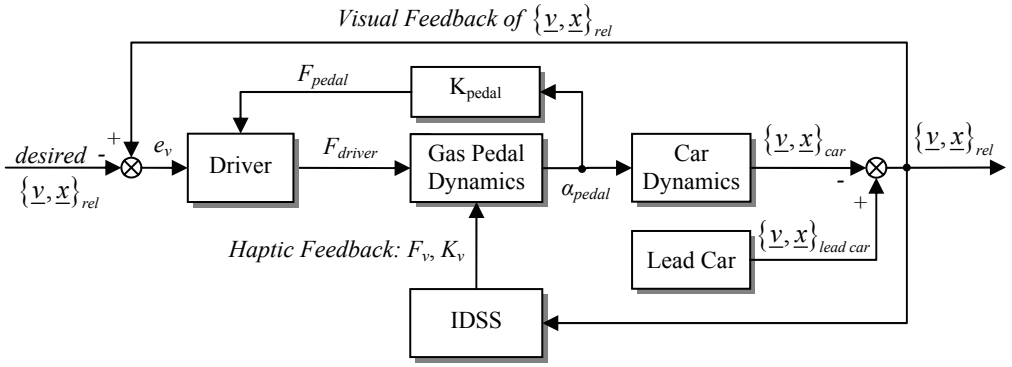


Figure 5: Block diagram of longitudinal control with haptic feedback. The Intelligent Driver Support System (IDSS) senses the lead car relative speed and distance. This information is then converted to a haptic feedback signal, force F_v or stiffness K_v, which is communicated to the driver through the gas pedal. Drivers perceive the haptic feedback through the forces (F_{pedal}) the gas pedal is now actively exerting on their foot. If drivers adopt a force task strategy, that is, if they try to maintain F_{pedal} constant, then a haptic feedback control loop is established which is related with the environment through the control logic of the IDSS.

To fulfil all the abovementioned properties of the haptic gas pedal it is important to know how humans perceive tactile information from the gas pedal and how they act through the gas

pedal to control the longitudinal motion of their vehicle. Section 2.2 therefore, explains the properties of the human interaction with the gas pedal, and the foot in particular, which is the main actor in both the perception of and the reaction to haptic information through the gas pedal. This interaction is modelled, such that it fits in a control theory model of car-following – the longitudinal control mode for which the haptic feedback system in this thesis is designed. In Section 2.3 the options for introducing virtual gas pedal dynamics to provide haptic feedback are discussed. During the development process two concepts, force feedback and stiffness feedback, have been worked out, implemented and tested. How both concepts change the car-following model will be shown at the end of Section 2.3. Finally, the benefits, disadvantages, possibilities, and limitations of providing haptic feedback through the gas pedal will be discussed in Section 2.4.

2.2 Dynamics of driver – gas pedal interaction

Drivers use their right foot to control the deflection of the gas pedal with which in turn the longitudinal dynamics of the car are controlled. Normally, to establish stable and comfortable gas pedal control, which requires the least amount of work, the heel is resting on the floor of the car and the ball of the foot is in contact with the gas pedal as shown in the left-hand side of Figure 6. The ankle joint functions as a hinge for the upward and downward motion of the foot to achieve gas pedal deflections. Upward and downward foot motion is produced by antagonistic pairs of (co)contracting muscles in the leg. The upward motion of the foot is achieved by contraction of the shin muscle (Tibialis Anterior) while the calf muscles (Gastrocnemius Medialis, Gastrocnemius Lateralis, and the Soleus) relax simultaneously, resulting in less gas pedal depression. Downward motion of the foot is the result of contraction of the calf muscles combined with relaxation of the shin muscles, yielding a depression of the gas pedal.

Both the foot and the gas pedal are dynamical systems, that is, the states of these systems are time-dependent. For a static condition to exist, the force the driver is exerting on the gas pedal must be equal to the force the gas pedal is exerting on the foot. Furthermore, both the foot and the gas pedal can be modelled as mechanical systems, with external forces acting on them to produce changes in foot and pedal position.

2.2.1 Passive gas pedal dynamics

The gas pedal as it is used in most cars is a simple mechanical mass, spring, damper system which can schematically be represented as shown in Figure 7. To produce a deflection $\alpha_p(t)$ of the gas pedal, the driver must exert a force $F_p(t)$ on the gas pedal that is linearly related to the dynamic properties of the pedal – stiffness K_p, damping B_p, and mass M_p:

$$F_p(t) = \alpha_p(t)K_p + \dot{\alpha}_p(t)B_p + \ddot{\alpha}_p(t)M_p \tag{2.1}$$

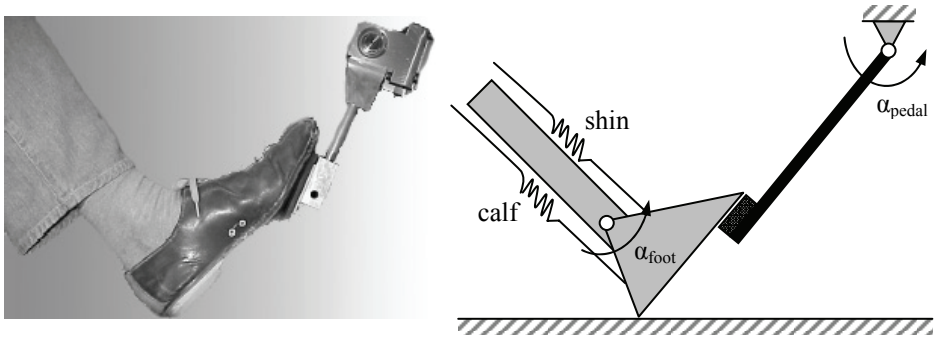


Figure 6: Foot – gas pedal combination, left, and schematic representation, right (pictures with courtesy of D.A. Abbink).

For most gas pedals, as well as the one that is used in the fixed base driving simulator that was used for this research, the mass and damping are negligibly small compared to the stiffness of the spring, reducing equation (2.1) to a mere spring. This spring, however, is pre-tensed. So, to produce a pedal deflection at all, an initial force F_i has to be overcome. Equation (2.1) becomes:

$$F_p(t) = \alpha_p(t)K_p + F_i \tag{2.2}$$

The spring is installed such that it will pull or push back the gas pedal to its zero deflection position. At zero deflection, there is no input to the engine. At maximum pedal deflection, input to the engine (throttle) is maximal. However, for the car that was used for this research, with automatic transmission, the maximum throttle opening is reached well before maximum gas pedal deflection, as can be seen in the right-hand graph of Figure 8. At approximately 60% gas pedal deflection, maximum throttle opening is reached. The 40% excess in pedal stroke is used when fast accelerations are required. The automatic gear transmission depends on the speed of the car and the gas pedal depression. At high speeds and high gear, there is little excess power to accelerate fast. Instead, when the gas pedal is depressed fully in fourth gear, the automatic transmission shifts back to third gear increasing engine rpm which results, thanks to the lower gear ratio, in a quick increase in speed (see left hand side of Figure 8). This implies that effective control of vehicle longitudinal motion is achieved in the first 60% of the gas pedal stroke, since the engine will be most responsive in that region. This is the first of two control characteristics of the gas pedal that will be important in the design of a haptic feedback system, since it determines the most important region of gas pedal positions during active control.

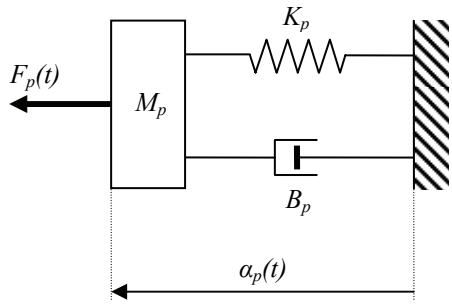


Figure 7: Schematic mechanical equivalent of the gas pedal: a mass, spring, damper system.

Constant gas pedal position is related to steady state vehicle speed, see left-hand graph of Figure 8. Drivers do not necessarily know (nor need to know) the exact pedal position for the speed they want to drive at. In fact, it is more likely that the correct pedal position is estimated from the speed information drivers get visually. Visual cues from outside the vehicle help drivers in determining their speed relative to other vehicles and objects in the environment. Furthermore, visual cues from the road and peripheral stationary objects might give an indication of absolute speed. For exact knowledge of the absolute speed the speed indicator is available. Other cues like acceleration, engine sounds, and vibrations might also help in building driver awareness of speed.

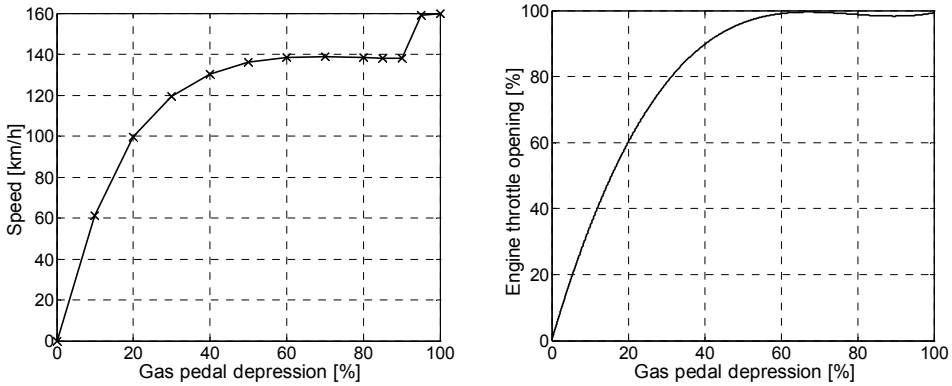
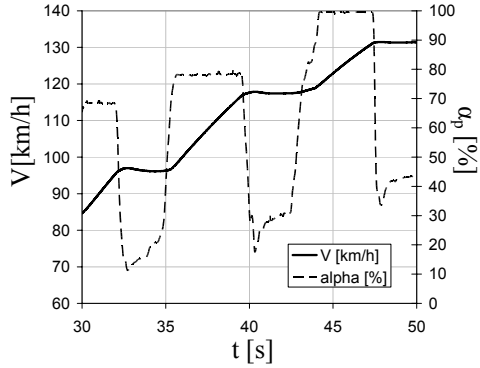


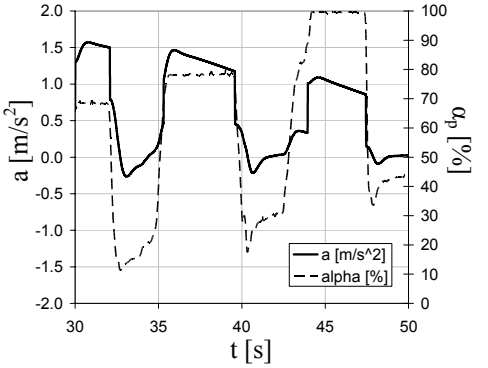
Figure 8: Gas pedal position vs. car speed at steady state (left). At approximately 60% pedal depression maximum throttle opening is reached (right; Pauwelussen, 2005) and no extra input to the engine can be given. However, an extra speed increase can be obtained by fully depressing the gas pedal, which will prompt the automatic transmission to shift back one gear. This increases rpm and releases some excess power to deliver the extra acceleration to increase speed.

In longitudinal control (e.g. speed control or separation regulation during car-following), drivers initially depress or release the gas pedal more than required for the steady state speed they want to reach. This speeds up the transition from the initial speed to the desired speed, but requires drivers to reverse their initial gas pedal command to prevent overshoot from the desired speed (Figure 9a). So, effectively, drivers command a desired acceleration with the gas pedal while actively controlling the vehicle (Figure 9b). This is the second important characteristic of the gas pedal, since it determines pedal movement patterns during active control.

Besides the control characteristics of the gas pedal, the human control characteristics with the inherent properties of the foot, which controls the movements of the gas pedal, are important to consider when designing haptic gas pedal feedback. Before discussing the implications of adding feedback signals to the gas pedal, the dynamics of the foot are described. Together, the dynamic properties of the gas pedal and the foot form an interacting system that can be described by mechanical representations. This simplification is useful in gaining an understanding of the complex interaction between the driver and the gas pedal. Furthermore, with this understanding it will be easier to investigate the available options for haptic gas pedal feedback.



a) Pedal position α_p and speed V as a function of time t.



b) Pedal position α_p and acceleration a as a function of time t.

Figure 9: Longitudinal speed control characteristics. To increase speed, the gas pedal is depressed relatively deep (a) to – effectively – command an acceleration (b). Once the desired speed is reached, the pedal is released and stabilized around the position for the steady state of the desired velocity (a).

2.2.2 Neuromusculoskeletal dynamics of the foot

The dynamics of the human foot are a complex interaction between muscles, passive tissues like the tendons, which connect the muscles to the bones of the skeleton, and reflexive and conscious control signals from the neural system. These dynamics are bi-directional, that is, drivers can exert forces and produce movement of the foot while at the same time, through proprioception, external forces and forced movement of the foot can be sensed. Furthermore, muscle activation can be voluntary through conscious control and reflexive through neural shortcuts that bypass the central nervous system. Voluntary muscle activation is initiated intentionally by the driver. Reflexive muscle activity is initiated by proprioceptive feedback of force, muscle stretch, and muscle stretch velocity. Muscle reflexes help humans to stabilize their limb movement or positioning and will be an important property to consider when designing a haptic feedback system. Generally, the combined intrinsic and neuromuscular dynamics are described by the mechanical admittance of a limb, which describes the limb position as a dynamic function of an external force (Abbink, van der Helm, and Boer, 2004). Proprioceptive reflexes and muscle (co)contraction offer mechanisms to adapt admittance to changing environmental conditions (van der Helm *et al.*, 2002; Abbink, van der Helm, and Boer, 2004).

Intrinsic musculoskeletal dynamics

During driving, the sole of the foot, usually embedded in footwear, is the contact endpoint with the gas pedal. Contact dynamics of the skin can be modelled as a spring-damper system with negligible mass as compared to the mass of the rest of the foot (which includes the footwear). The visco-elastic properties of the muscles and the mass of the foot are connected in series with the contact dynamics of the foot with the pedal (mainly skin dynamics, partly footwear dynamics), as represented in Figure 10. The properties of the skin dynamics are given by equation (2.3) and the lumped (all involved muscles and bones together) intrinsic mechanical properties of the leg/foot combination are described by equation (2.4). Due to reflexive muscle activity, a reflexive muscle force $F_{refl}(t)$ is produced besides the intrinsic muscle force $F_f(t)$, such that the total contact force of the sole is the result of intrinsic and reflexive muscle forces combined, see equation (2.5). If the contact force F_s is equal to the pedal force F_p, then the pedal position will be stationary. For $F_s > F_p$, the pedal depression will increase and for $F_s < F_p$ the pedal depression will be decreased.

$$F_s(t) = \left(\alpha_s(t) - \alpha_f(t)\right) K_s + \left(\dot{\alpha}_s(t) - \dot{\alpha}_f(t)\right) B_s \tag{2.3}$$

$$F_f(t) = \alpha_f(t) K_f + \dot{\alpha}_f(t) B_f + \ddot{\alpha}_f(t) M_f \tag{2.4}$$

$$F_s(t) = F_f(t) + F_{refl}(t) \tag{2.5}$$

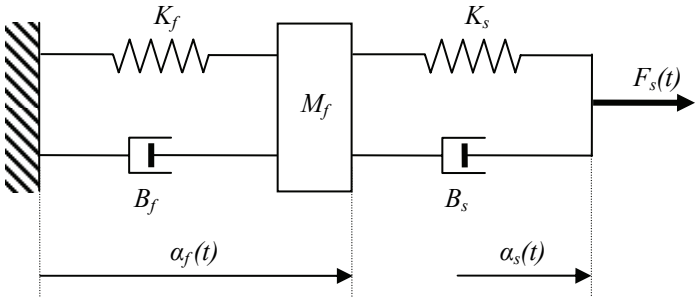


Figure 10: Mechanical representation of the contact and musculoskeletal dynamics of the foot. M_f, B_f, and K_f are the respective lumped mass and visco-elastic properties of the foot. The displacement of the foot is denoted α_f. In series with the dynamics of the foot are the visco-elastic properties K_s and B_s of the sole of the foot. The displacement α_s is the endpoint position of the foot (adapted from van der Helm *et al., 2002*).

Neuromuscular dynamics

Muscle force is dependent on muscle activation, length, and contraction velocity, that is, muscle stiffness and viscosity. The reflexive muscle force F_{refl} is the result of proprioception of muscle stretch, stretch velocity, and external forces. Reflexive muscle activity is generated by reflex loops in which muscle spindles provide sensory information on muscle stretch and velocity and Golgi tendon organs provide sensory information on active muscle force. Triggered by external forces acting on the foot, the reflexive neural input results in the activation of the muscles in the foot which try to counteract the disturbance. This self-stabilizing property of the neuromuscular system is effective up to the eigenfrequency of the

neuromusculoskeletal system of the foot, which is determined experimentally to be in the range of 6-8 Hz (Abbink, van der Helm and Boer, 2004).

The reader is also referred to the work of Abbink (2006) in which system identification techniques are applied to identify the parameters of the neuromuscular system. For the purpose of this discussion, it will suffice to conclude that the intrinsic musculoskeletal and neuromuscular dynamics can be represented by a mechanical endpoint admittance, which describes the position of the foot as a dynamic function of the force that is exerted on it.

Foot admittance

Abbink, van der Helm and Boer (2004) show that foot admittance is highly dependent on task interpretation. These findings correspond to admittance measurements on the arm (de Vlugt, Schouten and van der Helm, 2002). The smallest admittance is generally found for position tasks, in which drivers try to maintain position of the pedal as constant as possible, when external forces act on the gas pedal. The largest admittance is found for force tasks, in which drivers try to maintain a constant force on the gas pedal when the position of the gas pedal is disturbed.

Furthermore, admittance is influenced by the bandwidth of the external perturbation signal. Perturbations of the gas pedal with signals that have a bandwidth lower than the Eigen frequency of the foot (6 – 8 Hz) yield smaller admittances than perturbations of the pedal with signals that have a bandwidth higher than the Eigen frequency of the foot. This effect is most likely the result of increased reflexive muscle activity for perturbations below the Eigen frequency of the foot (Abbink, 2004; for the arm: de Vlugt *et al.*, 2002).

Finally, humans adapt their admittance to the system they are interacting with, such that the admittance of the combined limb and system dynamics yields optimal stability (de Vlugt *et al.*, 2002). Abbink *et al*. (2004) for example, show small decreases in admittance of the foot for three subsequent increases of pedal stiffness with 50% of nominal pedal stiffness.

2.2.3 Longitudinal control with a passive gas pedal

Now that the driver – gas pedal interaction characteristics have been discussed, the block diagram of Figure 4 can be drawn in more detail, distinctly showing the dynamics of the gas pedal, the skin, and the neuromusculoskeletal system (Figure 11). Driver processing of the visual feedback she/he is getting from the environment takes place in the central nervous system (CNS). Control decisions are made here, based on the desired separation the driver wishes to drive behind the lead vehicle and the visually perceived separation (e_v). These control decisions are passed on to the neuromuscular system to activate muscles for moving the foot to carry out the desired control actions. The dynamics of the gas pedal yield a gas pedal depression α_p as a result of the contact force F_s which the driver imposes on the gas pedal. Proprioception of muscle length, velocity, and force due to changes in pedal position (and hence foot contact position α_s and contact force F_s) result in reflexive muscle activity from the neuromuscular system that bypasses the CNS. Together with the reflexive muscle activation, the active control actions result in a foot position α_f. How is the perceived information feedback in this closed control loop utilised by drivers to deliver the required pedal depression?

Blaauw (1984) refers to Krendel and McRuer's theory of "Successive Organisation of Perception" to distinguish three levels of control:

1. Compensatory: drivers are constantly reacting to control information attempting to minimise the error in the tracking of a target. Control is closed-loop, e.g. car-following in heavy traffic, compensatory tracking of random side wind gusts.
2. Pursuit: drivers have preview information, which they can use to anticipate upcoming control actions. Includes closed-loop feed-forward control, e.g. preview through the windshield of cars ahead of a leading car.
3. Precognitive: drivers apply pre-learned control strategies to carry out manoeuvres without the need for constant information feedback from the environment. Basically intermittent open-loop control, e.g. speed control, passing manoeuvres.

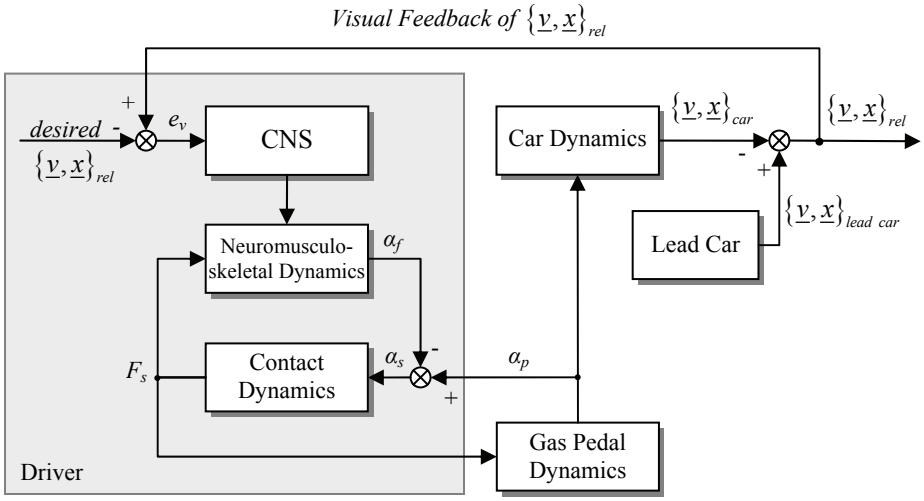


Figure 11: Block diagram of longitudinal control of the car, detailing the interaction between the foot and the gas pedal. The central nervous system (CNS) actively controls the foot through the neuromuscular system, resulting in movement α_f of the foot. The contact force F_s transmits the foot movement to the gas pedal. Due to the contact dynamics of the skin, a small difference α_s between pedal movement α_p and foot movement α_f exists.

These levels of control represent both the amount and kind of information that is necessary for control and the subsequent cognitive processing required by the driver. Note the similarity with the skills, rules, and knowledge taxonomy of Rasmussen (1983). He defined these three levels of operator behaviour based on the information needs required to control a system:

1. Skilled based behaviour represents sensory-motor performance which takes place almost without conscious control. Performance depends on a very flexible and efficient internal model of the controlled system.
2. Rule based behaviour represents the execution of stored rules of control which might have been derived empirically during previous occasions. This behaviour is activated in *familiar* situations.

3. Knowledge based behaviour is activated in *unfamiliar* situations for which no previous rules for control are available (yet). This level of control is goal-controlled and requires a thorough analytical evaluation of the control situation. It is unlikely that this kind of behaviour is encountered during car-following.

The three levels of control discussed by Blaauw (1984) correspond mainly to the first two levels of behaviour described by Rasmussen (1983). The compensatory level of control requires the most attention of the driver and a continuous stream of information. Drivers are most likely to be controlling at this level either when they are inexperienced or in unfamiliar or rapidly changing environments. On the pursuit level, drivers are able to use more information, allowing them to anticipate to changes in the environment, increasing the control performance at little extra processing demands. Finally, at the precognitive level of control, the amount of information required and the processing demands of this information is minimal, since control actions are based on learned manoeuvres. Only experienced drivers will be able to control their vehicle at this level.

With a passive gas pedal, no environmental information is communicated to the driver. That information is perceived visually only and the gas pedal is used only to act in that environment with the car the driver is controlling. The haptic feedback system that is proposed in this thesis, intends to provide environmental information that is relevant to the longitudinal control of the vehicle. Ideally, the interface provides for support at all levels of control. Whether this will be possible, depends on the possibilities the gas pedal offers to provide haptic feedback and how much it will enhance drivers' perception of the environment.

2.3 Virtual gas pedal dynamics

Unlike virtual reality or tele-manipulation, where haptic feedback needs to mimic real world properties of objects in the virtual or remote (real) world, haptic gas pedal feedback does not represent known haptic properties of the environment. Rather, the feedback system introduces a new haptic sensation that needs to communicate visually perceptible properties of the environment that are related to the safety boundaries of operation of the car in that environment: enhanced reality. While no direct equivalents exist that represent tactile sensations as driving safety boundaries, the dynamics of the gas pedal do offer possibilities for creating tactile sensations that are easily recognisable by humans.

In Section 2.2.1 the dynamics of the gas pedal were described as a mechanical mass, spring, damper system, with mass M_p, stiffness K_p, and damping B_p – equation (2.1). These are the inherent properties of a spring-loaded gas pedal. To create a haptic feedback system, the gas pedal lever is connected to an electric actuator which can deliver a precisely controlled torque to the gas pedal additional to the inherent pedal forces required to overcome the spring loading (and pre-tension forces). Depending on the direction of the applied torque, this results in the pedal being pushed back towards or pulled away from the driver. The haptic system is intended to provide information to the driver, not to automatically control the vehicle. Pulling of the gas pedal by the actuator, therefore, is not used. The driver is controlling the haptic gas pedal with an additional bias force. By letting the actuator push with a force F_v against the foot the driver may perceive this as an increase of pedal force $F_p(t)$, see equation (2.6). Whether this increased

pedal force is perceived depends on the Just-Noticeable-Difference (JND) threshold with which drivers can perceive force changes with their foot. Abbink and van der Helm (2004) show that in dynamically changing forces (presented to experiment subjects as sinusoids), frequency and amplitude of the changing forces have a significant influence on the JND. The higher the frequency and amplitude, the smaller the JND. The same experiment also showed that the type of footwear greatly influences JND.

Depending on the quality of the actuator and its control system, the force $F_v(t)$ can be made dependent on the position, velocity, and acceleration of the pedal, simulating a dynamic mass, spring, damper system with virtual mass $M_v(t)$, stiffness $K_v(t)$, and damping $B_v(t)$ properties. This means that the actuator enables active control of the dynamic properties of the gas pedal by the introduction of virtual dynamics (see equation (2.7) and right hand side of Figure 12).

$$F_p(t) = \alpha_p(t)K_p + \dot{\alpha}_p(t)B_p + \ddot{\alpha}_p(t)M_p + F_v(t) \tag{2.6}$$

$$F_p(t) = \alpha_p(t)\left(K_p + K_v(t)\right) + \dot{\alpha}_p(t)\left(B_p + B_v(t)\right) + \ddot{\alpha}_p(t)\left(M_p + M_v(t)\right) \tag{2.7}$$

Even when the forces $F_p(t)$ in equations (2.6) and (2.7) are equal numerically, they represent distinctly different dynamic systems, that is, the perception of $F_p(t)$ by the driver will be distinctly different with either system. The system represented by equation (2.6) is a pure force feedback system, which will be discussed in Section 2.3.1. Equation (2.7) represents a dynamic force feedback system, which, in reduced form, will be discussed in Section 2.3.2.

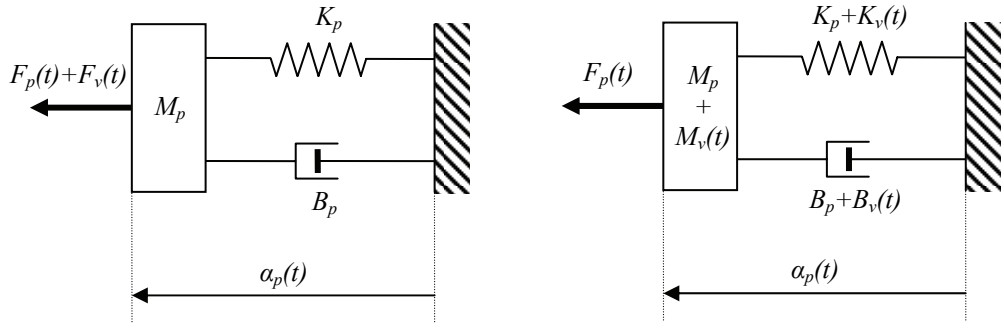


Figure 12: Schematic mechanical equivalent of the gas pedal with added virtual dynamics. With an actuator attached to the gas pedal it is possible to actively control an additional virtual force $F_v(t)$ (left figure) or additional virtual mass $M_v(t)$, stiffness $K_v(t)$, and damping $B_v(t)$ (right figure) of the gas pedal.

2.3.1 Force feedback

The force feedback system imposes a force $F_v(t)$ directly on top of the inherent characteristics of the gas pedal. For the same reasons as mentioned in Section 2.2.1 – negligible mass and damping of the gas pedal compared to the stiffness of the pedal from a pre-tensed (with force F_i) spring – equation (2.6) becomes:

$$F_p(t) = \alpha_p(t)K_p + F_i + F_v(t) \tag{2.8}$$

The force – position characteristic of the gas pedal with $F_v(t)=0$ is shown in Figure 13 by the solid line. When $F_v(t)>0$, shown in Figure 13 by the dashed line, it can be seen that the force –

position characteristic is translated upwards. This means that, for any given pedal position, the force required to hold that position is increased with magnitude $F_v(t)$. To change the pedal position with an amount $\Delta\alpha_p$ however, still the same change in pedal force ΔF_p is required compared to the nominal force – position characteristic of the gas pedal at $F_v(t)=0$, that is, the slope of the force – position characteristic remains the same. Thus, with force feedback, changes in gas pedal force can be perceived only when the force $F_v(t)$ is changed, and only then when these changes are above JND.

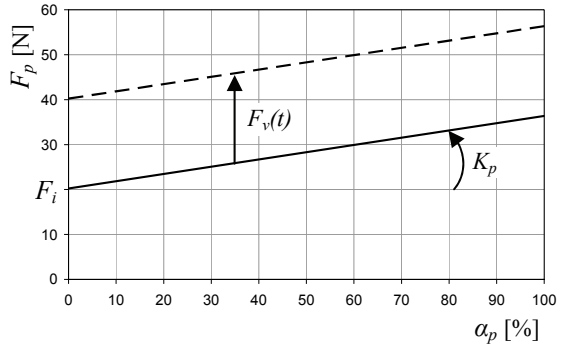


Figure 13: Gas pedal position – force relationship for the inherent gas pedal characteristics (solid line) and with added virtual force $F_v(t)$ (dashed line).

2.3.2 Stiffness feedback

Unlike the force feedback system, the dynamic feedback system of equation (2.7) does not increase the pedal force for any given pedal position, but it increases the pedal force depending on pedal position, velocity, and acceleration. Although it is possible to change all the dynamics of the gas pedal simultaneously, this might not be beneficial for a number of reasons.

First, simulating mass requires a highly accurate and powerful actuator and complicated control software. Furthermore, adding virtual mass M_v to the pedal increases its momentum, possibly making it too difficult to control. Ideally, the mass of the gas pedal should remain negligible. Added virtual damping could help make the pedal control more stable when fast pedal movements are required. For the benefit of communicating information, however, damping is not suited since it can only be perceived when the pedal is moved by the driver. It cannot be felt when the pedal is in a static position, that is, when the velocity of the pedal $\dot{\alpha} = 0$, nor when the pedal is moved by the actuator.

The only parameter with which information can be communicated effectively is the added virtual stiffness K_v. The added virtual stiffness can be felt as an increase in the pedal force $\Delta F_v(t)=K_v(t)\alpha_p(t)$ when the pedal is in a static position (see Figure 14). As an additional benefit, a change in pedal position $\Delta\alpha_p(t)$ now also yields an increase in pedal force $\Delta F_p(t)$ that is bigger than the increase in pedal force for the nominal pedal characteristic ($\Delta F_p(t)=K_p\Delta\alpha_p(t)$), since the slope of the force – position characteristic is increased from K_p to $K_p+K_v(t)$ ($\Delta F_p(t)=\Delta\alpha_p(t)(K_p+K_v(t))$. Equation (2.7) then becomes (including the pre-tensed spring):

$$F_p(t) = \alpha_p(t)\big(K_p + K_v(t)\big) + F_i \tag{2.9}$$

Thus, the dynamic feedback system is, for the practical reasons mentioned above, reduced to a stiffness feedback system, with an intrinsic minimum stiffness K_p and pre-tension F_i.

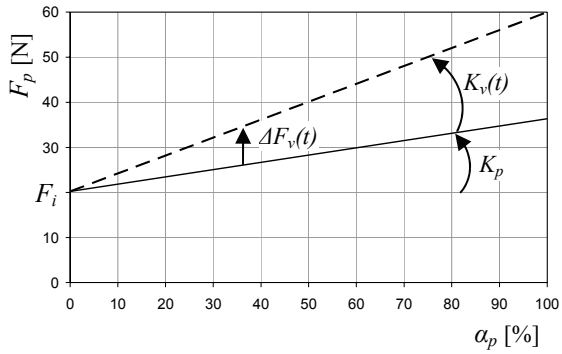


Figure 14: Gas pedal position – force relationship for the inherent gas pedal characteristics (solid line) and with added virtual stiffness $K_v(t)$ (dashed line).

2.3.3 Car-following control with an active gas pedal

With the knowledge of how the gas pedal dynamics can be influenced – by producing virtual forces and dynamics with an actuator – the longitudinal control model of Figure 11 can be extended with a haptic feedback loop. The haptic feedback loop duplicates the information that is already available visually, but it presents it in a complementary modality through the gas pedal.

A sensor system detects other vehicles in the environment. It is assumed for this research that the sensor system is available and capable of providing distance and speed information of leading vehicles. This information, together with the information on speed and acceleration of the own vehicle is the input to the control logic of the IDSS which determines the amount haptic feedback that is required for the current situation. The control logic of the IDSS is the topic of discussion of Chapter 3 of this thesis. For now, it is sufficient to state that the control logic determines either the magnitude of $F_v(t)$ or $K_v(t)$, depending on the choice of the designer.

The virtual force $F_v(t)$ or stiffness $K_v(t)$ is generated by an actuator attached to the gas pedal, which influences the force required of the driver to keep the pedal in an equilibrium position. Through proprioception of force and position changes of the gas pedal – if they are above JND – drivers can use these forces to infer what is happening in front of their own vehicle (see Figure 15), hence providing them with a haptic feedback control loop.

Because of the haptic feedback loop, the forces on and the position of the gas pedal are not merely the direct consequences of drivers' control actions. They now are also the consequence of changes in the environment. How the environment induces these changes depends on the control logic of the IDSS. This change in the meaning of pedal force and position is likely to have a profound impact in task interpretation by drivers in using the gas pedal.

As mentioned before in Section 2.2.2, humans adjust their admittance depending on the task. If the task is to maintain position of the gas pedal, drivers will adopt a very low admittance. If the task is to maintain the gas pedal force constant, drivers will adopt a relatively high admittance. Low admittance requires high muscle co-contractions and increased reflex

sensitivity to make the foot/leg combination as stiff as possible. This also requires more energy and effort than maintaining a high admittance, for which the muscles need to be relaxed. From an energy point of view it is therefore preferable to execute a force task, such that drivers can adopt a low admittance. Furthermore, a force task seems preferable from the control point of view, since drivers will have to yield, rather than counteract the force imposed on them through the gas pedal feedback. Yielding to additional pedal forces will automatically lead to a control action that promotes a decrease in speed, whereas counteracting additional forces will at best lead to no control action at all. Humans are very sensitive to changes in force, but are bad at estimating absolute forces, especially if they are to be maintained over a longer period of time. Yielding to a change in force requires drivers only to comply with the force change. Counteracting an increased pedal force requires drivers to maintain a higher force constantly, which is a more difficult task to perform accurately. It is therefore hypothesized that drivers will adopt a force task strategy to deal with the haptic information that is provided through the haptic feedback loop.

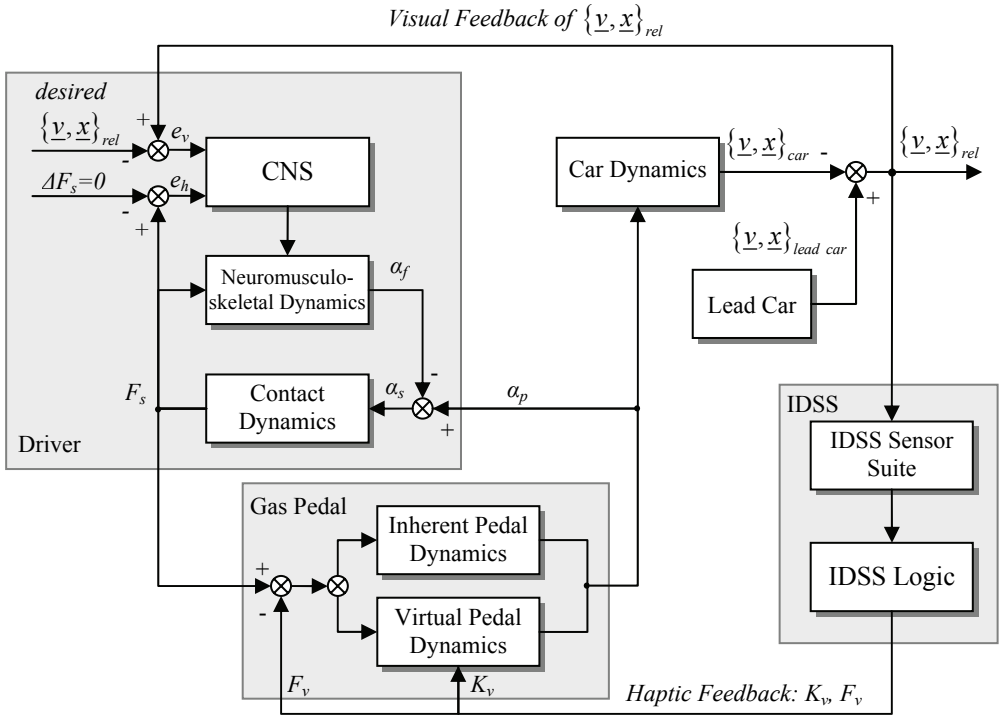


Figure 15: Block diagram of longitudinal control with haptic feedback. The haptic feedback is determined by the feedback logic, which receives information from the environment through a sensor suite. Force feedback F_v acts directly on the gas pedal, together with the contact force F_s which the driver exerts on the pedal, but does not change the dynamic characteristics of the pedal. The virtual stiffness K_v changes the dynamics of the gas pedal which is dependent on pedal position. Either force feedback or stiffness feedback is used. The driver can now base his control actions on both visual perception and haptic perception of the changes in the environment – e_v and e_h respectively.

2.4 From Force to Information

Haptic gas pedal feedback has been applied successfully before in speed adaptation and collision avoidance systems. As a car-following support system haptic gas pedal feedback has more or less been mentioned only as another driving situation in which it might be beneficial (in the GIDS and PROSPER projects mentioned in Section 2.1), but this apparently never resulted in more specific research. Recently, Continental (2004) has announced its Active Distance Support system (ACDIS) which most closely resembles the haptic feedback system which is the topic of this thesis. This system, however, gives haptic feedback information on the state of the Adaptive Cruise Control system, rather than information on the state of the inter-vehicle separation between the own vehicle and a leading vehicle.

This Chapter discussed the interaction between the human driver and the gas pedal with which the longitudinal motion of her/his vehicle is controlled. This interaction can be extended by introducing virtual forces or dynamics on the gas pedal, using an (electrical) actuator. The complementary haptic control loop (Figure 15) that is obtained by feeding back environmental parameters with these virtual forces or dynamics is based however, on one major assumption: environmental parameters can be converted into meaningful haptic information in a car-following context.

What is meaningful haptic information in a car-following context? No direct connections between haptic information and car-following exist. However, relations between the characteristics of the interpretation of haptic information and car-following information can be identified. First, an increase in force is easily identified with an object moving towards the observer and vice versa. Relative movement of the vehicle in front of the own vehicle is the most important environmental information during car-following. Hence, force should increase with a decrease in inter-vehicle separation and vice versa. Second, the change in force related to the change in vehicle separation should be correlated such that the magnitude of the required control action can be estimated. Too much change in force might result in too much control action, too little change in force might result in too little control action. Third, task interpretation plays an important role in the admittance humans will use for the required control task. From the perspective of comfort, it would be preferable to have a force task, such that admittance can be high, and effort low. If car-following can be interpreted as a compensatory task in which the separation with a leading vehicle needs to be kept constant, the first and second observations mentioned above fulfil the third observation. This is shown in Figure 16.

If it makes sense to let the required feedback force be a function of the separation[2] between the own vehicle and a leading vehicle, how does this feedback force make sense as a function of the gas pedal position? In Section 2.3 it was made clear that haptic feedback can be generated as an additional force on the gas pedal – which is independent of the gas pedal position – or as additional stiffness of the gas pedal – which is heavily dependent on the gas pedal position. The advantage of an additional force is that the increase in force can be chosen such that it is always well above JND. This assures that changes in the feedback can always be

[2] The term separation is used deliberately, so as not to make presumptions about which physical representation is best suitable to quantify it.

felt. When using additional pedal stiffness, the increase in force is smaller for low pedal depressions and bigger for high pedal depressions. Depending on the pedal position drivers may or may not detect these changes in force.

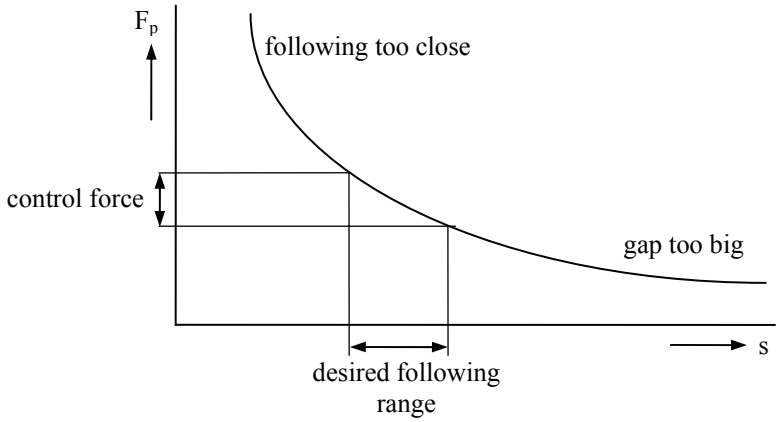


Figure 16: Inter-vehicle separation *s* related to feedback force F_p. The required car-following control force depends on the desired following separation. If the control force is kept more or less constant, the desired following range can be maintained. If the feedback force increases beyond the control force, drivers are likely to be following too close. Feedback forces below the control force are correlated with a big gap.

However, as was shown in Section 2.2.1, drivers depress the gas pedal deeply to command a relatively high acceleration in order to increase speed. Once the desired speed is reached, the gas pedal is released again to the approximate position for the desired steady state speed. When using an additional force as force feedback, drivers will not be informed immediately when they depress the gas pedal to accelerate, because, although the absolute force is higher due to the smaller inter-vehicle distance, the dynamic gas pedal characteristics remain the same. Only after the control actions have manifested themselves as changes in the environment will drivers experience an increase in force, since the inter-vehicle separation has changed. With the additional stiffness feedback, however, drivers will experience an immediate increase in force when they try to accelerate, because that is an inherent characteristic of increased stiffness: force increases proportionally to depression angle. In other words, drivers are instantaneously informed that the consequence of their control action (increased acceleration) will decrease the separation with the lead vehicle.

So, to finalize this discussion, three important design issues for a haptic gas pedal feedback system can be distinguished:

1. Type of haptic feedback: additional force or additional stiffness
2. The relation between the haptic feedback and inter-vehicle separation
3. Quantification of inter-vehicle separation parameters

These design issues cannot be viewed as separate design problems; rather, they are interrelated and must therefore be investigated as a whole. This Chapter intended to clarify the importance of these design issues and why they are interrelated. The derivation of algorithms that capture this interrelation is discussed in Chapter 3.

Chapter 3

Haptic Feedback Algorithms

The basic idea behind the intelligent driver support system (IDSS) as it was introduced in Chapter one is to provide the driver haptically with the same information she/he acquires visually that is necessary to control the separation with a leading vehicle during car-following. The haptically transmitted information may keep the driver aware of the situation in front of the own car when visual attention is temporarily directed to, for example, in-vehicle devices such as a car-stereo system, a mobile phone or a navigation display.

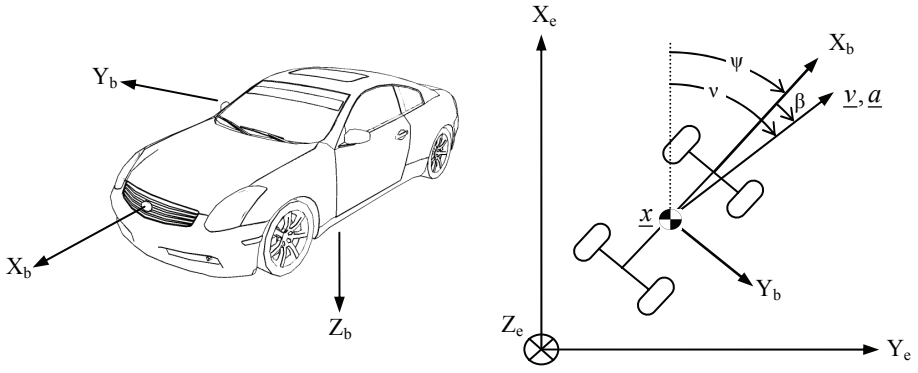
In practice, the implementation of all the required hardware to realise this idea does not pose any real problems. Actuators, sensor systems, and computer power to transform sensor information into actuator commands to the gas pedal are all readily available. The real challenge of this idea, however, is found in answering a single question – a question posed before, in Section 2.4 of the previous Chapter: 'What is meaningful haptic information in a car-following context?'

In the next Section, Section 3.1, the kinematics of car-following are discussed which determine the basic relations from which the haptic feedback algorithm is constructed. It will also be shown how the commonly used 'Newtonian' variables [1] to describe kinematic relationships can also be combined to yield variables that represent car-following behaviour in a consequent manner over a range of vehicle speeds. In Section 3.2 mathematical formalisms for obstacle avoidance control are reviewed. It is discussed how they can be applied to the particular situation of car-following. Finally, in Section 3.3 the resulting formulations of the haptic feedback algorithms that have been used in this research are derived.

[1] 'Newtonian' variables refer to position, speed, and acceleration, normally used to describe kinematic relationships of point masses.

3.1 Car-following kinematics

The kinematics of car-following can be defined in the horizontal plane of the world axis system $\{X_e, Y_e, Z_e\}$ (Figure 17b), by the position $\underline{x}$, speed $\underline{v}$, and acceleration $\underline{a}$, of two vehicles: the own vehicle ($\underline{x}_{car}$, $\underline{v}_{car}$, and $\underline{a}_{car}$, respectively) and the leading vehicle ($\underline{x}_{lead}$, $\underline{v}_{lead}$, and $\underline{a}_{lead}$, respectively). Since the haptic feedback system is installed in the own vehicle, it is convenient to base the origin of the observations of speed, position, and acceleration in the body axis system $\{X_b, Y_b, Z_b\}$ of the own car (Figure 17a). This means that all observations are relative to the position, speed, and acceleration of the own car.



(a) Car body-axis system (b) World-axis system

Figure 17: The car body-axis system (a) and the world-axis system (b). X_e is fixed to the North, Y_e is fixed to the East, Z_e is pointing towards the centre of the earth. The orientation of the car-body axis system is defined by the heading angle ψ. The speed vector orientation is defined by the course angle ν. The difference between the heading angle and the course angle is the slip angle: $\beta = \nu - \psi$ (adapted from Kruit, 2005).

Absolute position, speed, and acceleration of the vehicles are acting from their centre of gravity. Relative speed, and acceleration are thus acting from the centre of gravity of the lead vehicle (equations (3.1) to (3.3) respectively). The inter-vehicle separation distance x_{rel}, however, is defined as the distance from the front bumper of the own car to the rear bumper of the lead vehicle (see equation (3.1) and Figure 18).

$$x_{rel} = (x_{lead} - l_{lead}) - (x_{car} + l_{car}) \tag{3.1}$$

$$v_{rel} = v_{lead} - v_{car} \tag{3.2}$$

$$a_{rel} = a_{lead} - a_{car} \tag{3.3}$$

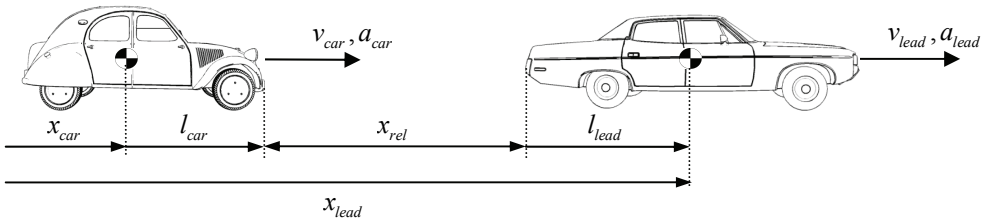


Figure 18: Definition of the direction of position x, speed v, and acceleration a, of the own car and the lead car in the horizontal plane of the world body axis system.

3.1.1 Following behaviour

Due to the coupling of equations (3.1) – (3.3) it is difficult to derive clear graphs that show the interactions between lead vehicle and following vehicle. Nevertheless, car-following research has shown (Goodrich and Boer, 2003; Piao and McDonald, 2003; Brackstone, Sultan, and McDonald, 2002; Ceder, 1979) that during a stable car-following situation, "*drivers cycle around an approximate equilibrium spacing*" (Ceder, 1979) when plotting the inter-vehicle separation distance x_{rel} against the relative velocity v_{rel}, see Figure 19. This phase-plane graph is both a very illustrating and useful graph, since it clearly shows the coupling of x_{rel} and v_{rel} such that it can be used for analyzing driver car-following behaviour. The most important observation from this cyclic behaviour was formulated by Rockwell (1972), who noted that maintaining a low relative velocity comes at the expense of more variance in the inter-vehicle separation distance and vice versa.

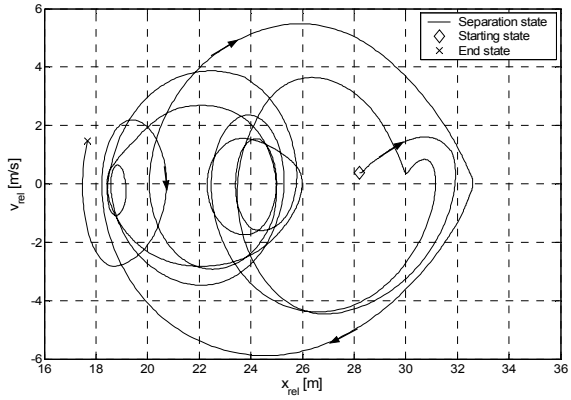
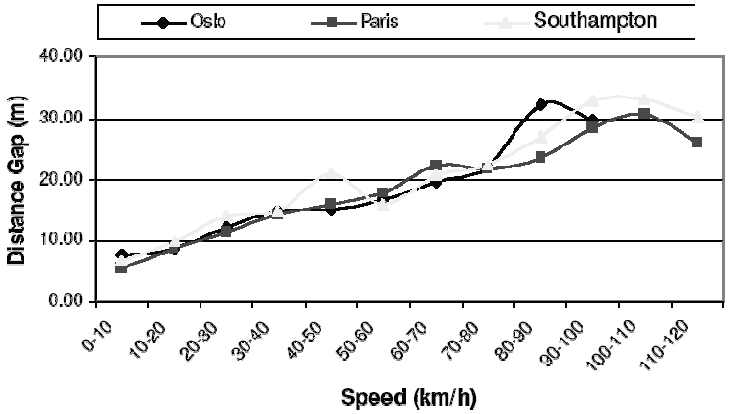


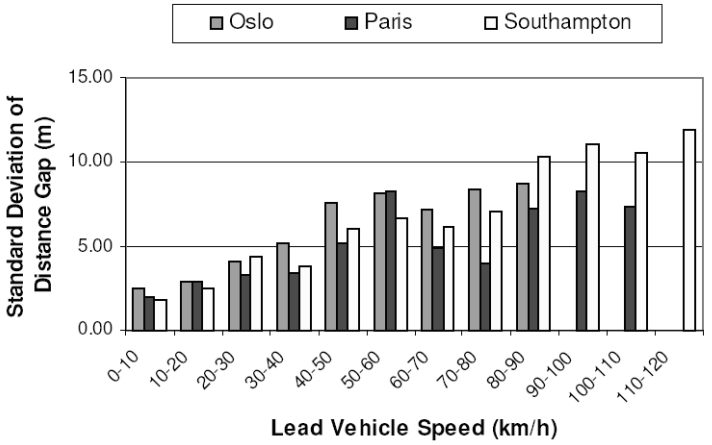
Figure 19: Cyclic phase-plane behaviour, observed during stable car-following. Data shown here was taken from a car-following experiment in a fixed base driving simulator.

More recent car-following research shows that the 'equilibrium spacing' mentioned by Ceder (1979) is a function of the speed at which drivers are driving (Piao and McDonald, 2003; McDonald *et al.*, 1997). Especially the findings of Piao and McDonald (2003) are interesting and provide an important impetus for application in the design of the haptic feedback algorithms, below in Section 3.3. They conducted an experiment with an instrumented vehicle, capable of detecting inter-vehicle separation and following vehicle speed and acceleration. The instrumented vehicle had measuring equipment mounted in the rear of the vehicle, such that it could observe the following vehicle. Observations were made of anonymous drivers, that is, drivers did not know they were being observed by the instrumented vehicle, during driving in continuous traffic streams. In total, over 65 hours of driving data were collected on urban motorways, arterial roads, and streets in the cities of Oslo, Paris, and Southampton, of which 1804 time series of car-following situations were extracted.

Two major findings of Piao and McDonald's experiment were that i) the inter-vehicle separation distance (x_{rel}) increased with driving speed (Figure 20a) and ii) the standard deviation of the inter-vehicle separation distance (x_{rel}) increased with increasing driving speed (Figure 20b). They hypothesised that these results might, for example, be explained by the capacity of drivers to estimate x_{rel}.



a) The distance gap (x_{rel}) in stable car-following increases with lead vehicle speed.



b) Standard deviation of distance gap (x_{rel}) increases with lead vehicle speed.

Figure 20: With increasing speed, drivers increase the inter-vehicle separation distance x_{rel} (a), yielding an increase in the variation in inter-vehicle separation distance (b). Reproduced from Piao and McDonald (2003).

Drivers are believed to be poor judges of longitudinal distance (Boer, 1999; Rockwell, 1972) and especially in changes in longitudinal distance. Rockwell (1972) provides an indication that the necessary change in x_{rel} before drivers can perceive a change at all obeys Weber's law:

$$\Delta x_{rel} \approx K x_{rel} \tag{3.4}$$

where Δx_{rel} is the change in separation distance, x_{rel} is the initial separation distance and where $0.1<K<0.2$, which means, for example, that at 30 [m] distance, drivers would need a 3 – 6 [m]

change in x_{rel} before they could detect the change. This is in accordance with Piao and McDonald's (2003) findings that the standard deviation of x_{rel} increases with increased driving speed and increased driving speed was also found to be correlated with an increase x_{rel}.

Even though drivers are poor judges of distance, they seem to be capable of quite accurately increasing the following distance with increasing speed (see Figure 20a). This suggests that drivers might not only perceive distance and speed separately, but also in a way that enables them to perceive directly what the following situation 'affords'[2] them in terms of keeping a safe inter-vehicle separation.

3.1.2 Time-headway and time-to-contact

A large volume of literature is available (see, for example, Vogel, 2003; Taieb-Maimon and Shinar, 2001; Gray and Regan, 1998; van Winsum and Heino, 1996; Hoffmann and Mortimer, 1994) that deals with the perception of inter-vehicle separation and the rate of change of inter-vehicle separation as defined by the variables time-headway (*THW*) and time-to-contact (*TTC*). Time-headway is defined as the time it takes for the following vehicle to travel the distance between the lead and following vehicle:

$$THW = \frac{x_{rel}}{v_{car}} \tag{3.5}$$

THW can be interpreted as an estimate of the safety margin, or safe-field-of-travel, drivers adopt during car-following (Boer, 1999), since it represents the maximum amount of time drivers have to react to a deceleration of the lead vehicle (Taieb-Maimon and Shinar, 2001). The time-to-contact is defined as the remaining time before the lead and following vehicle collide if nothing changes in the current situation:

$$TTC = \frac{x_{rel}}{v_{car} - v_{lead}} = \frac{x_{rel}}{-v_{rel}} \tag{3.6}$$

Boer (1999) characterizes *TTC* as the amount of time drivers have to "*intervene by employing a suitable skill to avoid an impending crash.*" For $TTC<0$, the lead vehicle is driving away from the following vehicle, increasing the inter-vehicle separation and no corrective action is necessary to improve the situation. When $TTC>0$, the lead vehicle is approaching the following vehicle (this can be the result of a decelerating lead vehicle, an accelerating following vehicle, or a combination of both), and a corrective action is required of the following driver, to avoid collision with the lead vehicle. In stationary car-following, $TTC \rightarrow \infty$ (since $v_{rel} \rightarrow 0$), and no corrective action is required.

Similar phase-plane graphs as shown above in Figure 19 can be made with *THW* and the inverse of *TTC*, see Figure 21. Because *TTC* is going to infinity when v_{rel} is going to zero, TTC^{-1} is used to draw the phase-plane graphs. Furthermore, since *TTC* was defined to be

[2] Gibson (1986) argued that humans do not necessarily perceive the environment in terms of the 'Newtonian' variables, used in physics, to describe the world we see, but also in terms of what the environment affords, depending on the context of the situation. Thus, a thirsty person, for example, does not only perceive a glass in terms of its dimensions and the material of which it is made, but also in terms of how it can satisfy her/his needs: a container for carrying a drink to quench thirst.

positive when the lead vehicle is moving towards the following vehicle, that is, $v_{lead}<v_{car}$, the sprirals in the $THW - TTC^{-1}$ phase-plane rotate counter-clockwise, rather than clockwise as in the $x_{rel} - v_{rel}$ phase-plane.

$$TTC^{-1} = \frac{-v_{rel}}{x_{rel}}$$

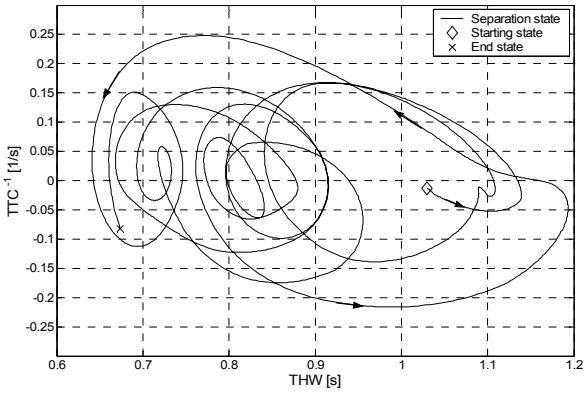


Figure 21: A phase-plane graph of stable car-following in the THW-TTC^{-1} space. Data shown here was taken from a car-following experiment in a fixed base driving simulator (same data as shown in Figure 19).

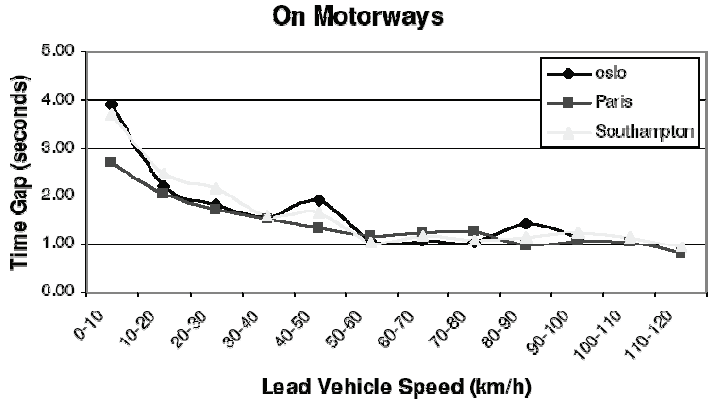
Driver time-headway perception characteristics

An important property of the *THW*, found in several investigations, is that it seems to be relatively constant (within drivers) over a broad range of following speeds. Van Winsum and Heino (1996) found that *THW* was not significantly affected by driving at speeds of 50, 60, and 80 [km/h]. Taieb-Maimon and Shinar (2001) evaluated drivers' *THW*'s at speeds ranging from 50 to 100 [km/h] and found that drivers adjusted their distance headways in relation to speed, such that THW remained constant. Similar results were found by Piao and McDonald (2003) as was shown above. They investigated a speed range from 10 to 120 [km/h] and found that for speeds >70 [km/h] *THW* was relatively stable and so was its standard deviation (see Figure 22a and Figure 22b respectively). From 10 to 60 [km/h] they noticed a clear trend of *THW* decreasing with increasing speed, and at speeds <10 [km/h] *THW* was largest and had the largest variability. From this experimental evidence it is concluded here, that for speeds at or above minimum highway speeds (>80 [km/h]), individual drivers maintain a constant *THW* strategy while car-following. This is a very useful driver characteristic during car-following since it yields a measure of the size of the safe-field-of-travel which is independent of driving speed when driving on a highway. It must be noted however, that the absolute value of the following THW varies significantly between drivers (van Winsum and Heino, 1996).

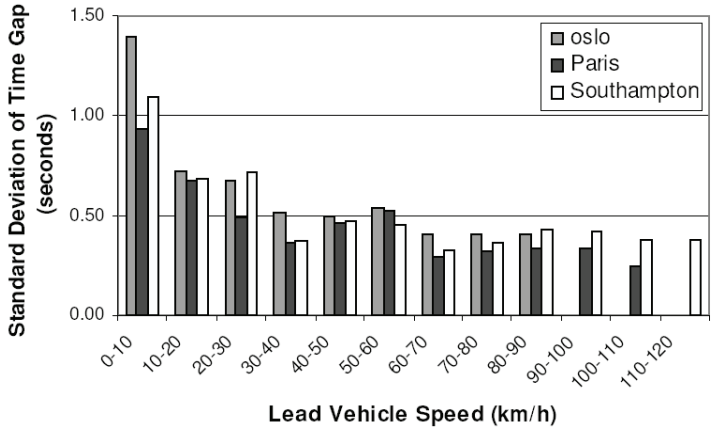
Driver time-to-contact perception characteristics

Since *TTC* influences the kind of control decisions drivers have to make to maintain their safe-field-of-travel, it has been hypothesised that *TTC*, and the perception of *TTC*, are directly related to corrective control actions. Cavallo and Laurent (1988) are very decisive and state that drivers "*must anticipate the moment of the impending collision in order to decide when to start braking…*" Lee (1976) believed drivers are able to control braking based on the TTC

information they get from the optic flow field. Van Winsum and Heino (1996) tested and confirmed the hypothesis that drivers use *TTC* information to determine when to start braking in a car-following situation that has a decreasing safe-field-of-travel for driving speeds of 50, 60, and 80 [km/h].



a) The time headway (*THW*) in stable car-following decreases with lead vehicle speed.



b) Standard deviation of *THW* decreases with lead vehicle speed.

Figure 22: For speeds >70 [km/h] the *THW* (a) and the standard deviation of *THW* (b) are relatively stable, independent of speed. For speeds between 10-60 [km/h] there is a clear trend of decreasing *THW* and σ_{THW} with increasing speed. At speeds lower than 10 [km/h] *THW* and σ_{THW} are relatively large. Reproduced from Piao and McDonald (2003).

A particular characteristic of drivers' ability to estimate *TTC* during car-following, which is consistently found in several investigations, is the fact that most drivers tend to underestimate *TTC* (Hoffmann and Mortimer, 1994; Cavallo and Laurent, 1988; Schiff and Detwiler, 1979). Beyond approximately 10 [s], underestimation of *TTC* increases rapidly. For car-following and taking the right corrective actions, however, especially the lower values (*TTC*<10 [s]) are of importance. Underestimations of *TTC* below 10 [s] have been shown to be about 40% of the actual *TTC*. This information must be taken into account when designing the feedback algorithms, to prevent drivers from mismatching haptic perception of the driving situation with visual perception of that same scene, when they have available both haptic and visual feedback.

Now, if *THW* and *TTC* are representative variables that drivers not only use to estimate their safe-field-of-travel and the rate of change of the safe-field-of-travel, but also to base their control actions on, how can that information be transformed into a meaningful force on the gas pedal?

3.2 Generalised obstacle avoidance algorithms

The key to realising the 'Magic Bumper' concept, and thus to answering the question of how to provide meaningful haptic information in a car-following context, is to formalise this concept mathematically. Different mathematical formalisms have been developed in the past to tackle similar problems, especially in the field of robotics (Gerdes and Rossetter, 1999; Hennessey, Shankwitz, and Donath, 1995; Ratering and Gini, 1995; Hennessey and Donath, 1992; Borenstein and Koren, 1991; Krogh, 1984). Most of the latter authors have created algorithms that apply to situations for obstacle avoidance in which obstacles can be located anywhere in the space around the own vehicle. This makes their application suitable for manoeuvring in environments and situations that are not known beforehand. The situations in which the IDSS is to function, however, are known exactly: during car-following. Thus, the application of these general theories may be simplified to this one particular case.

One of the most useful theories of obstacle avoidance, which might also be extended into the car-following domain, is Krogh's generalised potential field theory (1984). This theory is reviewed in Section 3.2.1 below. The major advantages and disadvantages of this theory in applying it to car-following will be discussed.

Another useful theory, which has already been modified to apply to obstacle avoidance control in highway vehicles, is impedance control (Hennessey, Shankwitz, and Donath, 1995). Impedance control uses virtual mechanics to represent the dynamics of the 'Magic Bumper', or 'Virtual Bumper' as Hennessey, Shankwitz, and Donath (1995) called their obstacle avoidance system, when a vehicle enters the safe-field-of-travel of the own vehicle. Their ideas are reviewed and discussed below in Section 3.2.2.

3.2.1 Generalised potential fields

The goal of the generalised potential field (GPF) that was derived by Krogh (1984) is to determine the magnitude and direction of the control actions that are required to manoeuvre an autonomous robotic vehicle through an obstacle filled course. To achieve this goal, each obstacle A_i (i indexes the obstacles) in the environment that is detected by the system is assigned a potential $P_i(\underline{x},\underline{v})$ based on the position $\underline{x}$ and the speed $\underline{v}$ of the controlled system relative to the obstacle. $P_i(\underline{x},\underline{v})$ is defined as in equation (3.7). The potential $P_i(\underline{x},\underline{v})$ defines the urgency with which the controlled system needs to accelerate away from the obstacle A_i.

$$P_i(\underline{x},\underline{v}) = \begin{cases} 0 & \forall\ v_i(t_0) \le 0 \\ \dfrac{1}{T_i - \tau_i} & \forall\ v_i(t_0) > 0 \end{cases} \tag{3.7}$$

T_i and τ_i are the maximum and minimum avoidance time respectively (see Appendix A.1 for the derivation of T_i and τ_i), defined by equations (3.8) and (3.9). The maximum avoidance time T_i

is defined as the time in which the vehicle comes to a stop without collision when an acceleration with a magnitude less than the maximum acceleration α is applied. The minimum avoidance time τ_i is defined as the time in which the vehicle comes to a stop without collision when the maximum acceleration of the vehicle, α, is applied.

$$T_i = \frac{2d_i(t_0)}{v_i(t_0)} \tag{3.8}$$

$$\tau_i = \frac{v_i(t_0)}{\alpha} \tag{3.9}$$

with $d_i(t_0)$ being the distance to the object A_i, along the obstacle normal $\underline{n}_i$, at time t_0; α the maximum deceleration of the controlled vehicle applied in the direction of $\underline{n}_i$; and $v_i(t_0)$ the approach velocity in the direction $\underline{n}_i$, at time t_0 (see Figure 23).

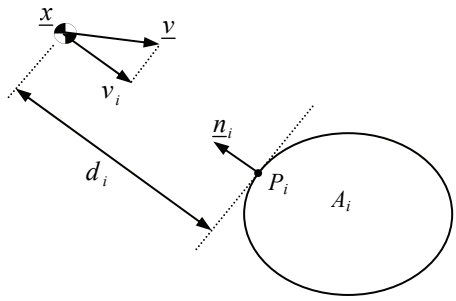


Figure 23: Definition of the relations between an obstacle A_i and the controlled element at $(\underline{x}, \underline{v})$, generating a potential P_i. Reproduced from Krogh (1984).

The gradient $\underline{c}_{0,i}$ of the potential $P_i(\underline{x}, \underline{v})$ with respect to the position $\underline{x}$ determines the direction and magnitude of the required control action to steer the controlled system away from this obstacle. It can be seen from equation (3.10) that the direction of $\underline{c}_{0,i}$ is indeed away from the obstacle, that is, in the direction of the obstacle normal $\underline{n}_i$ (see Appendix A.2 for the derivation of $\underline{c}_{0,i}$, the obstacle avoidance vector).

$$\underline{c}_{0,i} = -\underline{\nabla}_x P_i(\underline{x}, \underline{v}) = \begin{cases} 0 & \forall\ v_i(t_0) \le 0 \\ \dfrac{2P_i(\underline{x}, \underline{v})}{v_i(t_0)} \underline{n}_i & \forall\ v_i(t_0) > 0 \end{cases} \tag{3.10}$$

Because the gradient $\underline{c}_{0,i}$ is a vector, the total required control action $\underline{c}$ to steer the controlled system away from all obstacles in field with N obstacles A_i (with $i=1..N$) without colliding with any of the obstacles is the sum of all obstacle gradients $\underline{c}_{0,i}$, equation (3.11).

$$\underline{c} = \underline{c}_{0,1} + \underline{c}_{0,2} + \ldots + \underline{c}_{0,N} \tag{3.11}$$

To apply this method, the GPF needs to be calculated at every time step Δt for all obstacles that are within line-of-sight of the controlled system. In the case of autonomous vehicles, as Krogh (1984) describes in his paper, a final control action vector is necessary to keep the system going: the goal attraction vector $\underline{c}_g$. The goal attraction vector is, therefore,

always pointed towards the destination of the vehicle. Autonomous control is beyond the scope of this thesis, however, and the goal attraction vector will not be elaborated on any further.

The generalised potential field and car-following

One of the most important aspects of the GPF is its dependence on both position and velocity of the controlled system relative to the obstacles. As was mentioned earlier, in Section 3.1.1, car-following requires a weighing of maintaining low relative velocity at the cost of a higher relative position or vice versa (Rockwell, 1972). Thus, in order to provide drivers with the right kind of information it should contain both speed and position information. However, the GPF algorithms are based on static objects, whereas during car-following the 'obstacle' that needs to be avoided is the moving lead vehicle. This will make calculating the reserve avoidance time T_r more difficult, since movement towards or away from the lead vehicle does not just depend on the own vehicle any longer, but on the movement of the lead vehicle too. The assumption of constant acceleration away from the obstacle to determine equations (3.8) and (3.9) to calculate the potential of equation (3.7) does not hold anymore. The use of a limited available acceleration of the controlled element, which was assumed to be acting constantly in case of an avoidance manoeuvre is, nevertheless, useful in that it demonstrates the incorporation of the limits of system dynamics in the avoidance algorithm.

A feature of the GPF that is readily applicable to car-following is the fact that there is no potential $P_i(\underline{x}, \underline{v})$ in case $v_i(t_0) \leq 0$. So, when the lead vehicle is moving away from the following vehicle there is no feedback required, since the safe-field-of travel is already expanding, which is the goal the driver support system is trying to achieve.

The GPF was designed to handle multiple objects surrounding the own vehicle. In the case of car-following, there is, in general, only one 'obstacle' to avoid and that is the lead vehicle. Furthermore, the direction in which the avoidance vector $\underline{c}$ should be pointing is always in line with the obstacle normal vector $\underline{n}$ of the lead car. This greatly simplifies the GPF calculations, eliminating the need to determine the gradient of the potential field, since the direction of the avoidance vector $\underline{c}$ is known beforehand.

There are cases with multiple vehicles in front of the own car, where it is difficult to distinguish which vehicle is the lead vehicle. For example, when a vehicle is cutting in, or cutting out at highway entries and exits, respectively. These situations do require taking into account more than one 'obstacle'. But, since the gas pedal, as a haptic information channel and as the longitudinal control channel, cannot give directional information other than in the longitudinal direction of the car-body axis, a different solution to this multiple car problem is required. This problem has been investigated and a solution has been proposed and tested by de Winter (2004a; 2004b) and de Winter *et al.*, 2004. The solution de Winter (2004a; 2004b) proposes is based on the combination of the haptic feedback algorithms described below in Section 3.3 and 'vector field histograms' (Borenstein and Koren, 1991). The design of the vector field histogram that is used in the solution of de Winter assigns a local time-headway (*THW*) and time-to-contact (*TTC*) to all vehicles within the boundaries of the field. An algorithm is developed to determine the total weight of all vehicles, such that the result is a single *weighted THW* and a single *weighted TTC* that are representative of the entire situation in

front of the own vehicle. The results show that the introduction of weighted *THW* and *TTC* result in smooth transitions in force when another vehicle cuts in of moves out from in front of the own vehicle. Furthermore, drivers do not seem to change their driving behaviour due to this algorithm when multiple vehicles manoeuvre laterally in front of the own vehicle. This thesis, however, will not elaborate on this problem of multiple car situations but focuses on the single car-following problem.

Finally, the GPF was designed to calculate a control avoidance vector $\underline{c}$ which has a magnitude $||\underline{c}|| \rightarrow \infty$ when the distance to the obstacle $d_i \rightarrow 0$. Using this kind of algorithm for haptic feedback purposes is unacceptable and impossible. The goal is to provide informational haptic feedback, which means the amount of force on the gas pedal that can be used for feedback is very limited. Furthermore, if the amount of force on the gas pedal is allowed to increase such that drivers will not be able to depress the gas pedal anymore, the system is effectively telling the driver what to do. In other words, control authority is taken away from the driver. Also, a quick and substantial increase in force, that is well above the force drivers can resist might even lead to injury. Finally, from a technical point of view, delivering high forces with an electrically controlled actuator requires expensive equipment, which would make the system unattractive financially for potential customers.

Summarising, the beneficial features of the GPF that can be applied in haptic feedback for car-following are: i) speed and position dependence, ii) no feedback when the lead vehicle is moving away from the own vehicle, and iii) system dynamics included in the potential field.

3.2.2 Impedance control for obstacle avoidance

Hennessey, Shankwitz, and Donath's (1995) impedance control ideas for obstacle avoidance in vehicle collision avoidance originated from impedance control research in robot obstacle avoidance done by Hennessey and Donath (1992). Mechanical impedance is used to characterise the dynamic response of the controlled system to disturbances that act on its motion. For a mobile robot, this problem is dealt with at low speeds, static obstacles, and involves complicated path-planning algorithms. During driving, fast algorithm updates are required, since the dynamics of collision avoidance in traffic are high frequency and involve moving 'obstacles', while path planning is executed by the driver. Therefore, the concept of mechanical impedance was simplified from the 6 degrees of freedom (DOF) for robot arms, to a simple 1 DOF method that represents a 'virtual bumper' in front of the own vehicle.

The 'virtual bumper' is mechanically represented by a virtual spring-damper system that is attached to the front of the own vehicle. The undisturbed state of this spring-damper system is a computer-controlled boundary, which Hennessey *et al.* (1995) called the vehicle's personal space (note the similarity with Gibson and Crooks' (1938) safe-field-of-travel mentioned in Chapter 1). Whenever another vehicle enters the own vehicle's personal space, the virtual bumper is deflected and generates a virtual force F based on the dynamics of the virtual spring-damper system, acting on the own vehicle (see Figure 24). The magnitude of this virtual force F depends on the depression Δx, the rate of depression $\Delta \dot{x}$ and the stiffness k and damping b of the virtual bumper:

$$F = k\Delta x + b\Delta \dot{x} \tag{3.12}$$

The virtual force F can then be used as a command to move the own vehicle in the direction of the applied force, that is, away from the lead vehicle. A simple control law is proposed which commands an acceleration a_c away from the lead vehicle based on F:

$$a_c = -KF \tag{3.13}$$

in which K is a simple control gain.

The virtual bumper concept is extended further by Hennessey *et al.* (1995), to 2 DOF, such that lateral control can be included as well. Since lateral control is beyond the scope of this thesis, it will not be elaborated on.

Haptic feedback with impedance control

The virtual bumper concept based on impedance control seems to be readily applicable to haptic gas pedal feedback. Since the resulting impedance of the system due to an encroaching vehicle is expressed as a force, there should not be any difficulties in scaling this force such that it can be applied to the gas pedal. Position and velocity of the lead vehicle can be measured and used in the algorithm. However, as was shown in Section 3.1.2, inter-vehicle separation based on time-headway – equation (3.5) – and time-to-contact – equation (3.6) – rather than relative position and speed yield variables that represents car-following behaviour in a more useful manner over a range of vehicle speeds. This would require some modifications such that the virtual bumper virtual force F can be related to THW and TTC instead.

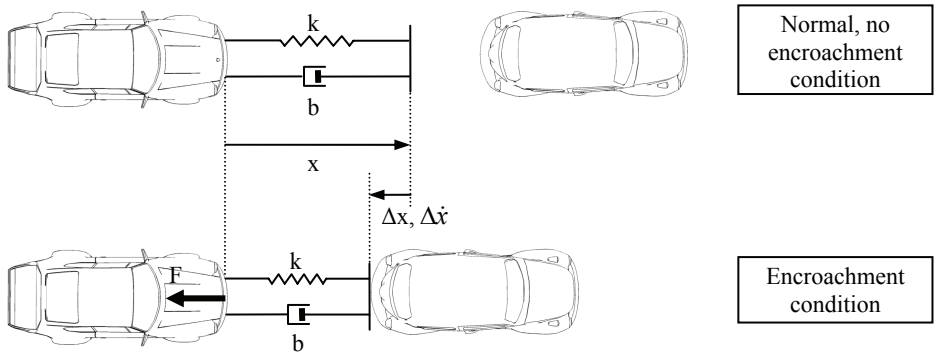
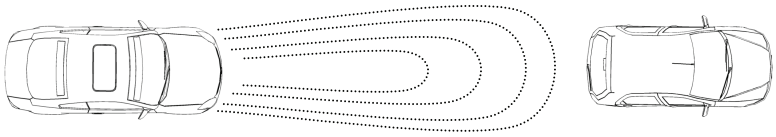


Figure 24: Virtual bumper example. The stiffness k and damping b of the virtual bumper will yield a virtual force F when a lead vehicle is moving into the own vehicle's personal space, causing a deflection Δx of the virtual bumper with undisturbed length x. Adapted from Hennessey, Shankwitz, and Donath (1995).

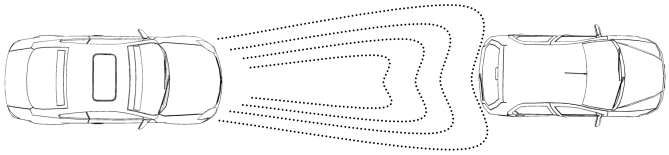
3.3 Haptic feedback algorithms

The implementation of the haptic feedback algorithm was envisaged by the Nissan Motor Company Ltd. engineers to be found in the metaphorical concept of the 'Magic Bumper', a virtual bumper similar to that described by Hennessey, Shankwitz, and Donath (1995) above. The own vehicle's material bumper would be extended with the metaphorical 'Magic Bumper' which would reach well ahead of the own car. Whenever another vehicle would enter the

operational boundaries of the 'Magic Bumper' this virtual bumper would deform, analogous to Gibson and Crooks' (1938) safe-field-of-travel. The amount of deformation would be a measure of the amount of required haptic feedback (Figure 25). Intuitively, this resembles the compression of an air-cushion attached to the front of the vehicle. The more the cushion is depressed by a leading vehicle closing in on the own vehicle, the more the tension, and hence the force on the own car, builds up in the cushion. Another intuitive example is the approach of two similar magnetic poles. The closer the poles come together, the higher the repulsive forces they experience, and the more difficult it becomes to make them move even closer together. These metaphorical concepts show that there are ways in which a, in reality non-existent, haptic relationship between an environment and the control of a vehicle can be established that intuitively makes sense for humans.



a) The 'Magic Bumper' extends in front of the own vehicle as a protective cushion.



b) The protective cushion deforms by the closing in of a lead vehicle.

Figure 25: Metaphorical concept of the 'Magic Bumper'. The 'Magic Bumper' extends in front of the own vehicle (a) as a safety cushion that deforms when a lead vehicle enters the operational boundaries of the 'Magic Bumper' (b), analogous with Gibson and Crooks' (1938) safe-field-of-travel and Hennessey, Shankwitz, and Donath's (1995) virtual bumper. The amount of deformation is a measure of the amount of haptic information that needs to be communicated to the driver.

3.3.1 Nissan force feedback

The force feedback algorithm that was derived by Nissan Motor Company Ltd. is an impedance based algorithm. The algorithm uses *THW* and *TTC* rather than x_{rel} and v_{rel} to generate a virtual force F_{PP} [N] acting on the own vehicle whenever a lead vehicle is entering the safe-field-of-travel:

$$F_{PP} = \left(\frac{a}{THW} + \frac{b}{TTC} \right) \cdot g \tag{3.14}$$

with constants $a=1$ [kgf/s] and $b=8$ [kgf/s], which are empirically determined from the distribution of measured *THW* and *TTC* during car-following – see Figure 26 and Figure 27 – and g=9.81 [m/s^2], the gravitational constant at sea-level. A $THW \leq 1$ represents the lowest 25% *THW*'s of the distribution, therefore a was chosen to be equal to one. A $TTC \leq 4$ represents the lowest 5% of the distribution of *TTC* at driving speeds >40 [km/h], but b was chosen to be eight

to include most observed situations. Since *THW* and *TTC* decrease when the lead vehicle is moving towards the following vehicle, the virtual force F_{PP} increases and vice versa.

The objective representation of an encroaching lead vehicle by a virtual force as defined by equation (3.14) might not be perceived as such by humans. From psychophysics it is known that subjective perception of force is related to the physical quantity through Stevens' power law (Stevens, 1957):

$$S = kI^n \tag{3.15}$$

in which S is the subjective sensation magnitude, k a constant depending on the sensed continuum, I the physical stimulus intensity, and n is a constant depending on the modality. When plotted on a log-log scale, the power law yields a straight line relating subjective sensation magnitude S to the objective stimulus intensity I with a slope n.

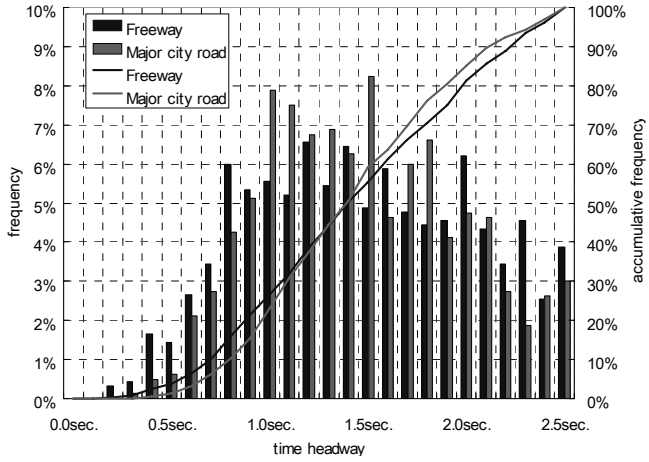


Figure 26: Distribution of measured time-headways during car-following on freeways and city-roads near Tokyo, Japan. Reproduced from Yamamura (2002).

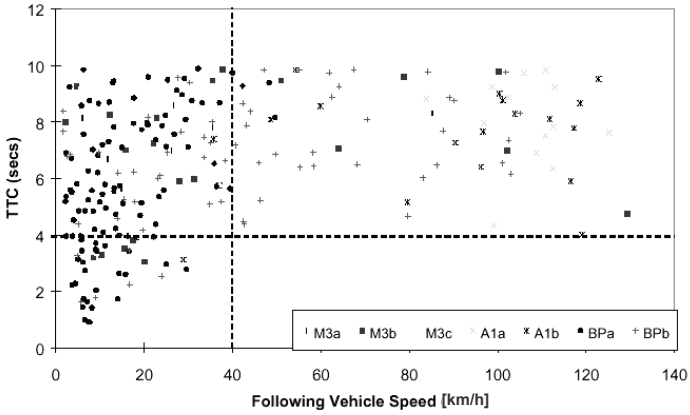


Figure 27: Distribution of measured time-to-contacts (TTC) during car-following on freeways and city roads in Europe: M3a-c (UK, London, M3), A1a-b (Germany, Hamburg, A1), and BPa-b (France, Paris, Boulevard Périferique), DIATS (1998).

Applying Stevens' power law to the feedback force F_{PP}, equation (3.14) can be written as F_{force} [N], with limitations on the minimum and maximum forces:

$$F_{force} = \begin{cases} 0 & \forall\ F_{PP} < F_{PP}^{\min} \\ kF_{PP}^{n} & \forall\ F_{PP}^{\min} \le F_{PP} < F_{PP}^{\max} \\ F_{\max} & \forall\ F_{PP} > F_{PP}^{\max} \end{cases} \tag{3.16}$$

The constant $n \approx 0.90$ is determined by equation (3.17), in which F_{min}=4.9 [N] and F_{max}=24.5 [N], the minimum and maximum forces applied by Nissan to the gas pedal respectively; and $F_{PP}^{\min} = 4.9$ [N] and $F_{PP}^{\max} = 29.4$ [N], the minimum and maximum virtual forces the car-following situation is allowed to generate respectively:

$$n = \frac{\log F_{\min} - \log F_{\max}}{\log F_{PP}^{\min} - \log F_{PP}^{\max}} \tag{3.17}$$

The constant $k \approx 0.93$ is determined by equation (3.18):

$$k = \frac{F_{\max}}{(F_{PP}^{\max})^{n}} \tag{3.18}$$

The feedback algorithm (3.16) yields the feedback force in [N] depending on *THW* and *TTC* as visualized below in Figure 28.

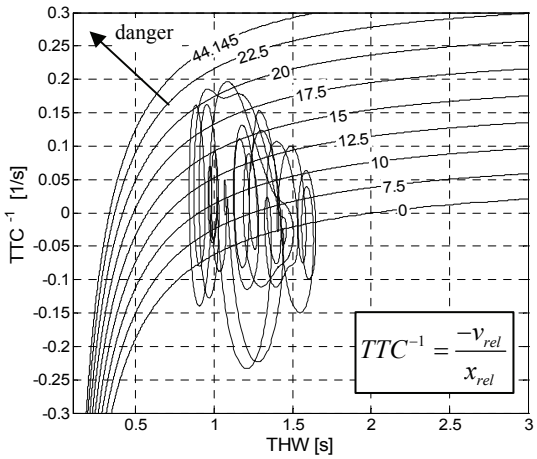


Figure 28: The force feedback profile as a function of *THW* and TTC^{-1}. The solid lines represent iso-force levels (in [N]). The spiraled lines are typical measured car-following data (60 seconds) from a fixed base driving simulator for a subject that was asked to maintain a *THW* of approximately 1 [s]. The haptic feedback system was not activated.

Discussion of the feedback algorithm

The Nissan force feedback algorithm makes use of position and velocity feedback, both expressed in the desired *THW* and *TTC*, as was discussed in Sections 3.2.1 and 3.2.2 above. There is, however, feedback when *TTC*<0, that is, when the lead car is moving away from the following car. In Section 3.2.1, it was argued that this is unnecessary since there is no movement towards increased criticality of the situation. The area for which the force feedback algorithm does provide feedback when *TTC*<0 is small, however. Only for *THW*<0.5 there is

considerable feedback due to negative *TTC*. Under normal driving conditions, this situation is not likely to occur very often. The urge to move away from the lead vehicle can be said to be strengthened for such small time-headways.

In Figure 28 above, typical car-following data from a fixed-base driving simulator experiment is plotted on the force feedback profile, to give an idea of the kind of feedback this particular driver would have experienced had this algorithm been active. The driver was asked to try and maintain a *THW* of 1 [s], the average highway *THW* adopted by drivers on roads in Paris, Oslo, and Southampton as was measured by Piao and McDonald (2003). As can be seen, most of the feedback would have been generated by $TTC>0$. Changes in *THW* have little effect for this particular situation. For following situations with higher time-headways ($THW>1$ [s]) little would change in the kind of feedback that would be generated, noting that the higher the *THW*, the less likely it is that *TTC* will become small, reducing the amount of feedback.

Applying a force task, that is, trying to maintain a constant force on the gas pedal, would, with this algorithm, be beneficial in maintaining TTC^{-1} as close to zero as possible (in other words, maintaining zero relative velocity), since there is a significant amount of feedback for increases in TTC^{-1}. However, maintaining a preferred *THW* by applying a force task strategy is, with this feedback algorithm, hardly beneficial. The algorithm will yield significant changes in force feedback with changes in *THW* only for very low values of *THW*. It is therefore expected that with this algorithm the benefits will be especially noticeable in the distribution of *TTC*.

3.3.2 THW-stiffness feedback

With the implementation of a *THW*-only feedback algorithm it is expected that drivers will be able to benefit more from the haptic feedback in the sense that it might better facilitate adopting a force task. By using feedback of *THW* only, the presentation of relative velocity information is sacrificed. However, because car-following is a dynamic process, the changes in *THW* during car-following are expected to compensate for not having any relative velocity information in the feedback algorithm.

It was also decided to provide stiffness feedback with the *THW* algorithm, rather than force feedback. Using stiffness feedback is expected to enhance the perception of *THW* changes since not only the actual environmental changes in *THW* will be perceptible, but the changed force slope of the gas-pedal characteristic is immediately perceptible too (see Section 2.3.2). Hence, the stiffness feedback characteristics are expected to strengthen the perception of the environmental characteristics.

The *THW*-stiffness feedback algorithm F_{THW} is defined by the maximum additional stiffness K_{max} on the gas pedal and a linear scaling function *P(THW)*. This function *P(THW)* is dependent on the actual *THW* and the maximum THW_{max} for which the algorithm will provide feedback.

$$P(THW) = 1 - \frac{THW}{THW_{\max}} \tag{3.19}$$

$$F_{THW} = \begin{cases} 0 & \forall \ P(THW) < 0 \\ K_{\max} P(THW) \alpha_{pedal} & \forall \ 0 \le P(THW) < 1 \end{cases} \tag{3.20}$$

THW_{max}=2.5 [s], and K_{max}=1000 [N/m]. The maximum feedback force the driver will be able to experience due to this maximum additional stiffness depends on the dimensions of the gas-pedal. The length of the gas-pedal arm, from the rotation axle to the position of the pedal-pad, l_{pedal}=0.18 [m]. At maximum gas-pedal depression (α_{pedal}=100 [%]) the angular displacement of the pedal A_{pedal} =20°. Thus, the maximum pedal stroke $s_{pedal}^{\max}$ =0.06 [m] is calculated with equation (3.21).

$$s_{pedal}^{\max} = \frac{\mathrm{A}_{pedal}\pi}{180} l_{pedal} \tag{3.21}$$

Thus, the maximum feedback force $F_{\max} = K_{\max} s_{pedal}^{\max} = 60$ [N].

The *THW*-stiffness feedback algorithm is visualized in Figure 29. The feedback force drivers experience is not only dependent on *THW* (see the iso-stiffness lines in the left hand graph of Figure 29), but also on the gas-pedal position α_{pedal} (see the iso-force lines in the right hand graph of Figure 29).

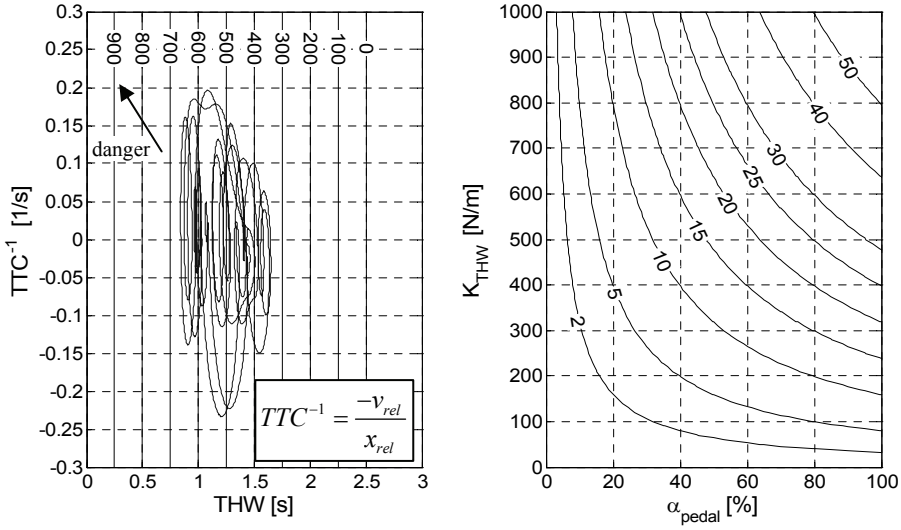


Figure 29: Iso-stiffness lines [N/m] of the *THW*-stiffness feedback algorithm as a function of *THW* and TTC^{-1} (left). A typical car-following spiral, measured during car-following in a fixed base driving simulator is shown in the *THW*-TTC^{-1} phase plot (left) as well. The force drivers experience from the pedal now depends not only on the *THW* but on the depression of the gas-pedal, α_{pedal}, as well – see the iso-force lines [N] in the right graph.

Discussion of the feedback algorithm

As can be seen from the left hand graph of Figure 29, the stiffness of the gas-pedal only changes when there is a change in *THW*. Clearly, this feedback is always present if *THW*<2.5 [s], whether *TTC*<0 [s] or not. This is a departure from the idea that no feedback is needed when the inter-vehicle separation is increasing, that is, when *TTC*<0 [s]. For every *THW* there is a constant feedback stiffness K_{THW}. This should stimulate the adoption of a force task strategy to control the inter-vehicle separation.

Since a decrease in *THW* yields an increase in stiffness, the driver is urged to release the gas pedal. Increased stiffness makes releasing the gas pedal easier, and depressing the gas pedal more difficult, since the change in force with a change in gas-pedal position is higher with an increased stiffness. The reason why stiffness-feedback is expected to be more beneficial in promoting a force task is that, if the driver response to an increase in stiffness is to decrease the gas-pedal depression, this also leads to a decrease in the pedal force. In other words, a force task strategy with stiffness feedback has inherent coherence with the required response of the driver to the changing following situation.

Still, the hypothesis that the dynamics of car-following will compensate for the lack of relative velocity feedback is a fragile one. Due to the nature of the design problem – creating a haptic feedback sensation that has no real-life equivalent – this hypothesis can only be verified experimentally. The design of the experiments to verify this hypothesis – amongst others – is described in Chapter four. The understanding that car-following is based on a balance between relative velocity and relative distance changes (Section 3.1.1) and that this should be incorporated in the feedback algorithm (Section 3.2.1) motivated the design of the algorithm discussed next.

3.3.3 TTC-stiffness feedback

Time-headway and time-to-collision are coupled through the inter-vehicle separation x_{rel}. Rewriting equation (3.5) to get x_{rel} and then substituting in equation (3.6) yields:

$$TTC^{-1} = \frac{-1}{THW}\frac{v_{rel}}{v_{car}} \tag{3.22}$$

Thus, TTC^{-1} is inversely proportional to *THW* for a given v_{rel} at a given driving speed v_{car}. Figure 30 shows for v_{car}=100 [km/h] and v_{rel}={-20, -15, -10, 5, -2.5, 2.5, 5, 10, 15, 20} [km/h] how TTC^{-1} changes with *THW* and vice versa (if v_{car} and v_{rel} do not change). It can be seen from this figure, which follows from equation (3.22), that the smaller the *THW*, the faster the TTC^{-1} increases (or decreases for TTC^{-1}<0). In other words, at smaller *THW's* the importance of reacting to changes in TTC^{-1} increases rapidly. This relationship between *THW* and TTC^{-1} is incorporated in the *TTC*-stiffness feedback algorithm.

The *TTC*-stiffness feedback algorithm F_{TTC} is defined by the maximum additional stiffness K_{max} on the gas pedal and a non-linear scaling function *P(THW,TTC)*. This scaling function is defined by equation (3.23), with THW_{max}=2.5 [s], THW_{min}=0.5 [s], TTC_{max}=10 [s] as the operational boundaries of the algorithm. K_{TTC} itself is defined as in equation (3.24). The algorithm is shown in Figure 31. The left hand side of Figure 31 shows iso-stiffness lines dependent on *THW* and TTC^{-1}. In the right hand side, iso-force lines [N] are drawn. The feedback force drivers experience with the stiffness algorithm depends on the feedback stiffness and the pedal position in the same manner as with the *THW*-stiffness feedback algorithm.

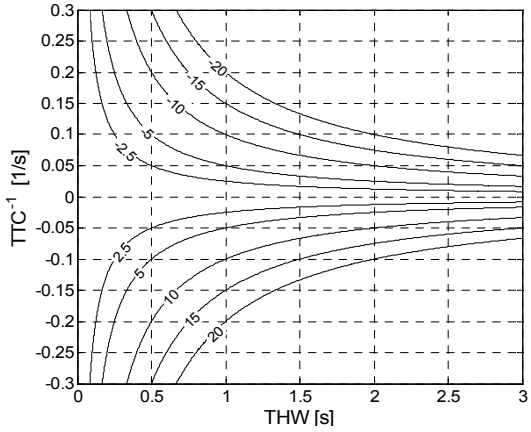


Figure 30: Iso relative velocity lines [km/h] at a driving speed of 100 [km/h] of the following vehicle, showing the increased importance of TTC^{-1} for decreasing *THW*.

$$P(THW,TTC)=\begin{cases}\dfrac{TTC_{\max}}{TTC} & \forall\ 0\le THW<THW_{\min}\\ THW_{\min}(THW_{\max}-THW)\dfrac{TTC_{\max}}{TTC} & \forall\ THW_{\min}\le THW\le THW_{\max}\end{cases} \tag{3.23}$$

$$F_{TTC}=\begin{cases}K_{\max}\alpha_{pedal} & \forall\ P(THW,TTC)>1\\ K_{\max}P(THW,TTC)\alpha_{pedal} & \forall\ 0<P(THW,TCC)\le 1\\ 0 & \forall\ P(THW,TTC)\le 0\end{cases} \tag{3.24}$$

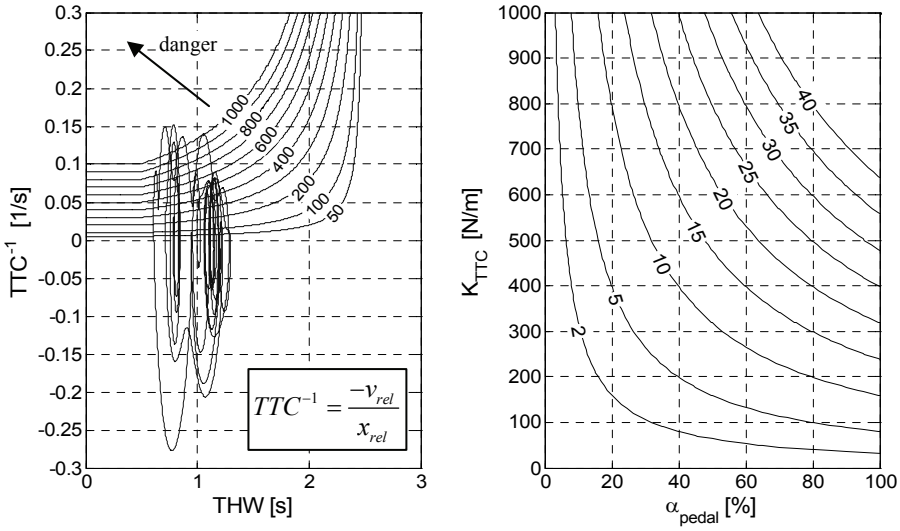


Figure 31: Iso-stiffness lines [N/m] of the *TTC*-stiffness feedback algorithm as a function of *THW* and TTC^{-1} (left). A typical car-following spiral, measured during car-following in a fixed base driving simulator is shown in the *THW*-TTC^{-1} phase plot (left) as well. The force drivers experience from the pedal now depends not only on the state of *THW* and *TTC*, but on the depression of the gas-pedal, α_{pedal}, too – see the iso-force lines [N] in the right graph.

Discussion of the feedback algorithm

As can be seen from the left hand graph of Figure 31, the *TTC*-stiffness feedback algorithm does not generate any feedback for $TTC<0$. The properties of the feedback algorithm are such that feedback is only given when the safe-field-of-travel is decreasing – with increasing intensiveness the smaller the *THW*. Because of the shape of the field, the dependence of the amount of feedback due to changes in the safe-field-of-travel, changes from mainly *THW* dependence for $THW \geq 2.0$ [s] to only *TTC* dependence for $THW \leq 0.5$ [s], and combined *THW* – TTC^{-1} dependence from $0.5<THW<2.0$. Thus, for example, in some 75% of the car-following situations measured near Tokyo, Japan (see Figure 26 above) drivers would experience haptic feedback based on the combination of *THW* and TTC^{-1}, only in the extreme 5% of cases would drivers experience feedback entirely based on *TTC*.

This feedback algorithm is expected to provide the best support for drivers to adopt a force task strategy in controlling their vehicle during car-following. At any given, stationary car-following situation, the pedal force the driver experiences is the same. Only due to changes in this car-following situation do the pedal forces change. The amount of change in the pedal force is situation-dependent. Thus, from any given stationary car-following situation, drivers receive properly scaled haptic feedback information that reflects the criticality of the impeding situation.

3.3.4 Human response to haptic gas-pedal feedback

It has been mentioned a couple of times before: the design of a haptic gas-pedal feedback sensation has no real-life equivalent. The design process has largely been an heuristic process, in which the development of the models of human interaction with a gas pedal contributed directly to gain more understanding in the complex coupling of intrinsic and reflexive limb dynamics, virtual gas-pedal dynamics, and driver perception and control of the car-following task. The resulting feedback algorithms, as presented in the previous sections, are derived from a number of assumptions that followed from the investigations that supported the design process. Three major assumptions, or hypotheses, have guided the design of the experiments that were conducted to test driver responses to driving with the proposed driver support system with any of the three described haptic feedback algorithms.

1. With the proper kind of haptic gas-pedal feedback during car-following, drivers will adopt a force-task in their interaction with the active gas pedal. In other words, when drivers experience haptic gas-pedal feedback the most optimal form to deal with this information is by trying to maintain the force on the gas pedal constant.
2. The use of stiffness feedback will increase the sensitivity of drivers to the support information as compared to using force feedback. Therefore, drivers are expected to adopt a force-task strategy more easily with stiffness feedback, than with force feedback.
3. The *THW* and *TTC* provide adequate information that can be transformed into haptic feedback, such that drivers intuitively understand the haptic information that is provided through the gas pedal. Furthermore, *THW* and *TTC* provide information that can be transformed into haptic feedback, such that drivers' haptic perception of the car-following situation matches their visual perception.

The design of the experiments that were conducted to find evidence in support of these hypotheses, and more particular sub-hypotheses, is the subject of the next Chapter. The detailed description of the particular design characteristics of each individual experiment, as well as the results, are described in Chapters 5 and 6.

Chapter 4

Experimental Method

Because there is no 'real-life' equivalent to communication of environmental information by haptic signals from the gas-pedal, the only way to learn about the effectiveness of this communication is by experimental investigation. Two experiment facilities have been constructed at Delft University of Technology which enable this specific type of research. At the department of Mechanical Engineering, section Man-Machine Systems, an electrical actuator is installed that is capable of producing accurate, high-bandwidth force and position control of a gas-pedal. The Human-Machine Laboratory of the Aerospace Engineering department, section Control & Simulation, facilitates a fixed-base driving simulator with electrically actuated steering-wheel and gas-pedal devices[1]. The software[2] with which both facilities are controlled is the same, which allows quick and easy updating as well as precise replication of simulation conditions in either laboratory.

Goal of the experiment facility of the department of Mechanical Engineering is to investigate the neuromusculoskeletal characteristics of the human leg/foot interaction with the haptic gas-pedal. The results of the experiments carried out with this facility are used to identify the parameters of the detailed neuromuscular model that has been described in Chapter 2 and in Abbink (2006), Abbink, van der Helm, and Boer (2004) in much greater detail.

With the fixed-base driving simulator at the department of Aerospace Engineering, the developed IDSS logic can be tested in a semi-realistic driving environment. Goal of the simulator experiments is to investigate the effects of the haptic feedback of environmental information on driver behaviour. In other words, *how* does driving behaviour change? Besides the effects that can be observed by looking at the statistics of the time domain data, the control

[1] Thanks to the generous support of Nissan Motor Company Ltd., which delivered in kind the driver seat, the actuated gas-pedal, the passive brake pedal, and the steering wheel, and provided funding for the procurement of the steering wheel actuator, dashboard LCD, and outside visual LCD projector.

[2] Delft University Environment for Communication and Activation (DUECA); a software architecture for real-time simulation. Developed by Dr. M.M. van Paassen of Delft University of Technology.

theory model from Chapter 2 is simplified to enable frequency domain analysis of driver behaviour. Frequency domain identification of driver behaviour is expected to give more insight into the underlying causes of observed changes in driving behaviour. In other words, *why* does driver behaviour change?

An extensive number of experiments has been carried out to test the developed IDSS logic. All the experiments described in this thesis have been executed in the fixed-base driving simulator. Although each experiment had different objectives and investigated different situations, there was one common condition: drivers were asked to perform a car-following task. This car-following task was conditioned in more or less the same way for each experiment. Therefore, the design of the car-following task will be discussed in this Chapter as the basis for all experiments that are described in the two subsequent Chapters.

4.1 Apparatus

The fixed-base driving simulator has been custom designed and built at the Aerospace Engineering department[3]. It is part of a Human-Machine Systems laboratory in which it shares a simulation platform with a flight simulator. The left-hand side of the platform is used for the driving simulator (see Figure 32).

Drivers are seated in an electrically adjustable car seat. They have at their disposal two active control devices and one passive control device. The steering wheel and the gas-pedal are fitted with electrical actuators. These actuators are software controlled and can be used to deliver the haptic feedback required for the experiments that were executed. The brake pedal is a passive control device. It is spring-loaded mechanically to provide some resistance to depression, but this characteristic cannot be altered during experiments.

Right behind the steering wheel, a 12" colour LCD screen is mounted on which the speed and rpm indicators are shown. Drivers have to look down, through the steering wheel to sample these indicators.



Figure 32: The Human-Machine laboratory fixed-base simulation facility. The right hand side of the simulation platform is used for flight simulation; the left-hand side for driving simulation.

[3] Thanks to the input of ing. Ruud van Olden and ing. Henk Lindenburg for the design and drawings, Ed Roessen for the fabrication and installation of the mechanical parts, and ing. Kees van Woerkom and ing. Adri Tak for the installation of all electronic equipment.

A Sanyo PLC-XU33 Multimedia projector projects the driving scene on the laboratory wall at a distance of 2.9 [m] from the driver-eye-reference-point (DERP). The projected screen is approximately 3.3 [m] wide and 2.1 [m] high. This results in a 60º horizontal and 40º vertical field-of-view (FOV). The graphical resolution of this projection is 1280x1024 pixels. This resolution is good enough for the purpose of the experiments conducted: car-following. The projector can be positioned such that the centre of the projection is in line with the DERP.

Around the platform, a five speaker surround sound system is installed which generates the engine sound and the sound of the wind, the volume of which depends on the speed of the car. At the back of the driver seat, two Aura AST-1B-4 Bass Shakers are attached to create a sensation of road and engine vibrations while driving the simulator. A subwoofer connected to the bass shaker system generates the low pitched rumble of the tyres on the road.

4.1.1 The active gas-pedal

The active gas-pedal is torque driven, that is, an electrical command to the actuator is converted into a torque on the gas-pedal. A pre-tensed (with force $F_i \approx 20$ [N]) passive mechanical spring (with stiffness $K_p \approx 0.17$ [N/m]) is also attached to the pedal lever, to always bring the pedal back to zero depression angle ($\alpha_p(t)=0$) when no force is exerted on it by the driver. This also makes the feedback system fail-safe: when the actuator fails, the gas-pedal still functions as a passive gas-pedal thanks to the mechanical spring (see Figure 33c). The characteristics of the passive spring were described in Section 2.2.1, equation (2.2):

$$F_p(t) = \alpha_p(t) K_p + F_i$$

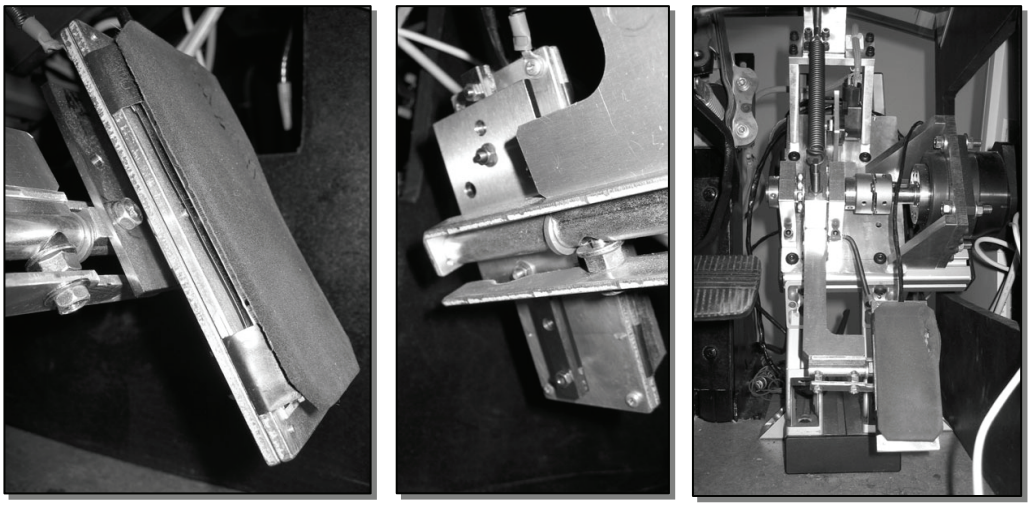
Torque is delivered at the pedal rotation point. The length of the pedal arm is $l_p = 0.18$ [m]. So, to deliver a force $F_p(t)$ on the foot of the driver the actuator must deliver a torque $T_p(t)$.

$$T_p(t) = l_p F_p(t) \tag{4.1}$$

To make sure the driver always experiences the same force F_p on her/his foot when a torque T_p is delivered, a sliding gas-pedal pad, developed by Nissan Motor Company, Ltd., has been installed that keeps the foot from sliding over the pad and thereby changing the position at which the feedback force acts on the foot. The foot is continuously positioned on the same position on the pad, while the pad slides up and down a small rail attached to the gas-pedal lever as the lever is rotated to depress or release the gas-pedal (see Figure 33a and Figure 33b).

The depression $\alpha_p(t)$ of the gas-pedal is measured with a position sensor which converts the angle of the pedal lever into a depression percentage of the maximum depression. The maximum rotation of the gas-pedal is 20º. This yields a maximum stroke $s_p^{\max}$ of the pedal at the contact point with the foot of $s_p^{\max} = 0.18 \cdot 2\pi \cdot 20/360 = 0.06\,[m]$. At both the minimum and maximum depression angles, pedal movement is blocked by a hard, mechanical stop.

Four Kyowa LM-5KA load cells (Figure 34) are mounted on the four corners of the gas-pedal pad to measure the force drivers are exerting on the gas-pedal. The four load cells are connected in parallel electrically to give one resultant pedal force. The point of application of the resultant force is in the focal point of the four load cells together, that is, in the middle of the gas-pedal pad.



a) side view sliding pad b) back view sliding pad c) front view gas-pedal

Figure 33: Photo details of the haptic gas-pedal (c) and the sliding pedal pad (a & b) as they are installed in the driving simulator.

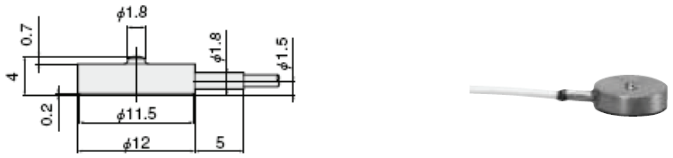


Figure 34: The Kyowa LM-5A miniature load cell (dimensions in mm). The load cell is placed on the four corners of the gas-pedal pad to measure the force drivers are exerting on the gas-pedal. The rated capacity of each load cell is 50 [N].

4.2 The car-following task

To investigate the effects of the use the haptic gas-pedal on driver behaviour and car-following performance, a specific procedure for the car-following task is developed. In short, during an experiment drivers are shown a lead vehicle which they are asked to follow at a certain time-headway (*THW*). At pre-determined intervals in time, the *THW* is visually indicated by a transparent rectangle – the THW-indicator (discussed in more detail below, in Section 4.2.1). At random 7-10 second intervals later, the THW-indicator disappears. The, up to then stationary speed of the lead vehicle, is then disturbed with a semi-random speed disturbance. After the trial the THW-indicator appears again. This process is repeated for as many times as specified in the particular experiment protocol. Drivers are instructed to maintain the indicated *THW* as good as possible, even when the THW-indicator is not visible and the lead vehicle speed is disturbed (see Appendix C for an example of driver task instruction).

Because the haptic feedback algorithms that were presented in Chapter 3 provide haptic feedback that is dependent on *THW* and/or *TTC*, it is important to make sure there is sufficient data available for analysis under similar driving conditions (in terms of *THW* and *TTC*), since similar driving conditions will produce similar feedback. Free driving conditions, where drivers

are allowed to choose their own following separation, require long driving periods for each participant in any one of the experiments to ensure enough comparable conditions are available for statistical analysis. This will first of all take too much time. Second, it is too monotonous a task for drivers to stay focused during the entire experiment. Third, a large amount of the collected data might not be suitable for analysis, because too little comparable data is recorded for large parts of the experiment run.

Thus, it was decided to instruct drivers to follow the lead vehicle at prescribed separations, expressed in seconds *THW*. From literature it is well known that most drivers naturally adopt a constant *THW* strategy while driving at speeds ≥60 km/h (Piao and McDonald, 2003; Brackstone, Sultan, and McDonald, 2002; McDonald *et al.*, 1997; Hogema, 1996; Fuller, 1984). Although the observed constant *THW* strategies in literature refer to free driving, where drivers choose a *THW* themselves, they can easily maintain a prescribed, non-preferred *THW*, as will be shown later in Chapters 5 and 6.

The problem, however, with requiring drivers to drive at a specific *THW* is that they need a reference to start with. This reference can be given as a rule of thumb, like 'keep the lead vehicle at two vehicle lengths from your own vehicle' or the 'two second rule' where lane markers can be used to count '21, 22' to verify the current separation (Verkeer en Waterstaat, 2000). Also, in Belgium, for example, specific Λ shaped symbols are painted on lanes at specific intervals that would then guarantee sufficient separation at highway speeds (100-120 km/h) if at all times two of these Λ shaped symbols are visible between the own vehicle and the lead vehicle.

In the driving simulator all of these solutions can be implemented, but they all have similar drawbacks. First of all, they are approximations of specific *THW* values. Second, they require some mental and visual effort of the drivers which distracts them from the following task. And third, for the 2 second rule and the Λ shaped symbols: they are visible all the time, allowing drivers to constantly monitor their performance visually, when the experiments are intended to investigate the benefit of using haptic feedback to support car-following. It was therefore decided to use an alternative indication of the required *THW*, which would set off the drivers very accurately at the specified *THW*, but which would not be visible during the actual experiment runs.

4.2.1 Time-headway indicator

To help drivers drive at any required *THW*, the capabilities of the powerful graphics cards[4] and software engines[5] available in the Human-Machine Laboratory were exploited to create a THW-indicator that was easy to understand by experiment subjects while yielding very accurate initial positioning results in terms of the required *THW*.

[4] NVIDIA GeForce 6800 GT.

[5] For the high performance rendering of the environment the open-source package called Maverik was used, developed by the Advanced Interface Group at the School of Computer Science, Manchester University, UK. This is an extension of the powerful OpenGL graphic library developed by Silicon Graphics.

Drivers are shown an infinitely thin (in longitudinal direction), partially transparent red rectangle of about the same width and height as the vehicle they are asked to follow. This rectangle, referred to as the THW-indicator, is programmed to stay ahead of the own vehicle at exactly the *THW* that is desired by the experimenter and required of the experiment subject to be maintained during the experiment run.

Because the rectangle is transparent, the lead vehicle can still be seen and tracked when that vehicle is driving further away than the required *THW*. The rectangle will move through and ahead of the lead vehicle if the lead vehicle is coming closer than the required *THW*. In case when the THW-indicator touches the rear bumper of the lead vehicle, the separation between the own vehicle and the lead vehicle is exactly the required *THW* for the concurrent experiment condition. These three states are illustrated in Figure 35 below.



a) Driving closer to the lead vehicle than required for the experimental condition.



b) Driving at the time-headway required for the experimental condition.



c) Driving further away from the lead vehicle than required for the experimental condition.

Figure 35: Examples of the use of the THW-indicator in the driving simulator.

Ten seconds after the experiment leader starts the experiment the THW-indicator disappears. All drivers are instructed to try and maintain the previously indicated *THW* as good as they possibly can. Meanwhile, a speed disturbance forcing function is superimposed onto the lead vehicle speed, forcing the drivers to actively accelerate or decelerate in order to maintain the required *THW*. Drivers are instructed to use the gas-pedal only. The THW-indicator reappears after a some interval of time (depending on the experiment protocol) to help drivers correct for any drift that might have driven them away too far from the lead vehicle. This process is repeated a number of times, depending on the experiment protocol.

The THW-indicator is shown from the start of each experiment. Both the experiment subject's car and the lead vehicle will start driving from zero velocity. The lead vehicle accelerates with a constant acceleration of 1.5 [m/s^2] to the speed that is specified in the

experiment protocol. Once the lead vehicle and the experiment subject are driving at stationary speeds at the *THW* indicated by the THW-indicator, that is, the THW-indicator is touching the rear bumper of the lead vehicle, the experiment leader would start the experiment.

4.2.2 Lead vehicle speed disturbance characteristics

A particularly important part of the experiment method is the use of a lead vehicle disturbance signal, constructed from a sum of sinusoids. This disturbance signal is the forcing function of the experiment and is constructed such, that it is possible to apply system identification techniques to identify the driver components of the car-following control-loop that was shown in Chapter 2 (this control loop had to be simplified, however, to allow identification of the entire loop – see Section 4.3.2 below). An example of a forcing function for the lead vehicle speed disturbance signal is given in Figure 36. The bandwidth of the lead vehicle speed disturbance was varied for some experiments, to investigate the effects on driver control behaviour. Most experiments however, used a bandwidth of 0.5 [Hz]. To avoid extreme changes in lead vehicle speed, cresting is applied to keep the amplitude of the sum of sinusoids signal within bounds (van der Ouderaa, Schoukens, and Renneboog, 1988).

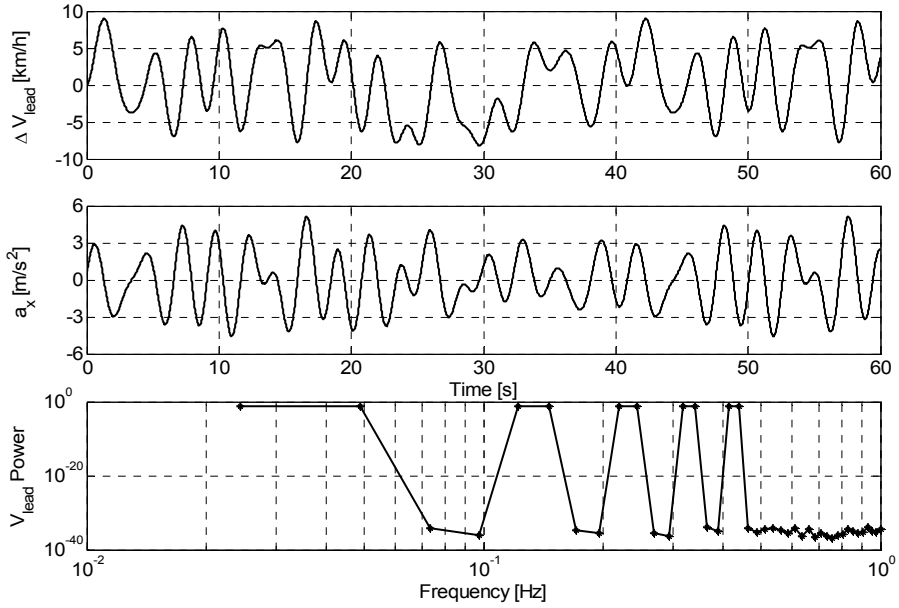


Figure 36: Lead vehicle speed disturbance example (top) with a bandwidth of 0.5 [Hz] (bottom). Cresting of the speed profile ensures that no speed and acceleration (middle) peaks are present which would require immediate braking. All speed changes can be dealt with by using the gas-pedal only.

One reason to use a sum of sinusoids forcing function is that the forcing function must appear to be a random signal to drivers. If the disturbance is predictable, drivers will be able to anticipate speed changes of the lead vehicle, which changes their control behaviour (Mulder, 1999; McRuer and Jex, 1967). Instead of a compensatory tracking task, they will then be able to execute a tracking task with preview information. Since the IDSS intends to support drivers

especially during unanticipated driving events, the goal of the experiments is to investigate compensatory control behaviour.

The use of sinusoidal forcing functions is also motivated from a practical point of view. Most importantly, sinusoidal signals are deterministic and periodic. This means that, if linear driver behaviour at the experimental conditions is assumed, the forcing functions will excite driver behaviour in a deterministic and reproducible way (Mulder, 1999). Furthermore, for a well-designed sinusoidal forcing function the Signal-to-Noise Ratio[6] (SNR) will be relatively high at the frequencies of the forcing function frequency set compared to driver induced control frequencies that are not part of the forcing function frequency set – the driver noise signal, or remnant (Mulder, 1999). The implication of this is that, if system identification techniques are used to identify driver control behaviour, identification can only be achieved at those frequencies at which the forcing function was applied. At other frequencies the SNR will be too low to determine accurate estimates of driver transfer.

4.3 Data acquisition and processing

To allow for any kind of analysis of the car-following task, a large set of variables needs to be collected. For the variables related to motion of the own vehicle and of the leading vehicle, it is important to use axis systems in which, position, speed, and acceleration will be defined. In Section 3.1 the body axis system $\{X_b, Y_b, Z_b\}$ of any car that is driving in the simulated environment was defined. This body axis system is fixed to the body of the car. The world axis system $\{X_e, Y_e, Z_e\}$ of the simulated environment, also defined in Section 3.1 is fixed to the driving scene, with the X_e axis pointing North, and the Y_e axis pointing East.

All experimental data are recorded on a dedicated computer at a sample rate of 50 Hz. For each experiment the required variables for data collection can be selected from the list of recordable variables as listed in Table 1. The data are written to a text file, which can be processed with MATLAB. The decomposition of a single experimental run into different events can be visualized as in Figure 37. Data are collected only during the relevant part of the experiment run, that is, during the time period where the lead vehicle speed is disturbed.

For the analysis of the data, first, all parts for which the THW-indicator has been visible are discarded in order not to bias the following performance results due to the greatly enhanced visual perception of the *THW* tracking error during those periods. Next, each section in between two consecutive appearances of the THW-indicator are labeled and saved as a separate section of recorded data. Each section is treated as a separate segment of data, that, from a statistical point of view, is taken as a measured instance of a single condition. Thus, if for a particular experimental condition, *n* sections are recorded in which the lead vehicle speed is disturbed, then *n* data sets will be available for statistical analysis for that particular experiment condition, and the particular driver, even though the driver would have driven all sections together in one run.

[6] The ratio between the forcing function and driver control input energy distributions in the frequency domain.

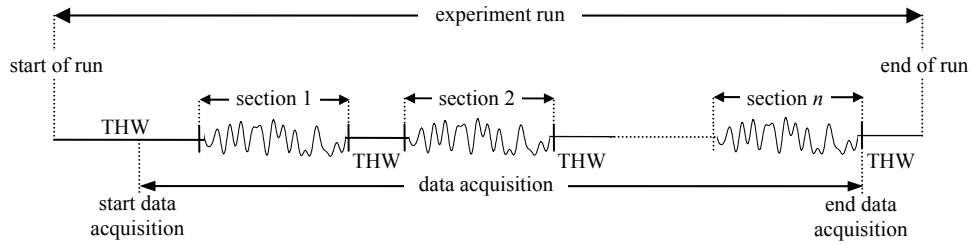


Figure 37: Visual representation of the construction of an experiment run. At the start of the run, the THW-indicator is visible. When the driver and the lead vehicle are following at stationary speeds, the data acquisition is started. Some 7-10 seconds later, the THW-indicator disappears and the lead vehicle speed (V_{lead}) is disturbed. After an experiment dependent time interval, the V_{lead} disturbance is stopped and the THW-indicator appears again for 10-15 seconds. Then, V_{lead} is disturbed again. This process is repeated *n* times, depending on the experiment protocol. The total experiment run thus yields *n* data sets for analysis.

Table 1: All variables available for data collection.

variable	dimension	Description
V	m/s	Speed of the own car
u	m/s	Speed component of the own car, along X_b
a_x	m/s^2	Acceleration component of the car, along X_b
v	m/s	Speed component of the own car, along Y_b
a_y	m/s^2	Acceleration component of the own car, along Y_b
RPM	-	Engine revolutions per minute
α_p	%	Gas-pedal depression: 0% – 100%
$\dot{\alpha}_p$	%/s	Gas-pedal depression rate: $\dot{\alpha}_p$ >0 depression; $\dot{\alpha}_p$ <0 release
F_p	N	Total endpoint force measured at gas-pedal pad
F_v	N	Feedback force applied to the gas-pedal
K_v	N/m	Feedback stiffness applied to the gas-pedal
β_p	%	Brake pedal depression: 0% – 100%
F_β	N	Total endpoint force measured at brake pedal pad
δ	º	Steering wheel angle: <0 left turn; >0 right turn
F_δ	N	Force applied to the steering wheel
V_{lead}	m/s	Speed of the leading vehicle
A_{lead}	m/s^2	Acceleration of the leading vehicle
X_{rel}	m	Distance between own car and leading car
V_{rel}	m/s	Speed difference between own car and leading car
THW	s	Time-headway
TTC	s	Time-to-contact

The disturbance signal for the lead vehicle speed is a sum of sinusoids, as was discussed in Section 4.2.2. Because the same sum of sinusoids is used for the lead vehicle speed disturbance in each section of an experiment run, and because these sum of sinusoids were assumed to excite repeatable behaviour, although they appeared to be random for the drivers, it is believed

that this segmentation of the experiment data strengthens the accuracy of the statistical analyses of the acquired data sets, since more comparable data sets become available.

4.3.1 Time domain data analysis

From the acquired datasets, a number of evaluation metrics are determined which are used in statistical analysis of the car-following task. Each separate section of data is processed to produce metrics on car-following performance, control effort, and physical load of the control task. These metrics are then evaluated with an analysis of variance (ANOVA) to test the hypotheses of the experiments described in Chapters 5 and 6 below.

Car-following performance

A particularly good starting point for the analysis of car-following performance is the THW-TTC^{-1} phase plane. *THW* ($=x_{rel}/v_{car}$)is a representation of the separation between the lead vehicle and the own vehicle. TTC^{-1} ($=-v_{rel}/x_{rel}$) represents the rate of change of that inter-vehicle separation. Together they yield typical spiralling plots (see for an example Figure 38) that have been found by many others (Goodrich and Boer, 2003; Piao and McDonald, 2003; Brackstone, Sultan, and McDonald, 2002). Some important characteristics of the THW-TTC^{-1} spiral plots follow. First, the spiral develops counter clockwise over time, since an increase in THW can only be achieved with a negative *TTC* ($V_{lead} > V_{car}$) and vice versa. Second, as Boer and Goodrich (2003) argue, drivers are likely to accelerate when $TTC^{-1} < 0$, dividing the THW-TTC^{-1} plane into driver accelerating ($TTC^{-1} > 0$) and driver decelerating ($TTC^{-1} < 0$) sections roughly at $TTC^{-1}=0$. They conclude that drivers use *THW* and *TTC* as "*speed independent variables for controlling the dynamics of...* [deceleration] *...as well as the set point for car following.*" Finally, the THW-TTC^{-1} phase plane nicely illustrates the interdependence of relative speed and the inter-vehicle distance. Rockwell (1974) noted that maintaining a low relative velocity (low TTC^{-1}) comes at the expense of more variance in the inter-vehicle distance (*THW*) and vice versa.

Because drivers are required to drive at a pre-determined *THW*, the mean *THW*, $\overline{THW}$, per section is determined as a measure of how well they are able to comply with this requirement. The standard deviation of the *THW*, σ_{THW}, and the TTC^{-1}, $\sigma_{TTC^{-1}}$, were calculated per section to determine the boundaries of the car-following spiral. This is what determines the car-following performance. The smaller and compacter the spiral (and thus the smaller σ_{THW} and $\sigma_{TTC^{-1}}$), the better the car-following performance.

Control effort

As much as *THW* and TTC^{-1} are inter-related in determining car-following performance, so is car-following performance inter-related to control effort. It is most likely in manual control tasks that improved performance comes at the expense of increased control effort of the driver. The longitudinal motion of the car is controlled by depressing and releasing the gas-pedal. The standard deviation σ_{α_p} or the variance $\sigma^2_{\alpha_p}$ of the gas-pedal depression α_p is therefore used as a measure of control effort. As will be shown in Section 4.3.2, a frequency

domain analysis yields a related measure of control effort, the cross-over frequency ω_c. Drivers increase their cross-over frequency to improve their performance. To increase the cross-over frequency, the control-effort needs to be increased.

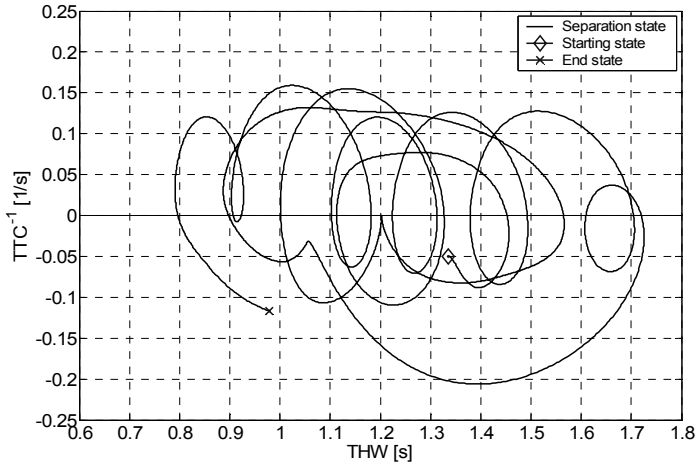


Figure 38: A typical car-following spiral, recorded during an experiment in the fixed-base driving simulator. The subject was asked to maintain a *THW* of 1 [s].

Another related measure that is used to determine control effort is the foot-off-gas-pedal time. The foot-off-gas-pedal time is the time, as a percentage of the total driving time per section, for which drivers did not have their foot on the gas-pedal. This is a representation of the percentage of driving time drivers were trying to get the highest deceleration possible of their car, without using the brakes. And, since the haptic gas-pedal feedback can only be perceived when the driver has her/his foot on the gas-pedal, it is also a measure of the percentage of time drivers were able to perceive the haptic gas-pedal feedback.

Physical load

Of course, when introducing additional forces on the gas-pedal, it is likely that drivers will have to deliver more muscle force to control the gas-pedal. As was stated in Chapter 2, it is expected that drivers will adopt a force task strategy to control the active gas-pedal, that is, they will try to keep the force on the gas-pedal constant. During car-following, the fluctuations of the pedal force due to the haptic feedback delivered by the driver support system will be relatively small compared to the static component of the pedal force, that is, the minimum force F_p drivers have to exert on the gas-pedal to depress the pedal to the desired α_p. So, it is mainly the static component of the pedal force determines the physical load. Abbink and van der Helm (2005) show that it is favourable energy wise, to have a static component of the pedal force that is at least as high as the force of the foot/leg combination of the driver at those pedal depressions $\alpha_{p,}$ that are used most during driving ($\alpha_p \approx 25\%$) when relaxed (30 – 60 N). For lower pedal forces, their experimental results show that drivers have to use both the shin muscles (Tibialis Anterior) and calf muscles (the Soleus, Gastrocnemicus Lateralis, and the Gastrocnemicus Medialis) to relieve the weight and stabilize the desired pedal position. In other words, drivers co-contract their leg muscles. This will lead to unnecessary fatigue. Higher mean

pedal force, due to haptic feedback, might therefore actually decrease rather than increase the physical load drivers experience during car-following.

The measures used to investigate the physical load are the mean endpoint contact force $\overline{F_p}$, and its standard deviation σ_{F_p}, exerted on the pedal by the driver. The mean endpoint contact force is used as an estimate of the average static component of the pedal force, and thus the biggest contributor to physical load of the driver. The standard deviation of the mean pedal force is used to test the hypothesis that drivers will adopt a force task strategy when driving with a haptic feedback system during car-following.

4.3.2 Frequency domain data analysis[7]

The car-following task is defined as a compensatory task in which tracking errors in relative speed and distance with a leading vehicle need to be minimized. Different drivers may adopt different strategies. However, maintaining a low relative velocity comes at the expense of more variance in the separation distance and vice versa (Rockwell, 1974). To reflect this in the car-following model presented in Chapter 2, the total driver frequency response $H_d(\omega)$ to relative velocity and inter-vehicle distance has been separated and represented in a serial multi-loop structure by $H_d^{in}(\omega)$ and $H_d^{out}(\omega)$ respectively, as depicted in Figure 39 (ω represents the frequency vector with the frequencies of the forcing function *D(ω)*). $H_c^{in}(\omega)$ represents the frequency response function of the car-dynamics that relates driver gas pedal input *U(ω)* to the speed of the vehicle *Y(ω)*. $H_c^{out}(\omega)$ is an integrator to yield the position of the vehicle, *X(ω)*.

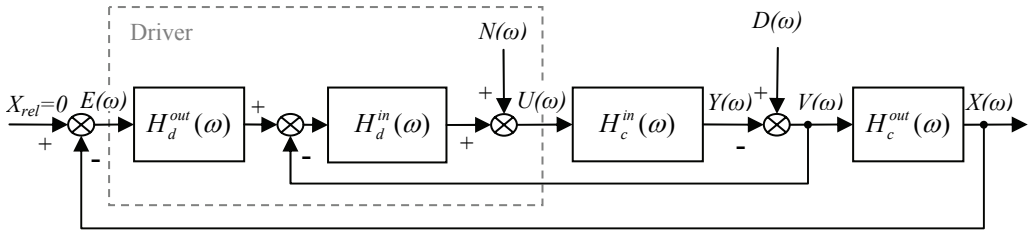


Figure 39: Quasi-linear, serial multi-loop car-following model structured as in McRuer and Krendel (1974). *D(ω)* is the lead vehicle speed, *N(ω)* is the driver remnant, representing all non-linearities in driver behaviour. *U(ω)* is the driver gas-pedal input to the car, *Y(ω)* is the resulting speed of the own car. *V(ω)* is the relative speed between the lead vehicle and the own vehicle, *X(ω)* is the vehicle separation distance. *E(ω)* represents the separation error drivers are minimizing during car-following. $H_d^{out}(\omega)$ and $H_d^{in}(\omega)$ outer- and inner-loop driver frequency response functions (FRF) respectively. $H_c^{in}(\omega)$ and $H_c^{out}(\omega)$ are the vehicle-dynamics FRF's for the inner- and outer-loops respectively.

For the identification of each loop in a multi-loop system, it is necessary to introduce a known forcing function with well-specified frequency domain properties in each loop (van Lunteren, 1979). In this model structure, however, inserting a forcing function in both the inner-loop and outer-loop will not lead to distinguishable disturbances to the driver, hence no

[7] This section has been published as part of a conference paper titled "Identification of Driver Car-Following Behaviour" (Mulder *et al.,* 2005a).

different control behaviour due to the forcing functions can be identified. It is therefore only possible to use a single forcing function, *D(ω)*, which represents the lead vehicle speed, with frequencies specified only at ω. Despite this limitation, can both the inner-loop and outer-loop still be identified?

Non-parametric identification

Identification of the inner-loop as well as the outer-loop is still possible, but not directly. Because only one forcing function can be used, the model structure that can be identified directly is shown in Figure 40. This is essentially the same model as Figure 39, with the contribution of $H_d^{out}(\omega)$, $H_d^{in}(\omega)$, and $H_c^{out}(\omega)$ lumped together in one transfer function $H_d^l(\omega)$. It is $H_d^l(\omega)$ that can be identified directly with frequency domain identification techniques.

When the signals *V(ω)* – the relative velocity – and *U(ω)* – the gas-pedal position – are measured during an experiment, and no correlation between driver remnant *N(ω)* and forcing function *D(ω)* is assumed, $H_d^l(\omega)$ can be estimated at frequencies ω using spectral densities obtained with the Fast Fourier Transform (FFT), see equation (4.2). The squared coherence function $\Gamma^2(\omega)$ (equation (4.3)) is an indication of the linearity of the identified system in responding to the forcing function *D(ω)* at the frequencies ω for which the transfer function is identified (Schouten, 2004; de Vlugt, 2004). $\Gamma^2(\omega)$ has a value of one at those frequencies for which the input-output relationship of the identified transfer function is perfectly linear (so there is no remnant nor noise) and zero when there is no linear relationship at all.

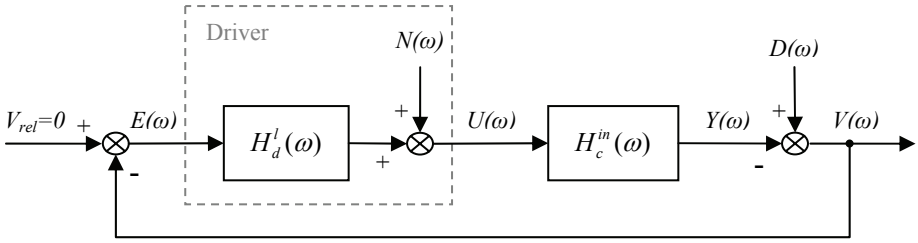


Figure 40: Modified driver model suitable for frequency domain identification with only one forcing function, *D(ω)*.

$$\hat{H}_d^l(\omega) = -\frac{\hat{S}_{d,u}(\omega)}{\hat{S}_{d,v}(\omega)} \tag{4.2}$$

$$\hat{\Gamma}^2(\omega) = \frac{\left|\hat{S}_{d,u}(\omega)\right|^2}{\hat{S}_{d,d}(\omega)\hat{S}_{u,u}(\omega)} \tag{4.3}$$

If *Y(ω)* is measured too, or calculated from *V(ω)* and *D(ω)*, then $H_c^{in}(\omega)$ can be estimated as well, as a verification of the linearization of the non-linear car dynamics:

$$\hat{H}_c^{in}(\omega) = \frac{\hat{S}_{d,y}(\omega)}{\hat{S}_{d,u}(\omega)} \tag{4.4}$$

With the estimates of the model's frequency response functions known, the next step is to identify the model parameters by fitting a parametric model on the FRF estimates.

Parametric identification

The relationship between $H_d^l(\omega)$ from the model in Figure 40 and $H_d^{in}(\omega)$ and $H_d^{out}(\omega)$ from the model in Figure 39 is given by equation (4.5) which follows from writing out the lumped model $H_d^l(\omega)$ as a system with the relations between *V(ω)* and *U(ω)* expressed as shown in Figure 39.

$$H_d^l(\omega) = H_d^{in}\left(1 + H_c^{out}(\omega)H_d^{out}(\omega)\right) \tag{4.5}$$

With help of the known properties of pilot/driver control behaviour, formulated in the early 1970s by McRuer and Krendel (1974), well known as the cross-over model, assumptions can be made of the structure of $H_d^{in}(\omega)$ and $H_d^{out}(\omega)$:

$$H_d^{out}(\omega) = K_d^{out} \tag{4.6}$$

$$H_d^{in}(\omega) = K_d^{in}\frac{(1+j\omega\tau_L)}{(1+j\omega\tau_I)}e^{-j\omega\tau_e} \tag{4.7}$$

$H_c^{in}(\omega)$ and $H_c^{out}(\omega)$ are the linear representations of the known dynamics of the own vehicle:

$$H_c^{out}(\omega) = \frac{1}{j\omega} \tag{4.8}$$

$$H_c^{in}(\omega) = \frac{K_c^{in}}{(1+j\omega\tau_c)} \tag{4.9}$$

Substitution of equations (4.6) to (4.9) into equation (4.5) yields a parameterised expression of $H_d^l(\omega)$.

$$H_d^l(\omega) = K_d^{out}K_d^{in}\frac{(1+j\omega\tau_L)}{(1+j\omega\tau_I)}\frac{(1+j\omega\frac{1}{K_d^{out}})}{j\omega}e^{-j\omega\tau_e} \tag{4.10}$$

Estimations of the parameter vector $\underline{\theta} = \{K_d^{out}, K_d^{in}, \tau_I, \tau_L, \tau_e\}$ are be obtained by fitting equation (4.10) through the estimated FRF determined with equation (4.2). Finding the best fit is done by minimizing a cost function $L(\omega;\underline{\theta})$ (see de Vlugt, 2004). The cost function makes use of the squared coherence, so that the estimates at each frequency ω_k (k indexes the frequency vector ω), which are less accurate (lower signal-to-noise ratio), are weighed less.

$$L(\omega;\underline{\theta}) = \sum_k \hat{\Gamma}^2(\omega_k)\left|\ln \hat{H}_d^l(\omega_k) - \ln H_d^l(\omega_k;\underline{\theta})\right|^2 \tag{4.11}$$

Time-domain verification

When the parameters of the driver model have been identified in the frequency domain, it is possible to simulate the car-following situation with the developed model in the time domain. To verify the validity of the identified model, the model outputs $\hat{y}(t)$ (where t denotes time) are compared with measured experimental outputs *y(t)* under the same conditions. The variance accounted for (VAF) is used to quantify the accuracy of the model in producing output that

represents (experimentally) measured output (Schouten, 2004; de Vlugt, 2004; van der Helm *et al.*, 2002).

$$VAF = 1 - \frac{\sum_{k=1}^{n} \left| y(t_k) - \hat{y}(t_k) \right|^2}{\sum_{k=1}^{n} \left| y(t_k) \right|^2} \tag{4.12}$$

The time domain measurements were done in equally spaced, finite intervals in time. The total time vector t is indexed by k, such that t_k represents the k^{th} time interval of a total of n intervals in equation (4.12). A value of one for the VAF represents exact reproduction of measured driver output to a forcing function; values lower than one down to zero represent decreasing accuracy in reproducing measured driver output with the used model structure. Because in reality, the remnant $n(t) \neq 0$, the VAF's that are determined from the identified model of Figure 39 will always be smaller than one.

Cross-over frequency and phase-margin

With the help of the identification techniques described above, two important parameters concerning the controllability of the car-following task become available: the cross-over frequency and phase-margin. The cross-over ω_c frequency is a measure of the bandwidth up to which drivers are controlling the closed loop system shown in Figure 39. The phase-margin φ_m is a measure of the stability of the closed-loop system.

The cross-over frequency and phase-margin can be determined for both the inner- as well as the outer-loop of the car-following model of Figure 39 yielding control effort and stability measures with respect to regulation of relative velocity (ω_c^{in} and φ_m^{in}) and relative distance respectively (ω_c^{out} and φ_m^{out}). With help of the cross-over frequencies and the phase-margins more insight is expected to be gained as to *why* driver behaviour changes if changes are found with the statistical time domain analyses.

Chapter 5

Car-following Experiments with Maximal Visual Attention

Implementation of new in-vehicle support systems requires a thorough investigation of the benefits and the effects on driver behaviour the system induces when it is in use. The proposed haptic driver support system is designed to be active during car-following situations. That is, when there is another vehicle in front of the own vehicle within range of the haptic feedback algorithm's operational boundaries. Within these boundaries, the haptic feedback is generated continuously, when the driver is fully concentrated on her/his driving task, or when the driver is distracted and is not paying full attention (visually) to the driving task. This continuous activation of the haptic feedback system, therefore, demands investigation during both non-distracted driving – maximal car-following – and during (visually) distracted driving – sub-maximal car-following.

The experiments presented in this chapter are designed to investigate the influence of the three support algorithms (presented in Chapter 3, Section 3.3) on driver behaviour during non-distracted driving. Second, the first experiment, presented in Section 5.1, is designed to show the differences between using force feedback and stiffness feedback. Third, the experiments in Sections 5.2 and 5.3 are designed to investigate the usefulness of the THW-stiffness and TTC-stiffness feedback algorithms respectively under different car-following conditions.

Although each experiment presented in this Chapter has its particular sub-hypotheses, they were all designed with two major hypotheses in mind:

1. The use of haptic gas pedal feedback during car-following will lead to drivers adopting a force task in using the gas pedal, that is, they will try to maintain the force on the gas pedal as constant as possible in order to try to maintain a constant inter-vehicle separation.

2. The use of haptic gas pedal feedback during car-following will lead to at least similar and at best improved car-following performance compared to car-following using a normal gas pedal in similar car-following conditions.

5.1 Comparison between force feedback and stiffness feedback

Two possible options for providing haptic feedback were discussed in Section 2.3 – force feedback or stiffness feedback. Force feedback imposes a force $F_v(t)$ directly on top of the inherent characteristics of the gas pedal, translating these inherent characteristics along the force axis. In other words, the dynamics of the gas pedal, that is, the force – position relationship of the gas pedal, do not change. Stiffness feedback, however, changes the gas pedal characteristics, by introducing an additional stiffness $K_v(t)$ on top of the inherent gas pedal characteristics. The result is a change in the force – position relationship of the gas pedal.

From the discussion that followed in Section 2.3.3, it was argued that the addition of haptic feedback to the gas pedal would lead drivers to adopt a force-task strategy in using the haptic gas pedal. From literature (Abbink, van der Helm and Boer, 2004) it is known that when humans adopt a force-task strategy in control, they will try to maintain a very high admittance, that is, they will try to yield to forces that are disturbing the equilibrium they are trying to maintain. Thus, for drivers to adopt a force-task strategy with the haptic gas pedal, they are expected to yield as much as possible to the feedback forces, such that the experienced gas pedal force remains as constant as possible. In practical control actions this means that when the force on the pedal increases, drivers are expected to release the gas pedal to lower the force they experience and when the force on the pedal decreases again, drivers are expected to depress the gas pedal again to increase the force they experience, back to the equilibrium level.

If the haptic feedback algorithm is providing the proper kind of feedback, this kind of force-task behaviour should, in theory, occur. This experiment and the subsequent two experiments were set-up to investigate whether this hypothesis can be validated.

In the particular experiment described in this section, the driver responses and control behaviour when using force feedback or THW-stiffness feedback during car-following are investigated. A base-line condition, without haptic feedback is tested as well, for comparison.

5.1.1 Method

Subjects

Twenty-one subjects participated in this experiment: 2 females and 19 males. Their average age was 26.3 years, the oldest subject being 30 years old, the youngest 24 years. All subjects had valid driving licenses with an average driving experience of 7.1±2.2 years, driving approximately 3 times a week.

Task instruction

Subjects were instructed to maintain a prescribed inter-vehicle separation as good as they possibly could. This separation was visually indicated by the THW-indicator (see Section 4.2.1 for a description of the THW-indicator). The THW-indicator was not visible when the lead

vehicle speed was disturbed. Furthermore, the subjects were instructed to make as much use of the gas pedal as possible to control their separation with the lead vehicle. They were told to use the brake only in the extreme case in which collision with the lead vehicle would be unavoidable without using the brakes.

Apparatus

The experiment was carried out in the fixed-base driving simulator described in Section 4.1. None of the drivers had previous experience driving in this simulator.

Independent variables

Only one independent variable was varied in the experiment – between subjects, that is, each subject was given just one of the following three conditions to drive:

1. The haptic feedback system, *S*: *None*, *force feedback*, and *THW-stiffness feedback*.

Experiment design

A between-subjects design was used, in which 6 subjects (1 female; 5 males) were given the base-line condition without the haptic feedback system (*S*=*none*); 8 subjects (all male) were given the force feedback (*S*=*force feedback*); and 7 subjects (1 female; 6 males) were given the THW-stiffness feedback (*S*=*THW-stiffness feedback*).

All subjects were given a 5 minute training run to familiarise themselves with driving in the driving simulator and the driving task. After the training run, drivers were given 20 subsequent intervals of one minute of car-following time without the THW-indicator. Each interval was separated by 10 seconds of visibility of the THW-indicator. Thus, 20 sections of 1 minute of driving time were recorded for each subject. Total driving time per subject was approximately 30 minutes.

Drivers were directed with the THW-indicator to drive at a desired time-headway THW_d=1.5 [s]. The lead vehicle speed disturbance was constructed as described in Section 4.2.2. The bandwidth of the frequency spectrum that was used to generate the sum of sinusoids signal, f_d=0.5 [Hz]. The lead vehicle speed disturbance amplitude A_d=10 [km/h].

Dependent measures

In order to determine the car-following performance, *THW* and TTC^{-1} were measured, from which the mean and standard deviation of *THW*, $\overline{THW}$, and σ_{THW} respectively, and the standard deviation of TTC^{-1}, $\sigma_{TTC^{-1}}$, are calculated. For the control effort, the gas pedal depression angle, α_p, is measured, from which the mean, $\overline{\alpha}_p$, and standard deviation, σ_{α_p}, are calculated. To determine the physical load, the force F_p, the driver exerts on the gas pedal is measured, from which the mean, $\overline{F_p}$, and standard deviation, σ_{F_p}, are calculated. The calculated variables represent the experiment results in the time-domain. No frequency-domain analysis was done.

5.1.2 Hypotheses

The main hypothesis for this experiment follows from Chapter 2 where the application of force feedback and stiffness feedback is discussed. Drivers are expected to adopt a force task strategy to benefit from the provided haptic feedback, and for this experiment it is hypothesised that stiffness feedback will show to support the adoption of this strategy better than force feedback. This is expected to be evident from the standard deviation and distributions of the pedal forces. If drivers adopt a force-task, the standard deviation will be relatively small and the distribution will be concentrated around the mean much more than when no force-task is adopted. Both haptic feedback systems are expected to yield similar or better car-following performance compared to the base-line condition without haptic feedback. Also, both haptic feedback conditions are expected to decrease the amount of control effort displayed by drivers. Due to the presentation of extra forces/stiffness on the gas pedal, the physical load is expected to be increased by the haptic feedback systems. The stiffness feedback system is, however, expected to increase the physical load less than the force feedback system. Summarized, the hypotheses are formulated as follows:

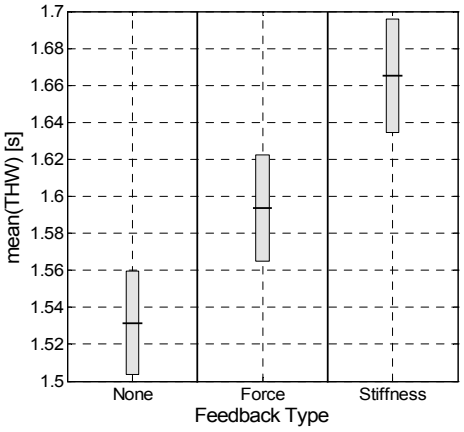
1. Both feedback systems yield similar or better car-following performance than driving without haptic feedback.
2. Both feedback systems will decrease control effort compared to driving without haptic feedback.
3. Haptic feedback will increase the physical load of the driver.
4. The stiffness feedback algorithm will increase the physical load less than the force feedback algorithm.
5. The stiffness feedback algorithm will yield a more force-task like strategy than the force feedback algorithm.

5.1.3 Results

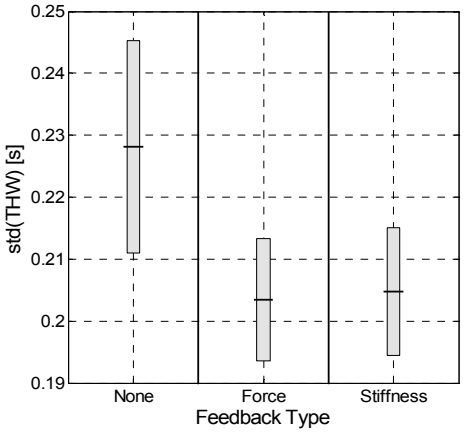
Car-following performance

Drivers were asked to drive at a desired THW_d=1.5 [s]. From Figure 41a it can be seen that drivers that used the haptic feedback system increased their $\overline{THW}$ compared to the base-line condition without haptic feedback. These increases are significant for each condition ($F_{2,397}$=19.856; p<0.01). The σ_{THW} is significantly lower, however, for the haptic feedback systems compared to the base-line condition ($F_{2,397}$=4.647; p<0.01), as can be seen in Figure 41b. This is remarkable, since visual perception of changes in separation distance decreases with increasing separation (Evans, 1991). It appears that the addition of haptic feedback has increased drivers' sensitivity to changes in *THW*, allowing them to maintain better *THW* control even at larger *THW*'s compared with no haptic feedback. However, the decrease in σ_{THW} is very small – only 0.03 [s]. No significant difference in σ_{THW} is found between the haptic feedback systems. The σ_{TTC}^{-1}, is significantly different for each condition ($F_{2,397}$=38.785; p<0.01), with the base-line condition having the highest σ_{TTC}^{-1} and the stiffness condition the lowest σ_{TTC}^{-1}, see Figure 41c. This effect seems to be inversely proportional to the increased *THW* at which drivers

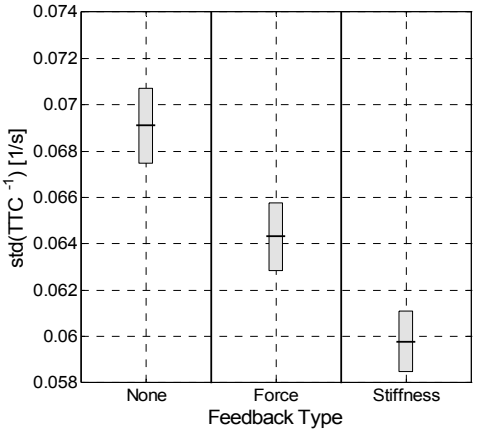
were driving due to the presence of haptic gas-pedal feedback. The further away the lead vehicle, that is, the higher the *THW*, the smaller the effects of *TTC*.



a) mean *THW*



b) standard deviation of *THW*



c) standard deviation of TTC^{-1}

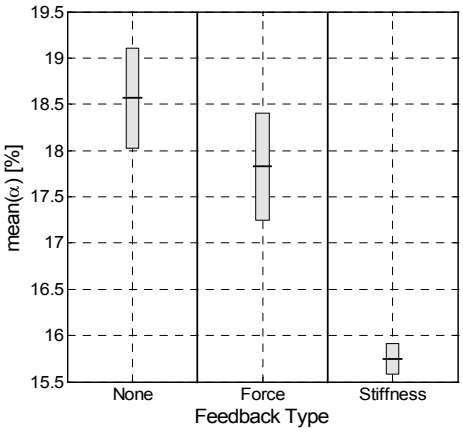
Figure 41: The means (horizontal lines) and 95% confidence intervals (gray bars) of the car-following performance indicators.

Control effort

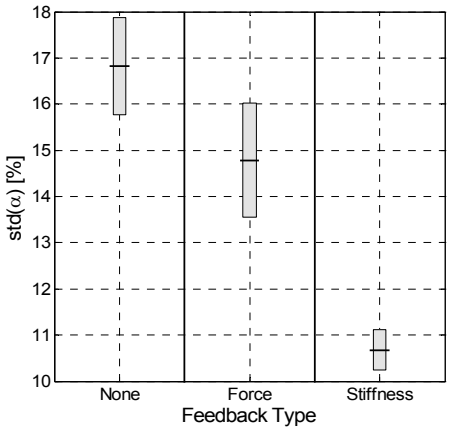
The effort displayed by drivers to deliver the discussed car-following performance is mainly measured by the standard deviation of the gas pedal depression α_p. From Figure 42b it can be seen that the use of haptic gas pedal feedback reduces σ_{α_p} significantly ($F_{2,397}$=40.721; p<0.01). Especially the stiffness feedback condition yields a great reduction in σ_{α_p} – almost half that of the condition without haptic feedback, and almost a third less than the force feedback condition. Furthermore, $\overline{\alpha_p}$ is also significantly ($F_{2,307}$=39.359; p<0.01) lower for the haptic feedback conditions, with the stiffness again having the lowest value (see Figure 42a). Even though $\overline{\alpha_p}$ is the lowest for the stiffness feedback condition, due to the small standard

deviation this also yields the least amount of time for which the gas pedal was completely released, t_r (see Figure 42c). Compared to the base-line condition without haptic feedback, both the force feedback and stiffness feedback condition yield significantly ($F_{2,397}$=48.477; p<0.01) lower times t_r.

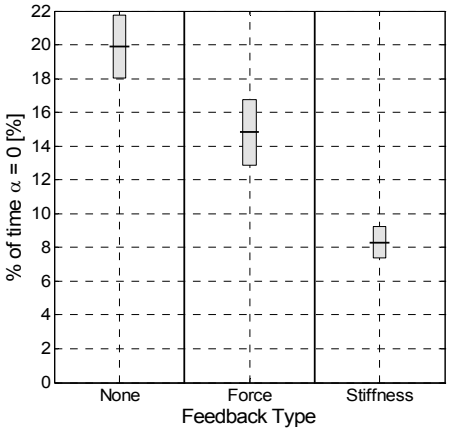
It seems from these data that haptic feedback not only reduces the control effort to maintain car-following performance, but that it also leads to less time during which the pedal is not depressed. This means that drivers keep their foot on the gas pedal longer periods of time, during car-following with haptic feedback, thus increasing the time during which they can benefit from the information that is provided haptically.



a) mean gas pedal depression α_p



b) standard deviation of the gas pedal depression α_p



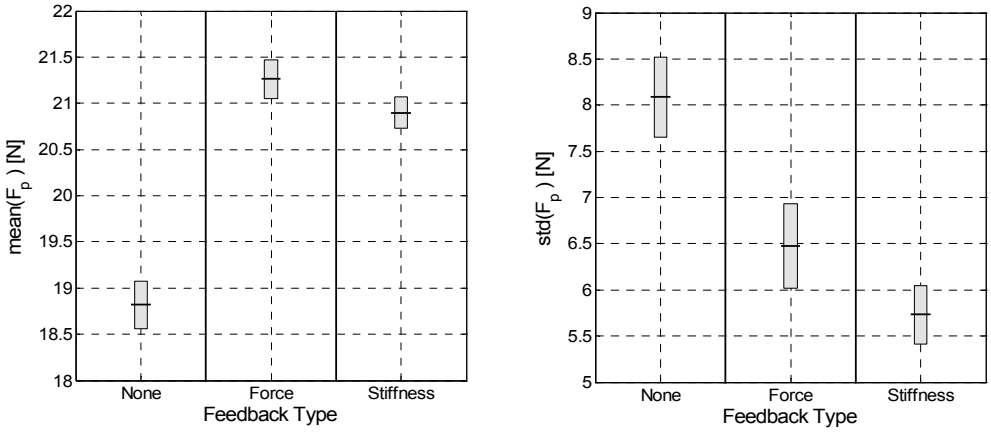
c) % of time the gas pedal was not depressed

Figure 42: The means (horizontal lines) and 95% confidence intervals (gray bars) of the car-following control effort indicators.

Physical load

As could be expected, $\overline{F_p}$ increased significantly ($F_{2,397}$=145.134; p<0.01) when using haptic feedback. The force feedback condition yielded significantly higher pedal forces than the

stiffness feedback condition, although the difference is only approximately 0.5 [N] (see Figure 43a). The σ_{F_p} of the haptic feedback conditions, also as expected, are significantly ($F_{2,397}$=184.861; p<0.01) lower compared to the base-line condition without haptic feedback, with the stiffness condition having the lowest σ_{F_p}. This seems to confirm the hypothesis that the use of haptic gas pedal feedback during car-following induces drivers to adopt a force-task in using the gas pedal.



a) mean gas pedal force, F_p, exerted by drivers

b) standard deviation of gas pedal force, F_p

Figure 43: Means (horizontal lines) and 95% confidence intervals (gray bars) of the car-following physical load indicators.

5.1.4 Discussion of the results

From Table 2 it is clear that the addition of haptic feedback had significant effects on all dependent measures, for the conditions tested. Despite the fact that drivers drove significantly further from the THW_d=1.5 [s] they were asked to drive when using haptic feedback, the σ_{THW} and $\sigma_{TTC^{-1}}$ for both haptic feedback conditions are significantly lower. The differences in $\sigma_{TTC^{-1}}$ are very small, though, and therefore are more likely due to the increase in $\overline{THW}$ only. The differences in σ_{THW}, however, are more likely to be caused by the presence of haptic feedback on the gas pedal, since the further away the lead vehicle, the less visible changes in lead vehicle speed, and therefore the higher the σ_{THW}. With the haptic feedback, the perception of changes in THW seems to have improved, which resulted in slightly more accurate tracking of the lead vehicle – even though $\overline{THW}$ was higher than the base-line condition without haptic feedback.

Table 2: Summary of the results of the One-way-ANOVA statistical analysis of the dependent measures, with significance level α=0.05. In the table, •••, ••, and • denote a significance of $p\leq0.01$, $0.01<p\leq0.05$, and $0.05\leq p<0.1$ respectively and '-' denotes no significance. S is the support system state.

	Following performance			Control effort			Physical load	
	$\overline{THW}$	σ_{THW}	$\sigma_{TTC^{-1}}$	$\overline{\alpha_p}$	σ_{α_p}	t_r	$\overline{F_p}$	σ_{F_p}
Main effects								
S	•••	•••	•••	•••	•••	•••	•••	•••

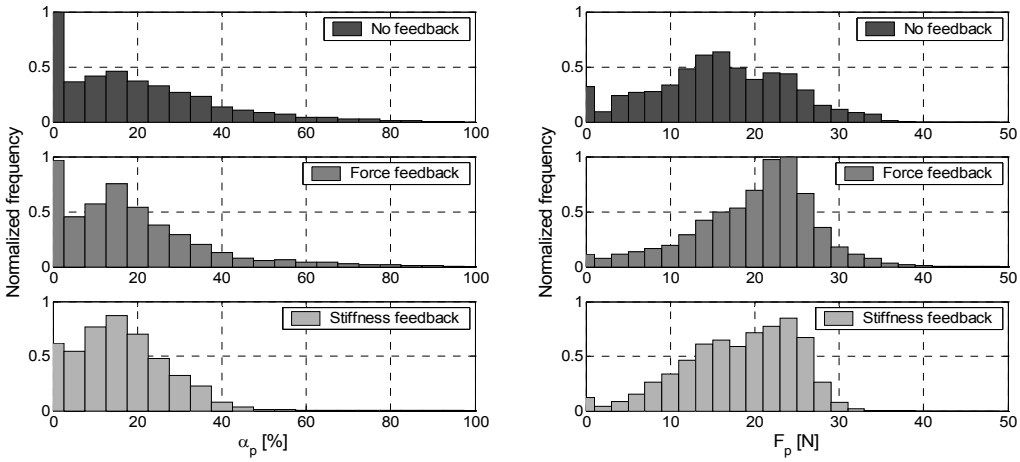
More dramatic effects are found for the control effort. With haptic feedback, drivers displayed much less control activity than without haptic feedback. Especially the stiffness feedback condition yielded very low control activity compared to the other two conditions – as much as approximately one third less than the base-line condition without haptic feedback. Thus, drivers seem to be controlling their vehicle in a much more relaxed manner, without sacrificing performance. Added benefit is that the percentage of time t_r drivers have their foot off the gas pedal, and therefore cannot receive any haptic information, reduces almost as much as the control activity.

The significant reductions in control activity for the haptic feedback systems show that most is gained in increasing driver comfort during car-following control. It is believed, however, that these results cannot entirely be ascribed to the presence of haptic gas pedal feedback. Because of motion cues, in a moving-base simulator, or a real car, the difference in control effort for the condition without haptic feedback and the conditions with haptic feedback is expected to be smaller. The absence of motion in the driving simulator, and hence the absence of accelerations, has likely played a role in this reduction in control activity too. Due to the sluggish dynamics of the simulated vehicle the subjects were driving, the visual cues due to big, rapid changes in pedal position – manifested as high $\overline{\alpha}_p$ and high σ_{α_p} – are hardly different from the visual cues due to smaller, less fast changes in pedal position. Rockwell and Snider (as mentioned in Rockwell, 1972) indicate that humans can sense ±0.01 [g] of vehicle acceleration. This is well above the accelerations drivers would have experienced had the simulator been able to provide motion. Because the sluggish vehicle dynamics filtered out most effects of the high frequency inputs from the gas pedal, drivers would, with motion cues, have been able to notice the ineffectiveness of their high frequency control actions better.

Nevertheless, when looking at the distribution of gas pedal positions and the resulting gas pedal forces for the three conditions of *S*, it can be seen that drivers have been concentrating their control actions within a smaller area (see Figure 44a). Furthermore, despite the higher mean pedal forces that were experienced by drivers when driving with the haptic feedback systems, the distribution of the pedal forces shows that the pedal force is also more concentrated around the mean pedal force, especially so for the force feedback (see Figure 44b).

5.1.5 Conclusions

1. The results of the experiment show that there is a minimal improvement in car-following performance for the haptic feedback conditions, at the required THW_d=1.5 [s].
2. Control effort decreased significantly for both haptic feedback systems compared to using no haptic feedback.
3. The physical load of the drivers was, as expected, significantly increased by the application of haptic feedback.
4. It is believed that the stiffness feedback algorithm is more advantageous in promoting a force-task strategy and hence easier to use for drivers.



a) distribution of the gas pedal positions. b) distribution of the gas pedal forces.

Figure 44: Distributions of the measured gas pedal depressions (a) and the forces drivers exerted on the gas pedal (b), for each condition, all drivers, and all recorded driving time.

5.2 Supported car-following at different time-headways

Unsupported car-following behaviour depends greatly on the visual perception of changes in lead vehicle speed and position. In Chapter 3, Section 3.1.2, it was argued that drivers use the time-headway (*THW*) and time-to-contact (*TTC*) to make judgements of their so-called safe-field-of-travel (Gibson and Crooks, 1938). It was shown how car-following behaviour displays typical spiralling graphs in the THW-TTC^{-1} phase-plane, illustrating the inter-dependence of *THW* and *TTC*. As Rockwell mentioned in 1972, and Ceder later in 1979, car-following is a balancing act around an approximate equilibrium spacing by minimising the deviations in *THW* at the cost of more variations in *TTC* or vice versa.

Since the accuracy of visual perception of changes in *THW* and *TTC* increases when *THW* decreases, there is a need to investigate how the presence of haptic gas pedal feedback affects driver car-following behaviour for different *THW*'s. Because the haptic feedback algorithms have been designed to increase the perceptibility of the feedback forces with decreasing *THW*, possible mismatches in visual and haptic perception might influence driver behaviour more for low values of *THW* than for high values of *THW*. An experiment was, therefore, conducted to investigate the effects of the presence of haptic feedback at different *THW*'s, ranging from dangerously close (*THW*=0.5 [s]) to the advised 2-second-rule separation (*THW*=2.0 [s]).

5.2.1 Method

Subjects

In this experiment, ten subjects participated. All subjects were male. Average age of the subjects was 25±2.1 years old. They had an average driving experience of 6.5±2.4 years, with an average driving frequency of 4.1±2.9 times per week. None of the drivers were paid for their participation. Nine participants had driven in the driving simulator before.

Task instruction

Drivers were instructed to try and maintain the *THW* as indicated by the THW-indicator (see Section 4.2.1) as good as they possibly could, whenever the THW-indicator had disappeared and the lead vehicle speed was disturbed. They were explicitly instructed to maintain separation as much as possible with the gas pedal only. In the case of impending collision, drivers were permitted to use the brake pedal.

Apparatus

The experiment was conducted in the fixed-base driving simulator, described in detail in Section 4.1.

Independent variables

Two independent variables were varied during the experiment, to yield the fully randomized experiment design. The driver support system algorithm that was used was the THW-stiffness feedback algorithm. The two independent variables were:

1. The *THW* at which drivers were asked to drive, *T*: 0.5, 1.0, 1.5, and 2.0 [s].
2. The driver support system state, *S*: No haptic feedback (*off*), THW-stiffness feedback (*on*).

Experiment design

Both independent variables were randomly combined to yield a full-factorial, within-subjects experiment design. Thus, in total, 8 conditions were tested. Drivers were given a car-following task for each *THW* for 8 minutes. In between each minute the THW-indicator was visible for 10-15 seconds. During the entire run of 8 minutes, the requested *THW* did not change. The support system state *S*, however, varied randomly from minute to minute. This yielded 4 minutes per *THW* of driving with *S*=*on* and 4 minutes of driving with *S*=*off* for each run. Every run was randomly repeated once, yielding a total of 8 minutes of data for each of the 8 conditions.

The lead vehicle speed was disturbed with a forcing function constructed from a sum of sinusoids with bandwidth f_d=0.3 [Hz] and amplitude A_d=8 [km/h]. This disturbance manifested itself to the drivers as a random disturbance of the lead vehicle speed.

Dependent measures

THW and TTC^{-1} were measured to determine the car-following performance indicators – the mean and standard deviation of *THW*, $\overline{THW}$ and σ_{THW} respectively, and the standard deviation of TTC^{-1}, $\sigma_{TTC^{-1}}$. For the control effort, the gas pedal depression angle, α_p, is measured, from which the mean, $\overline{\alpha}_p$, and standard deviation, σ_{α_p}, are calculated. To determine the physical load, the force F_p, the driver exerts on the gas pedal is measured, from which the mean, $\overline{F_p}$, and standard deviation, σ_{F_p}, are calculated.

5.2.2 Hypotheses

The hypotheses for this experiment focus on the effects of *THW* on car-following behaviour, especially when the THW-stiffness feedback support is used. It is expected that: When using the driver support system (*S=on*), car-following performance will improve for all *THW*'s.

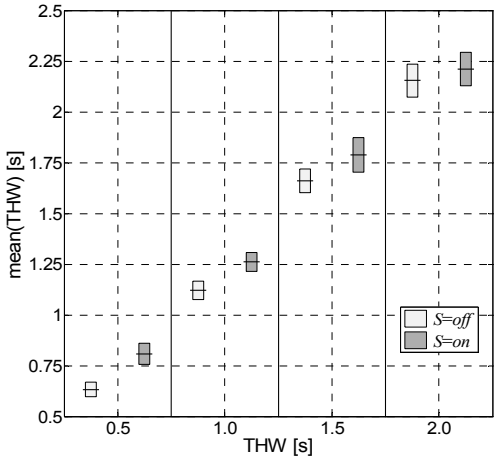
1. Control effort will decrease when *S=on* for all *THW*'s.
2. The physical load will increase when using the driver support system (*S=on*), and when *THW* decreases, due to the design of the THW-stiffness algorithm.
3. Due to the presence of haptic feedback (*S=on*), drivers will adopt a force-task strategy in using the gas pedal.

5.2.3 Results

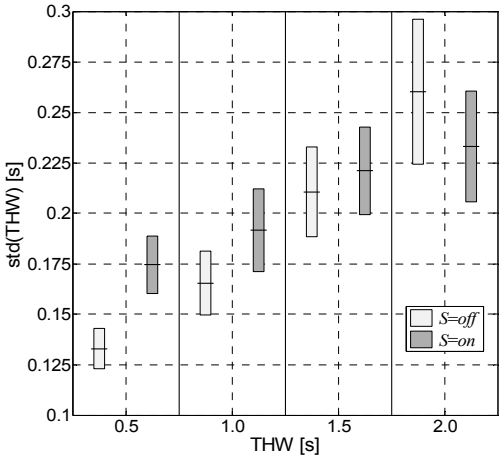
Car-following performance

Car following performance was positively influenced by the driver support system (DSS) in that drivers drove at significantly ($F_{1,9}$=29.400; p<0.01) higher *THW*'s when the haptic feedback was on (see Figure 45a). This effect decreased with increasing *THW*'s. A reverse effect is shown for σ_{THW}. The DSS yielded marginally significant ($F_{1,9}$=4.618; 0.05<p≤0.1) different σ_{THW} compared to driving without DSS. The σ_{THW} increased significantly ($F_{3,27}$=10.891; p<0.01) with increased *THW*. However, for *THW*=0.5 [s] σ_{THW} is higher when driving with DSS, but this difference decreases with increasing *THW* and even reverses for *THW*=2.0 [s], leading to a significant ($F_{3,29}$=7.847; p<0.01) two-way interaction between *S* and *T* (see Figure 45b).

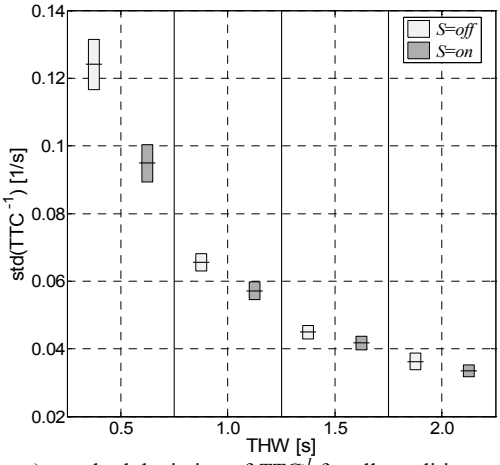
As for $\sigma_{TTC^{-1}}$, the DSS yielded significant ($F_{1,9}$=32.869; p<0.01) lower values for all *T*. The $\sigma_{TTC^{-1}}$ decreased significantly ($F_{3,27}$=162.072; p<0.01) for both conditions of *S* with increasing *THW*. The difference in $\sigma_{TTC^{-1}}$ for each *S* decreased with increasing *THW*, yielding a significant ($F_{3,28}$=16.932; p<0.01) two-way interaction between *S* and *T*.



a) mean *THW* for all conditions



b) standard deviation of *THW* for all conditions

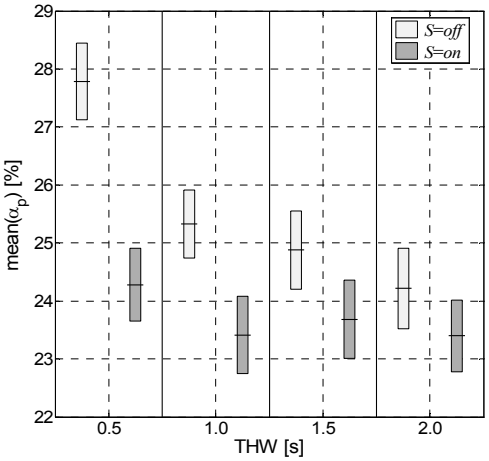


c) standard deviation of TTC^{-1} for all conditions

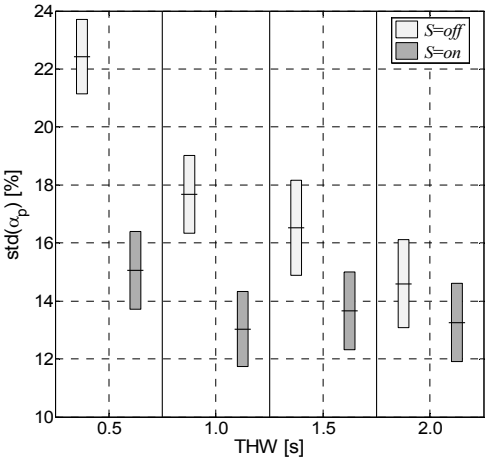
Figure 45: Means (horizontal lines) and 95% confidence intervals (gray bars) of the car-following performance indicators. The results are clustered (shades of gray of the bars) by the state *S* of the haptic feedback system: *on* or *off*.

Control effort

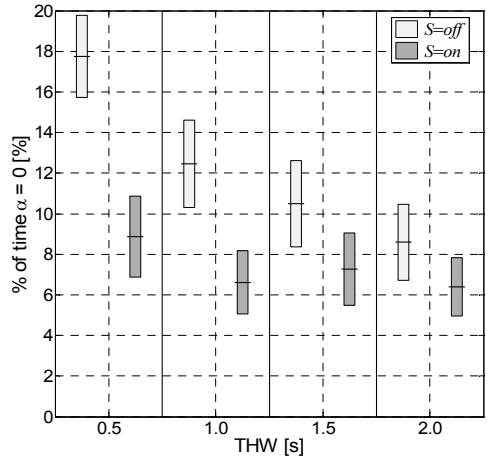
The $\overline{\alpha_p}$ has been significantly ($F_{1,9}$=31.005; p<0.01) lower for *S*=*on* for all *THW*'s (see Figure 46a). The higher the *THW*, the lower $\overline{\alpha_p}$, this effect was significant ($F_{3,28}$=10.970; p<0.01), but less pronounced for *S*=*on* than for *S*=*off*. This led to a significant ($F_{3,28}$=16.499; p<0.01) two-way interaction between *S* and *T* for $\overline{\alpha_p}$. Similar significant effects and trends have been found for σ_{α_p} and t_r (see Figure 46b and Figure 46c).



a) mean gas pedal depression, α_p, for all conditions



b) standard deviation of the gas pedal depression for all conditions



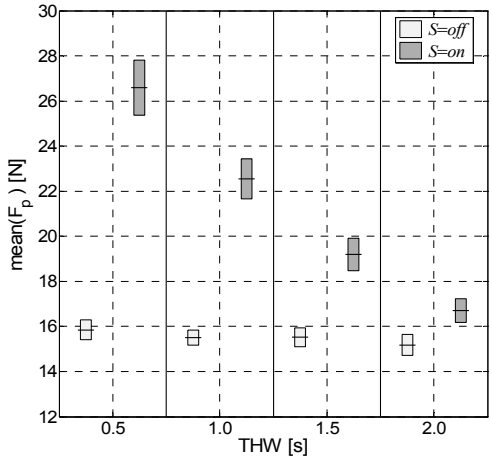
c) percentage of time for which the gas pedal was not depressed for all conditions

Figure 46: Means (horizontal lines) and 95% confidence intervals (gray bars) of the car-following control effort indicators. The results are clustered (shades of gray of the bars) by the state *S* of the haptic feedback system: *on* or *off*.

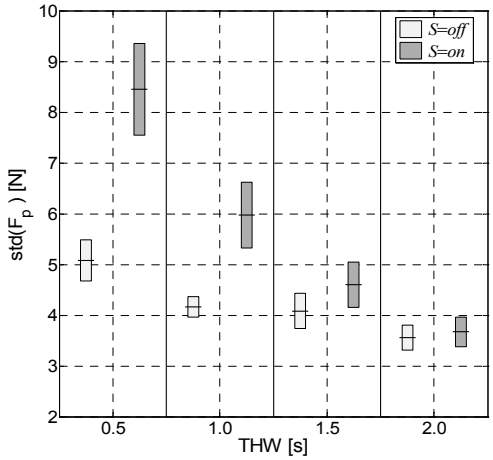
Physical load

The $\overline{F_p}$ was significantly ($F_{1,9}$=47.409; p<0.01) higher for *S=on* and decreased significantly ($F_{3,27}$=47.050; p<0.01) with increasing *THW* (see Figure 47a). For *S=off* there is no significant change $\overline{F_p}$ with changes in *T*. The different trends for $\overline{F_p}$ with *T* for *S* leads to a significant ($F_{3,28}$=64.425; p<0.01) interaction between *S* and *T*. In fact, the decrease appears to be linear, quite like the THW-stiffness algorithm. The σ_{F_p} also decreases significantly ($F_{3,28}$=11.716; p<0.01) with increasing *THW* (see Figure 47b). The decrease in σ_{F_p} is significant ($F_{1,9}$=121.051; p<0.01) for both *S=on* and *S=off*. The difference in σ_{F_p} between *S=on* and *S=off*

becomes smaller with increasing *THW*, yielding a significant ($F_{3,28}$=10.047; p<0.01) interaction between *S* and *T*.



a) mean gas pedal force, F_p, exerted by drivers for all conditions



b) standard deviation of gas pedal force, F_p, for all conditions

Figure 47: Means (horizontal lines) and 95% confidence intervals (gray bars) of the car-following physical load indicators. The results are clustered (shades of gray of the bars) by the state *S* of the haptic feedback system: *on* or *off*.

5.2.4 Discussion of the results

The results of the ANOVA's are summarised in Table 3. No increase in car-following performance due to the presence of haptic feedback was found. In fact for the most critical situation, *THW*=0.5 [s], the performance (σ_{THW}) decreased significantly. This decrease in performance for *THW*=0.5 [s], however, did not lead to less safe driving, as drivers have also increased their $\overline{THW}$'*s* when *S*=*on*, which compensates for the lesser following performance. The improvement in σ_{TTC}^{-1} for the haptic feedback conditions is most likely caused by the increase in $\overline{THW}$ rather than the presence of the haptic feedback, because the improvements are relatively small. Still it is interesting to note that at *THW*=0.5 [s] the increase in σ_{THW} for *S*=*on* is much higher than for all other *T*, while at the same time, the decrease in σ_{TTC}^{-1} is also the highest for *S*=*on*. It appears as if drivers shifted the balance from maintaining low variations in *THW* to maintaining low variations in *TTC* at *THW*=0.5 [s] when using haptic feedback. This effect of the support system seems to be confirmed by the significant interaction that was found between *S* and *T* for σ_{THW} and σ_{TTC}^{-1}. When using haptic feedback, drivers appear to be controlling more with *TTC* for lower values of *THW* (0.5 and 1.0 [s]), while at higher values of *THW* (1.5 and 2.0 [s]) that control shifts from *TTC* to *THW*, as the difference between σ_{THW} for *S*=*on* and *S*=*off* changes from better for *S*=*off* to better for *S*=*on*. The differences between σ_{TTC}^{-1} for *S*=*on* and *S*=*off* become smaller for increasing *THW*. This is qualitatively illustrated in Figure 48a-h, in which the distributions of the car-following spirals are plotted for all drivers and all conditions (see Appendix C.1 for an explanation of how these distributions were determined). Figure 48a and b show most clearly the change in balance between correcting *THW* errors and *TTC* errors. Furthermore, it can be seen that the criticality of the situation is much

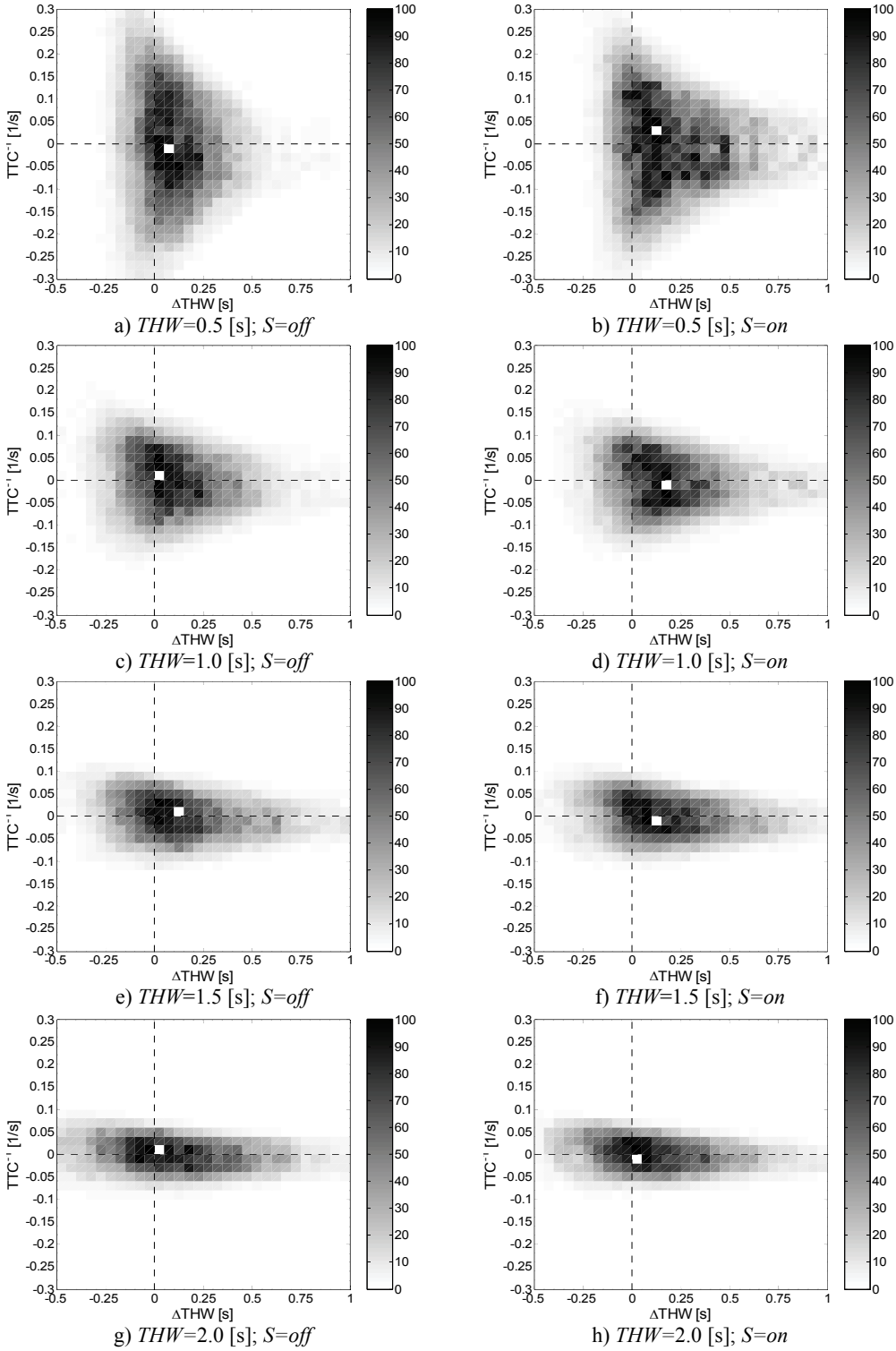
higher for *THW*=0.5 [s] because the shape of the car-following spirals is more oriented along the TTC^{-1} axis than the *THW* axis, whereas for *THW*=1.0, 1.5, and 2.0 [s] the orientation of the spiral shifts more towards the *THW* axis.

Table 3: Summary of the results of the univariate ANOVA statistical analysis of the dependent measures, with significance level α=0.05. In the table, •••, ••, and • denote a significance of $p \leq 0.01$, $0.01 < p \leq 0.05$, and $0.05 \leq p < 0.1$ respectively and '-' denotes no significance**.** *S* is the support system state, *T* are the *THW* levels at which drivers were asked to drive.

	Following performance			Control effort			Physical load	
	$\overline{THW}$	σ_{THW}	$\sigma_{TTC^{-1}}$	$\overline{\alpha}_p$	σ_{α_p}	t_r	$\overline{F_p}$	σ_{F_p}
Main effects								
S	•••	•	•••	•••	•••	•••	•••	•••
T	•••	•••	•••	•••	•••	•••	•••	•••
2 way interaction								
SxT	-	•••	•••	•••	•••	•••	•••	•••

Control effort decreased when using the haptic feedback. In general, the control effort varied little with *THW* when using haptic feedback. Only for *THW*=0.5 [s] does control effort increase a little. This is in contrast with the big changes in control effort without haptic feedback with changes in *THW*. It seems that the presence of haptic feedback reduces the gain between visual perception of the changes in the environment and the resulting control actions. In other words, the extra haptic information available to drivers when the haptic feedback system is active, allows drivers to relax their control actions. This has little effect on following performance and could hence be said to improve car-following comfort. It must be noted here again, though, that the absence of motion cues might also have played a part in the big differences in control effort between *S=on* and *S=off*. On the other hand, it also is an indication of the potential of the haptic feedback information, which might have effectively replaced the absence of motion cues in comfortably controlling the vehicle.

As expected, the presence of haptic feedback significantly increased the physical load which drivers experienced during the experiment. What is remarkable however, that, unlike in the results presented in the previous Section, the standard deviations of the pedal forces are significantly higher with haptic feedback compared to no feedback. Still, the higher forces on the gas pedal yield similar σ_{F_p} for both conditions of *S* for *THW*=1.5 and 2.0 [s]. For the two lower *THW*'s, the differences in σ_{F_p} increase quickly. It appears as if it is more difficult to maintain a force-task strategy with the THW-stiffness algorithm at smaller *THW*'s. Apparently, the higher $\overline{F_p}$ allows for less accurate implementation of the force-task strategy. Another factor that might have influenced the proper adoption of a force-task strategy is the fact that the system was turned on and off randomly for each driving minute, which could have made the transitions too difficult, allowing too little time for drivers to adapt their driving strategy to the change in pedal feedback. Thus, the drivers may have continued using the gas pedal as a 'normal' gas pedal, even when they were experiencing haptic feedback, hence not fully benefiting from the information they were provided with through the gas pedal feedback.



a) *THW*=0.5 [s]; *S=off*

b) *THW*=0.5 [s]; *S=on*

c) *THW*=1.0 [s]; *S=off*

d) *THW*=1.0 [s]; *S=on*

e) *THW*=1.5 [s]; *S=off*

f) *THW*=1.5 [s]; *S=on*

g) *THW*=2.0 [s]; *S=off*

h) *THW*=2.0 [s]; *S=on*

Figure 48: Distribution of the car-following spirals for all conditions. Shades of gray represent normalized frequency (between 0 and 100). The white dot shows the center of the spirals.

5.2.5 Conclusions

1. The results of the experiment show that the car-following performance was not improved by using the THW-stiffness feedback algorithm.
2. Control effort was shown to decrease significantly with haptic feedback, without sacrificing car-following performance.
3. The physical load, as expected, increased significantly for the haptic feedback condition and more so with decreasing *THW*.
4. The hypothesis that drivers adopt a force-task strategy cannot be confirmed for the conditions tested.

5.3 Lead vehicle speed effects on supported car-following[1]

Highway traffic flow depends on the speed and occupation density of the vehicles. The ability of drivers to deal with different kinds of traffic flow depends on experience and skill. In the more and more congested highways all over the world, this ability is becoming increasingly more important.

An experiment was conducted to investigate the effects of lead vehicle speed changes and following separation on driver behaviour when using the TTC-stiffness feedback algorithm. The experiment was designed such that system identification techniques could be applied to examine the driver characteristics which mainly depend on driver skills, that led to changes that might be found in driver behaviour in this experiment (see Section 4.3.2 for a comprehensive description of these system identification methods).

5.3.1 Method

Subjects

Ten subjects participated in the experiment, 5 males and 5 females. Average age of the participants was 23 years. Mean driving experience was 3.5 years, with an average driving frequency of 2.5 times per week (± 0.5-1.0 hour per ride). All subjects were paid €5.- per hour for their participation.

Task instruction

The driving task given to the subjects, in written instructions, was to "try to maintain the separation with the yellow [lead] car as previously indicated by the red translucent rectangle as good as you can by accelerating when the yellow car is speeding up and by decelerating – with the gas pedal only – when the yellow car is slowing down." Drivers were explicitly instructed to use the brake pedal only to avoid imminent collision. This allowed for the investigation of the limits of vehicle control with the gas-pedal only.

[1] Parts of the results in this section have been published in a conference paper titled "Effects of Lead Vehicle Speed and Separation Distance on Driver Car-Following Behaviour" (Mulder *et al.*, 2005b).

Apparatus

The fixed based driving simulator described in Section 4.1 was used to carry out the car-following experiment. The vehicle dynamics were those of a powerful, but heavy car, yielding sluggish dynamics, which were linearized around the vehicle following speed of 100 [km/h]. At this speed the longitudinal dynamics of the vehicle can be approximated by the Frequency Response Function (FRF) $H_{car}(\omega)$ of equation (5.1), in which ω denotes the frequency vector, V_{car} the speed of the car (in m/s), and α the pedal depression (in % of the maximum). Figure 49 shows a Bode plot of the speed response of the car to gas pedal inputs.

$$H_{car}(\omega) = \frac{V_{car}}{\alpha} = \frac{0.37}{(1 + j\omega \cdot 17.5)} \tag{5.1}$$

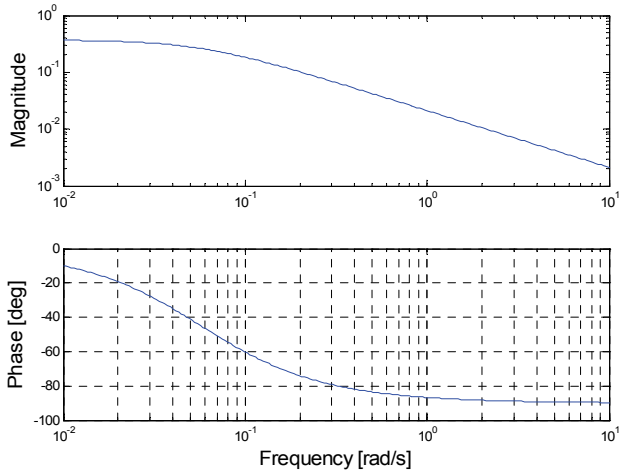


Figure 49: Bode plot of the speed response of the car to gas pedal inputs.

Independent variables

Three independent variables defined the conditions under which drivers were tested. Lead vehicle speed disturbance bandwidth f_d [Hz] and amplitude A_d [km/h] were varied, such that the total power in the disturbance remained the same for all three conditions:

1. The *THW* at which drivers were asked to drive, *T*: 0.5, 1.0, and 1.5 [s].
2. The lead vehicle speed disturbance characteristics, *D*: f_d=0.3 [Hz]; A_d=14 [km/h], f_d=0.5 [Hz]; A_d=10 [km/h], f_d=0.7 [Hz]; A_d=7 [km/h].
3. The TTC-stiffness feedback state, *S*: No haptic feedback (*off*); TTC-stiffness feedback (*on*).

Experiment design

The three independent variables – *T*, *D*, and *S* – were combined to yield a randomized factorial experiment design. However, the design was not completely randomized. In order to prevent drivers from having to switch between using a DSS and not using a DSS (which might require drivers to adopt different driving strategies), all nine combinations of *T* and *D* were first

driven with *S=on* and then with *S=off*, or vice versa. The DSS state order was alternated between drivers.

The experiment that was set up to investigate the effects of lead vehicle speed changes and following separation on driver behaviour was designed such that it would be possible to apply system identification techniques to identify driver Frequency Response Functions (FRF) to changes in relative velocity (V_{rel}) and relative distance (X_{rel}). The complete identification procedure is described in Section 4.3.2.

Driving time for each condition was 5 minutes, during which the THW-indicator was not visible. All conditions were repeated once. Total driving time per condition, including positioning at the required THW behind the lead vehicle and the repetition, amounted to ±13 minutes. Average driving time per subject was 3.9 hours. Drivers had two short breaks of 5-10 minutes and one long brake of 15-20 minutes to prevent fatigue.

Dependent measures

To determine control effort and following performance a number of measures were used in conjunction. First, car-following performance is expressed by the mean and standard deviation of *THW*. From the parameterized model, that was identified, total time-delays τ_e could be calculated, which together with the phase margins φ_m show the capability of drivers to follow the lead vehicle disturbance. The higher the time-delays and the smaller phase margins, the more trouble drivers have had in following the lead vehicle speed and vice versa. Furthermore, φ_m is a measure of the stability of the control loop. Second, control effort is both described in terms of the time-domain statistics standard deviation of α_p, and the percentage of time the gas pedal was not depressed t_r (maximum deceleration without using the brakes). System identification yields driver crossover frequencies ω_c which give an indication of the tracking performance drivers achieved. In order to improve tracking performance drivers have to increase ω_c. This usually comes at the expense of less phase margin, hence less stability. Third, the physical load is described by time-domain statistics alone, using the mean and standard deviation of the pedal force F_p drivers exerted on the gas pedal. The combined system identification results give an indication of the skill drivers displayed in executing the car-following task they were asked to perform during the experiment.

5.3.2 Hypotheses

Purpose of the experiment was to investigate the effects of lead vehicle speed and separation distance on driver behaviour, with and without using the earlier described DSS.

Because of the sluggish longitudinal dynamics of the car (low-pass bandwidth of 0.06 [rad/s]), it is expected that increased control effort necessary to follow increased lead vehicle disturbance bandwidth will mostly be filtered out, and therefore will not increase following performance. Increased *THW* will lower the perceptibility of lead vehicle speed changes (Rockwell, 1972) and therefore the driver control effort, consequently also lowering following performance. The DSS is expected to increase the perceptibility of lead vehicle speed changes, since it adds a second perceptual channel with which changes in lead vehicle speed can be

detected (Mulder *et al.*, 2004a and Mulder *et al.*, 2004b). In short, the hypotheses can be formulated as follows:

1. Increased lead vehicle speed disturbance (higher disturbance bandwidth f_d; lower disturbance amplitude A_d) will increase control effort; following performance will remain the same or decrease.
2. Increased following *THW* will decrease control effort and following performance.
3. Use of the TTC-stiffness gas-pedal feedback will decrease control effort and increase following performance, especially for the larger time-headways.

5.3.3 Time-domain results

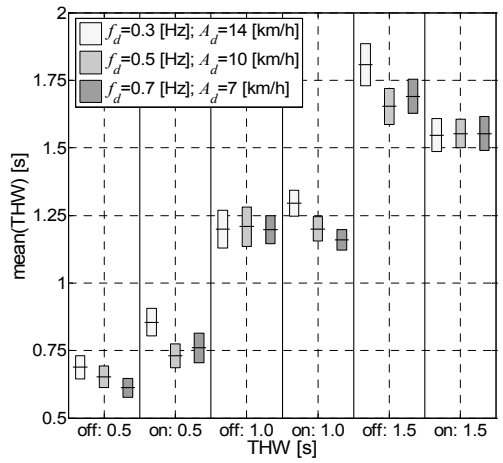
Car-following performance

Drivers were asked to follow a lead vehicle at *THW*=0.5, 1.0, and 1.5 [s]. For each of these conditions drivers tended to drive approximately 0.2 – 0.25 [s] further away from the lead vehicle than required (see Figure 50a). ANOVA shows that the $\overline{THW}$'*s* are significantly ($F_{2,18}$=3.742; 0.01<p≤0.05) influenced by the lead vehicle speed disturbance *D*. Generally, the lower the disturbance bandwidth f_d (and the higher the disturbance amplitude A_d), the larger the bias from the required *THW*.

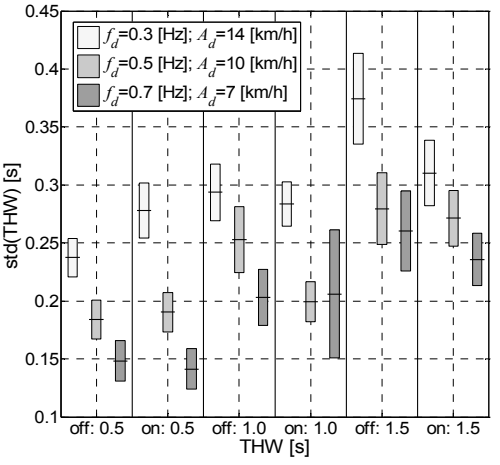
Further, a highly significant interaction ($F_{2,18}$=14.0; p<0.01) between *T* and *S* was found. For *THW*=0.5 [s] the driving with the DSS yields a larger bias from the required *THW* – towards increased safety. For *THW*=1.0 [s] driving with the DSS did not have a significant influence. However, for *THW*=1.5 [s] the bias is smaller when using the DSS and constant for all lead vehicle speed disturbances. This might indicate that for the latter conditions the extra separation information provided by the DSS could have helped improve drivers' perception of changes in V_{lead}.

Although, when using the DSS, drivers were driving significantly further away from the lead vehicle at *THW*=0.5 [s] and significantly closer at *THW*=1.5 [s], this did not lead to significant differences in σ_{THW} compared to using no DSS (see Figure 50b). *D* did have a significant ($F_{2,18}$=73.571; p<0.01) effect on following performance. The lowest bandwidth disturbance consistently yielded the highest σ_{THW}, the highest bandwidth disturbance the lowest. This effect is most likely to be caused by the amplitude of *D*, A_d, which was highest for the lowest bandwidth, and lowest for the highest bandwidth. A higher required *THW* also increased σ_{THW} significantly ($F_{2,18}$=28.724; p<0.01), due to decreasing perceptibility of changes in V_{lead}.

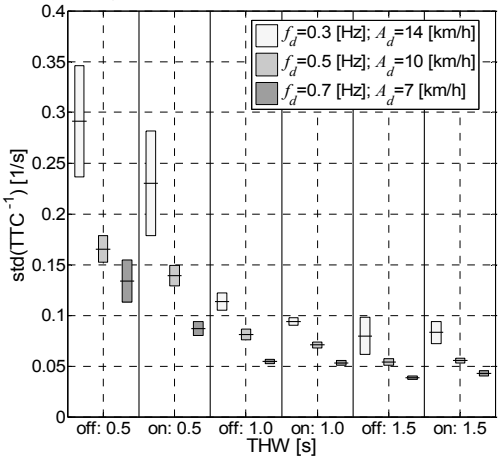
The $\sigma_{TTC^{-1}}$ increased significantly ($F_{2,18}$=38,209; p<0.01) with decreasing *THW* and decreased significantly ($F_{2,18}$=36.623; p<0.01) with increasing lead vehicle speed disturbance bandwidth f_d (and decreasing amplitude A_d). These effects are clearly visible in Figure 50c. Both effects are related, since a significant ($F_{2,18}$=9.759; p<0.01) interaction effect between *T* and *D* is found. *S* has only borderline significance ($F_{1,9}$=3.494; 0.05<p≤0.1) on reducing the magnitude of TTC^{-1}. Case by case investigation of the DSS contributions in reducing TTC^{-1} (and hence improving safety), shows that only for *THW*=1.0 [s] there is a significant ($F_{1,9}$=15.149; p<0.01) reduction in TTC^{-1} and then only for the lead vehicle speed disturbances *D*={0.3 Hz, 14 km/h; 0.5 Hz, 10 km/h}.



a) mean *THW* for all conditions



b) standard deviation of *THW* for all conditions



c) standard deviation of TTC^{-1} for all conditions

Figure 50: The means (horizontal lines) and 95% confidence intervals (gray bars) of the car-following performance indicators. The results are clustered by the different lead vehicle speed disturbances (shades of gray of the bars) and by the state of the haptic feedback system: *on* or *off*.

Control effort

With decreasing *THW*, $\overline{\alpha_p}$ increases significantly ($F_{2,18}$=25.669; p<0.01). With increasing lead vehicle speed disturbance bandwidth f_d, $\overline{\alpha_p}$ decreases significantly ($F_{2,18}$=131.513; p<0.01) (see Figure 51a). This effect is probably caused by the fact that the sluggish car dynamics of the own vehicle could not respond fast enough to the rapid changes in velocity of the lead car. It is believed that drivers therefore choose to ignore high frequency, low amplitude lead vehicle speed changes, and respond only to the lower frequencies. This is confirmed when looking at σ_{α_p} (see Figure 51b). The *T* and *D* effects also have a significant ($F_{4,36}$=2.68; 0.01<p≤0.05) interaction. For higher *THW*'s the differences in $\overline{\alpha_p}$ for each *D* become smaller. The DSS had only a marginally significant ($F_{1,9}$=3.593; 0.05<p≤0.1) effect of decreasing $\overline{\alpha_p}$. There is a

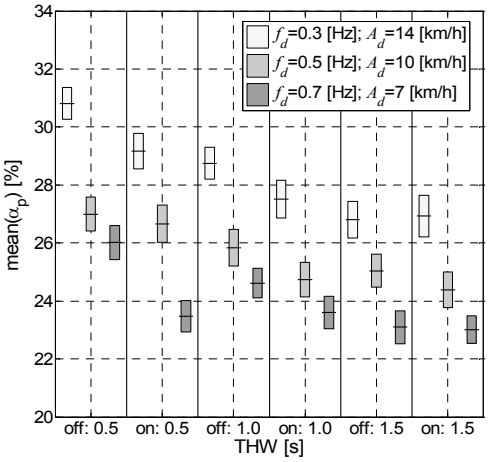
significant ($F_{4,36}$=3.263; 0.01<p≤0.05) three-way interaction between *S*, *D*, and *T*. Besides the previously mentioned interaction between *D* and *T*, the DSS reduction of the mean gas pedal depression decreases with increasing *THW*.

The σ_{α_p} decreases significantly ($F_{2,18}$=25.713; p<0.01) with increasing *THW*. Furthermore, σ_{α_p} decreases significantly ($F_{2,18}$=94.335; p<0.01) also with increasing lead vehicle speed disturbance bandwidth f_d (which has decreasing amplitude A_d) as can be seen in Figure 51b. The DSS only had a marginally significant ($F_{1,9}$=3.380; 0.05<p≤0.1) effect on reducing σ_{α_p}, which was greatest for *THW*=0.5 [s].

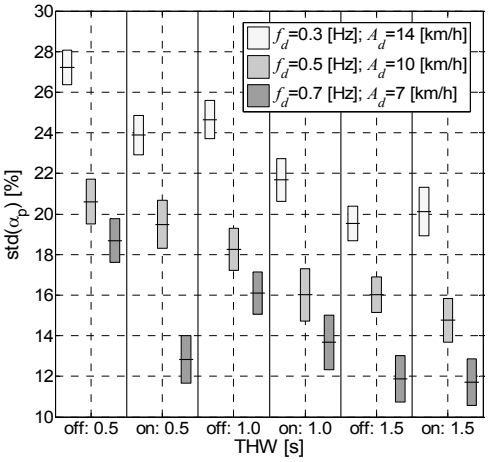
The DSS did yield significantly ($F_{1,9}$=14.386; 0.01<p≤0.05) less time t_r in which drivers did not press the gas pedal, that is, the amount of time drivers required maximum deceleration without using the brakes (see Figure 51c). This effect was smaller for increasing *THW*'s and increasing f_d. It seems that the DSS effectively prevents drivers from over-accelerating towards a lead vehicle, since that would then require more deceleration, hence more foot-off-pedal time, when getting too close. Increased *T* and *D* both significantly lowered t_r ($F_{2,18}$=25.504; p<0.01 and $F_{2,18}$=97.657; p<0.01 respectively).

Physical load

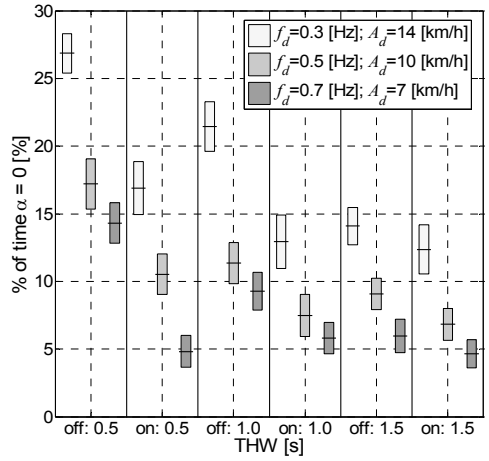
Due to the haptic feedback, $\overline{F_p}$ increased significantly ($F_{1,9}$=49.805; p<0.01) when using the DSS (see Figure 52a). Increased *THW* also lowered $\overline{F_p}$ significantly ($F_{2,18}$=58.260; p<0.01), as well as decreased f_d ($F_{2,18}$=48.121; p<0.01). These latter two effects are most likely to be directly related to the lower $\overline{\alpha_p}$ for increased *THW* and decreased f_d. There are two-way and three-way interactions for $\overline{F_p}$. Marginally significant interactions are found for the *S* and *D* and for *S* and the *T* ($F_{2,18}$=3.109; 0.05<p≤0.1 and $F_{2,18}$=2.879; 0.05<p≤0.1 respectively). When the DSS is not used, at a *THW*=0.5 [s], only the low-bandwidth disturbance f_d=0.3 [Hz] yields a higher $\overline{F_p}$. With the DSS, at *THW*=0.5 [s] only the high-bandwidth disturbance f_d=0.7 [Hz] yields a lower $\overline{F_p}$. With an increase in *THW*, the differences between $\overline{F_p}$ for the different *D* increase, both for driving with or without DSS, leading to the significant ($F_{4,36}$=4.014; p<0.01) three-way interaction between *S*, *D*, and *T*.



a) mean gas pedal depression α_p for all conditions



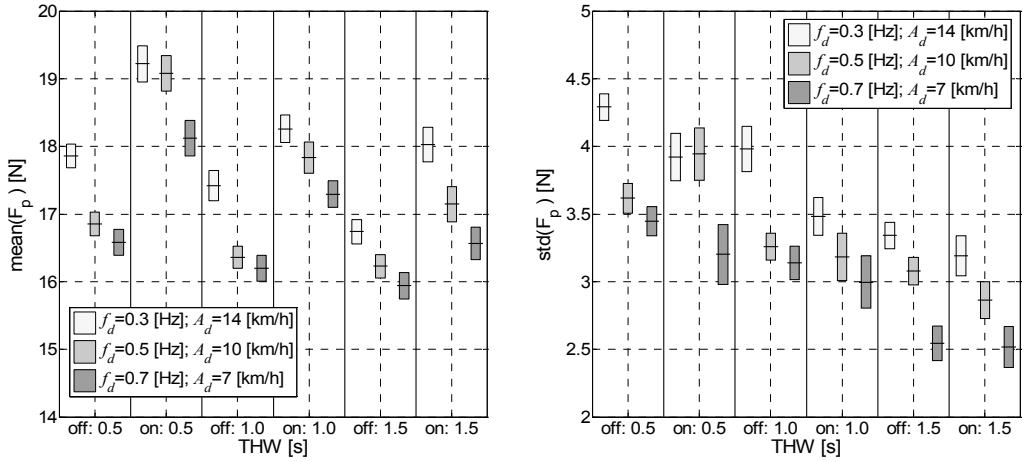
b) standard deviation of the gas pedal depression for all conditions



c) % of time the gas pedal was not depressed for all conditions

Figure 51: The means (horizontal lines) and 95% confidence intervals (gray bars) of the car-following control effort indicators. The results are clustered by the different lead vehicle speed disturbances (shades of gray of the bars) and by the state of the haptic feedback system: *on* or *off*.

For $\overline{\sigma_{\alpha_p}}$, only D and T have significant ($F_{2,18}$=39.824; p<0.01 and $F_{2,18}$=26.190; p<0.01) effects (see Figure 52b). $\overline{\sigma_{\alpha_p}}$ decreases with increasing f_d and with increasing THW. A two-way interaction ($F_{2,18}$=4.276; 0.01<p≤0.05) between S and D is found for $\overline{\sigma_{\alpha_p}}$. Because the two-way interaction between S and D changes with increasing THW, there is also a three-way interaction between S, D, and T ($F_{4,36}$=2.708; 0.01<p≤0.05).



a) mean gas pedal force, F_p, exerted by drivers for all conditions

b) standard deviation of gas pedal force, F_p, for all conditions

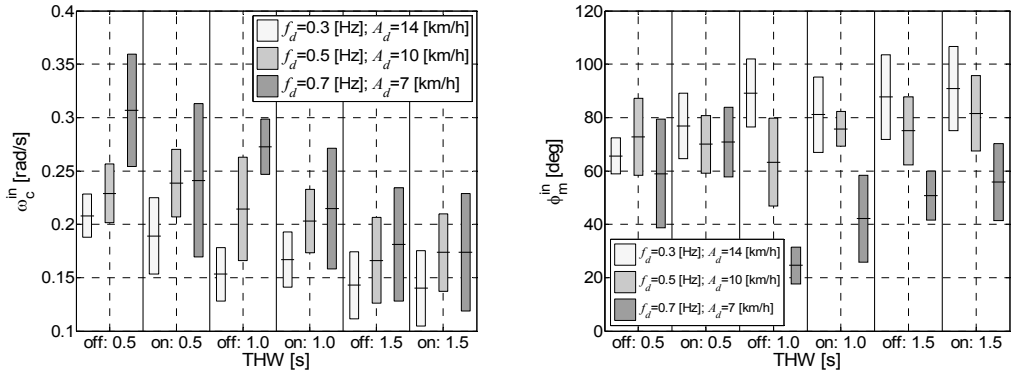
Figure 52: Means (horizontal lines) and 95% confidence intervals (gray bars) of the car-following physical load indicators. The results are clustered by the different lead vehicle speed disturbances (shades of gray of the bars) and by the state of the haptic feedback system: *on* or *off*.

5.3.4 Frequency-domain results

Parametric identification of the car-following model as formulated by equations (4.6) and (4.7) resulted in a wide range of values for the parameters K_d^{out}, K_d^{in}, τ_l, τ_L, τ_e. Further analysis of the Cramer-Rao lower bounds revealed the insensitivity of the cost function which was minimized to estimate the model parameters to changes in these parameters. Consequently, it is not possible to formulate single sets of parameters to represent each driving condition. Still, the crossover frequencies and phase margins of the inner- and outer-loops could be determined. However, with increase of *THW* and decrease of f_d, the perceptibility of changes in V_{lead} diminished which greatly decreased the displayed control activity of the drivers. This seriously impaired the application of system identification techniques, since driver behaviour was increasingly non-linear for these conditions.

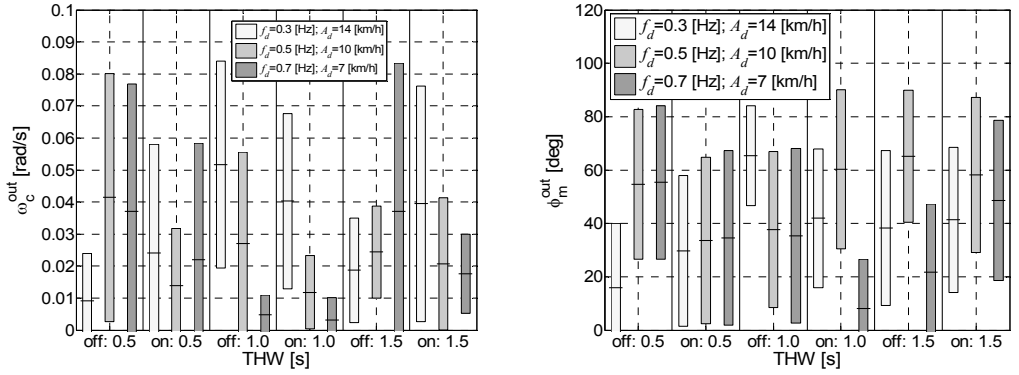
First, the inner-loop crossover frequencies ω_c^{in} (see Figure 53a) are remarkably low ($\omega_c^{in} \ll f_d$). Nevertheless, ω_c^{in} increases significantly ($F_{2,18}$=24.713; p<0.01) when the V_{lead} disturbance bandwidth f_d is increased. Increased *THW* significantly reduces ω_c^{in} ($F_{2,18}$=21.641; p<0.01).

The corresponding inner-loop phase margins are shown in Figure 53b. In contrast with the crossover frequencies, the phase margins are remarkably high, some even showing signs of crossover regression (ϕ_m^{in} >90º). For *THW*=1.0 and 1.5 [s] and V_{lead} disturbance bandwidth f_d=0.7 [Hz] the phase margins are significantly ($F_{2,18}$=50.077; p<0.01) lower. For these conditions the amplitude A_d of the V_{lead} disturbance was smallest, which resulted in the lowest perceptibility of changes in V_{lead}.



a) inner-loop cross-over frequency

b) inner-loop phase margin



c) outer-loop cross-over frequency

d) outer-loop phase margin

Figure 53: Identified frequency-domain characteristics of the car-following model inner-loop (a and b) and outer-loop (c and d).

Outer-loop crossovers and phase margins were difficult to determine, especially since the inner-loop crossovers were already very low and phase margins very high. On average, ω_c^{out}, when possible to determine, was more than three to four times lower than ω_c^{in} (see Figure 53c), but the spread in ϕ_m^{out} was so high that it is impossible to say anything conclusive (see Figure 53d). Since the outer-loop crossover frequencies seem to be so low, it is most likely that drivers hardly used X_{rel} ($\approx THW$) to control their following separation. It is mainly V_{rel} ($\approx TTC$) that was used to control car-following separation and even then it does not seem to require much effort, while stability of the control loop is high.

The effective time-delays τ_e found through the system identification (Figure 54) for THW=1.0 and 1.5 [s] and f_d=0.3 and 0.5 [Hz] are significantly lower when using the DSS ($F_{1,9}$=13.834; p<0.01 and $F_{1,9}$=3.785; 0.05<p≤0.1, respectively). For THW=1.0 and 1.5 [s] and f_d=0.7 [Hz] τ_e is higher when using the DSS. These values of τ_e are, however only marginally supportive, since drivers showed very little control activity at THW=1.5 [s], making the identification of driver behaviour very difficult. For THW=0.5 [s] τ_e is significantly lower when using the DSS for all lead vehicle disturbances ($F_{1,9}$=38.479; p<0.01).

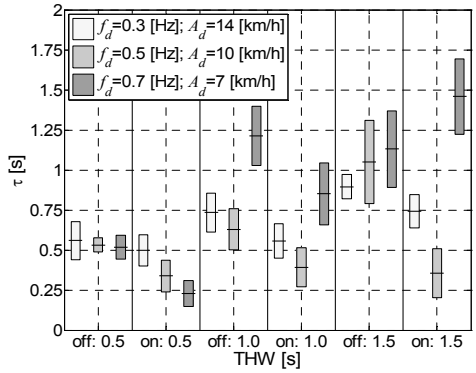


Figure 54: Identified effective time delay of the car-following model inner-loop.

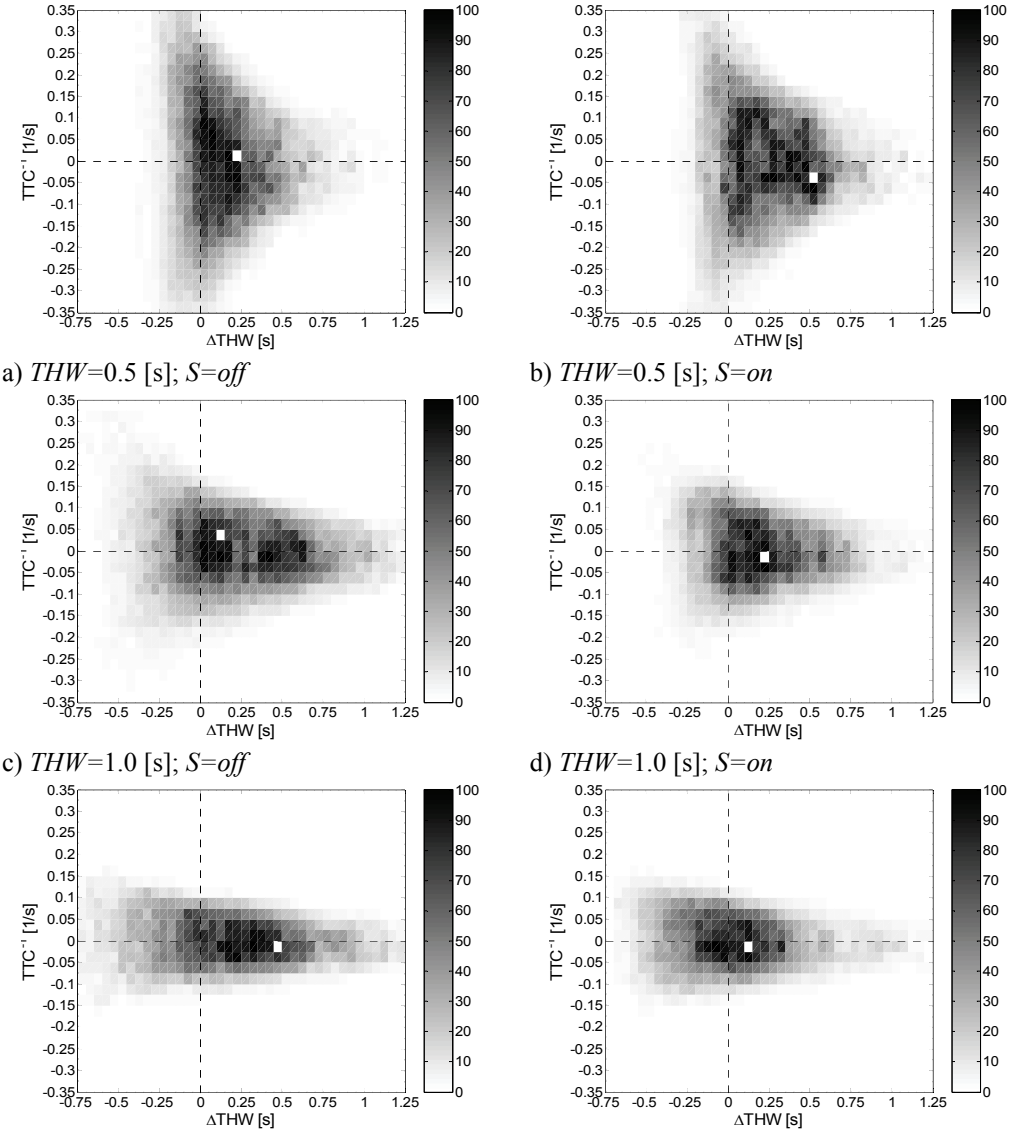
5.3.5 Discussion of the results

The results of the ANOVA's are summarized in Table 4. From the car-following performance statistics it seems that the haptic feedback is least effective for *THW*=0.5 [s], the most critical car-following condition. Drivers tend to driver further away from the THW_d they were asked to drive and significantly more so with DSS than without. This compensates for the increase in σ_{THW} at *THW*=0.5 [s] when driving with the DSS. The $\sigma_{TTC^{-1}}$ is significantly lower for all *THW* when driving with DSS, which might indicate that drivers tend to control more with TTC^{-1} rather than with *THW*. However, it might also be the result from driving at higher *THW*'s when using the DSS. The former hypothesis is strengthened, nevertheless, by the results of the system identification, which show that control is mainly the result of regulating the error in V_{rel} ($\approx TTC$). However, the results of the identification were very noisy, making it difficult to interpret them properly. To get more qualitative insight in drivers' control strategy, the distributions of the car-following spirals in the THW-TTC^{-1} phase-plane are shown in Figure 55.

Table 4: Summary of the results of the univariate ANOVA statistical analysis of the dependent measures, with significance level α=0.05. In the table, •••, ••, and • denote a significance of $p \leq 0.01$, $0.01 < p \leq 0.05$, and $0.05 \leq p < 0.1$ respectively and '-' denotes no significance. *S* is the support system state, *D* are the lead vehicle speed characteristics and *T* are the *THW*'s at which drivers were asked to drive.

	Following performance			Control effort			Physical load	
	$\overline{THW}$	σ_{THW}	$\sigma_{TTC^{-1}}$	$\overline{\alpha_p}$	σ_{α_p}	t_r	$\overline{F_p}$	σ_{F_p}
Main effects								
S	-	-	•	•	•	•••	•••	-
D	••	•••	•••	•••	•••	•••	•••	•••
T	•••	•••	•••	•••	•••	•••	•••	•••
2 way interaction								
SxD	-	-	-	-	-	-	•	••
SxT	•••	-	•	-	-	•••	•	-
DxT	-	-	•••	••	-	••	-	-
3 way interaction								
SxDxT	-	••	-	••	••	-	•••	••

From the car-following spiral distributions in Figure 55 it can be seen that, for different *THW* the car-following spirals are somewhat smaller when using the DSS compared to not using the DSS. Only for *THW*=0.5 [s] there appears to be a shift. There, the car-following spiral distribution appears more vertical, that is, more variation in TTC^{-1} than in *THW*, whereas this is opposite for *THW*=1.0 and 1.5 [s]. When using the DSS, this shift is less pronounced. In Appendix C.1.1 the car-following spiral distributions for the other two conditions of *D* are given, which show similar results.



a) *THW*=0.5 [s]; *S=off* b) *THW*=0.5 [s]; *S=on*

c) *THW*=1.0 [s]; *S=off* d) *THW*=1.0 [s]; *S=on*

e) *THW*=1.5 [s]; *S=off* f) *THW*=1.5 [s]; *S=on*

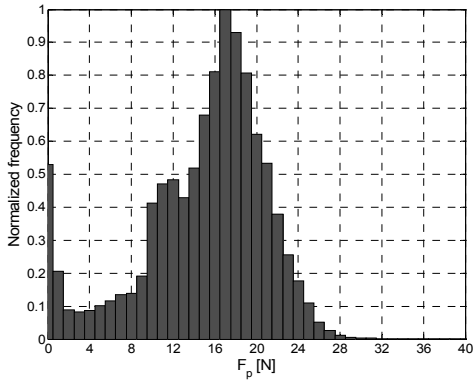
Figure 55: Distribution of the car-following spirals for all combinations of *T* and *S*, and *D*={f_d=0.5 [Hz]; A_d=10 [km/h]}. Shades of gray represent normalized frequency (between 0 and 100).

Like the inner-loop crossover frequency, the standard deviation of the gas pedal depression, σ_{α_p}, decreases significantly with increasing THW. Furthermore, σ_{α_p} decreases also with increasing V_{lead} disturbance bandwidth f_d, which has decreasing amplitude A_d. These results indicate that drivers are capable of detecting the characteristics of *D* quite accurately, both in magnitude as well as frequency. However, for the high *THW*'s (1.0s and 1.5s) and high bandwidth disturbances f_d=0.7 Hz, drivers displayed increasingly less control activity. Part of this can be explained by poor perceptibility, but based on the previous conclusion that both changes in frequency and magnitude seem to have been perceived correctly, this cannot explain the decreased control activity entirely. It is suggested that for the conditions mentioned above the need to accurately follow the lead vehicle is simply less than for the low *THW*=0.5 [s], low bandwidth disturbance f_d=0.3 [Hz] since these conditions do not impose any safety impairments. As f_d increases (and A_d decreases), control activity is more focused around the mean pedal position (see also Appendix C.2). In other words, control activity decreases with increasing f_d. It is most likely, however, that this effect is caused by the combination of the decrease in A_d and the relatively increasing uselessness to react to the high frequency changes in lead vehicle speed – probably because drivers do not see the need to react to such small changes in velocity.

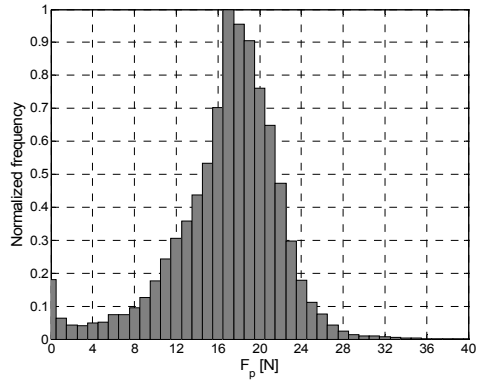
The significant increase in physical load due to haptic feedback, did not lead to an increase in σ_{F_p}, but to a decrease in σ_{F_p}, although this effect was not significant anymore for *THW*=1.5 [s]. From these results it is rather difficult to make a clear judgement whether the haptic feedback yielded force-task like behaviour. It is, therefore, illustrative to investigate the distributions of the pedal forces F_p. What can be seen from Figure 56 is that the measured force distributions of the forces F_p which drivers have exerted on the gas pedal, at *THW*=1.0 [s], are more concentrated around the $\overline{F_p}$. This followed from the σ_{F_p} already, but the distributions clearly show how well this behaviour could be maintained for different lead vehicle speed disturbances compared to driving without haptic feedback (*S=off*). The symmetry of the distribution for *S=on* clearly shows that drivers have properly yielded to the imposed feedback forces. There is no indication drivers have counteracted the feedback forces, which would have created an asymmetry in the force distribution towards higher forces.

The asymmetry of the force distributions for *S=off* in Figure 56a, c, and e, is probably caused by the hysteresis of the normal gas pedal characteristics: when drivers are actively releasing the gas pedal, the force exerted on the gas pedal will be significantly lower than when drivers are actively depressing the gas pedal. Releasing the gas pedal when no haptic feedback is present will, therefore, cost relatively more energy than when haptic feedback is present. In that case, the foot is supported much better all the way through the release movement of the foot, probably requiring less co-contraction of the shin and calf muscles. This is expected to have a positive effect on driver comfort and fatigue. Of course, the duration of this experiment has been too short to say anything conclusive about fatigue.

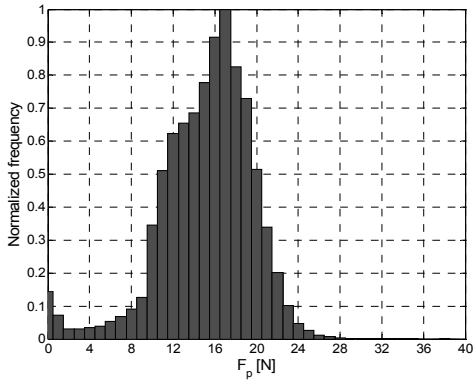
In Appendix C.3, the force distributions for *THW*=0.5 and 1.5 [s] show similar trends for the conditions of *S* and *D*. The impact of *D* seems to be small, and limited to a widening of the base of the distribution.



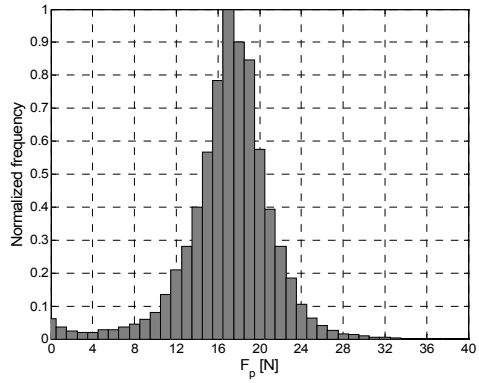
a) *S*=*off*; f_d=0.3 [Hz], A_d=14 [km/h]



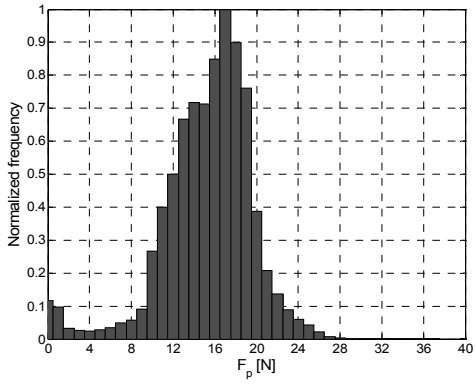
b) *S*=*on*; f_d=0.3 [Hz], A_d=14 [km/h]



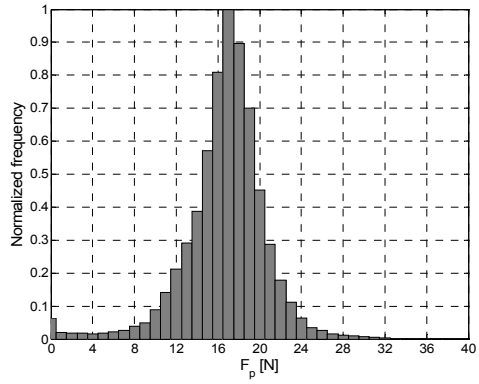
c) *S*=*off*; f_d=0.5 [Hz], A_d=10 [km/h]



d) *S*=*on*; f_d=0.5 [Hz], A_d=10 [km/h]



e) *S*=*off*; f_d=0.7 [Hz], A_d=7 [km/h]



f) *S*=*on*; f_d=0.7 [Hz], A_d=7 [km/h]

Figure 56: Measured gas pedal force distributions for all conditions of *S* and *D*, at *THW*=1.0 [s], for all drivers together.

5.3.6 Conclusions

1. Increased bandwidth of the V_{lead} disturbance decreases control effort, although inner-loop crossover frequencies increase with an increase of f_d.
2. Increased *THW* yielded decreased performance.
3. A decrease in disturbance bandwidth f_d yielded a decrease in performance for all support system states S.
4. The driver support system (TTC-stiffness algorithm) had no significant effects on following performance
5. Crossover frequencies were not influenced by the DSS, but the σ_{α_p} decreased with marginal significance, which led to significantly reduced foot-off-pedal times, t_r – an indication that drivers were reacting more relaxed to lead vehicle speed changes.
6. The DSS does not seem to interfere, nor improve car-following performance when drivers are paying full (visual) attention to the driving scene.

5.4 Overall discussion and conclusions

In this Chapter three maximal car-following experiments are presented, that is, experiments in which drivers could fully concentrate (visually) on the car-following task. The experiments were designed to investigate the effects of different environmental conditions, such as different *THW*'s and lead vehicle speed disturbances. Furthermore, the different haptic feedback algorithms were also tested under different conditions, to investigate their proficiency in different circumstances.

When introducing a new driver support system, it is important that, besides giving the driver the support for which the system was designed, driver behaviour is not negatively influenced. This is especially the case for the haptic support system discussed in this thesis, since it is to operate continuously from the boundaries of the safe-field-of-travel as defined by each haptic feedback algorithm.

Drivers are expected to benefit from this continuous haptic feedback in that they will be able to interpret the car-following task as a force-task in their use of the haptic gas pedal. This is one of the two major hypotheses that was tested by the experiments in this Chapter.

Based on the results from the three discussed maximal experiments, this hypothesis is accepted, although the evidence in support of this hypothesis is thin. The use of haptic feedback, whether this is force feedback or stiffness feedback, seems to result in significant reductions in the standard deviations σ_{F_p} of the measured gas pedal forces F_p. Investigation of the distributions of the measured gas pedal forces shows a symmetric distribution around the mean measured pedal force, $\overline{F_p}$. This indicates that drivers yield properly to the imposed feedback forces on the gas pedal.

It was attempted to find differences in the use of force and stiffness feedback. These differences were found to be small. Based on the σ_{F_p} of both the force feedback algorithm and the THW-stiffness feedback algorithm, the latter produced better results. However, the distribution of the measured pedal forces is more symmetrical for the force feedback condition,

indicating better yielding to the imposed haptic feedback. It is believed however, that stiffness feedback will be more beneficial because it has more information content. Since only one driving condition was tested, preference was given to the stiffness feedback for further experiments.

Car-following performance was hardly improved when using haptic feedback. There was some evidence, quantitatively from the system identification data and qualitatively from the car-following spiral distributions, that the use of TTC-stiffness feedback shifted the preference to minimise errors in *THW* to minimising errors in *TTC*. This was especially visible for small *THW*'s, that is, for *THW*=0.5. Overall, it can be said that car-following performance is not improved when haptic feedback is presented to drivers when they are (visually) paying attention to the driving scene.

The reduction in control effort, however, is significant, and was found for almost all conditions tested. It appears that the haptic feedback prevents drivers from over accelerating towards the lead vehicle, which in turn reduces the need to compensate by (over)decelerating. The differences in control effort that were found between the conditions with and the conditions without haptic feedback are believed to be partly due to lack of motion cues in the fixed-base driving simulator. However, the differences that were found were of such a magnitude that even in the presence of motion cues – either in a moving-base simulator or a real car – haptic feedback is expected to be beneficial in reducing the control effort. Hence, an improvement of driver comfort.

When using haptic feedback, the physical load increases, as expected. The increase is, however, not that big that it poses problems for drivers. In fact, there is some evidence that it might actually be beneficial. Abbink and van der Helm (2005) show that there is an optimal force, which is equal to the weight of the foot at rest on the pedal, where muscle contraction is minimal. In this position, drivers can be most relaxed. If the force on the gas pedal is too low, drivers will have to maintain their shin and calf muscles co-contracted to maintain the desired pedal position.

With haptic feedback, as was shown in the results of the described experiments, the mean pedal force is higher than without haptic feedback. However, the measured force distributions are more symmetric. The force distributions without haptic feedback show a-symmetry towards the lower end of the distribution due to hysteresis in the gas pedal. The absence of hysteresis in the haptic feedback conditions could mean that even when drivers are moving their foot off the gas pedal, they are better supported, hence the need for co-contraction of the shin and calf muscles is reduced. Less shin and calf muscle co-contraction means, in the long run, less fatigue. The experiment runs were of too short duration to say anything conclusive about this, however.

Finally, to conclude this Chapter, it can be said that the tested haptic feedback algorithms did not interfere with the car-following task for the tested conditions. The real benefit seems to come from more relaxed driving behaviour. If the haptic gas pedal feedback can improve driving comfort when drivers are (visually) fully concentrated on the driving task, can it help improve car-following performance when drivers are visually distracted? With two experiments, presented in the next Chapter, it is attempted to provide more insight into this research question.

Chapter 6

Car-following Experiments with Secondary Tasks

Driving is a visually demanding task. It is believed that, by far, the majority of information feedback to drivers which is used in controlling the vehicle is visual (Rockwell, 1972; Evans, 1991). Unfortunately, as noted by Rockwell (1972), visual perception is "…*very sensitive to changes in the roadway environment, vehicular design, and particularly to changes in the driver's psychological and physiological state*…"

Driver inattention to the driving scene causes drivers to lose valuable response time in unexpected situations. Time, which could have prevented a normal car-following situation from developing into a potential rear-end collision situation. It is then hardly surprising that driver inattention is a major cause of over 60% of all rear-end collisions (Knipling *et al.*, 1993). Several rear-end collision avoidance systems (RCAS) are under investigation, e.g. (Tijerina *et al.*, 2000; Godthelp and Schumann, 1993). Driver support system research is motivated by the expectancy that these systems will help improve traffic safety. Jagtman, et al. (2001) mention that it is believed that "*large-scale implementation of collision avoidance systems* […] *could reduce road fatalities up to 45%.*" However, most collision avoidance systems are still in the development phase, far from being implemented on a large-scale. Therefore, like Jagtman *et al.* (2001) point out too, many uncertainties still exist regarding the relationship between collision avoidance systems and driver response to these systems.

The goal of this research is to investigate the effects of the haptic driver support system during normal car-following situations. Nevertheless, this research was part of a larger research effort to investigate the possibilities of supporting drivers with haptic gas pedal feedback in a range of driving situations. Driver inattention during car-following in normal situations will most likely not lead directly to rear-end collisions, but easily degrades driver reaction to abrupt changes in the car-following situation, for example when the lead vehicle suddenly brakes hard. Instead of focussing on providing driver support during these emergency braking reactions, the

philosophy that has driven the research network is that continuous feedback of environmental information will keep drivers more aware of their driving situation and their control task. This will allow them to better interpret the information they receive from their support system and may lead to improved reaction times in emergency situations. Driver behaviour during these emergency situations has been studied in detail by our research partners of Nissan Motor Company, the University of Minnesota (Manser, Ward and Kuge, 2004a & b; Ward, Manser and Kuge, 2004), and the University of Iowa.

The strength of using continuous haptic gas pedal feedback not only during emergency situations, but also during normal car-following, is the fact that drivers experience the information the support system is generating during prolonged driving hours in a multitude of driving situations. This will allow drivers to learn how to use the haptic information most effectively and how to respond to the feedback properly. Because of this frequent exposure to the haptic feedback information, reacting to this information may become more intuitive and natural during emergency situations.

In order to provide drivers with continuous haptic feedback during normal car-following conditions, drivers must feel comfortable with the system and it must not interfere with their visual processing of environmental information. The experiments in this Chapter are designed to investigate the effects of the haptic feedback system on driver behaviour when they are engaged in a secondary task that demands visual attention. In other words, drivers are visually distracted while they are following a lead vehicle. It is investigated whether or not they benefit from the provided haptic information under these conditions.

As with the experiments described in Chapter 5, the experiments discussed in this Chapter have a common hypothesis too. It is expected that haptic gas pedal feedback will allow drivers to better divide their attention between the car-following task and a secondary task demanding visual attention than when driving without haptic gas pedal feedback. When drivers are capable of dividing their attention more strategically, it is expected that performance on the secondary task improves when compared to driving without haptic feedback.

Two experiments were conducted in the fixed-base driving simulator (see Section 4.1 for a description of the driving simulator) to investigate the usefulness of the discussed haptic feedback system when drivers are visually distracted. The first experiment, described in Section 6.1, investigated visual distractions in the driving scene. While driving, drivers frequently have to look at road signs, check their mirrors, read traffic announcements, etcetera, distracting visual attention from the road and other traffic. Drivers were asked to respond to (abstract) visual stimuli that were presented in the central and peripheral field of view, while following a lead car. The reaction times were measured and car-following behaviour was investigated with and without the support of the haptic feedback system.

The second experiment investigated in-car visual distraction, with and without using haptic gas pedal feedback. Drivers were given a task in which they had to relocate their visual attention from the driving scene into the car to execute a track-selection task with their CD-player. Besides task-completion time, the precision with which the task was completed and the driving behaviour, before, during, and after the task were analysed. This experiment is described and discussed in detail in Section 6.2.

6.1 Reaction-time task with central and peripheral visual stimuli[1]

The haptic gas pedal support system presented in this thesis, is believed to be useful when drivers are not paying attention (visually) to the driving scene. Nevertheless, it should not interfere with the driving task when drivers *are* paying attention. The goal of this Section is to present a simulator study of the haptic feedback system which investigated the influence of haptic feedback on the processing of visual information of the driving scene. Ideally, the haptic support system alleviates the driver's car-following task, while allowing her/him at least equal or more time to divide attention to other tasks, such as checking mirrors, looking at road signs, etcetera. It is therefore expected that the driving conditions with the haptic feedback system engaged will yield lower reaction times to randomly presented visual stimuli, while car-following behaviour would be similar or better compared to driving without the haptic feedback (Borra, 2003).

6.1.1 Method

Subjects

In total, 28 subjects participated in the experiment – 6 female and 22 male. Average age was 26 years old, with an average driving experience of 6.7 years. Ten participants (2 female, 8 male) were given the base-line condition to carry out the experiment – no haptic feedback; eight participants (1 female, 7 male) performed the experiment under a force feedback condition; and ten participants (3 female, 7 male) drove the car under a stiffness feedback condition.

Task instruction

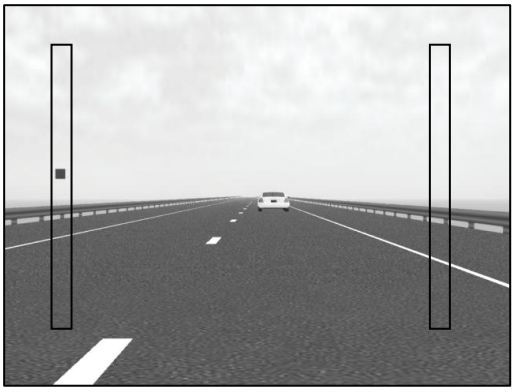
Subjects were given two tasks. The primary task was to follow a lead vehicle at a prescribed separation THW of 1.5 seconds. The lead vehicle speed (V_{lead}) was disturbed by a randomized sum of sinusoids (see Section 4.2.2). The secondary task was a reaction-time task: reacting as quickly as possible to small purple rectangles that appeared in the driving scene in the central and peripheral fields of view (see Figure 57).

All subjects were explicitly instructed not to use the brake pedal: all corrections were to be made with the gas pedal. During driving, the visual stimuli were presented randomly on a radius of 50 pixels ($\approx \frac{1}{20}$ of screen width) from the centre of the screen (see Figure 57b) and peripherally on a vertical line 400 pixels ($\approx \frac{2}{5}$ of screen width) from the centre of the screen (see Figure 57a). Subjects were asked to respond as quickly as possible to the visual stimuli by pressing the spacebar of a keyboard that was located to the right of the steering wheel. No stimuli were presented while the THW-indicator was visible.

[1] This experiment has been part of the work of the Master Thesis of Borra (2003). Part of the results of this experiment have also been published in a conference paper titled "Car-Following Support With Haptic Gas Pedal Feedback" (Mulder *et al.*, 2004a) and in a conference paper titled "Reaction-Time Task During Car-Following with an Active Gas Pedal" (Mulder *et al.*, 2004b).

Apparatus

The fixed-base driving simulator, described in Section 4.1, was used for this experiment. Some software adjustments were made to present the visual stimuli on the same screen as the driving scene. The maximum accuracy with which the reaction times could be detected was 10 [ms]



a) the peripheral visual stimuli were shown randomly on a vertical line 400 pixels from the screen centre (vertical bars not shown in actual driving scene).



b) the central visual stimuli were shown on a circle with a radius of 50 pixels from the screen centre (circle not shown in actual driving scene).

Figure 57: Driving simulator screen shots of the driving scene in which the peripheral (a) and central (b) field of view visual stimuli are shown.

Independent variables

Three different driver support system conditions, *S*, were tested between drivers. The first, base-line condition was the condition in which no haptic feedback was presented to drivers, i.e. the pedal was passive, just like in a normal car. Both other conditions presented haptic feedback to the driver, but differed in the way the feedback was generated and presented to drivers. The first haptic feedback condition presented drivers with an increase of the force on the gas pedal as a function of time-headway (THW) and time-to-contact (TTC) as described in Section 3.3.1. The second haptic feedback condition presented drivers with an increase of the stiffness of the gas pedal as a function of THW only, as described in Section 3.3.2.

The visual stimuli, *V*, were presented either in the central field of view (FOV) or in the peripheral FOV. Summarising the independent variables and their levels:

1. Driver support system state, *S*: *off*; *force-feedback*; *THW-stiffness feedback*.
2. Visual stimuli, *V*: *central* and *peripheral*.

Experiment design

The experiment was a within-subjects design for the driver support system conditions and a between-subjects design for the visual stimuli. In other words, some drivers (10) were assigned the condition without the haptic feedback system engaged, some (8) with the force-feedback system, and some (10) with the stiffness-feedback system. All drivers had to respond to all the visual stimuli.

Drivers were required to continuously maintain a *THW* of 1.5 [s]. The characteristics of the lead vehicle speed disturbance were constant throughout the experiment. Around a stationary speed of 80 [km/h] the lead vehicle speed was disturbed with a signal that was constructed as a sum of sinusoids with a bandwidth f_d=0.5 [Hz] and an amplitude A_d=10 [km/h]. To the subjects this signal manifested itself as an unpredictable speed disturbance of the lead vehicle speed. The total number of visual stimuli that were presented in total was one hundred: fifty were projected in central field of view, and fifty in the peripheral field of view. These stimuli were presented at random in time and position.

Each driver was given approximately 25 minutes of driving time, in which 20 sections of one minute were separated with the appearance of the THW-indicator (see Section 4.2.1). Each time, the THW-indicator was visible for 10-15 seconds. Before starting the experiment, drivers were given a 5 minute training session to get used to driving in the simulator and the reaction-time task.

Dependent measures

From the data recorded during the experiment, a number of variables were derived with which the hypotheses were tested. These derived variables are: (1) performance, (2) control effort, (3) physical load, and (4) reaction times to visual stimuli. How these variables were derived has been discussed in Section 4.3.

6.1.2 Hypotheses

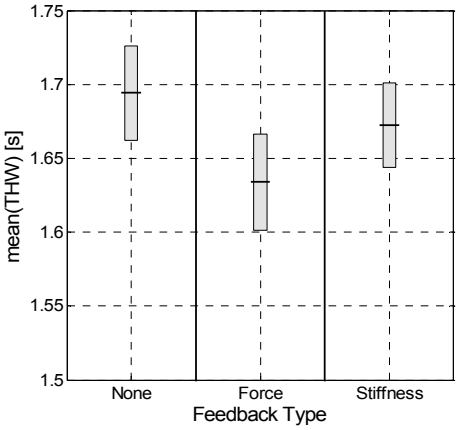
It was hypothesized that if the reaction times to the visual stimuli increased for driving with haptic feedback compared to the base-line condition without haptic feedback, this would be either because the haptic feedback loop required additional attention or because there was a modality interference due to similar response mapping (McLeod, 1977). If there were no difference in reaction times for the haptic feedback conditions, this could mean a number of things. First, it could indicate that there was no competition for attentional resources between the visual and haptic processes. Second, it could indicate that there are no modality interference effects. Third, it could hint at rapid task-switching of the drivers. Finally, a decrease in reaction times was hypothesized to be caused by the haptic feedback supporting drivers in their driving task, making more attentional resources available for other tasks, for example, responding to visual stimuli.

6.1.3 Results

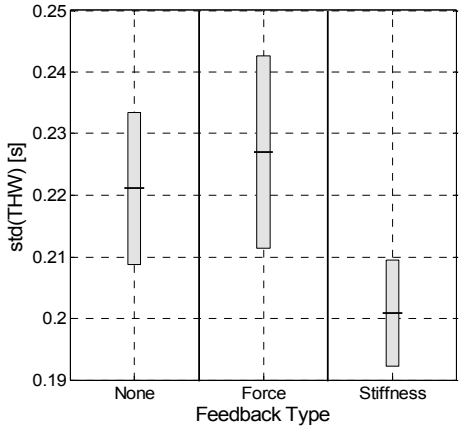
Two subjects showed relatively high *THW*'s (mean > 2.0 [s]) over the duration of the experiment. In numerous car-following experiments it is found that the ability to judge relative speed is approximately inversely proportional to inter-vehicle spacing (Evans, 1991). Judgement of relative speed has been shown to be of significant importance in headway estimation (Rockwell, 1972). Therefore, these two subjects were removed from the dataset, since their car-following behaviour was too much influenced by their high *THW*'s.

Car-following performance

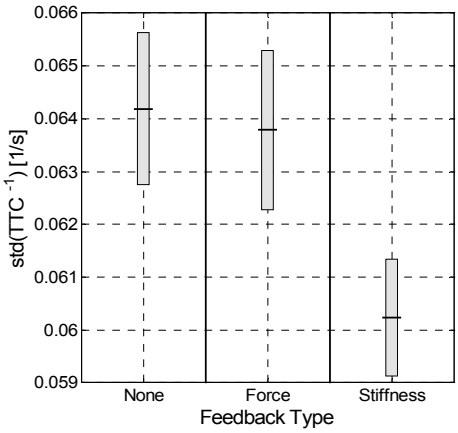
Mean measured *THW* was higher for all conditions than the 1.5 [s] at which drivers were instructed to drive (see Figure 58a). A significant ($F_{2,505}$=3.392; 0.01<p≤0.05) difference in *THW* was found for *S*. Tukey-b post-hoc analysis yielded two subsets of *S* for which *THW* was different. The force feedback and stiffness feedback conditions yielded significantly lower *THW* compared to the subset of stiffness feedback and no feedback. For σ_{THW}, however, only the stiffness feedback condition yielded significantly ($F_{2,505}$=5.394; p<0.01) lower values than force feedback and the base-line, no feedback condition (see Figure 58b). This also resulted in significantly ($F_{2,505}$=11.179; p<0.01) lower $\sigma_{TTC^{-1}}$ for the stiffness feedback (see Figure 58c).



a) mean *THW* for all conditions



b) standard deviation of *THW* for all conditions



c) standard deviation of TTC^{-1} for all conditions

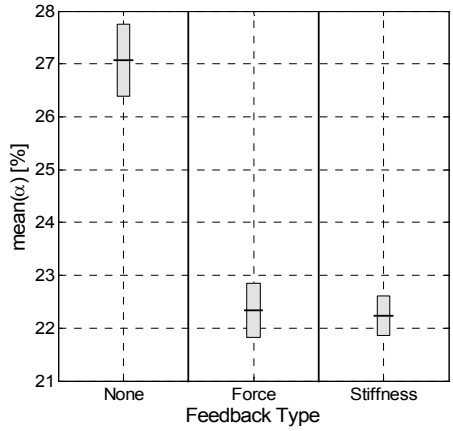
Figure 58: The means (horizontal lines) and 95% confidence intervals (gray bars) of the car-following performance indicators.

Control effort

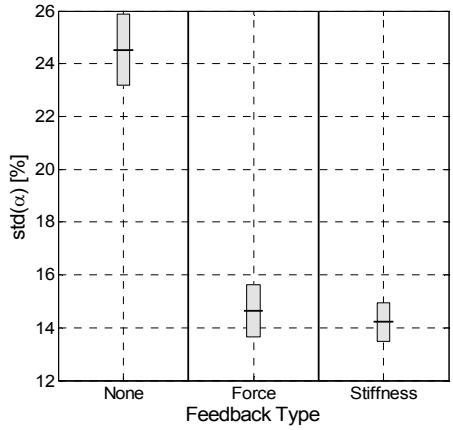
Figure 59a shows the highly significant ($F_{2,505}$=106.480; p<0.01) reduction in mean gas pedal depression, $\overline{\alpha}_p$, resulting from the use of haptic gas pedal feedback. Furthermore, a highly significant ($F_{2,505}$=124.488; p<0.01) reduction in σ_{α_p} is achieved with haptic gas pedal feedback (see Figure 59b), leading to significant ($F_{2,505}$=92.198; p<0.01) less foot-off-pedal time (α_p=0) as compared to the condition without haptic feedback (see Figure 59c).

Physical load

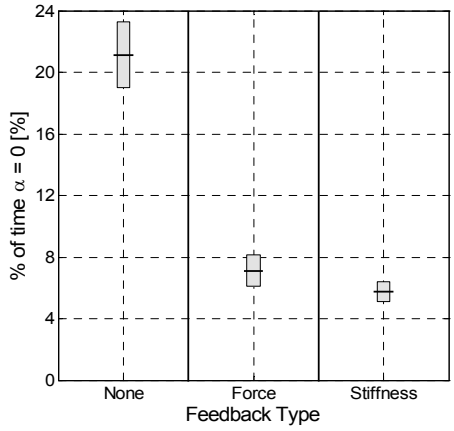
It is interesting to notice that the mean force, $\overline{F_p}$, exerted on the gas pedal by the drivers, did not change significantly (see Figure 60a). The standard deviation, σ_{F_p}, did change significantly ($F_{2,505}$=92.198; p<0.01), with the stiffness condition having the lowest and the condition without haptic feedback the highest σ_{F_p} (see Figure 60b).



a) mean gas pedal depression, α_p, for all conditions

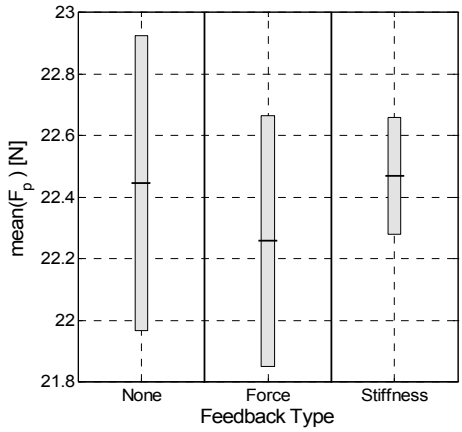


b) standard deviation of the gas pedal depression for all conditions

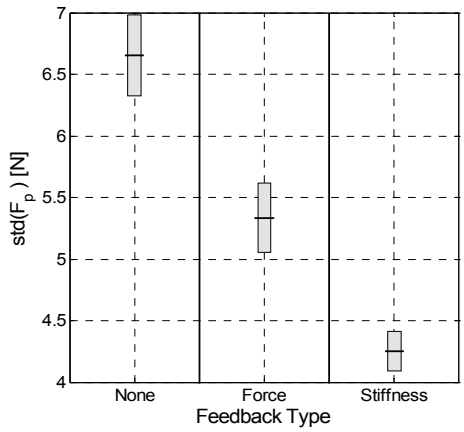


c) percentage of time the gas pedal was not depressed for all conditions

Figure 59: The means (horizontal lines) and 95% confidence intervals (gray bars) of the car-following control effort indicators.



a) mean force, F_p, exerted on the pedal by the drivers, for all conditions



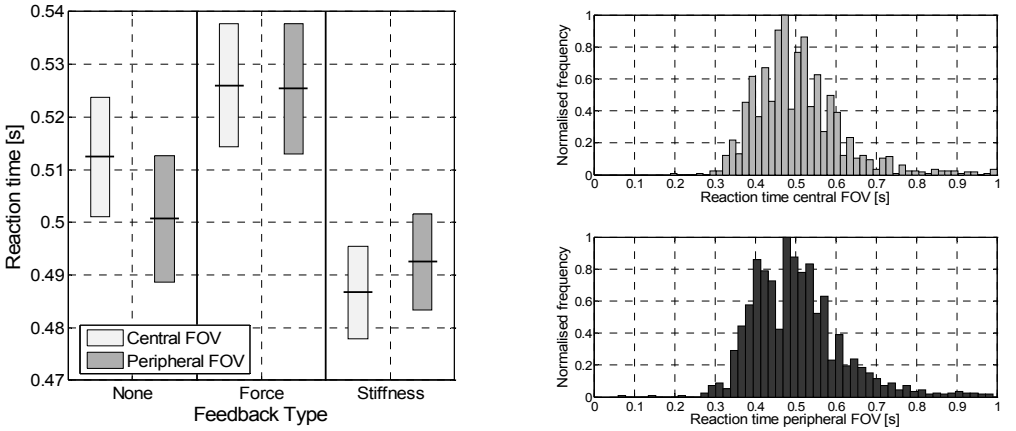
b) standard deviation of the gas pedal force, F_p, exerted on the pedal by the drivers, for all conditions.

Figure 60: The means (horizontal lines) and 95% confidence intervals (gray bars) of the car-following physical load indicators.

Reaction times

From the difference in visual stimulus onset-time and subject reaction-time the reaction time to the visual stimuli was calculated. Stimuli were presented to drivers for a maximum time of three seconds. From literature it is known that a simple visual reaction-time task yields reaction times between 0.15 [s] (Evans, 1991) and 0.18 [s] (Brebner and Welford, 1980). Because the reaction-time task was given as a secondary task, it was expected that reaction times would be higher than in simple reaction-time experiments. For this experiment, reaction times less than 1.00 [s] were considered to be valid reaction times (see Figure 61b). Reaction times between 1.00 [s] and 2.99 [s] were considered late detections. Above 3.00 [s] reaction times were considered missed detections.

ANOVA statistics revealed significant differences in reaction times to stimuli in the central field of view (T_{CFOV}) conditions ($F_{2,1229}$=12.872; p<0.01). A Tukey-b post-hoc analysis showed that the stiffness condition had significantly lower central FOV reaction times compared to the base-line and force feedback condition as can be seen in Figure 61a. Also, for the peripheral stimuli, a significant difference in reaction times (T_{PFOV}) was found ($F_{2,1276}$=8.110; p<0.01). The force feedback condition yielded a higher peripheral FOV reaction-time as compared to the base-line and stiffness condition. No significant differences between central and peripheral reaction times were found. Ando *et al.* (2002) refer to a body of literature that show reaction times to stimuli in the peripheral FOV generally are higher than reaction times to visual stimuli in the central FOV. The absence of differences might be explained by the minimum accuracy with which reaction times that could be measured with the available equipment: 10 ms. This measuring accuracy is in the order of magnitude of the differences between central and peripheral FOV reaction times generally found for simple-reaction time tasks Ando *et al.* (2002).



a) mean reaction times (horizontal lines) and 95% confidence intervals (gray bars) for the central and peripheral FOV for all conditions

b) reaction time distributions for the central and peripheral FOV for all conditions combined.

Figure 61: The mean reaction times for each condition separately (a) and the distributions (b) of the reaction times for the central and peripheral field of view (FOV), combined for all conditions.

Very few late detections were recorded and even less missed detections: 35 and 8 out of 2761 recorded detections, respectively. False detections were not recorded. The visual stimuli were rather big, had a high contrast with the background, and, since a one second detection time is long considered the average detection time of 0.15 – 0.18 [s] for a simple reaction task (Brebner and Welford, 1980) these low counts on late and missed detections can be explained.

6.1.4 Discussion of the results

The results of the ANOVA statistical analysis are summarised in Table 5. Haptic feedback did not change the car-following strategy in this particular experiment, that is, the trade-off between minimising *THW* and *TTC* errors, since neither haptic feedback condition shows a different weighing of either term. The stiffness condition shows small, but significant reductions in both variables, suggesting a slight overall improvement in car-following performance for this experiment condition.This is an interesting result, since the reaction times to stimuli in the central FOV are lower for the stiffness feedback condition. At the same time, the control activity that was found for the stiffness feedback condition is similar to that of the force feedback condition. However, the force feedback condition did not yield improved reaction times to the central FOV stimuli. More importantly, the force feedback condition actually resulted in significantly higher reaction times to the peripheral FOV stimuli compared to the other two conditions. This appears to suggest that haptic feedback influences the processing of visual information and that the type of feedback influences the way the processing of visual information is affected.

The significant reductions in control activity for the haptic feedback systems show that most is gained in increasing driver comfort during car-following control. However, since the fixed-base driving simulator that was used in this experiment does not have a motion system – hence drivers did not experience any acceleration cues – this big reduction in control effort

cannot entirely be ascribed to the presence of haptic feedback. Rockwell and Snider (as mentioned in Rockwell, 1972) indicate that humans can sense ±0.01 [g] of vehicle acceleration. As can be seen in Figure 62, standard deviation of the acceleration of the own vehicle (a_{car}) is well above that threshold. What can be seen too, is that the standard deviation of the acceleration for the condition without the haptic feedback has been significantly ($F_{2,505}$=124.583; p<0.01) higher than for the haptic feedback conditions.

Table 5: Summary of the results of the One-way-ANOVA statistical analysis of the dependent measures, with significance level α=0.05. In the table, •••, ••, and • denote a significance of $p\leq0.01$, $0.01<p\leq0.05$, and $0.05\leq p<0.1$ respectively and '-' denotes no significance.

	Following performance			Control effort			Physical load		Reaction time	
	$\overline{THW}$	σ_{THW}	$\sigma_{TTC^{-1}}$	$\overline{\alpha_p}$	σ_{α_p}	t_r	$\overline{F_p}$	σ_{F_p}	T_{CFOV}	T_{PFOV}
Main effects										
S	••	•••	•••	•••	•••	•••	-	•••	•••	•••

Neither haptic feedback condition showed negative influences on the physical load drivers experienced during the experiment. Nevertheless, it is expected that driving at shorter time-headways will increase the physical load experienced by drivers since the corresponding feedback forces will be higher. The standard deviations of the pedal forces indicate that drivers have an inclination to adopt a more force-task like strategy when the haptic feedback system is active, since for both systems the standard deviations of the pedal force are significantly lower than for no haptic feedback condition. This effect is of course partly due to the higher control activity displayed by drivers in the no feedback condition.

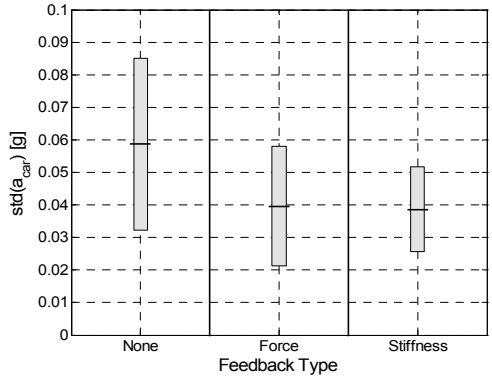


Figure 62: Standard deviation of the acceleration of the own car (horizontal lines) and 95% confidence intervals (gray bars) for all conditions.

6.1.5 Conclusions

1. It is believed, based on the observed decrease in control effort and standard deviation of the forces exerted on the gas pedal, that drivers adopt a force-task strategy for the tested conditions when provided with haptic feedback.
2. The hypothesis that an increase in reaction times is caused by modality interference is rejected on the grounds that the stiffness feedback condition decreased the reaction times to central visual stimuli, even though the force feedback condition increased the reaction times to peripheral stimuli.
3. It was concluded that, under the conditions of the experiment, the results showed that the force feedback condition required additional attention of the drivers.
4. The combined decrease in reaction times and increase in car-following performance resulted in the acceptance of the hypothesis that the stiffness feedback condition helped drivers in their car-following task allowing them more time for other attentional processes.

6.2 Audio system track selection task

All the experiments described so far have focussed on car-following while drivers are constantly looking at the driving scene. Even in the previously discussed experiment of Section 6.1, drivers were given a reaction-time task with visual stimuli in the driving scene. The major problem of course is when drivers are *not* looking at the driving scene, but are directing their attention elsewhere, for example, to their mobile phone, their navigation system, or their stereo system.

Traffic accident statistics show that driver inattention is a major cause of over 60% of all rear-end collisions (Knipling, *et al*., 1993). Development of driver support systems is therfore, not surprisingly, focussing on rear-end collision avoidance systems (for example, Tijerina, *et al.*, 2000; Godthelp and Schumann, 1993). The DSS discussed in this thesis is not primarily designed to be an active rear-end collision support system, but the haptic feedback does extend into critical areas where rear-end collisions can be eminent. The haptic information drivers receive through the gas pedal, might prompt drivers earlier to redirect their (visual) attention to the driving scene when they are engaged in a non-driving related task for which they are directing their (visual) attention away from the driving scene.

An experiment was set-up to create just such kind of driving scenarios. In the fixed base driving simulator a car-following task was prepared during which drivers were frequently asked to change the track that was playing on the simulated car-stereo system. Even though the controls to manipulate the cd-player are mounted on the steering wheel, such that drivers do not have to move their hand from the steering wheel, they will need to monitor their cd-player display frequently to check whether they have selected the right track. In other words, drivers are frequently asked to engage in a secondary task, that requires them to remove their visual attention from the driving scene into the car, to look at the cd-player display.

The goal of this experiment is to investigate whether the haptic feedback systems that have been discussed in this thesis (Section 3.3.1, 3.3.2 and 3.3.3) are effective in supporting the driver in maintaining proper separation with a lead vehicle when also engaged in an in-vehicle task. Furthermore, the three algorithms are compared with a base-line condition, in which no haptic feedback is available, to determine which changes in driver behaviour can be ascribed to the presence of haptic feedback. In the next subsections, the experiment will be described in detail, with a statistical analysis of the results.

6.2.1 Method

Subjects

Nine subjects participated in the experiment, eight of whom had driven in the driving simulator before. Three subjects were female, six male. Average age of the subjects was 26±2.2 years old. Driving experience ranged from 1 to 10 years, averaging 6.6±2.5 years. Subjects reported an average driving frequency of 3±2.4 times per week, totalling approximately 6500 [km] a year.

Task instruction

Drivers were instructed to follow the lead vehicle at the, by the THW-indicator indicated, *THW* as good as they possibly could. Drivers were *not* explicitly instructed on the use of the gas pedal and brake pedal, other than that the haptic feedback would be most beneficial when yielding to the imposed pedal forces.

For the secondary task, drivers were instructed on how to use the CD-player controls that were mounted on the steering wheel. It was explained that when a "beep" was heard, they should initiate the CD-player task by selecting the track indicated on the display, below the picture of the CD-player. When the correct track was chosen, the time, to which to forward the selected track appeared and drivers were instructed to fast-forward to this particular time. To indicate the completion of the CD-player task, the middle mouse button needed to be clicked. The instructions said the objective was to complete the secondary task as quickly and as accurately as possible, that is, finish the task when the track is at the desired track and the track is fast-forwarded to the desired time.

Drivers were implicitly instructed that their main task was to maintain the proper separation with the lead vehicle. The secondary task needed to be completed as fast and accurately as possible, *without* compromising the primary task of car-following.

All drivers received their instructions in digital form, through e-mail, some days before the experiment. On the day of the experiment they were given the opportunity to read the instructions again.

After the completion of each run, drivers were asked to fill out a short six-question questionnaire with which they had to rate the usefulness of the haptic feedback while not engaged in the cd-task and while they were engaged during the cd-task. The ratings were given on a scale from one to nine, with five always the neutral answer. The scores have been

normalised by subtracting five and then dividing by four. Thus yielding a maximum score of one, a neutral score of zero, and a minimum score of minus one.

Apparatus

The fixed-base driving simulator, described in Section 4.1, was used to carry out the experiment. For this particular experiment, a mouse was mounted upside-down on the steering wheel to provide the controls for the CD-player (see Figure 63). The upper and lower mouse buttons were used to control the CD-player. A click (pressing less than 0.5 [s]) of either the upper or lower mouse button, would respectively increase or decrease the track currently playing. By pressing (longer than 0.5 [s]) either the upper or lower mouse button, drivers could respectively fast-forward or fast-rewind in track-time of the currently playing song. Fast-forwarding or fast-rewinding had two speed stages. After 2.5 [s] the forwarding or rewinding speed doubled. With the middle button, drivers could mark the completion of a task.



a) position of the mouse as it was mounted on the steering wheel

b) the CD-player as it was displayed in the driving simulator, with track-time on the left and track number on the right

Figure 63: Driving simulator additions to enable the secondary CD-player task. The steering wheel (a) was extended with an upside-down computer mouse. To the right of the driver, at approximately the same height as the steering wheel axle, the CD-player was displayed (b).

The CD-player was displayed on an LCD-screen to the right of the driver. A picture of a real car CD-player was placed in such a position on the screen that it more or less resembled the location where, in a real car, a CD-player can normally be found. Only track and track-time were shown in the CD-player display. The required track and track-time to be selected by the driver were shown below the picture of the CD-player.

Independent variables

The independent variables in this experiment are *THW* and the type of haptic feedback *S*. *THW* has two levels, *S* has four levels:

1. Required *THW, T*: 0.5 and 1.0 [s].
2. Support system, S: *off*; *force*; *THW-stiffness*; *TTC-stiffness*

Experiment design

A within subjects design was used to carry out the experiment. In other words, each driver was subjected to each combination of the independent variables – which yielded 3x4=12 conditions. These conditions were randomly presented to each driver, with the exception that first every level of *T* was driven before the level of *S* was changed. This was done to prevent drivers from having to switch between driver support system every time a different level of *T* was selected. The order in which the levels of *S* were presented to drivers was randomized between drivers.

For each condition, that is, each combination of *T* and *S*, drivers were given 10 minutes of driving time. Each minute of these 10 minutes of driving time was separated by 10-15 seconds in which the THW-indicator (see Section 4.2.1) was visible – 're-calibrating' drivers at the required *THW* of 0.5 or 1.0 [s]. During each minute drivers would hear a short "beep", some 15±5 seconds after the THW-indicator had disappeared, which was the starting signal for the secondary cd-task. Thus, for each condition, drivers executed the cd-task ten times.

Dependent measures

For this experiment, the car-following performance, control effort, and physical load indicators were determined before, during, and after the execution of the cd-task. By splitting up the dependent measures in these three segments, the influence of the task on driving behaviour can be investigated as well – besides the influence of the independent measures on the driving task as a whole.

From the data collected on the performance of the cd-task, task-completion time is the most important measure. Task-completion time is defined as the elapsed time since the moment the "beep" was sounded and the moment a subject clicks the middle mouse button to indicate she/he has completed the cd-task. Two other measures are recorded to give an indication of the accuracy with which drivers complete the cd-task. They are, first, the track-error, which is the difference between the selected track and the track that is required of the drivers to be selected. Second, the track-time-error is measured too, which is the difference (in seconds) between the selected track-time and the track-time that is required of the driver.

Finally, a short questionnaire (6 questions) is given to drivers after each condition, in which drivers have to rate the driving task and the usefulness of haptic feedback when concentrating only on the car-following task (before and after the cd-task) and while performing the secondary task (during the cd-task). The results of the questionnaire are used as a subjective evaluation of the tested conditions.

6.2.2 Hypotheses

It is expected that drivers, when haptic feedback is available, will show better car-following performance compared to using no haptic feedback. Furthermore, the best performance is expected from the TTC-stiffness feedback, as it combines the most salient haptic information (stiffness) with, what is believed to be, the most useful environmental information – *TTC*. All haptic feedback conditions are expected to show the adoption of force-task strategies in controlling the gas pedal. Based on the results of the previously discussed

experiments, it is expected that the force feedback condition and the TTC-stiffness conditions will show the force-task strategy most clearly.

With respect to the cd-task, it is expected that the presence of haptic feedback will allow drivers to spend more time away from the driving scene, diverting more time to the cd-task, while not compromising car-following performance. This is expected to be evident in shorter task-completion times and more accurate task performance (less track and track-time errors). Summarised, the hypotheses are formulated as follows:

1. The presence of haptic feedback will improve car-following performance.
2. The TTC-stiffness feedback algorithm will show the best car-following performance
3. The presence of haptic feedback will lead drivers to adopt a force-task strategy in controlling the gas pedal.
4. With haptic feedback performance of the cd-task will improve, leading to shorter task-completion times and less track and track-time errors.

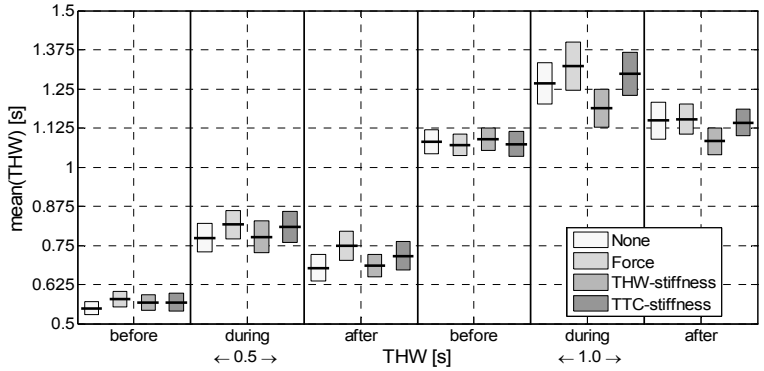
6.2.3 Results

Car-following performance

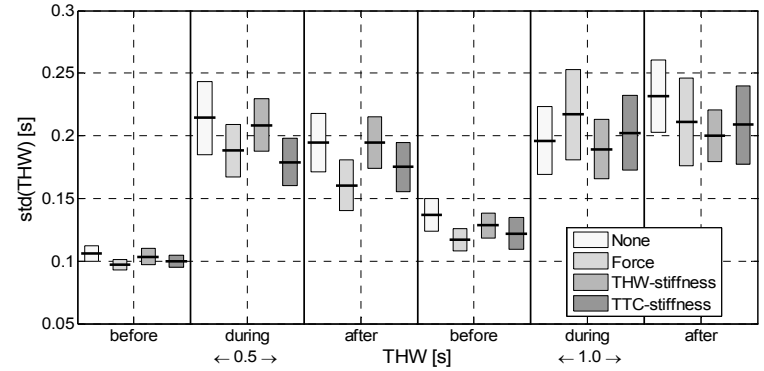
From the statistical analysis of the dependent measures (univariate ANOVA), it follows that *S* did not have a significant effect on the mean *THW*, $\overline{THW}$. The $\overline{THW}$ was, however, significantly ($F_{5,40}$=169.411; p<0.01) influenced by the cd-task. Drivers tend to drive further from the required *THW* during and after the execution of the cd-task, but even more so during the cd-task. A Tukey-b post-hoc analysis of the ANOVA results show that the $\overline{THW}$ at which drivers end up driving after the cd-task is lower than during the cd-task, but higher than before the cd-task (see Figure 64a).

The standard deviation of *THW*, σ_{THW}, was significantly ($F_{5,40}$=15.887; p<0.01) increased by both the cd-task as well as the *THW* at which drivers were asked to drive (see Figure 64b). Post-hoc analysis revealed that, contrary to the mean *THW*, the standard deviation of *THW* did not decrease significantly anymore after the cd-task. No significant influence of the support system *S* was found.

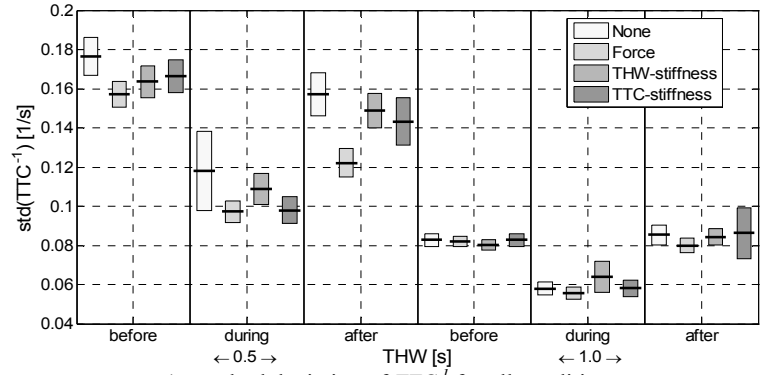
Even though car-following performance does not seem to have been improved by the presence of haptic feedback, some small improvements were found for the standard deviation of TTC^{-1}. The $\sigma_{TTC^{-1}}$ significantly ($F_{5,40}$=144.119; p<0.01) decreased during the cd-task, for both *THW*'s at which drivers were asked to drive (see Figure 64c). This is mainly due to the significant increase in $\overline{THW}$ during the cd-task. Nevertheless, a significant ($F_{3,24}$=3.569; 0.01<p≤0.05) effect of *S* was found. Post-hoc analysis shows that the force feedback yields the lowest $\sigma_{TTC^{-1}}$ and the condition without haptic feedback the highest. Both stiffness conditions yielded a $\sigma_{TTC^{-1}}$ in between the two other levels of *S*. Furthermore, a significant ($F_{15,120}$=1.983; 0.01<p≤0.05) interaction between *S* and *T* was found because the differences in $\sigma_{TTC^{-1}}$ between the conditions with haptic feedback and the one without become smaller with the increase in *THW*. Appendix B.1.2 shows the distributions of *THW* and TTC^{-1} in the THW-TTC^{-1} phase plane.



a) mean *THW* for all conditions



b) standard deviation of *THW* for all conditions



c) standard deviation of TTC^{-1} for all conditions

Figure 64: Car-following performance indicators for all conditions. The x-axis levels of *T*, the required *THW*, are divided into three sections: before, during, and after the cd-task. The clustered levels of *S*, the support system type, are shown in shades of gray.

Control effort

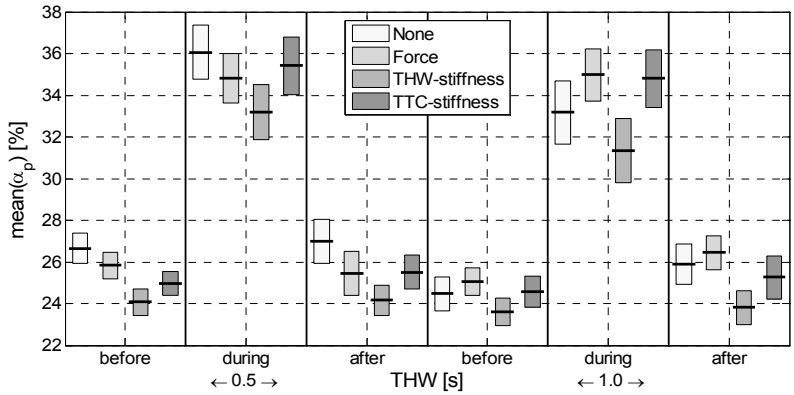
Mean gas pedal depression $\overline{\alpha}_p$ increases significantly ($F_{5,40}$=118.868; p<0.01) during the cd-task, but upon completion, comes back to the level at which it was before the cd-task was initiated (see Figure 65a). Only the THW-stiffness level of *S* has a significant ($F_{3,24}$=8.023; p<0.01) lower $\overline{\alpha}_p$ compared to the other levels of *S*. This difference increases for the increase in *THW* from 0.5 to 1.5 [s], leading to a significant ($F_{15,120}$=2.061; 0.01<p≤0.05) interaction between *S* and *T*.

The standard deviation of the gas pedal depression decreases significantly ($F_{5,40}$=7.847; p<0.01) with increasing *THW*. Also, significant ($F_{3,24}$=13.743; p<0.01) differences in σ_{α_p} are found for different *S* (see Figure 65b). From the Tukey-b post-hoc analysis it is found that the THW-stiffness yielded the lowest and the force feedback the highest σ_{α_p}. The condition without haptic feedback and the TTC-stiffness yielded similar σ_{α_p}, with values in between the other two levels of *S*.

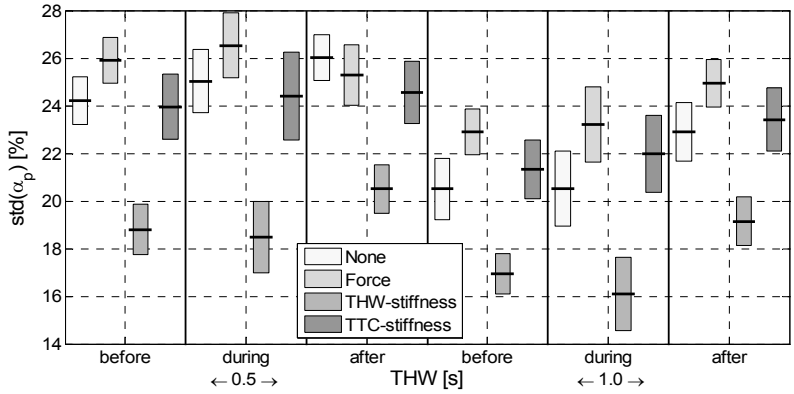
The percentage of time drivers have their foot off the gas pedal, t_r, decreases significantly ($F_{5,40}$=65.963; p<0.01) during the cd-task and with an increase in *THW* (see Figure 65b). Furthermore, the different support systems have had a significant ($F_{3,24}$=12.668; p<0.01) influence on t_r as well. With Tukey-b post-hoc analysis it was found that the THW-stiffness condition has the lowest value of t_r, the TTC-stiffness the second lowest, lower than the condition without haptic feedback. The force feedback condition yielded the highest values for t_r.

Physical load

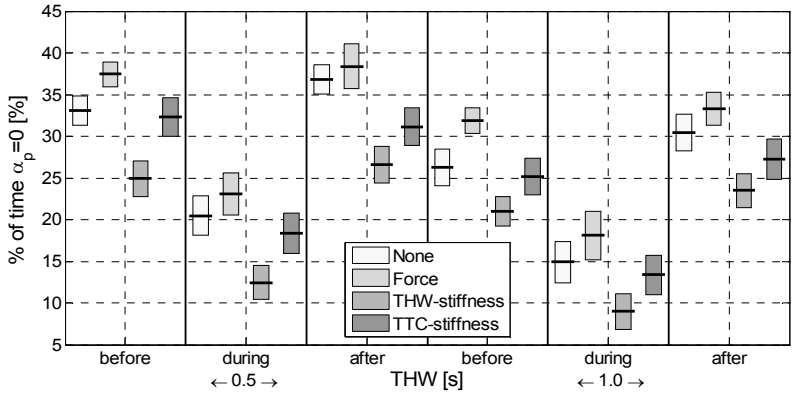
From Figure 66a it is easily seen that the force feedback and THW-stiffness conditions yielded the highest mean pedal forces $\overline{F}_p$ – significantly ($F_{3,24}$=108,300; p<0.01) higher than for the TTC-stiffness condition and the condition without haptic feedback. *THW* also has a significant ($F_{5,40}$=18.817; p<0.01) effect on $\overline{F}_p$ – an increase in *THW* leads to a decrease in $\overline{F}_p$. The cd-task also influence the $\overline{F}_p$. During the task drivers increases the $\overline{F}_p$. This is especially the case for the THW-stiffness condition. From post-hoc analysis it follows that the order, from low to high $\overline{F}_p$ is: no haptic feedback, TTC-stiffness feedback, force feedback, THW-stiffness feedback.



a) mean measured gas pedal depression, for all conditions

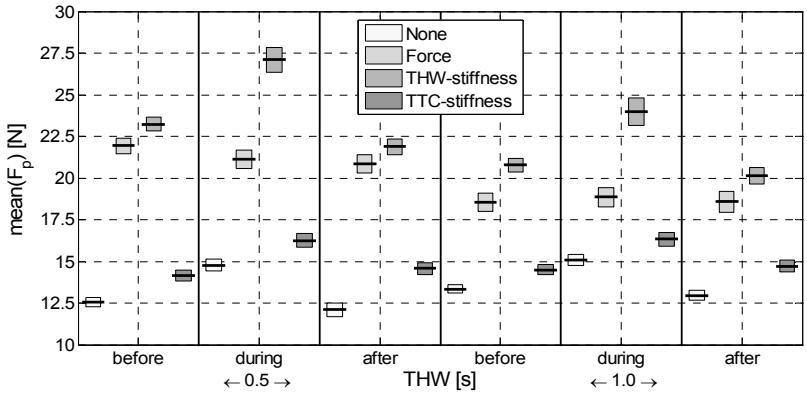


b) standard deviation of the gas pedal depression, for all conditions

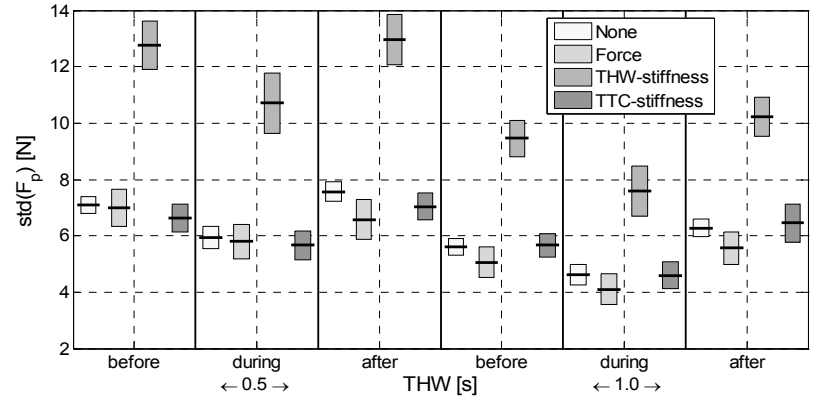


c) percentage of total driving time drivers did not depress the gas pedal

Figure 65: Control effort indicators for all conditions. The x-axis levels of *T*, the required *THW*, are divided into three sections: before, during, and after the cd-task. The clustered levels of *S*, the support system type, are shown in shades of gray.



a) mean measured pedal force for all conditions



b) standard deviation of the measured pedal force, for all conditions

Figure 66: Physical load indicators for all conditions. The x-axis levels of *T*, the required *THW*, are divided into three sections: before, during, and after the cd-task. The clustered levels of *S*, the support system type, are shown in shades of gray.

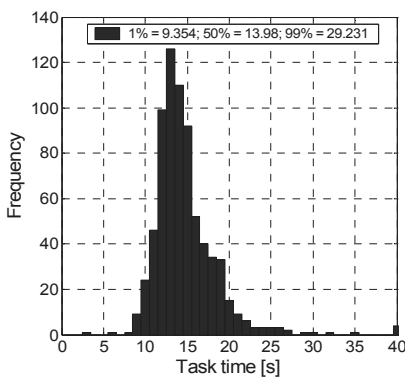
The standard deviation σ_{F_p} of the gas pedal force does not seem to be influenced by the cd-task, except for the THW-stiffness condition ($F_{5,40}$=41.107; p<0.01). Post-hoc analysis shows that this is the case (see Figure 66b). Significant ($F_{3,24}$=24.160; p<0.01) differences due to the different haptic feedback systems are found, with the force feedback condition yielding the lowest σ_{F_p}, the THW-stiffness condition the highest, and the no-feedback and TTC-stiffness conditions yield values in between. Because the differences in σ_{F_p} between the levels of *S* become smaller with increasing *THW*, a significant ($F_{15,120}$=4.604; p<0.01) interaction is found between *S* and *T*.

Task performance

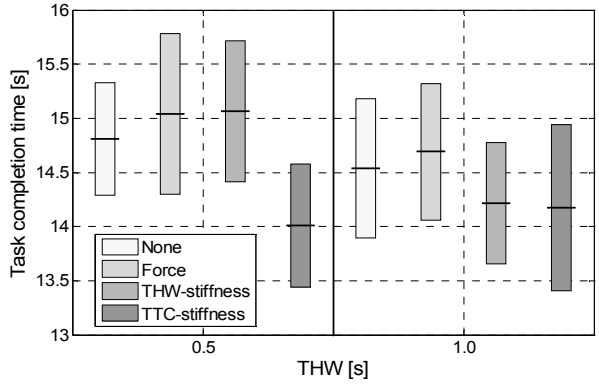
When looking at the distribution of the task-completion times (see Figure 67a), it can be seen that 99% of the responses are within 29.2 seconds. Only 1% of the responses are faster then 9.4 seconds. Therefore, for the statistical analysis of the task performance, task-completion times higher than 29 [s] are counted as not completed and task-completion times faster than 9 [s] are counted as completed too early.

Although it looks (in Figure 67b) like the TTC-stiffness condition has yielded a lower task-completion time for *THW*=0.5 [s], ANOVA reveals that this is not a significant difference. Furthermore, the task-completion times seem to be a little bit lower for *THW*=1.0 [s] as compared with *THW*=0.5 [s], but this is also found not to be significant.

The accuracy of the cd-task was high, as the mean track error over all results is only 0.056, with a standard deviation of 0.91. So, on average drivers made no errors in selecting the right track. If they did select the wrong track, this was most of the time not more than one track off the track they were required to select. No significant differences between the conditions of *S* and *T* were found. Also, the track-time errors were very small. The mean error over all results is 0.05 [s], with a standard deviation of only 1.9 [s]. In other words, most of the time, drivers selected the required track-time. If they selected the wrong track time, this was on average only 1.9 [s] from the track-time they were required to select. No significant differences between the different conditions of *T* or *S* were found.



a) distribution of the task-completion times for all conditions together



b) mean task-completion times for each level of *T* and each level of *S* (shades of gray)

Figure 67: Statistics of the task-completion times: distribution (a) of the task-completion times and mean task-completion times for each condition (b).

Subjective evaluation

Drivers were given 3 different questions to rate their task during normal car-following and during car-following while executing the cd-task (see Table 6). The results of the driver scores are presented in Figure 68a and Figure 68b.

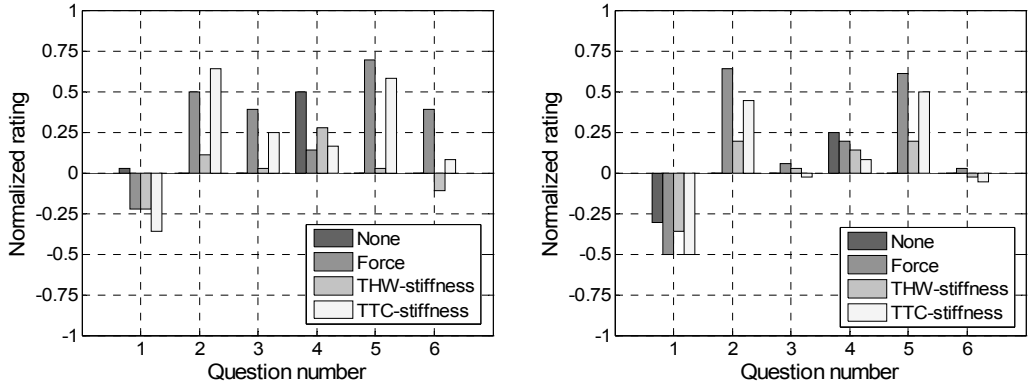
Table 6: The three questions that were asked after each driving condition was tested. The questions were asked for normal car-following (1-3) and for car-following while executing the cd-task (4-6).

No.	Question
1 & 4	How difficult was the car-following task?
2 & 5	How helpful was the feedback force on the gas pedal for the car-following task?
3 & 6	How high was the feedback force-level you felt from the gas pedal?

At *THW*=0.5 [s], drivers rated the car-following task as easy (question 1), but less easy than at *THW*=1.0 [s]. With the presence of haptic feedback the car-following task seems to be rated as easier for both levels of *T* compared to the base-line condition without haptic feedback, but this difference was not found to be significant. The force feedback and the TTC-stiffness

feedback were rated as giving the most helpful (question 2) haptic feedback at both *THW*=0.5 [s] as well as *THW*=1.0 [s]. The THW-stiffness feedback was rated neutral. Drivers experienced the forces (question 3) of the force feedback and TTC-stiffness feedback to be too high at *THW*=0.5 [s], though. At *THW*=1.0 [s] the forces for all feedback algorithms were rated as good.

The ratings of the difficulty of the car-following task while executing the cd-task (question 4) were positive for both levels of *T*, that is, difficult. Only for *THW*=0.5 [s] it seems that drivers rated the car-following task to be more difficult when not benefiting from haptic feedback, but this result is not significant. Both the force feedback and the TTC-stiffness feedback were rated to be the most helpful algorithms (question 5), for either *THW*. Only the force feedback force-level was rated (question 6) to be too high at *THW*=0.5 [s]. The other feedback algorithm force-levels were rated as good for both *THW*'s.



a) *THW*=0.5 [s] b) *THW*=1.0 [s]

Figure 68: Normalized responses to the questionnaire for the two *THW*'s at which drivers were required to drive (figures a and b) and all levels of *S* (shades of gray). The questions 1-3 for normal car-following (and 4-6 for car-following while executing the cd-task) that were asked were formulated as follows. 1&4) How difficult was the car-following task 2&5) How helpful was the feedback force on the gas pedal for the car-following task 3&6) How much was the feedback force-level you felt from the gas pedal?

6.2.4 Discussion of the results

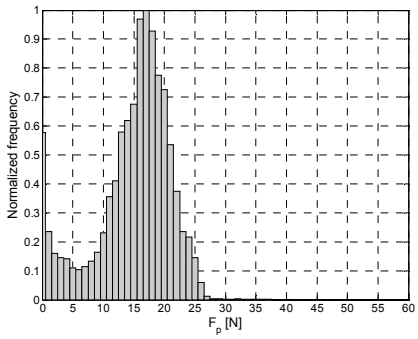
The results of this experiment show that the cd-task has had a highly significant influence on the car-following behaviour of the drivers that participated. While drivers are approximately only 0.1 seconds off the required *THW* before they commenced the cd-task, during the cd-task this bias increases to more than 0.25 seconds and is only reduced a little to approximately 0.15 seconds after completion of the task – for both required *THW*'s of 0.5 and 1.0 seconds. The bias is towards increased *THW* in both cases, which is a logical strategy when combining the car-following task with a secondary in-vehicle task, since increased headway increases the available time to react to unexpected changes in the lead vehicle speed. However, it was expected that due to the presence of haptic feedback drivers would have redundant information on their car-following situation which would have allowed them to maintain better car-following performance. This did not happen. Even with haptic feedback, providing

complementary car-following information, drivers increased their headways so as to increase their safety boundary while carrying out the secondary in-vehicle task.

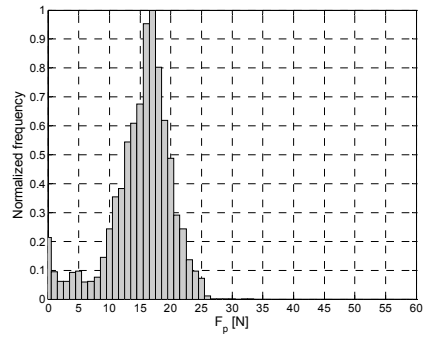
It is interesting to note that car-following performance not only changes during the cd-task, but remains at a similar level even when drivers have completed their cd-task. There is no experimental data to explain this result, but it is speculated here that this is an artefact created by the design of the experiment. Since there is no other traffic but the lead vehicle, drivers might not have any incentive or suitable reference to go back to the *THW* they were instructed to drive at after completion of the cd-task. Hence the visual bias went unnoticed. Not until the THW-indicator (see Section 4.2.1) came back on did drivers acquire a good frame of reference again.

Despite the increase in *THW* during the execution of the cd-task, driver control behaviour does not show significant changes in σ_{α_p} - the control effort. Thus, the much greater mean pedal depression, $\overline{\alpha}_p$, and the less foot-off-pedal time during the cd-task, indicate that drivers control with the same magnitude, but less frequent, that is, drivers show longer intervals of constant pedal activity while they are carrying out the cd-task. The THW-stiffness condition shows a significantly lower control effort than all the other levels of *S*. The force feedback algorithm shows a consistent higher control effort than all the other levels of *S* (except for *THW*=0.5 [s], after the cd-task). This pattern is repeated in the percentage of time for which drivers had their foot off the gas pedal. So, the presence of haptic gas pedal feedback significantly changes control behaviour but the findings of this experiment are only consistent with the findings of previous experiments for the THW-stiffness algorithm. For the other two haptic feedback algorithms no reduction is found in control effort, while this was consistently found in the experiments described in Section 6.1 and Chapter 5, even before the cd-task had started. Perhaps because most drivers that participated in the experiment (9 out of 10) had driven in the simulator before, in similar experiments, they were less inclined to change their driving strategies when the haptic gas pedal feedback was present compare to when it was not present. The results of the gas pedal force analysis is also not giving any conclusive evidence on this matter.

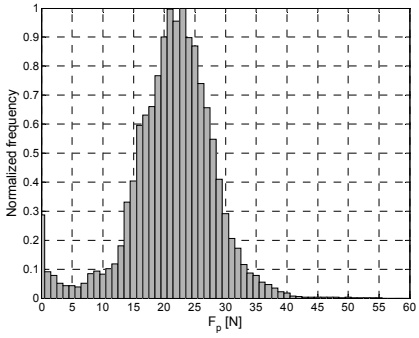
One of the central hypotheses of this dissertation is that drivers adopt a force task strategy in controlling the gas pedal when haptic feedback is available. The physical load indicators do no show much differences in σ_{F_p} except for the THW-stiffness condition, which has an exceptionally high σ_{F_p} for both *THW*=0.5 and 1.0 [s]. The cd-task also does not seem to have had much influence on the σ_{F_p}. So, did drivers adopt a force task strategy when haptic feedback was available? A tentative conclusion from the statistical analysis would be that drivers hardly adopted a force task strategy under the conditions of this experiment, because the σ_{F_p} did not change significantly for each of the levels of *S*, except for the THW-stiffness algorithm, which had greatly increased σ_{F_p} for all levels of *T*. Further analysis of the distributions of the exerted pedal forces might help to reach a more conclusive answer.



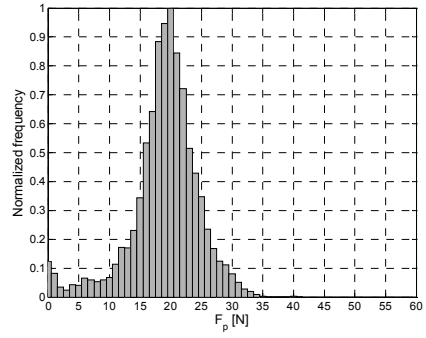
a) *THW*=0.5 [s]; No haptic feedback



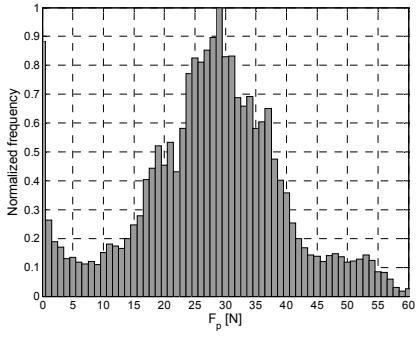
e) *THW*=1.0 [s]; No haptic feedback



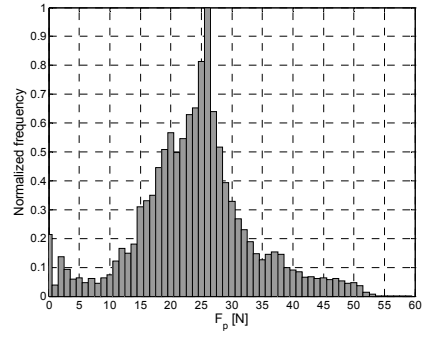
b) *THW*=0.5 [s]; force feedback



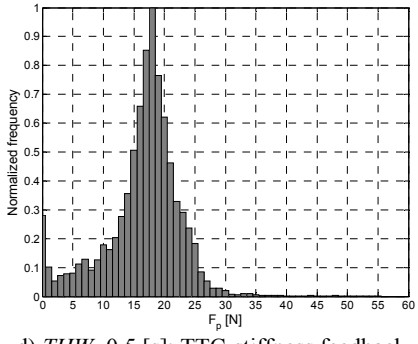
f) *THW*=1.0 [s]; force feedback



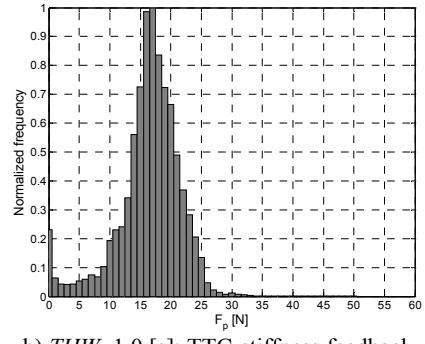
c) *THW*=0.5 [s]; THW-stiffness feedback



g) *THW*=1.0 [s]; THW-stiffness feedback



d) *THW*=0.5 [s]; TTC-stiffness feedback



h) *THW*=1.0 [s]; TTC-stiffness feedback

Figure 69: Distributions of the gas pedal forces exerted on the gas pedal by all drivers together, for all conditions during the cd-task.

Figure 69a to h show the distributions of the pedal forces exerted on the gas pedal by the drivers for all conditions during the cd-task. It can be seen from these distributions that only the THW-stiffness condition has a markedly different distribution, especially for *THW*=0.5 [s]. The maximum forces are much higher and the distribution is much flatter than in the other conditions. The other two haptic feedback conditions show little differences compared to the condition without haptic feedback. Both force and TTC-stiffness feedback conditions show distributions with narrow bases and a large concentration of force around the mean. The TTC-stiffness condition distributions appear to be a little more concentrated around the mean than the force feedback and no feedback conditions, but as was found in the statistical analysis, this is not significant. The distributions of the forces before and after the cd-task can be found in Appendix B.3.2. They show similar distributions as during the cd-task. Thus, it must be concluded that there is no conclusive evidence found for the conditions tested in this experiment that indicates whether drivers adopted a force task strategy when haptic feedback was available.

In this experiment, car-following performance was hardly influenced by the availability of haptic feedback. Even during the cd-task, drivers displayed the same kind of car-following performance and behaviour as when there was no haptic feedback provided. Drivers increased their following separation in order to create a safety boundary to execute the cd-task. The results of the cd-task show that the presence of haptic feedback also had little influence on this task. No improvements in task-completion time were found. There appears to be a slight improvement for the TTC-stiffness condition at *THW*=0.5 [s], but from the ANOVA it was found that this result was not significant. Furthermore, there were no significant changes in accuracy in completing the cd-task.

These results might be explained by the fact that the strategy drivers applied – increasing their following *THW* during the execution of the cd-task – allowed drivers to execute their task in the same manner for all conditions that were tested. In other words, the application of this strategy of increasing *THW* when an in-vehicle task demands attention has most likely been the preferred strategy, rather than to depend on the complementary haptic information that was provided when the haptic gas pedal feedback was activated. Nevertheless, the haptic information could have been used by drivers to allow themselves more time to look away from the driving scene and to spend it on the cd-task instead. Apparently drivers have not done this, although this cannot be decisively concluded since no eye tracking equipment was available to determine gaze direction. Table 7 summarizes the statistical analysis results.

Despite the lack of improved cd-task performance or car-following performance, subjects evaluated the presence of haptic feedback as being helpful and making the car-following task easier, especially at *THW*=0.5 [s]. However, at this same *THW* drivers evaluated the force-levels to be too high for the force feedback and the TTC-stiffness feedback, which is remarkable because the data suggests that it is the THW-stiffness feedback which yielded the highest forces exerted on the gas pedal by drivers. At the same time, however, drivers rated the force feedback and the stiffness feedback as most helpful both before and after and especially during the execution of the cd-task. At a *THW*=1.0 [s] drivers rate the level of haptic feedback for all haptic feedback conditions as good – not too high, not too low. The levels of usefulness

before, during and after the cd-task are rated similar as for *THW*=0.5 [s], but the differences are less pronounced.

Table 7: Summary of the results of the univariate ANOVA statistical analysis of the dependent measures, with significance level α=0.05. In the table, •••, ••, and • denote a significance of $p \leq 0.01$, $0.01 < p \leq 0.05$, and $0.05 \leq p < 0.1$ respectively and '-' denotes no significance.

	Following performance			Control effort			Physical load		CD-task time
	$\overline{THW}$	σ_{THW}	$\sigma_{TTC^{-1}}$	$\overline{\alpha_p}$	σ_{α_p}	t_r	$\overline{F_p}$	σ_{F_p}	t_{cd}
Main effects									
S	-	-	••	•••	•••	•••	•••	•••	-
T	•••	•••	•••	•••	•••	•••	•••	•••	-
2 way interaction									
SxT	-	-	••	••	-	-	•••	•••	-

6.2.5 Conclusions

1. The results of this experiment show that none of the developed algorithms yielded performance improvements (nor did performance decrease) during the execution of the secondary in-vehicle task (the cd-task).
2. There is no evidence for the conditions tested in this experiment that allows for the conclusion that drivers adopted a force-task strategy in controlling the gas pedal when haptic feedback is available.
3. The subjective evaluation of the driving conditions yielded favourable results for the haptic feedback conditions.

6.3 Overall discussion and conclusions

The experiments that were presented in this Chapter were both designed to investigate the effects of haptic gas pedal feedback on driver behaviour during car-following while drivers are visually distracted from the car-following task. The first experiment, presented in Section 6.1, required from drivers to react to visual distractions in the driving scene. In the second experiment, discussed in Section 6.2, the visual attention of drivers was directed away from the driving scene, into the car, by requiring them to pay attention to a cd-player. Although the tasks are artificial and do not exactly replicate real situations drivers deal with in every day driving, they are believed to be representative of real day-to-day driving tasks in an abstract manner, for example, checking road signs above the road or on the side of the road, using mobile phones, looking at navigation systems, etcetera.

The expectation was that with the presentation of car-following information through a complementary modality drivers will benefit from this non-visual information when they have to direct their visual attention away from their car-following task, such that they can perform better in their secondary task, while not degrading their primary task – car-following. The results in this Chapter show that at a *THW*=1.5 [s] drivers decreased their reaction times to central field of view (FOV) visual stimuli in the driving scene when using the THW-stiffness

feedback as compared to driving without haptic feedback. The force feedback condition showed an increase in reaction times to peripheral FOV visual stimuli. Car-following performance was neither improved nor degraded. It was concluded that haptic feedback influenced driver reaction times to visual stimuli in the environment, but the results of the influence depends on the type of haptic feedback.

In the cd-task experiment, all three haptic feedback algorithms were tested, but none was shown to improve task completion times, nor task accuracy. This was believed to be due to the strategy that drivers adopted in all conditions when they were executing the cd-task: increase the car-following headway.

In the reaction-time task, drivers did not have to change their driving strategy and were therefore able to benefit more from the haptic information that was prevented to them. Or, more precisely, in the reaction-time task, drivers did not change their following headway to increase their safety boundaries to carry out the secondary task, which is a very suitable strategy for carrying out in-car tasks. But, this strategy is also a strategy which is very much based on the fact that, when no haptic information is present, directing visual attention into the car, away from the driving scene, poses a real threat to the safety of the driver and her/his vehicle. In the time the driver is looking away from the driving scene she/he cannot receive any information from the driving scene. It appears from the results of the cd-task experiment that this strategy is so dominant that drivers apply it even when they still have a non-visual source of information – the haptic gas pedal feedback – to keep track of what is happening in front of their car while they are directing their visual attention to the secondary task in the vehicle. Because of this result it is difficult to come to more specific conclusions on which feedback algorithm is providing the best support during visually distracted driving. Subjective rating of the usefulness of the haptic feedback algorithms, however, yielded favourable results for the force feedback and TTC-stiffness feedback algorithms.

During distracted driving, drivers appear to be less willing to adopt a force-task strategy when haptic gas pedal feedback is presented during car-following. The σ_{F_p} decreased significantly during the reaction-time task, but in the cd-task experiment no evidence was found that could confirm the adoption of a force-force task strategy in controlling the gas pedal. It must therefore be concluded that during the cd-task that drivers were asked to perform, the haptic gas pedal feedback did not provide the kind of support that was expected. Therefore, the expected results – improved car-following performance with increased cd-task performance – as compared to driving without haptic feedback were not found. The strategy to deal with in-vehicle tasks is to increase following headway – with extra information or not. Drivers were unable, or did not feel comfortable enough to rely on the force-task strategy while visually distracted, as they did when they were not visually distracted.

Chapter 7

Conclusions

This dissertation set out to describe and discuss the development of a driver support system that presents car-following information from the driving environment directly ahead of the own vehicle by means of haptic gas pedal feedback. In Chapter 2 the dynamics of human leg/foot interaction with the gas pedal were investigated. From this investigation two different approaches were found to be suitable for implementation as haptic information providers through the gas pedal. The first approach was to add a force to the gas pedal dynamics which would have to be related to the safe-field-of-travel ahead of the own vehicle and changes therein. The gas pedal dynamics, that is, the force/pedal-position relationship is not changed by this approach. The second approach was to change the stiffness of the gas pedal by adding a virtual stiffness to the inherent stiffness of the gas pedal. By doing so, the dynamics of the gas pedal are changed depending on the changes detected in the safe-field-of-travel. In both approaches, an electrical actuator provides the additional force or stiffness. In the first approach, drivers receive information through changes in force on the gas pedal. With the second approach, drivers do not only experience changes in force on the gas pedal when there are changes in the safe-field-of-travel, but also changes in the rate of change of the pedal force when they change the pedal position. Hence the second approach, using additional stiffness should, in theory, provide more salient information to the driver.

Although it was discussed in Chapter 2 how haptic feedback could be presented to drivers by way of the gas pedal, it was left open, still, which environmental information would be used to represent drivers' safe-field-of-travel. This was discussed in Chapter 3. From the kinematics of car-following it was argued that there are different representations possible for the safe-field-of-travel. A strictly physical representation, by so-called 'Newtonian' variables was shown to be equivalent to the more useful variables *THW* and *TTC* which are shown in literature to yield more constant descriptions of driver behaviour under different conditions. From literature, experiments have indicated that the variable time-headway (*THW*) is a particularly suited

variable for use in support algorithms, since at highway speeds (>80 [km/h]) drivers tend to adopt a constant *THW* with increasing speed.

From the investigations into the environmental variables that are most suitable to represent the safe-field-of-travel and its changes, the link between the mechanisms to provide haptic gas pedal feedback and these environmental variables was established by three haptic gas pedal feedback algorithms. One of these algorithms, developed by Nissan Motor Company Ltd., was designed to provide force feedback with environmental information based on *THW* and *TTC*. This algorithm was called the force feedback algorithm. The other two algorithms used stiffness feedback as their means of generating haptic feedback and differed only in the use of the environmental variables. One of the algorithms, which made use of *THW* only as the source of environmental information was called the THW-stiffness algorithm. The other stiffness algorithm made use mainly of *TTC*, which was scaled, however, by *THW*. This algorithm was called the TTC-algorithm.

Because the transformation of environmental information (*THW* and *TTC*) into a haptic feedback signal does not have any natural equivalents, it was impossible to know beforehand how drivers would respond to this kind of support. Analogies can be made to explain the principles of the idea, such as similar magnetic poles pushing each other away, but the exact responses and amount of detectable information content remains unknown. Therefore, the different algorithms were tested in a number of experiments under a variety of environmental conditions.

In Chapter 4 the general procedure that was applied to all experiments in this thesis was explained. In each experiment, drivers were required to follow a lead vehicle at a prescribed separation. This separation would be indicated at the start and at selected points during the experiment by a visual aid: the THW-indicator. The THW indicator is a transparent red rectangle that is held at precisely the *THW* that drivers are required to drive at for a particular experiment condition. If the THW-indicator touches the rear-end bumper of the lead vehicle, the driver is driving at exactly the required separation. The THW-indicator is only visible for short periods of time during the experiment runs to allow drivers to position themselves at the right separation with the lead vehicle. When the THW-indicator is not visible, the lead vehicle speed is disturbed with a disturbance signal that is composed of a specifically designed set of sinusoids. The lead vehicle speed disturbance appears to be a random disturbance to the drivers. The sum of sinusoids is designed in the frequency domain, such that specific frequency bands can be selected with which the signal is constructed. This allows for the application of frequency-domain system identification procedures.

The experiments that were presented in Chapter 5 were set up to investigate the effects of the support system on driver behaviour when drivers can direct their full visual attention to the car-following task. Because the haptic gas pedal feedback provides similar information about the safe-field-of-travel as what is available visually, it is important to investigate whether the additional information channel could possibly interfere with the processing of the visual information. Three experiments were presented that each investigated different environmental conditions when using the different haptic feedback algorithms.

Because the support system is expected to be most beneficial when drivers are temporarily not paying attention to the car-following task visually, two experiments were conducted to investigate the effects on driver behaviour during visually distracted driving as well. One experiment investigated visual distractions in the driving scene and the other experiment investigated in-vehicle distractions, requiring drivers to temporarily direct their visual attention into the vehicle.

7.1 The use of haptic feedback in car-following

It was expected first and most importantly that drivers would adopt a force-task strategy in controlling the gas pedal when haptic feedback was available. The force task strategy entails that drivers try to maintain the force they experience from the gas pedal at a constant level. Because the haptic feedback algorithms are designed to increase the amount of haptic feedback with decreasing separation with a lead vehicle, trying to keep the force constant will automatically lead to drivers applying the desired control input to their vehicle: reducing gas pedal input when a lead vehicle approaches and increasing gas pedal input when a lead vehicle moves away again.

No significant differences between force and stiffness feedback could be detected in car-following performance in the two experiments (see Section 5.1 and Section 6.2) in which both the force and feedback algorithms were evaluated together. The most noticeable differences between the stiffness and force feedback algorithms were found in the reduction of control effort. In general, the control effort was reduced by all three haptic feedback algorithms discussed in this thesis compared to the condition when no haptic feedback was present. The THW-stiffness algorithm, however, greatly reduced the control effort even when compared to the force feedback algorithm.

This reduction of control effort when using haptic feedback, which was found in all experiments that were conducted, shows that drivers obtain valuable information not only of the changes in the safe-field-of-travel based on the movement of the lead vehicle alone, but also based on the dynamics of the own vehicle. This conclusion can be drawn because when no haptic feedback was present, drivers tended to overreact to the lead vehicle speed disturbance, which led to a sort of “bang-bang” control: over-acceleration when the lead vehicle accelerates followed by over-deceleration to compensate when the lead vehicle slows down again. This kind of control when no haptic feedback is present is believed to have been enhanced because of the absence of motion cues in the fixed-base driving simulator. Had these cues been available, drivers might have had a better sense of their unnecessary large accelerations and decelerations. The haptic feedback appears to have successfully replaced the information that was lost because of the absence of motion in the driving simulator. Thus, it can be concluded that the information that the haptic feedback is providing contains enough content for drivers to become more aware of the magnitude of the required control actions, greatly reducing the control effort in car-following, and hence improving car-following comfort.

The cost of reducing control effort is, however, paid in increased physical load during close following with the haptic feedback support system activated. All haptic feedback algorithms showed a highly-significant increase in the physical load. Especially at close

following separations ($THW \leq 1.0$ [s]) the THW-stiffness algorithm stands out in demanding a much higher physical load of the driver than with the force feedback or TTC-stiffness feedback algorithms. At higher *THW*'s the increase in physical load converges to similar levels for all three haptic feedback algorithms.

Because the THW-stiffness algorithm has a significantly higher physical load at close following separations, this has a negative impact on the capability of drivers to adopt a force task strategy. When visually distracted, drivers even seem to have difficulty in using the THW-stiffness feedback information at all, because the standard deviations of the pedal forces exerted on the pedal by the drivers are much higher than for the other two feedback algorithms.

Analysis of the distributions of the measured gas pedal forces, together with the statistical analysis of variance of the standard deviations, show there is reason to accept the hypothesis that drivers adopt a force task strategy in driving with haptic gas pedal feedback. Not for all haptic feedback algorithms, though. As mentioned before, the THW-stiffness algorithm shows little signs of force task strategy in the close following conditions. The differences between the force feedback and the TTC-stiffness feedback seem negligible and both algorithms might be concluded to lead to the adoption of a force-task strategy in controlling the gas pedal during car-following.

However, when drivers are executing an in-vehicle task, such as tuning their car-stereo system, they seem to fall back on driving behaviour that is very strongly rooted in the assumption that no information of the car-following situation is available when paying attention to in-vehicle devices. No force-task like strategy can be found anymore during such tasks, neither any benefit of reduced control effort. The reliance on previously learned strategies for dealing with driving and in-vehicle tasks at the same time, based on the availability of visual control information only, is so dominant that the effect of haptic feedback is rendered virtually zero. No improvements in secondary task performance have been found either, which would have suggested otherwise. Nevertheless, some improvements in the reaction times to visual stimuli in the driving scene were found when using haptic feedback, suggesting that the execution of tasks that demand less attention might also rely less on driving strategies that are based on the availability of visual control information only. It can only be speculated whether more driving experience with the haptic feedback support would, in time, increase drivers' trust and competence in using the haptic feedback information during the execution of non-driving related tasks that require them to divert their visual attention away from the driving scene.

7.2 Haptic feedback information content

Besides the different types of haptic feedback that can be generated by an electrical actuator attached to the gas pedal – stiffness feedback and force feedback – the type of environmental information mainly determines the content that is communicated to the driver. From the discussion of the visual perception of car-following information, it was concluded that the time-headway (*THW*) and the time-to-contact (*TTC*) are two environmental variables that best describe the car-following situation from the driver's perspective. The combination of *THW* and *TTC* to generate haptic feedback, however, is not easily determined.

Through an heuristic process three algorithms were determined to represent the safe-field-of-travel. The force feedback algorithm combines *THW* and *TTC* as the sum of each variable inverted. A scale factor determines the relative importance of either variable. The consequence of combining *THW* and *TTC* this way is that within the *THW* operating range, the driver always experiences haptic feedback, regardless of the inverse of *TTC*, which fluctuates around zero.

The THW-stiffness algorithm has the same characteristic as the force feedback algorithm in that haptic feedback is always present within the *THW* operating range of the algorithm, regardless of *TTC*. The use of stiffness was expected to compensate for the absence of *TTC* information, since stiffness would provide gradient information with respect to *THW*. From experiment results, however, no evidence for this hypothesis has been found. The THW-stiffness algorithm yielded no improvement in car-following performance over the force feedback algorithm and in almost all experiment conditions tested was found to have the highest physical load, except for relatively high *THW*'s (≥1.5 [s]). The high continuous stiffness did lead to significant control effort reductions. This control effort reduction is most likely the result from the high stiffness feedback rather than from high information content, since for lower *THW*'s (≤1.0 [s]) the force distributions show a relatively flat distribution compared to the concentrated distributions of the force feedback and TTC-stiffness feedback algorithms.

Finally, the TTC-stiffness algorithm is based on the feedback of *TTC* alone, although the strength of the feedback is amplified by *THW*. Thus, a compensatory feedback algorithm is created, which allows drivers to adopt a force-task strategy easily because feedback is felt whenever the lead vehicle is moving towards the own vehicle. When there is no change in the safe-field-of-travel, there is no force feedback. System identification of a simple linear model of the car-following situation shows that *TTC* is the most prominent source of information drivers use to determine their car-following control behaviour in the condition that were tested in the fixed-base driving simulator (*THW*=0.5, 1.0, and 1.5 [s]).

The results of the experiments show that the force feedback and TTC-stiffness feedback algorithms yield the least increase in physical load with similar reductions in control effort as the THW-stiffness algorithm compared to the base-line no feedback condition. The fact that due to the absence of motion cues drivers might have over-reacted in their accelerations and decelerations during the experiments driving the no feedback conditions, but not while driving the haptic feedback conditions leads to the belief that the information content of the haptic feedback for all algorithms was good enough to compensate for this lack of motion cueing.

7.3 The future of haptic gas pedal feedback

While the results of the experiments show that the one major improvement in car-following behaviour due to the use of haptic gas pedal feedback is the decrease in control effort, there are but few indications that there are other benefits such as improved following performance or relaxation of the demand on visual processing of the driving scene. If there is only an improvement in control effort, which might be interpreted as an improvement in comfort during car-following, can the instalment of haptic gas pedal feedback systems in future generation cars be justified?

This question can be answered with a 'yes', not in the first place because of this improvement in control effort during car-following. The research presented in this thesis focused on car-following situations that were limited to those situations which could, under most circumstances, be controlled with the gas pedal only. In other words, no extreme situations, in which the lead vehicle speed changed abruptly, like in an emergency braking situation, were investigated. The potential for extending the use of haptic gas pedal feedback into this domain of driving situations is likely to be the natural progress of this research. The benefits of providing haptic gas pedal feedback during car-following will most likely prove beneficial for extension into emergency situation alerting for a number of reasons.

First, by keeping the haptic gas pedal feedback part of the control loop during car-following, drivers will learn to benefit more easily from the environmental information they receive through the complimentary modality of haptics. This will only facilitate the extension of the use of haptic feedback into the emergency domain. Second, since the haptic gas pedal feedback is continuous, extension into the emergency domain will also yield a continuous transition of the haptic feedback information from normal following to emergency signalling – preventing drivers from experiencing emergency information activation too infrequently to be able to react instinctively and thereby saving valuable reaction time. Third, even though the results of the experiments discussed in this thesis do not show any major improvements in car-following performance, nor in reaction times to secondary tasks, neither do they indicate there are reasons to believe that haptic gas pedal feedback impairs car-following behaviour. Therefore, it is believed that, if the haptic gas pedal is to be used as an emergency aid, that is, as a collision warning aid, it would be beneficial to have drivers use haptic gas pedal feedback before they find themselves in an emergency situation such that they understand the meaning of the information that is provided them intuitively. Finally, to conclude this thesis, drivers have indicated subjectively to feel that they benefit from the presence of haptic feedback during car-following, indicating the trust they have in the information that is transmitted through to them via the haptic gas pedal. The combination of increased driver confidence and decreased control effort could well be an excellent combination in the increased complexity and busyness of our highway traffic today and in the future.

Appendix A

Derivation of generalized potential field parameters

A.1 The reserve avoidance time

The potential of the generalised potential field (GPF) as defined by Krogh (1984) is generated by, what he called, the reserve avoidance time T_r. This is the amount of time the controlled element has left to start taking action to avoid collision with an obstacle that is in its current path of motion (see Figure 70 for the geometric relations between the controlled element and an obstacle A_i).

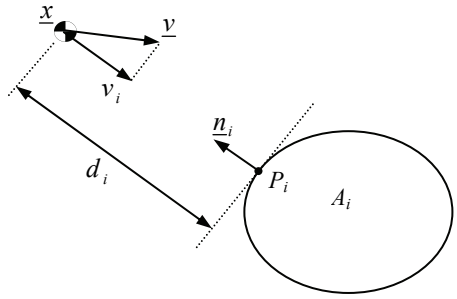


Figure 70: Definition of the relations between an obstacle A_i and the controlled element at $(\underline{x}, \underline{v})$, generating a potential P_i. Reproduced from Krogh (1984).

If action is taken after T_r amount of time, collision is unavoidable. If proper action is taken within T_r amount of time, then collision is avoidable. T_r is defined as the difference between the maximum avoidance time T_i and the minimum avoidance time τ_i:

$$T_r = T_i - \tau_i \tag{A.1}$$

If the maximum amount of (constant) acceleration α is applied in the direction of the normal $\underline{n}_i$ of obstacle A_i, then the velocity $v_i(t) \rightarrow 0$ in the minimum avoidance time τ_i. The velocity $v_i(t)$ determined by equation (A.2) in which t is the current time and t_0 the time at which the acceleration α was applied first:

$$v_i(t) = v_i(t_0) - \alpha t \tag{A.2}$$

So, at time τ_i:

$$v_i(\tau_i) = 0 = v_i(t_0) - \alpha \tau_i \tag{A.3}$$

yielding the expression for τ_i:

$$\tau_i = \frac{v_i(t_0)}{\alpha} \tag{A.4}$$

If, however, a constant amount of acceleration is applied in the direction of $\underline{n}_i$ that is less than α, then collision can only be avoided if $v_i(t) \rightarrow 0$ before $d_i(t)=0$, where $d_i(t)$ is the distance to the object A_i along the obstacle normal $\underline{n}_i$ at time t. This means that a minimum acceleration α_0, away from the obstacle, is required:

$$v_i(T_i) = 0 = v_i(t_0) - \alpha_0 T_i \;\Leftrightarrow\; \alpha_0 = \frac{v_i(t_0)}{T_i} \tag{A.5}$$

so that the maximum avoidance time T_i can be calculated from:

$$d_i(t) = d_i(t_0) + v_i(t)t - \tfrac{1}{2}\alpha_0 t^2 \tag{A.6}$$

when $d_i(T_i)=v_i(T_i)=0$ and substituting equation (A.5) for α_0:

$$T_i = \frac{2d_i(t_0)}{v_i(t_0)} \tag{A.7}$$

The reserve avoidance time T_r can thus be written as:

$$T_r = T_i - \tau_i = \frac{2\alpha d_i(t_0) - v_i^2(t_0)}{v_i(t_0)\alpha} \tag{A.8}$$

A.2 The obstacle avoidance vector

The gradient $\underline{c}_{0,i}$ of the GPF, with respect to the position $\underline{x}$, determines the direction and magnitude of the required control away from an obstacle A_i. The gradient is determined with the nabla operator $\underline{\nabla}_x$:

$$\underline{c}_{0,i} = -\underline{\nabla}_x P_i(\underline{x}, \underline{v}) = \begin{cases} 0 & \forall\ v_i(t_0) \le 0 \\ -\left(\dfrac{\partial}{\partial x}\underline{e}_x + \dfrac{\partial}{\partial y}\underline{e}_y\right)\left(\dfrac{\alpha v_i(t_0)}{2d_i(t_0)\alpha - v_i^2(t_0)}\right) & \forall\ v_i(t_0) > 0 \end{cases} \tag{A.9}$$

See Figure 70 above for the definition of the variables. Writing out equation (A.9) for $v_i(t_0)>0$ yields:

$$-\underline{\nabla}_x P_i(\underline{x},\underline{v}) = -\left\{\frac{\alpha\left(2d_i(t_0)\alpha - v_i^2(t_0)\right)\frac{\partial v_i(t_0)}{\partial x} - \alpha v_i(t_0)\left(2\frac{\partial d_i(t_0)}{\partial x}\alpha - 2v_i(t_0)\frac{\partial v_i(t_0)}{\partial x}\right)}{\left(2d_i(t_0)\alpha - v_i^2(t_0)\right)^2}\right\}\underline{e}_x$$
$$-\left\{\frac{\alpha\left(2d_i(t_0)\alpha - v_i^2(t_0)\right)\frac{\partial v_i(t_0)}{\partial y} - \alpha v_i(t_0)\left(2\frac{\partial d_i(t_0)}{\partial y}\alpha - 2v_i(t_0)\frac{\partial v_i(t_0)}{\partial y}\right)}{\left(2d_i(t_0)\alpha - v_i^2(t_0)\right)^2}\right\}\underline{e}_y \tag{A.10}$$

and since $\frac{\partial v_i(t_0)}{\partial x} = \frac{\partial v_i(t_0)}{\partial x} = 0$,

$$-\underline{\nabla}_x P_i(\underline{x},\underline{v}) = \frac{-2\alpha^2 v_i(t_0)\left(\frac{\partial d_i(t_0)}{\partial x}\underline{e}_x + \frac{\partial d_i(t_0)}{\partial y}\underline{e}_y\right)}{\left(2d_i(t_0)\alpha - v_i^2(t_0)\right)^2} \tag{A.11}$$

with $\frac{\partial d_i(t_0)}{\partial x}\underline{e}_x + \frac{\partial d_i(t_0)}{\partial y}\underline{e}_y = 1\cdot\underline{n}_i$,

$$\underline{c}_{0,i} = -\underline{\nabla}_x P_i(\underline{x},\underline{v}) = \begin{cases} 0 & \forall\ v_i(t_0) \le 0 \\ \frac{-2\alpha^2 v_i(t_0)}{\left(2d_i(t_0)\alpha - v_i^2(t_0)\right)^2}\underline{n}_i = \frac{2P_i(\underline{x},\underline{v})}{v_i(t_0)}\underline{n}_i & \forall\ v_i(t_0) > 0 \end{cases} \tag{A.12}$$

Appendix B

Car-following data distributions

B.1 Calculation of the car-following spiral distributions[1]

The car-following spirals found in the *THW-TTC* $^{-1}$ phase-plane graphs are important visualisations of car-following behaviour. In order to get a qualitative picture of these spirals for a multitude of car-following data, it is more illustrative to look at the distribution of these spirals, rather than at the spirals themselves, which would yield nothing more but a single cluster of overlapping spirals.

To determine the distribution of *THW-TTC* $^{-1}$ car-following data, a grid is created, dividing the phase-plane in equally spaced rectangles, which fill up the area of interest like a chess board. For each rectangle in the grid, the amount of data-points that are within its borders are counted. The total count for each rectangle in the grid is a measure of frequency, that is, it represent how often that particular grid-area has been crossed by the car-following spiral data.

In order to be able to compare different sized data-sets, the grid-counts are normalized by dividing the grid-counts by the maximum grid-count for a particular data-set. The entire grid is then multiplied by 100 to get a differentiation in grid-counts from 0-100%.

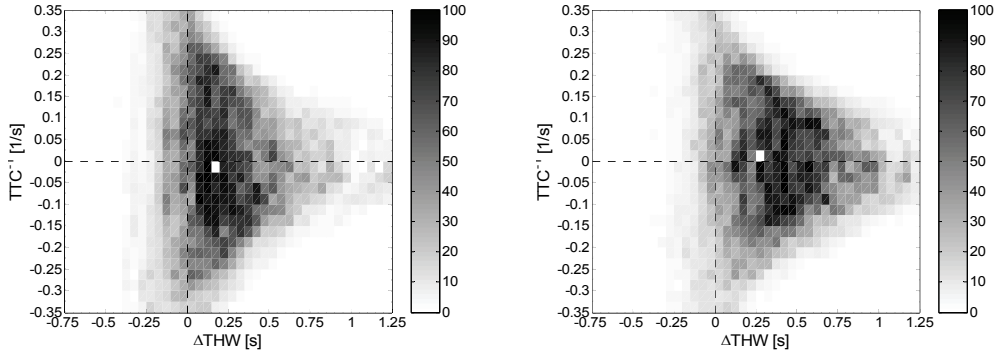
B.1.1 Distributions for different lead vehicle speed disturbances

The experiment described in Section 5.2 examined driver behaviour with and without THW-stiffness driver support at different *THW*'s, *T*, and different lead vehicle speed disturbances, *D*. Below, in Figure 71a-f and Figure 72a-f, the distributions for different levels of *T* and *D* with the DSS activated (*S=on*) and the DSS deactivated (*S=off*).

As can be seen from these figures, the effects of *THW* are manifested by a shift from a variation mostly in *THW* to a variation more pronounced in *TTC* $^{-1}$. This shift is visible for all the different lead vehicle speed disturbances. The effects of the lead vehicle speed disturbances

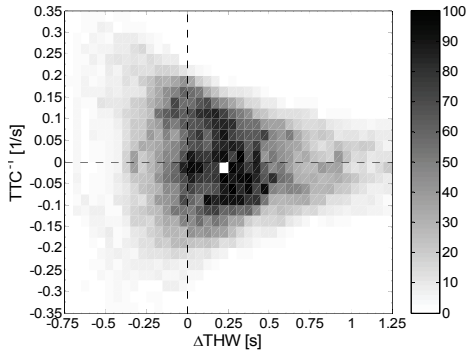
[1] As proposed by Dr. T. Yamamura of Nissan Motor Company, Ltd.

are found in the spread of the car-following spirals. The lower the bandwidth f_d of the lead vehicle speed disturbance (and therefore the higher the amplitude A_d), the bigger the spread in the car-following THW-TTC^{-1} distributions.

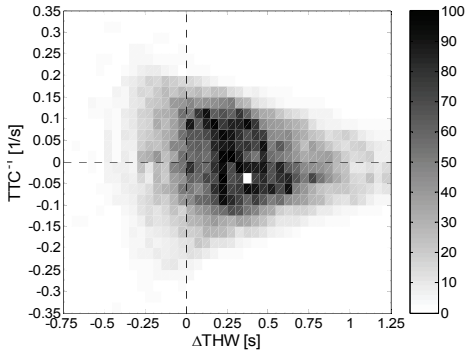


a) THW=0.5 [s]; S=*off*

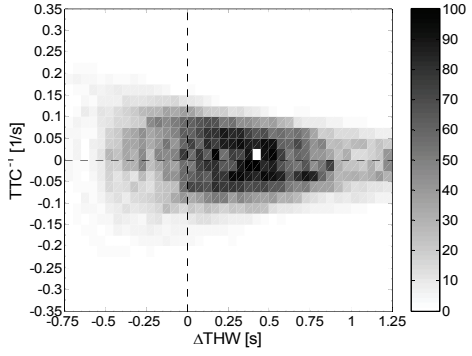
b) THW=0.5 [s]; S=*on*



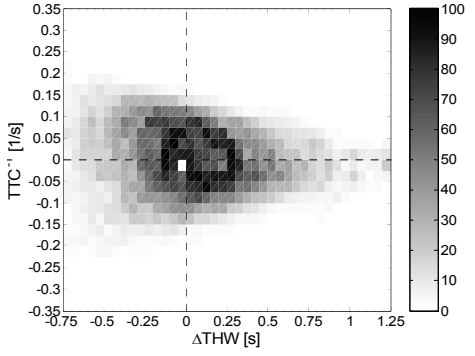
c) THW=1.0 [s]; S=*off*



d) THW=1.0 [s]; S=*on*

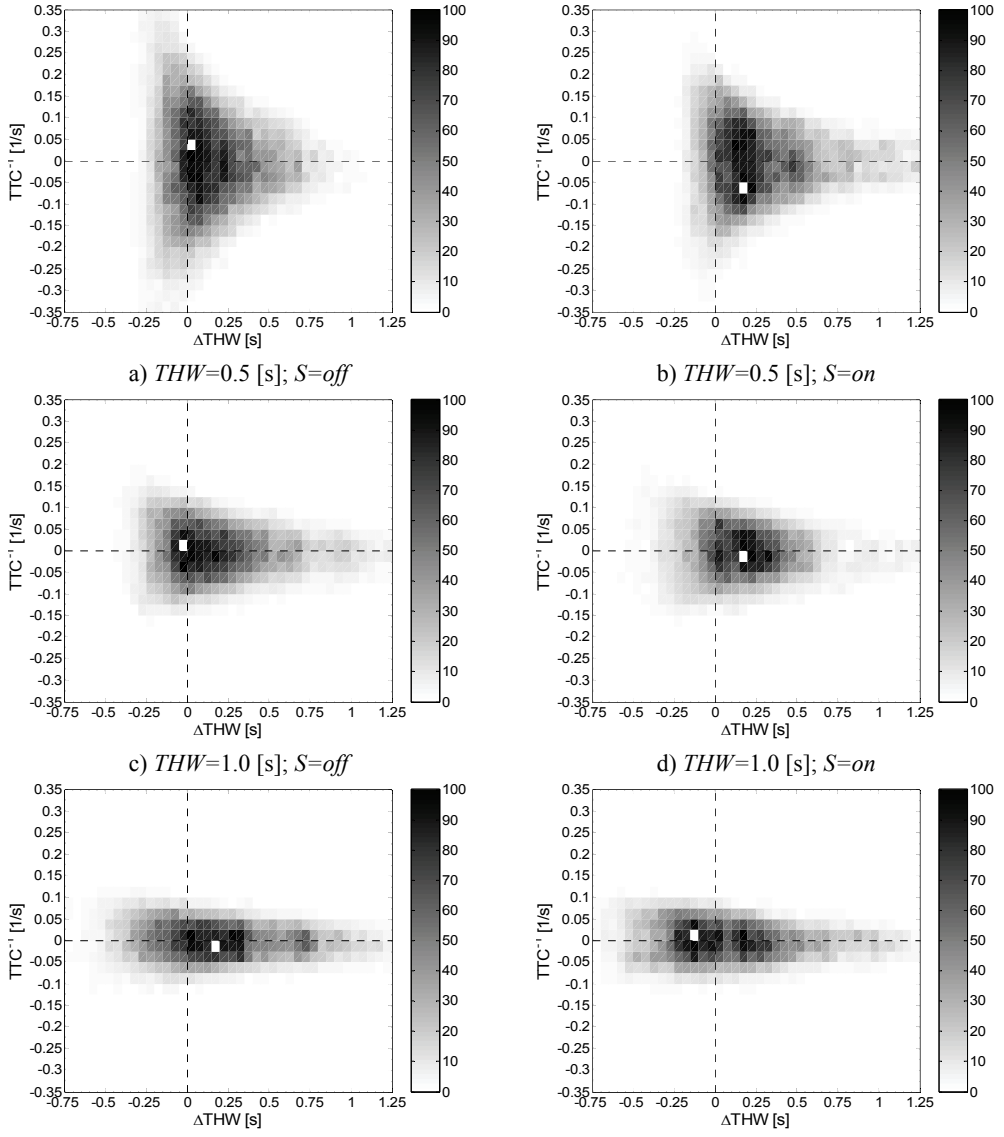


e) THW=1.5 [s]; S=*off*



f) THW=1.5 [s]; S=*on*

Figure 71: Calculated distribution of the car-following spirals for all conditions of T and S, and D=$\{f_d$=0.3 [Hz]; A_d=14 [km/h]$\}$. Shades of grey represent normalized frequency (between 0 and 100%).



a) *THW*=0.5 [s]; *S*=*off*

b) *THW*=0.5 [s]; *S*=*on*

c) *THW*=1.0 [s]; *S*=*off*

d) *THW*=1.0 [s]; *S*=*on*

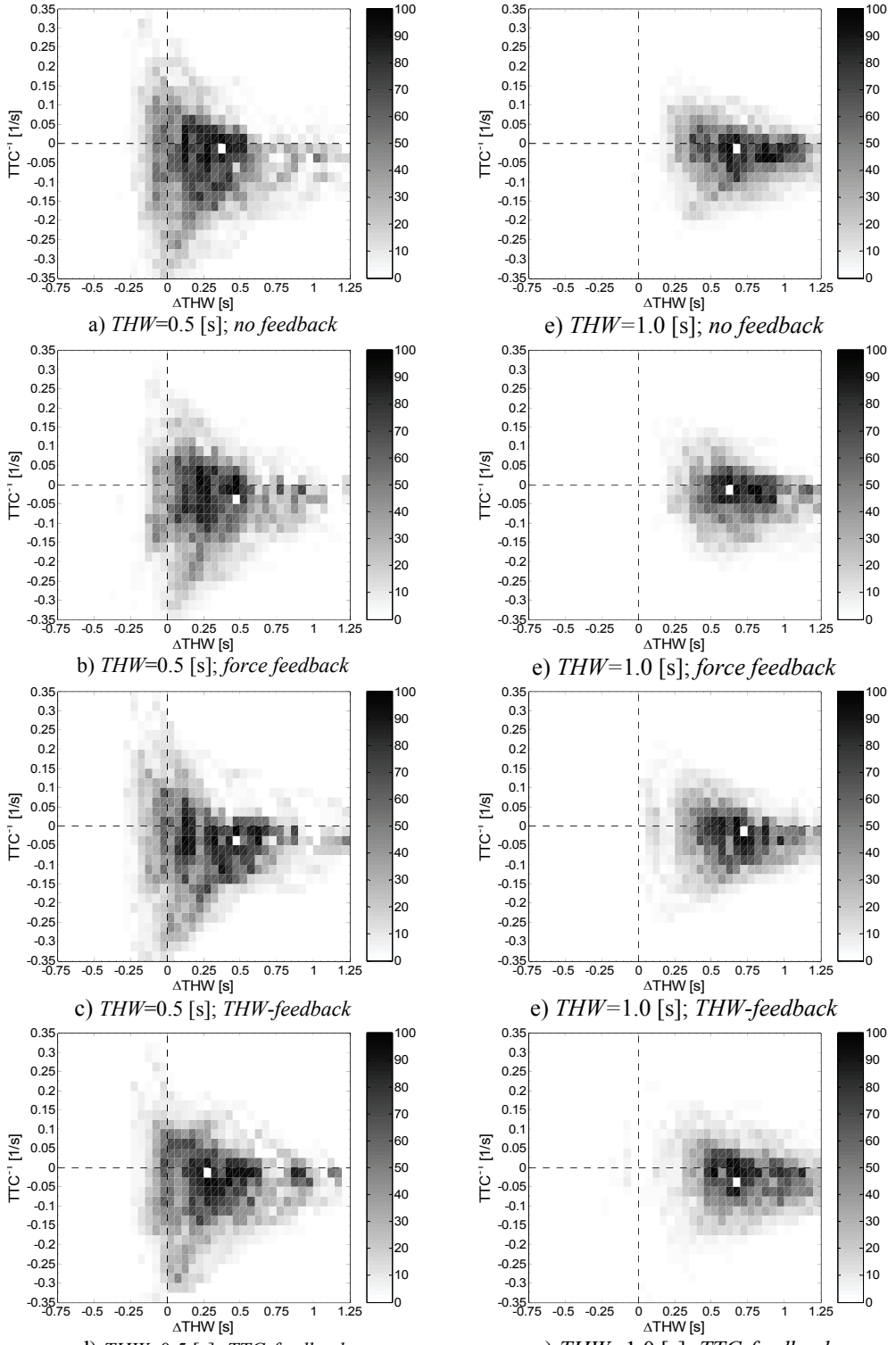
e) *THW*=1.5 [s]; *S*=*off*

f) *THW*=1.5 [s]; *S*=*on*

Figure 72: Calculated distribution of the car-following spirals for all conditions of *T* and *S*, and $D=\{f_d=0.7$ [Hz]; $A_d=7$ [km/h]$\}$. Shades of gray represent normalized frequency (between 0 and 100%).

B.1.2 Distributions for different feedback algorithms

In the car-following experiment with the cd-task, described in Section 6.2, all three haptic feedback algorithms were compared. The resulting car-following spirals in the THW-TTC^{-1} phase plane are shown for all tested conditions in Figure 73. No significant difference in *THW* or σ_{THW} were found. Only small differences between the feedback algorithms in $\sigma_{TTC^{-1}}$ were found.



a) *THW*=0.5 [s]; *no feedback*

e) *THW*=1.0 [s]; *no feedback*

b) *THW*=0.5 [s]; *force feedback*

e) *THW*=1.0 [s]; *force feedback*

c) *THW*=0.5 [s]; *THW-feedback*

e) *THW*=1.0 [s]; *THW-feedback*

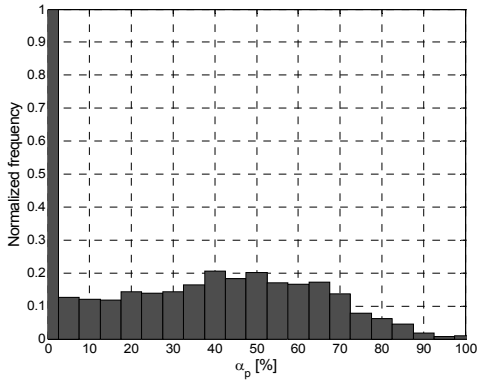
d) *THW*=0.5 [s]; *TTC-feedback*

e) *THW*=1.0 [s]; *TTC-feedback*

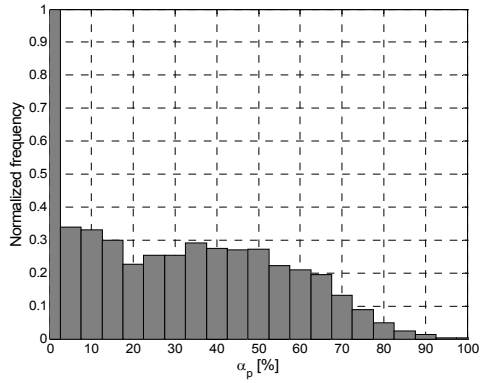
Figure 73: Calculated distribution of the car-following spirals for the different feedback algorithms.

B.2 Distribution of gas pedal characteristics

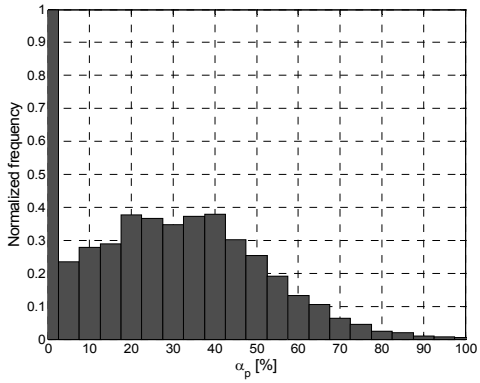
The distributions of the gas pedal depression α_p have been obtained for all conditions, that is, for all levels of T (*THW*), S (DSS state), and D (disturbance type). All measured data per condition has been grouped together for all drivers. From these datasets, the histograms that are shown in Figure 74, Figure 75, and Figure 76, have been created.



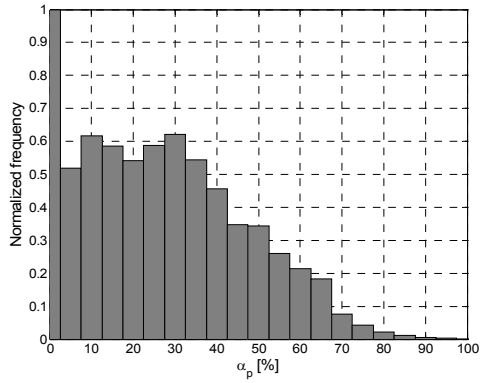
a) *S*=*off*; f_d=0.3 [Hz], A_d=14 [km/h]



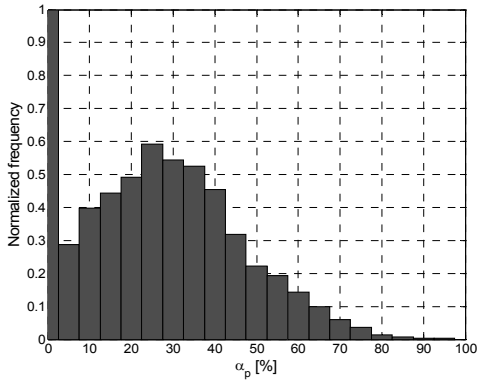
b) *S*=*on*; f_d=0.3 [Hz], A_d=14 [km/h]



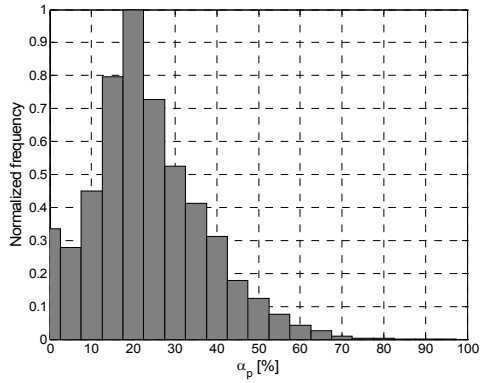
c) *S*=*off*; f_d=0.5 [Hz], A_d=10 [km/h]



d) *S*=*on*; f_d=0.5 [Hz], A_d=10 [km/h]

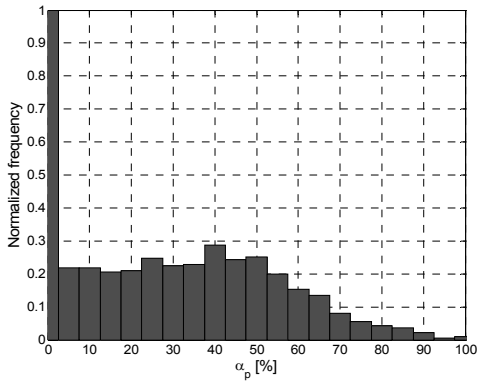


e) *S*=*off*; f_d=0.7 [Hz], A_d=7 [km/h]

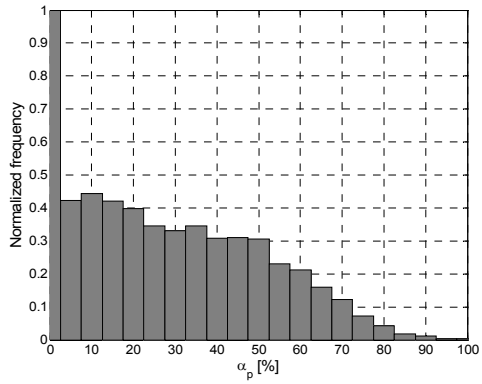


f) *S*=*on*; f_d=0.7 [Hz], A_d=7 [km/h]

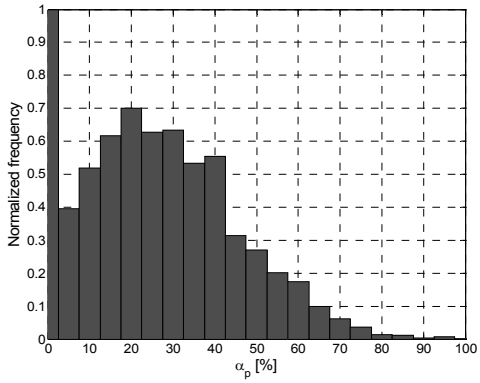
Figure 74: Measured gas pedal position distributions for all conditions of *S* and *D*, at *THW*=0.5 [s], for all drivers together.



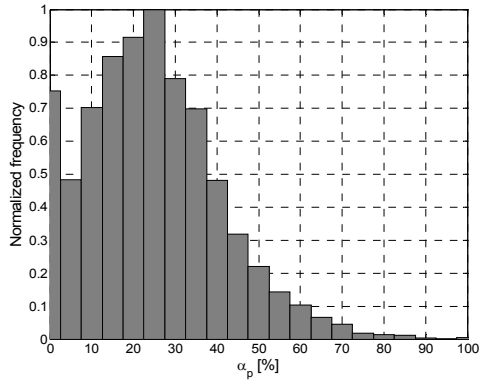
a) *S*=*off*; f_d=0.3 [Hz], A_d=14 [km/h]



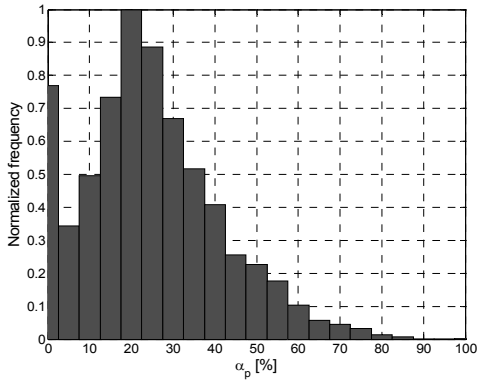
b) *S*=*on*; f_d=0.3 [Hz], A_d=14 [km/h]



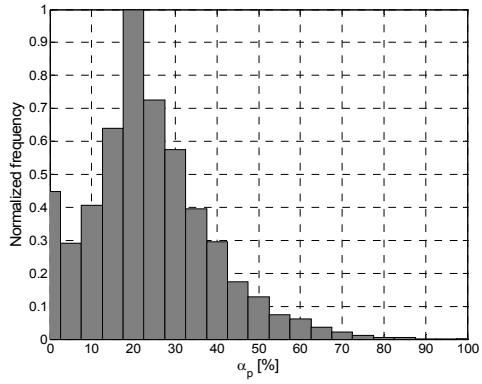
c) *S*=*off*; f_d=0.5 [Hz], A_d=10 [km/h]



d) *S*=*on*; f_d=0.5 [Hz], A_d=10 [km/h]

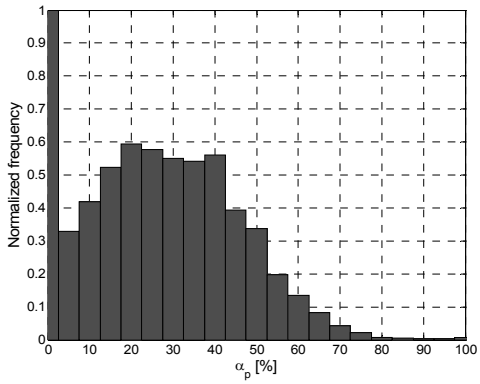


e) *S*=*off*; f_d=0.7 [Hz], A_d=7 [km/h]

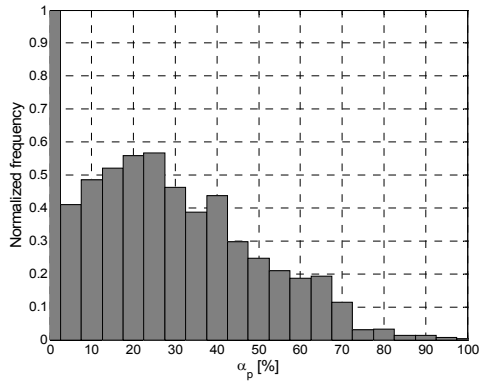


f) *S*=*on*; f_d=0.7 [Hz], A_d=7 [km/h]

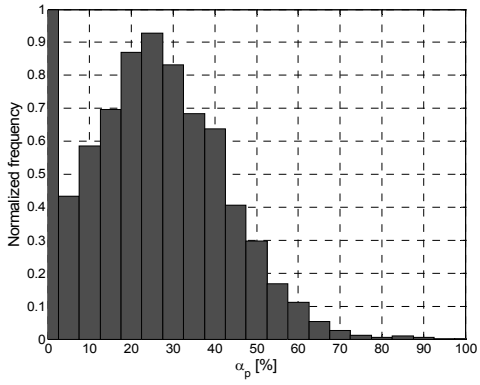
Figure 75: Measured gas pedal position distributions for all conditions of *S* and *D*, at *THW*=1.5 [s], for all drivers together.



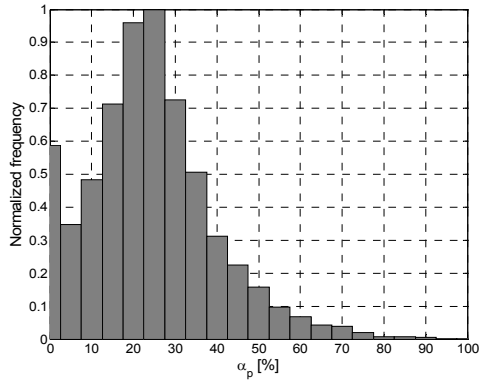
a) *S*=*off*; f_d=0.3 [Hz], A_d=14 [km/h]



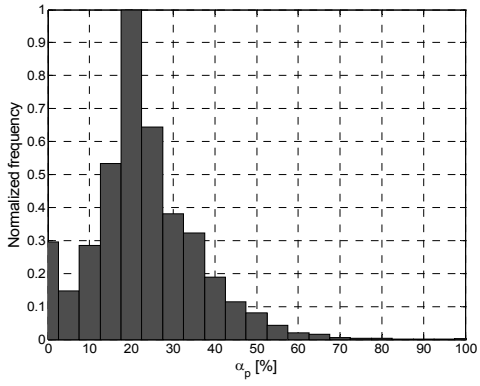
b) *S*=*on*; f_d=0.3 [Hz], A_d=14 [km/h]



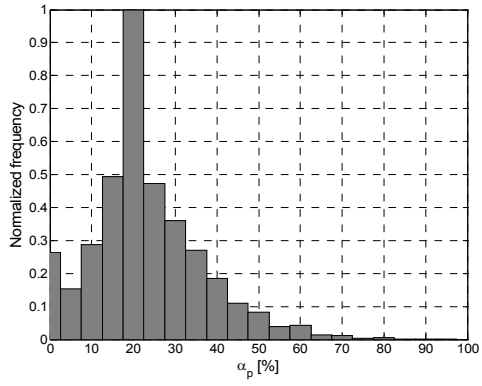
c) *S*=*off*; f_d=0.5 [Hz], A_d=10 [km/h]



d) *S*=*on*; f_d=0.5 [Hz], A_d=10 [km/h]



e) *S*=*off*; f_d=0.7 [Hz], A_d=7 [km/h]



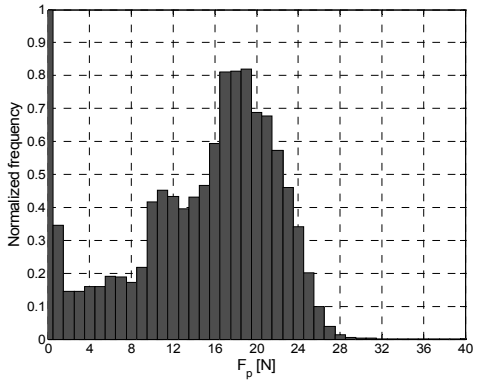
f) *S*=*on*; f_d=0.7 [Hz], A_d=7 [km/h]

Figure 76: Measured gas pedal position distributions for all conditions of *S* and *D*, at *THW*=1.5 [s], for all drivers together.

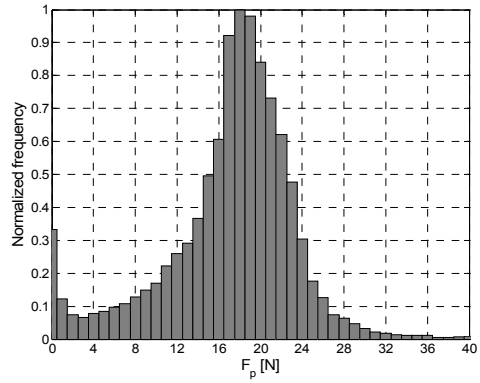
B.3 Distribution of gas pedal forces

B.3.1 Distributions for different lead vehicle speed characteristics

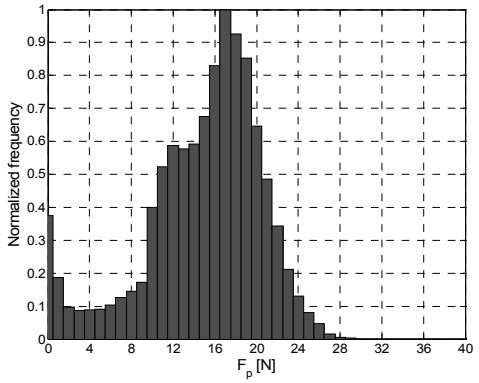
The distributions of the gas pedal depression F_p have been obtained for all conditions, that is, for all levels of T (*THW*), S (DSS state), and D (disturbance type). All measured data per condition has been grouped together for all drivers. From these datasets, the histograms that are shown in Figure 78 and Figure 78, have been created.



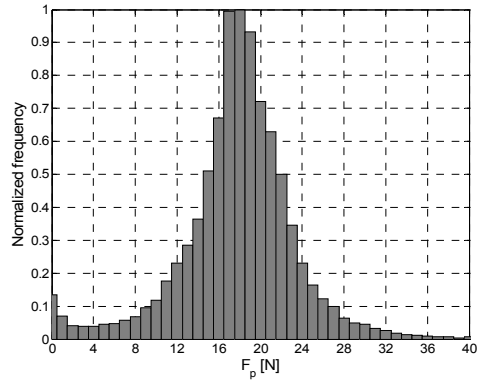
a) S=*off*; f_d=0.3 [Hz], A_d=14 [km/h]



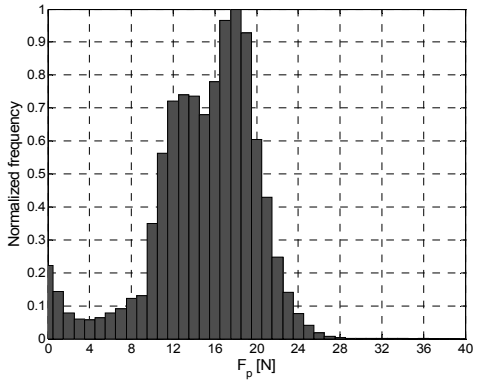
b) S=*on*; f_d=0.3 [Hz], A_d=14 [km/h]



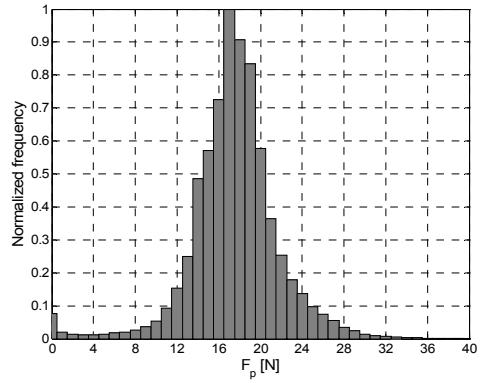
c) S=*off*; f_d=0.5 [Hz], A_d=10 [km/h]



d) S=*on*; f_d=0.5 [Hz], A_d=10 [km/h]

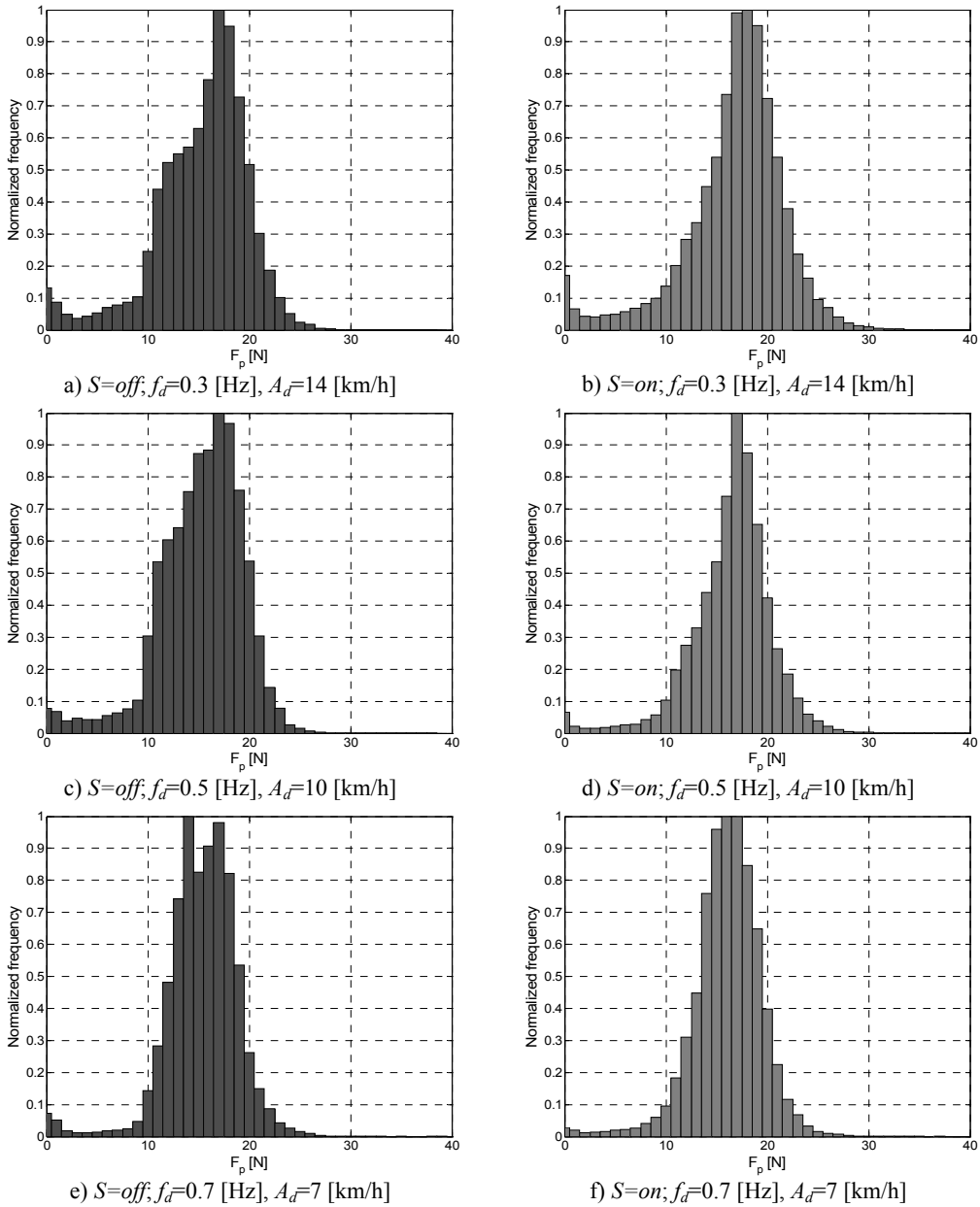


e) S=*off*; f_d=0.7 [Hz], A_d=7 [km/h]



e) S=*on*; f_d=0.7 [Hz], A_d=7 [km/h]

Figure 77: Measured gas pedal force distributions for all conditions of S and D, at *THW*=0.5 [s], for all drivers together.



a) *S*=*off*; f_d=0.3 [Hz], A_d=14 [km/h]

b) *S*=*on*; f_d=0.3 [Hz], A_d=14 [km/h]

c) *S*=*off*; f_d=0.5 [Hz], A_d=10 [km/h]

d) *S*=*on*; f_d=0.5 [Hz], A_d=10 [km/h]

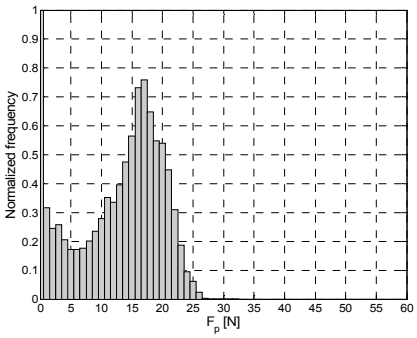
e) *S*=*off*; f_d=0.7 [Hz], A_d=7 [km/h]

f) *S*=*on*; f_d=0.7 [Hz], A_d=7 [km/h]

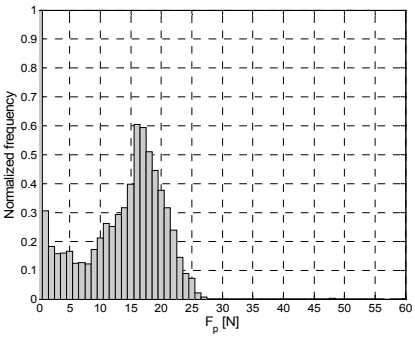
Figure 78: Measured gas pedal force distributions for all conditions of *S* and *D*, at *THW*=1.5 [s], for all drivers together.

B.3.2 Distributions for different haptic feedback algorithms

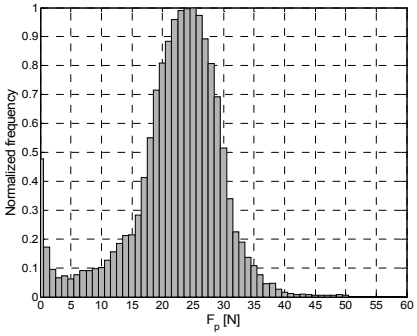
For the analysis of the results of the experiment discussed in Section 6.2, the data-minutes that were recorded were split in 3 sections: before the start of the cd-task, during the task and after the task until the THW-indicator appeared. Figure 79 and Figure 80 show the resulting force distributions before and after the drivers completed the cd-task.



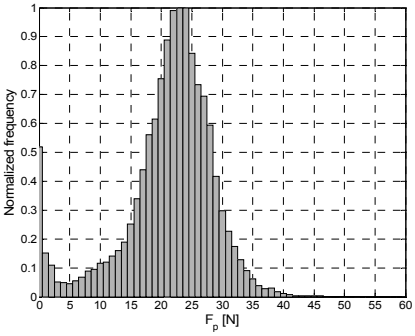
a) *No haptic feedback*; before cd-task



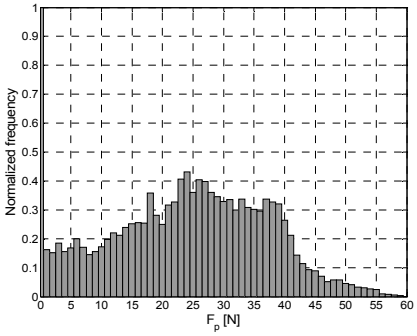
e) *No haptic feedback*; after cd-task



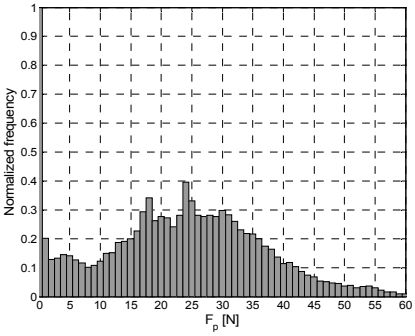
b) *Force feedback*; before cd-task



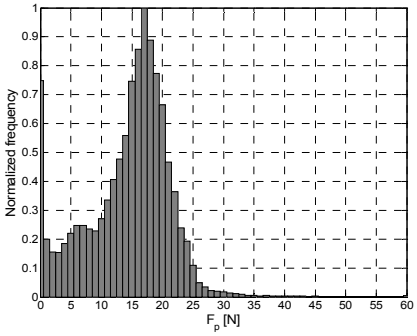
f) *Force-feedback*; after cd-task



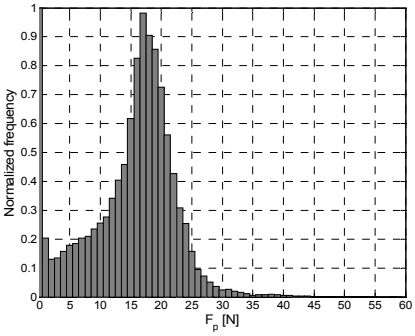
c) *THW-feedback*; before cd-task



g) *THW-feedback*; after cd-task

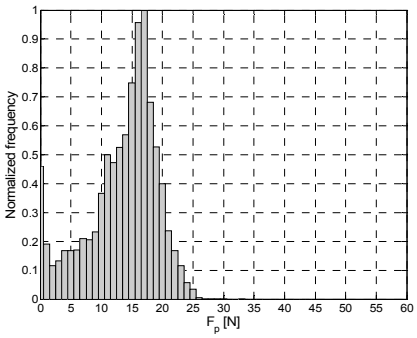


d) *TTC-feedback*; before cd-task

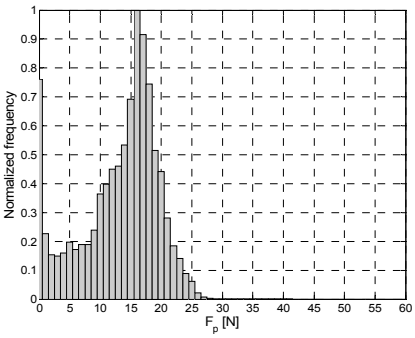


h) *TTC-feedback*; after cd-task

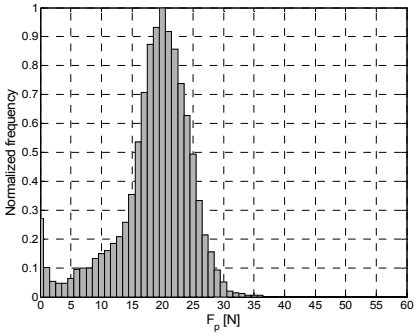
Figure 79: Distributions of the gas pedal forces exerted on the gas pedal by all drivers together, for *THW*=0.5 [s] - before the cd-task (left) and after the cd-task (right).



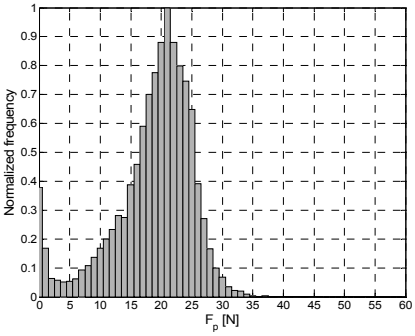
a) *No haptic feedback*; before cd-task



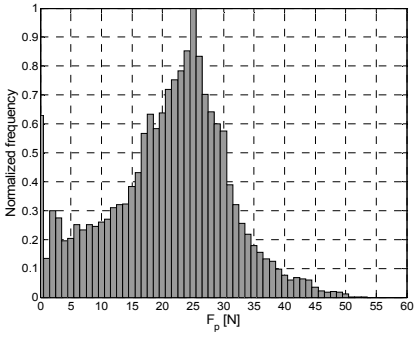
e) *No haptic feedback*; after cd-task



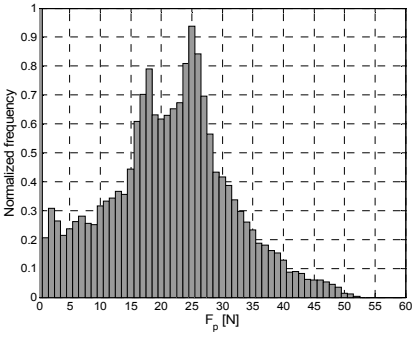
b) *Force feedback*; before cd-task



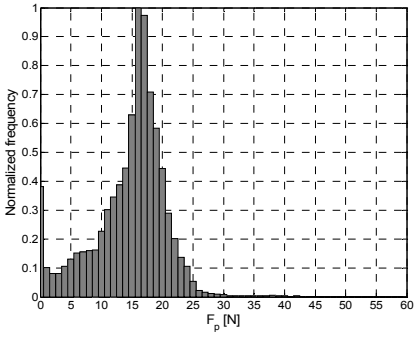
f) *Force-feedback*; after cd-task



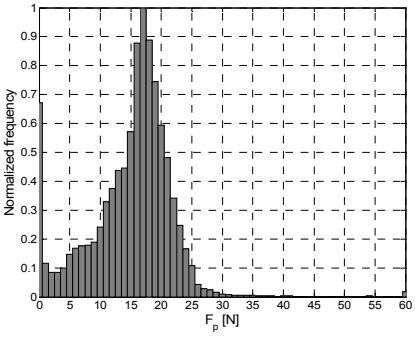
c) *THW-feedback*; before cd-task



g) *THW-feedback*; after cd-task



d) *TTC-feedback*; before cd-task



h) *TTC-feedback*; after cd-task

Figure 80: Distributions of the gas pedal forces exerted on the gas pedal by all drivers together, for *THW*=1.0 [s] - before the cd-task (left) and after the cd-task (right).

Nomenclature

Symbols

α	pedal position, %
α	maximum acceleration, m/s^2
α_f	foot displacement, %
α_p	pedal displacement, %
α_s	endpoint displacement of the foot (including skin deformation), %
a	acceleration, m/s^2
a_c	commanded acceleration, m/s^2
A	angular displacement, degrees
A_i	obstacle from a collection of obstacles, indexed by I
A_d	speed disturbance amplitude, m/s
β	slip angle, rad
β_p	brake pedal depression, %
b	damping of a virtual bumper, Ns/m
B	damping, Ns/m
B_f	damping of the muscle force, Ns/m
B_p	damping of the gas pedal, Ns/m
B_s	damping of the contact point, Ns/m
B_v	virtual damping, Ns/m
$\underline{c}$	total obstacle avoidance vector
$\underline{c}_{0,i}$	obstacle avoidance vector of obstacle A_i
$\underline{c}_g$	goal attraction vector
Δ	delta, infinitesimal increase
d_i	distance of the own vehicle to an obstacle A_i along $\underline{n}_i$, m
D	frequency transformation of the lead vehicle velocity
D	lead vehicle speed disturbance characteristics set
e	error
E	frequency transformation of the error
f_d	speed disturbance bandwidth, Hz

F	force, N
F	= between treatments mean square / Residual mean square
F_β	break pedal end force, N
F_δ	steering wheel force, N
F_f	muscle force, N
F_p	pedal force, N
F_{refl}	reflexive force, N
F_p	pedal force, N
F_s	contact force, N
g	gravitational constant, 9.81 m/s^2
Γ	coherence function in frequency domain
$\underline{\theta}$	parameter vector
H	frequency response function
I	physical stimulus intensity
j^2	= -1
k	stiffness of a virtual bumper, N/m
k	sensed continuum constant in Stevens' law
K	stiffness, N/m
K	Weber's law constant
K	control gain
K_f	muscle stiffness, N/m
K_p	pedal stiffness, N/m
K_s	contact point stiffness, N/m
K_v	virtual stiffness, N/m
l	distance from center of gravity to vehicle bumper, m
l	length of gas-pedal arm, m
L	cost function
M	mass, kg
M_f	muscle masse, kg
M_p	pedal mass, kg
M_v	virtual mass, kg
n	modality constant in Steven's law
$\underline{n_i}$	obstacle normal vector
N	index maximum
N	frequency transformation of driver remnant
p	significance
P	potential
P_i	potential of an obstacle A_i
σ	standard deviation
S	pedal stroke, m
S	subjective sensation magnitude
S	spectral density
S	haptic feedback system set
τ_c	time delay of the vehicle dynamics
τ_i	minimum avoidance time, s
τ_I	lag time
τ_L	lead time
t_r	time the pedal is not depressed, s
t_{CD}	CD task-time, s
T	time headway set
T	reaction time, s

T_{CFOV}	reaction time to stimuli presented in central field of view, s
T_i	maximum avoidance time, s
T_{PFOV}	reaction time to stimuli presented in peripheral field of view, s
THW	time headway, s
TTC	time-to-contact, s
U	frequency transformation of α
φ_m	phase margin
v	course angle, rad
v	speed, m/s
v_i	approach velocity in direction of $\underline{n}_i$, m/s
V	speed, m/s
V	frequency transformation of the relative velocity
V	visual stimuli set
ω_c	cross-over frequency
Ω	frequency vector
ψ	heading angle, rad
x	position, m
X	frequency transformation of the relative distance between vehicles
y	measured experimental output
$\hat{y}$	model output
Y	frequency transformation of the own vehicle speed

Subscripts

β	of the brake pedal
c	car
car	of the own vehicle
$CFOV$	central field of view
δ	of the steering wheel
d	driver
d	disturbance
$driver$	of the driver
f	muscle force
h	haptic
i	initial
i	index of a collection
in	inner loop
k	index of a collection
l	lumped
$lead$	of the lead vehicle
$lead\ car$	of the lead vehicle
max	maximum
min	minimum
out	outer loop
p	of the gas pedal
$PFOV$	peripheral field of view
pp	potential power
$pedal$	of the gas pedal
r	reaction
$refl$	reflexive

rel	relative
s	contact force
t	time
THW	time headway
TTC	time-to-contact
v	visual
v	virtual

Acronyms

ABS	Anti-lock Braking System
ACC	Advanced Cruise Control
ANOVA	Analysis of Variance
CWS	Collision Warning System
DERP	Driver Eye Reference Point
DOF	Degrees of Freedom
DSS	Driver Support System
EBD	Electronic Brake Distribution
FFT	Fast Fourier Transform
FOV	Field of View
FRF	Frequency Response Function
GPF	Generalized Potential Field
IDSS	Intelligent Driver Support System
ITS	Intelligent Transportation System
JND	Just Noticeable Difference
LCD	Liquid Crystal Display
LDWS	Lane Departure Warning System
RCAS	Read-End Collision Avoidance System
RPM	Revolutions per Minute
SIPS	Side Impact Protection System
SNR	Signal to Noise Ratio
THW	Time Headway
TTC	Time to Contact
VAF	Variance Accounted For
VDC	Vehicle Dynamics Control

References

Abbink, D.A. (2006) "*Neuromuscular Analysis of Haptic Gas Pedal Feedback during Car-Following*" PhD dissertation, Department of Mechanical Engineering, Delft University of Technology, the Netherlands.

Abbink, D.A., and van der Helm, F.C.T. (2005) "*Muscle Activity Measurements during Gas Pedal Manipulation*" *Unpublished*.

Abbink, D.A., and van der Helm, F.C.T. (2004) *"Force Perception Measurements at the Foot"* Proceedings of the IEEE International Conference on Systems, Man, and Cybernetics, Den Haag, the Netherlands, October 10-13.

Abbink, D.A., van der Helm, F.C.T., and Boer, E.R. (2004) *"Admittance Measurements of the Foot during 'Maintain Position' and 'Relax' Tasks on a Gas Pedal"* Proceedings of the IEEE International Conference on Systems, Man, and Cybernetics, Den Haag, the Netherlands, October 10-13.

Abbink, D.A., and Mulder, M. (2003) *"Final Report on The (Haptic) Presentation of Spatio-Temporal Affordances in Car Driving"* Unpublished, confidential year report for Nissan Research Center, Delft University of Technology, Delft, the Netherlands.

Ando, S., Kida, N., and Oda, S. (2002) "*Practice Effects on Reaction Time for Peripheral and Central Visual Fields*" Perceptual and Motor Skills, Vol. 95, No. 3, pp. 747-751.

Billings, C.E. (1997) *"Aviation Automation – The Search for a Human-Centered Approach"* Mahwah, NJ. Lawrence Erlbaum Associates.

Blauw, G.J. (1984) "*Car Driving As A Supervisory Control Task*" PhD Thesis, Institute for Perception TNO, Soesterberg, the Netherlands.

Boer, E.R. (1999) *"Car Following from the Driver's Perspective"* Transportation Research – Part F: Traffic Psychology and Behaviour, Vol. 2, No. 4, pp. 201-206.

Borenstein, J., and Koren, Y. (1991) *"The Vector Field Histogram – Fast Obstacle Avoidance for Mobile Robots"* IEEE Transactions on Robotics and Automation, Vol. 7, No. 3, pp. 278-288.

Borra, T. (2003) *"The Load of Haptic Feedback on Attentional Processes – A study into the effect of haptic feedback on reaction time in a car-simulator"* Master thesis, Leinden University, department of Cognitive Psychology, Leiden, the Netherlands.

Brackstone, M., Sultan, B., and McDonald, M. (2002) *"Motorway driver behaviour: studies on car following"* Transportation Research Part F, Vol. 5, pp. 329-344. Elsevier.

Brebner, J.M.T., and Welford, A.T. (1980) "*Introduction: An Historical Background Sketch*" In: Reaction Times (A.T. Welford, Ed.), Academic Press, New York, pp. 1-23.

Campbell, B.N., Smith, J.D., and Najm, W.G. (2003) *"Examination of Crash Contributing Factors Using National Crash Databases"* Technical Report No. DOT HS 809 664, U.S. Department of Transportation, Cambridge, MA.

Cavallo, V. and Laurent, M. (1988) *"Visual Information and Skill Level in Time-to-Collision Estimation"* Perception, Vol. 17, pp. 623-632.

Ceder, A. (1979) *"Stable Phase-Plane and Car-Following Behavior as Applied to a Macroscopic Phenomenon"* Transportation Science, Vol. 13, No. 1, pp. 64-78.

Continental (2004) *"Adaptive Cruise Control with intuitive feedback"* Press release, Continental Temic, Division Continental Automotive Systems, Nuremberg, Germany.

DIATS – Deployment of Inter-urban ATT Test Scenarios (1998)*"User Preference and Behavioural changes from ATT systems."* Deliverable 13-14, October 1998, CEC Brussels, Belgium.

Dingus, T.A., McGehee, D.V., Manakkal, N., Jahns, S.K., Carney, C., and Hankey, J.M. (1997) *"Human Factors Field Evaluation of Automotive Headway Maintenance/Collision Warning Devices"* Human Factors, 39 (2), pp. 216-229.

Fuller, R. (1984) *"A conceptualization of driving behaviour as threat avoidance"* Ergonomics, Vol. 27(11), pp. 1139-1155.

Gerdes, J.C., Rossetter, E.J. (1999) *"A Unified Approach to Driver Assistance Systems Based on Artificial Potential Fields"* Proceedings of the International Mechanical Engineering Congress and Exposition, Nashville, TN, USA, November 14-19.

Gibson, J.J. (1986) *"The ecological approach to visual perception"* Hillsdale, NJ: Lawrence Erlbaum Associates (originally published in 1979).

Gibson, J.J. and Crooks, L.E. (1938) *"A Theoretical Field-Analysis of Automobile-Driving"* Journal of Psychology, Vol. 51, No. 3, pp. 453-471.

Godthelp, J., and J. Schumann (1993) *"Intelligent Accelerator: an Element of Driver Support"* In: Driving future vehicles, Parkes, A. M. and Franzén, S. (Eds.), pp. 265-275. London: Taylor & Francis.

Goodrich, M.A., and Boer, E.R. (2003) *"Model-Based Human-Centered Task Automation: A Case Study in ACC System Design"* IEEE Transactions on Systems, Man, and Cybernetics – Part A: Systems and Humans, Vol. 33, No. 3, pp. 325-336.

Goodrich, M.A., and Boer, E.R. (2000) *"Designing Human-Centered Automation: Tradeoffs in Collision Avoidance System Design"* IEEE Transactions on Intelligent Transportation Systems, Vol. 1, No. 1, pp. 40-54.

Goodrich, M.A., and Quigley, M. (2004) *"Learning Haptic Feedback for Guiding Driver Behaviour"* Proceedings of the IEEE International Conference on Systems, Man, and Cybernetics, Den Haag, the Netherlands, October 10-13.

Gordon, D.A. (1971) *"The Driver in Single Lane Traffic"* Highway Research Record 349, pp. 31-41.

Gray, R. and Regan, D. (1998) *"Accuracy of Estimating Time to Collision using Binocular and Monocular Information"* Vision Research, Vol. 38, No. 4, pp. 499-512.

van der Helm, F.C.T., Schouten, A.C., de Vlugt, E., and Brouwn, G.G. (2002) *"Identification of Intrinsic and Reflexive Components of Human Arm Dynamics During Postural Control"* Journal of Neuroscience Methods, 119, pp. 1-14.

Hennessey, M.P. and Donath, M. (1992) *"Distributed Impedance Control of an N DOF Serial Link Manipulator Using Interpolation Theory"* Advances in Robotics, Dynamic Systems and Control, ASME, Vol. 42, pp. 169-180.

Hennessey, M.P., Shankwitz, C., and Donath, M. (1995) *"Sensor based 'virtual bumpers' for collision avoidance: configuration issues"* Proceedings of the International Society for Optical Engineering SPIE, Vol. 2592, pp. 48-59.

Higashimata, A., Adachi, K., Hashizume, T., and Tange, S. (2001) *"Design of a headway distance control system for ACC"* JSAE Review 22, No. 1, pp. 15-22.

Hjälmdahl, M., and Várhelyi, A. (2004) *"Speed regulation by in-car active accelerator pedal. Effects on driver behaviour"* Transportation Research Part F, Vol. 7, pp. 77-94. Elsevier.

Hjälmdahl, M., Almqvist, S., and Várhelyi, A. (2002) *"Speed regulation by in-car active accelerator pedal – effects on speed and speed distribution"* IATSS Research, Vol. 26(2), pp. 60-67.

Hoffmann, E.R. and Mortimer, R.G. (1994) *"Drivers' Estimates of Time to Collision"* Accident Analysis and Prevention, Vol. 26, No. 4, pp 511-520.

Hogema, J.H. (1996) *"Modelling of Individual Car-Following Behaviour"* Proceedings of the XV European Annual Conference on Human Decision Making and Manual Control. TNO, The Netherlands.

Horowitz, A.D., and Dingus, T.A. (1992) *"Warning Signal Design: a Key Human Factors Issue in an In-Vehicle Front-to-Rear-End Collision Warning System"* Proceedings of the Human Factors Society 36th Annual Meeting, pp. 1011-1013.

Jagtman, H.M., V.A.W.J. Marchau, and T. Heijer (2001) "*Current Knowledge on Safety Impacts of Collision Avoidance Systems (CAS)*" In: Critical Infrastructures – 5th International Conference on Technology, Policy and Innovation (P.M. Herder, and W.A.H. Thissen, Ed.). Delft.

Kitazaki, S. (2002) *"Nissan Intelligent Driver Support System: Magic Bumper. What Nissan Tries to Achieve and What Has Been Found so Far"* Unpublished, confidential 1st Nissan Workshop introduction presentation, Nissan Research Center, Yokohama, Japan.

Knipling, R.R., M. Mironer, D.L. Hendricks, L. Tijerina, J. Everson, J.C. Allen, and C. Wilson (1993). "*Assessment of IVHS Countermeasures for Collision Avoidance: Rear-end Crashes*" Report No. DOT HS 807 995. National Highway Traffic Safety Administration, Washington, D.C.

Krogh, B.H. (1984) *"A Generalized Potential Field Approach to Obstacle Avoidance Control"* International Robotics Research Conference, Bethlehem, PA, USA, August 14-16.

Kruit, J.D. (2005) *"Design of a Rally Driver Support System"* MSc. thesis, Department of Aerospace Engineering, Control & Simulation Division, Delft University of Technology.

Lee, D.N. (1976) *"A Theory of Visual Control of Breaking Based on Information about Time-to-Collision"* Perception, Vol. 5, pp. 437-459.

Manser, M.P., Ward, N.J., & Kuge, N. (2004a). Magic Bumper and Virtual Bumper Usability and Driver Stress Evaluation. Contract 20077114-A01 (Nissan Motor Company, LTD, Japan), HumanFIRST Program, University of Minnesota.

Manser, M.P., Ward, N.J., & Kuge, N. (2004b). Field Test Evaluation of Magic Bumper Usability and Stress Constructs. Contract 20077114-A01 (Nissan Motor Company, LTD, Japan), HumanFIRST Program, University of Minnesota.

McDonald, M., Brackstone, M.A., Sultan, B., and Roach, C. (1997) *"Close Following on the Motorway: Initial Findings of an Instrumented Vehicle Study"* Proceedings of the 7th Vision in Vehicles Conference, Marseille, France.

McLeod, P.D. (1977). "*A Dual Task Response Modality Effect: Support for Multi-Processor Models of Attention*" Quarterly Journal of Experimental Psychology, Vol. 29, pp. 651-667.

McRuer, D.T., and Jex, H.R. (1967) *"A Review of Quasi-Linear Pilot Models"* IEEE Transactions on Human Factors in Electronics, HFE-8(3), pp. 231-249.

McRuer, D.T., and Krendel, E.S. (1974) *"Mathematical Models of Human Pilot Behaviour"* AGARD-AG-188.

Mulder, M. (1999) *"Cybernetics of Tunnel-in-the-Sky Displays"* Ph.D. dissertation, Department of Aerospace Engineering, Control & Simulation Division, Delft University of Technology, the Netherlands.

Mulder, M., Mulder, M., van Paassen, M.M., Kitazaki, S., Hijikata, S, and Boer, E.R. (2004a) *"Car-Following Support With Haptic Gas Pedal Feedback"* Proceedings of the IFAC Symposium on Analysis, Design, and Evaluation of Human-Machine Systems, Atlanta, GA, USA, September 7-9.

Mulder, M., Mulder, M., van Paassen, M.M., Kitazaki, S., Hijikata, S., and Boer, E.R. (2004b) "*Reaction-Time Task During Car-Following with an Active Gas Pedal*" Proceedings of the IEEE International Conference on Systems, Man, and Cybernetics, Den Haag, the Netherlands, October 10-13.

Mulder, M., Mulder, M., van Paassen, M.M., and Abbink, D.A. (2005a), "*Identification of Driver Car-Following Behaviour*" Proceedings of the IEEE International Conference on Systems, Man, and Cybernetics, Hawaii, USA, October 10-12.

Mulder, M., Mulder, M., van Paassen, M.M., and Abbink, D.A. (2005b), "*Effects of Lead Vehicle Speed and Separation Distance on Driver Car-Following Behaviour*" Proceedings of the IEEE International Conference on Systems, Man, and Cybernetics, Hawaii, USA, October 10-12.

National Highway Traffic Safety Administration (1992) *"NHTSA IVHS Plan"* Publication No. DOT HS 807 850, NHTSA Office of Crash Avoidance Research.

van der Ouderaa, E., Schoukens, J., and Renneboog, J. "Peak Factor Minimization Using a Time-Frequency Domain Swapping Algorithm" IEEE Transactions on Instrumentation and Measurement, Vol. 37, No. 1, pp. 145-147.

Pauwelussen, J.J.A. (2005) *"Design of an Intelligent Driver Support System Including Deceleration Control"* Master thesis, Department of Aerospace Engineering, Control & Simulation Division, Delft University of Technology, the Netherlands.

Piao, J., and McDonald, M. (2003) *"Low speed car following behaviour from floating vehicle data"* Proceedings of the IEEE Intelligent Vehicles Symposium, Columbus, Ohio, USA.

Rasmussen, J. (1983) *"Skills, Rules, and Knowledge: Signals, Signs, and Symbols, and Other Distinctions in Human Performance Models"* IEEE Transactions on Systems, Man, and Cybernetics, SMC-13, no. 3, pp. 257-266.

Ratering, S., and Gini, M. (1995) *"Robot Navigation in a Known Environment with Unknown Moving Obstacles"* Autonomous Robots, Vol. 1, No. 2., pp. 149-165.

Rockwell, T.H. (1972) *"Skills, Judgment and Information Acquisition in Driving"* In: Human Factors in Highway Traffic Safety Research (T.W. Forbes, Ed.), pp. 133-164. Wiley-Interscience, New York.

Rudin-Brown, C.M., and Parker, H.A. (2004) *"Behavioural Adaptation to Adaptive Cruise Control (ACC): Implications for Preventive Strategies"* Transportation Research Part F, Vol. 7, pp. 59-76. Elsevier.

Schiff, W. and Detwiler, M.L. (1979) *"Information Used in Judging Impending Collision"* Perception, Vol. 8, pp. 647-658.

Schouten, A.C. (2004) "*Proprioceptive reflexes and neurological disorders"*, Ph.D. dissertation, Department of Mechanical Engineering, Delft University of Technology, the Netherlands.

Sheridan, T.B., and Ferrell, W.R. (1974) *"Man-Machine Systems: Information, Control, and Decision Models of Human Performance"* Cambridge, Massachusetts: MIT Press.

Smiley, A. (2000) *"Behavioral Adaptation, Safety, and Intelligent Transportation Systems"* Transportation Research Record 1724, pp. 47-51.

Stevens, S.S. (1957) *"On the Psychophysical Law"* Psychology Review, Vol 64, No. 3, pp. 153-181.

Taieb-Maimon, M. and Shinar, D. (2001) *"Minimum and Comfortable Driving Headways: Reality versus Perception"* Human Factors, Vol. 43, No. 1, pp. 159-172.

Tijerina, L., S. Johnston, E. Parmer, H.A. Pham, and M.D. Winterbottom (2000), *"Preliminary Studies in Haptic Displays for Rear-End Collision Avoidance System and Adaptive Cruise Control System Applications"*. Report No. DOT HS 808 (TBD)National Highway Traffic Safety Administration, Washington, D.C.

Treat, J.R., Tumbas, N.S., McDonald, S.T., Shinar, D., Hume, R.D., Mayer, R.E., Stansifer, N. J., and Castellan, N. J. (1979) *"Tri-level study of the causes of traffic accidents: final report"* Final Report DOT HS-805 085, Washington, DC: United States Department of Transportation.

USDoT (1996) *"Preliminary Human Factors Guidelines for Crash Avoidance Warning Systems"* NHTSA Project No. DTNH22-91-C-07004, U.S. Department of Transportation, National Highway Traffic Safety Administration.

Várhelyi, A. (2002) "*Speed management via in-car devices: effects, implications, perspectives"* Transportation, Vol. 29, pp. 237-252. Kluwer Academic Publishers.

Verkeer en Waterstaat (2000) *"Houd 2 seconden afstand"* Press release (in Dutch only), Dutch Ministry of 'Verkeer en Waterstaat'.

Verwey, W.B., Alm, H., Groeger, J.A., Janssen, W.H., Kuiken, M.J., Schraagen, J.M., Schumann, J., van Winsum, W., and Wontorra, H. (1993) *"GIDS functions"* In: Generic Intelligent Driver Support, Michon, J.A. (Ed.), pp. 113-146. London: Taylor & Francis.

de Vlugt, E., Schouten, A.C., and van der Helm, F.C.T. (2002) *"Adaptation of reflexive feedback during arm posture to different environments"* Biological Cybernetics, Vol. 87, pp. 10-26.

de Vlugt, E. (2004) *"Identification of Spinal Reflexes"*, Ph.D. dissertation, Department of Mechanical Engineering, Delft University of Technology, the Netherlands.

Vogel, K. (2003) *"A Comparison of Headway and Time to Collision as Safety Indicators"* Accident Analysis and Prevention, Vol. 35, pp. 427-433.

Wang, J.S., Knipling, R.R., and Goodman, M.J. (1996) *"The Role of Driver Inattention in Crashes; New Statistics from the 1995 Crashworthiness Data System"* 40th Annual Proceedings of the Association for the Advancement of Automotive Medicine, pp. 377-392.

Ward, N.J., Manser, M.P., & Kuge, N. (2004). Evidence of Behavioral Adaptation with MB and the Effect of System Failures Contract 20077114-A01 (Nissan Motor Company, LTD, Japan), HumanFIRST Program, University of Minnesota.

Wickens, C.D. (1992) *"Engineering psychology and human performance"* Second edition. New York: HarperCollins.

van Winsum, W. and Heino, A. (1996) *"Choice of Time-Headway in Car-Following and the Role of Time-to-Collision Information in Braking"* Ergonomics, Vol. 39, No. 4, pp. 579-592.

de Winter, J.C.F. (2004a) *"IDSS 2D Impedance Field"* Preliminary graduation thesis, Department of Aerospace Engineering, Control & Simulation Division, Delft University of Technology, the Netherlands.

de Winter, J.C.F. (2004b) *"A Two Dimensional Weighting Function for the Intelligent Driver Support System"* Master thesis, Department of Aerospace Engineering, Control & Simulation Division, Delft University of Technology, the Netherlands.

de Winter, J.C.F., Mulder, M., Mulder, M., Yamamura, T. (2005) *"Weighted Two-Dimensional Longitudinal Impedance for Driving Support System"* Proceedings of the 23rd European Annual Conference on Human Decision Making and Manual, Den Haag, the Netherlands.

Yamamura, T. (2002) *"Definition of the Potential Field for IDSS"* Unpublished, confidential presentation at Delft University of Technology.

Young, M.S., and Stanton, N.A. (2004) *"Taking the load off: investigations of how adaptive cruise control affects mental workload"* Ergonomics, Vol. 47, No. 9, pp. 1014-1035.

Samenvatting

De auto wordt steeds meer gezien als het verlengstuk van de huiskamer. Dientengevolge vragen in de auto aanwezige apparaten, zoals radio's, mobiele telefoons, en tegenwoordig ook navigatie systemen, steeds meer aandacht van de bestuurder die daardoor steeds meer afgeleid wordt van zijn primaire bronnen van informatie om de auto goed te kunnen besturen: de weg en andere weggebruikers. Verkeersongevallen statistieken wijzen onoplettendheid van de bestuurder aan als één van de grootste ongevallen veroorzakers (Campbell, Smith en Najm, 2003; Wang Knipling, en Goodman, 1996; Treat *et al.*, 1979). Dus het groeiende gebruik van apparaten in de auto is een zorgzame, misschien zelfs gevaarlijke ontwikkeling.

Om het gat te dichten dat is ontstaan tussen veiligheidsverbeteringen door de ontwikkeling van passieve veiligheidssystemen (bijvoorbeeld airbags en kreukelzones) en de toenemende ontwikkeling en toepassing van niet aan het besturen van de auto gerelateerde toepassingen van elektronica in de auto, wordt het onderzoek naar veiligheidssystemen steeds meer gericht op de ontwikkeling van actieve systemen. Deze actieve systemen zijn erop gericht bestuurders te helpen ongelukken te voorkomen, in plaats van de gevolgen van een ongeluk te verzachten zoals passieve systemen doen.

De Intelligente Transport Systemen (ITS) die momenteel beschikbaar zijn kunnen gecategoriseerd worden door wat Goodrich en Boer (2000) het primaire doel van taakautomatisering noemen: "veilig het comfort verbeteren". Door routine taken te automatiseren, die voorheen door de bestuurder uitgevoerd werden (bijvoorbeeld het reguleren van de snelheid, wat door Adaptive Cruise Control (ACC) kan worden overgenomen), wordt het besturen van een auto vereenvoudigd voor de bestuurder. Taak automatisering voert bestuurderstaken uit die automatisch de veiligheid garanderen in een gelimiteerde set van condities. Recentelijk is de aandacht verschoven naar de ontwikkeling van actieve systemen, die Goodrich en Boer (2000) reactieautomatisering noemen: "comfortabel de veiligheid verbeteren". Dit type automatisering geeft de bestuurder automatisch informatie wanneer de veiligheid in gevaar komt. Dus, in plaat van een bestuurderstaak over te nemen, houdt

reactieautomatisering de omgeving in de gaten en geeft dan, op basis van die informatie, veiligheidswaarschuwingen aan de bestuurder. De bestuurder blijft de eindverantwoordelijke voor het uitvoeren van de juiste regelacties om de veiligheidssituatie te verbeteren.

Het onderzoek dat in deze dissertatie gepresenteerd wordt richt zich op het ondersteunen van bestuurders in hun longitudinale regeltaak tijdens het volgen van een voorligger. In april 2002 is de Technische Universiteit Delft een samenwerkingsverband aangegaan met Nissan Motor Company Ltd., door deel te nemen aan een rond de mens gecentreerde ontwikkeling van een toekomstig intelligent bestuurder ondersteuningssysteem (IDSS). Het doel van het project is de ontwikkeling van een systeem dat samenwerkt met de bestuurder om op een comfortabele manier een veilige afstand te waarborden tussen het eigen voertuig en een voorligger. Het doel van deze dissertatie is een rond de mens gecentreerde ontwikkeling van een haptisch gas pedaal ter ondersteuning van het houden van afstand bij het volgen van een andere auto.

Twee verschillende aanpakken zijn uitgeprobeerd en geschikt bevonden voor het overbrengen van haptische informatie via het gas pedaal. De eerste aanpak was het toevoegen van een kracht op het gas pedaal als maat voor de verandering in de volgafstand. De dynamica van het gas pedaal, dat wil zeggen, de kracht/positie relatie van het pedaal, wordt hierdoor niet veranderd. De tweede aanpak was het veranderen van de stijfheid van het gas pedaal ten gevolge van veranderingen in de volgafstand. Hierdoor verandert de gas pedaal dynamica. In beide aanpakken wordt de kracht of stijfheid door een elektrische actuator geleverd.

De toegevoegde haptisch regellus die ontstaat door de terugkoppeling van omgevingsinformatie via het gas pedaal is gebaseerd op één aanname: informatie uit de omgeving kan geconverteerd worden naar betekenisvolle haptische informatie via het gas pedaal.

Uit het onderzoek naar de meest geschikte omgevingsvariabelen die de veranderingen in volgafstand het beste weergeven en de constatering dat zowel kracht als stijfheid teruggekoppeld kan worden zijn drie algoritmen ontstaan. Één algoritme is ontworpen om kracht terugkoppeling te genereren, gebaseerd op informatie uit de omgeving uitgedrukt in *time-headway* (*THW*) en *time-to-contact* (*TTC*). Dit algoritme is het *force feedback* algoritme genoemd. De andere twee algoritmen maakten gebruik van stijfheidterugkoppeling. Een maakt alleen gebruik van *THW* informatie – het *THW-stiffness* algoritme. Het andere stijfheidalgoritme maakt gebruik van *TTC* en de *THW* wordt gebruikt als schaalfactor.

Omdat de transformatie van omgevingsinformatie (*THW, TTC*) naar haptisch informatie geen natuurlijk equivalent heeft was het van te voren onmogelijk om te weten hoe bestuurders zouden reageren op deze vorm van ondersteuning. Analogieën kunnen wel worden gemaakt om het principe uit te leggen, zoals gelijke polen die elkaar afstoten, maar de exacte reacties van de bestuurders en de mate van waarneembaarheid van de informatie blijven onbekend. Daarom zijn de ontwikkelde algoritmen onderzocht en getest in een aantal experimenten met een groot aantal verschillende omgevingscondities.

De verwachting was, ten eerste, dat bestuurders de stuurtaak met haptische feedback als een krachttaak zouden opvatten. Dat wil zeggen dat bestuurders zullen proberen de kracht, die zij voelen via het gas pedaal, zoveel mogelijk constant te houden. Omdat de haptische feedback algoritmen ontwikkeld zijn om meer kracht te bieden als de volgauto dichterbij komt, resulteert

een krachttaak automatisch in de gewenste regelactie: gas terug als de volgauto dichterbij komt; gas indrukken als de volgauto van de eigen auto weg rijdt.

Uit de statistische analyse van de resultaten van de uitgevoerde experimenten blijkt dat deze krachttaak hypothese geaccepteerd kan worden maar niet voor alle drie de algoritmen. Voor het *THW-stiffness* algoritme is nauwelijks een krachttaak waar te nemen in het pedaalgebruik van de bestuurders van de auto simulator. De verschillen tussen het *force-feedback* en het *TTC-stiffness* algoritme zijn verwaarloosbaar. Het kan geconcludeerd worden dat ze beiden tot een krachttaak regeling door de bestuurders leiden tijdens volgsituaties.

Uit het feit dat in alle experimenten volgt dat bestuurders met minder regelinspanning dezelfde volgprestatie konden leveren, blijkt dat bestuurders waardevolle omgevingsinformatie met betrekking tot de volgtaak verkrijgen uit de haptische feedback, evenals informatie over de voertuigdynamica van de auto die ze besturen.

De prijs voor de lagere regelinspanning is echter een verhoging van de fysieke belasting tijdens de volgtaak en de haptische feedback actief. Alle drie de algoritmen lieten een significante verhoging van de fysieke belasting zien. Uit de experimenten blijkt verder wel, dat het *force-feedback* en het *TTC-stiffness* algoritme de minste verhoging van de fysieke belasting laten zien, terwijl ze wel dezelfde verlaging van de regelinspanning opleveren als het *THW-stiffness* algoritme.

Ter afsluiting, de bestuurders gaven subjectief gezien te kennen dat ze baat hebben bij de haptische informatie die ze via het gas pedaal ontvingen tijdens het volgen van een voorligger. Dit geeft aan dat bestuurders vertrouwen hebben in het systeem. De combinatie van vertrouwen en verminderde regelinspanning zou wel eens een prima combinatie kunnen zijn in het steeds chaotischer en drukker wordende verkeer van vandaag en in de toekomst.

Acknowledgements

The work in this thesis has first and most important of all been the result of the sponsorship of Nissan Motor Company Ltd., Japan. Their support of and participation in an international, multi-university research effort to investigate the human-machine issues related to their innovative 'Magic Bumper' concept has been a very interesting and rewarding academic experience for me personally, and Delft University of Technology as one of the participating universities. I would specifically like to thank Mr. Y. Akatsu, Mr. K. Doi, Dr. S. Kitazaki, Dr. T. Yamamura, and Mr. S. Hijikata of Nissan Motor Company for their cooperation, their professional input and feedback and their company during our meetings and workshops. We are very much obliged to their dedication to make the project and the cooperation work.

Of course, this whole project would not have functioned as well as it did without the impressive 24 hour, 7 days a week input of Dr. Erwin Boer either. His efforts to coordinate a scientifically, professionally, culturally and linguistically diverse group of equally diverse personalities have been astonishing. His secret of not suffering from jet-lag must be to travel continuously, thus entering a state of perpetual jet-lag. I would like to call this 'the art of project maintenance'.

I would also like to thank Prof. John Lee, Prof. Mike Goodrich, Dr. Nicholas Ward, Dr. Mike Manser, MSc. Heather Stoner, MSc. Bobbie Seppelt, MSc. Deborah Forster, MSc. David Whipf, MSc. Jonathan Levy and all other colleagues of the 'Magic Bumper' project with whom I had the pleasure of working.

Closer to home, at Delft University of Technology, my gratitude is going to my supervisors Dr. Max Mulder and Dr. René van Paassen for taking me onboard this project. Our cooperation with Prof. Frans van der Helm and Dr. David Abbink from the department of Mechanical Engineering has been the driving force for me to make this project a success both personally as well as professionally.

If boring people complain about their professional life, the song is always only work and no play; I think that it speaks for itself when I say that working with David was quite the

opposite! Max, Rene and Frans had to be more professional due to their positions (of course…), but their personal involvement and commitment to the project has been of invaluable importance for my successful and enjoyable three and a half years of working with them.

Those three and a half years would have been three and a half years only if it wasn't for Max and Frans to convince me of writing this thesis. I am grateful to Prof. Bob Mulder and Prof. Frans van der Helm for having them as my promoters. Dr. Hans van der Vaart reviewed some of my first Chapters, for which I would like to thank him.

The work that I accomplished is not my personal achievement alone. I made use of delicate and specialistic equipment built and maintained by a number of people from the department of Aerospace Engineering at Delft University of Technology. I have made frequent use of the time, expertise and patience of Ing. Kees van Woerkom who proved to be invaluable in creating and trouble-shooting the electronics of our driving simulator. Of course, Adri Tak and Ing. Henk Lindenburg had part in this work too, but most importantly, they helped me getting the driving simulator built in the first place. All construction work was designed by Ruud van Olden and constructed by Ed Roessen. For all my computer related problems I could always count on Ing. Peter Kraan and Ing. Andries Muis to get things solved.

Besides help in getting the hardware up and running, I also had help with my research from Master students and interns. Tobias Borra, psychology student from Leiden University, was the first to work with me on his graduation project, followed by Joost de Winter, currently a PhD. student at the department of Mechanical Engineering, here at Delft University of Technology. João da Silva came all the way from Portugal and Jasper Pauwelussen was happy to find a project on cars, rather than airplanes, at our department. Julian de Pool Diaz, Rob Brink, and Wytze Hoekstra completed their internship with me by taking some of the development tasks out of my hands.

A great part of my work consisted of experiments in the driving simulator. I am much obliged to all of those who – voluntarily (most of the time) – participated.
And last, but not least, I would like to thank all my colleagues simply for being my colleagues.

Mark Mulder Delft, November 2006

Curriculum vitae

Mark Mulder was born on January 20, 1974 in the Holy hospital, Vlaardingen, the Netherlands. He grew up in Puttershoek, a small village south of Rotterdam. From 1980 – 1984 he attended the 'Baanbreker' primary school, which, after moving to Strijen, he completed in 1986 at the 'Patrijspoort'. From 1986 – 1992, daily cycling some 18 km to and fro the 'RSG Oud Beijerland', he got his secondary *VWO* education in preparation of his academic adventure in Delft.

Choosing to pursue an academic degree in Aerospace Engineering in 1992, Mark moved to Delft in 1993, after commuting to Delft in his first year at Delft University of Technology. Life as a university student didn't prove to give all the answers to the questions of life, which led to the first of a number of yearlong journeys around the world in 1997.

Life was beautiful, easy and fun when travelling, but cash was short and hard to get. A return to academics was the end of what had been a year of broadening of horizons and the foundation of great friendships which resulted in a new zest to succeed in graduating from the department of Aerospace Engineering at Delft. In 2000 Mark obtained his Masters in Aerospace Engineering, graduating on the 'Integration of Aircraft Warning Systems'. This research was supervised by Prof. Bob Mulder , Dr. Max Mulder and Dr. René van Paassen.

After yet another trip around the world, Mark found himself back in Delft again, working with Dr. Max Mulder, Dr. René van Paassen, Prof. Frans van der Helm and Dr. David Abbink at Delft University of Technology on the development of a new driver support system – the research of which this thesis is the result.

In the year preceding the defence of this thesis, Mark worked for Médecins Sans Frontières as a field logistician in Sierra Leone.